Universidade do Minho
Escola de Engenharia

Bárbara Daniela da Costa Ferreira

Resilience of concrete structures in the marine environment through microstructural innovation

dezembro de 2015

Resilience of concrete structures in the marine environment through microstructural innovation
Bárbara Daniela da Costa Ferreira
UMinho | 2015

Universidade do Minho
Escola de Engenharia

Bárbara Daniela da Costa Ferreira

Resilience of concrete structures in the marine environment through microstructural innovation

Dissertação de Mestrado
Ciclo de Estudos Integrados Conducentes ao
Grau de Mestre em Engenharia Civil

Trabalho efectuado sob a orientação do
Professor Doutor Eduardo Nuno Borges Pereira
Professor Doutor Vítor Manuel Couto Fernandes Cunha

dezembro de 2015

ACKNOWLEDGEMENTS

This dissertation would not have been possible without the help of so many people in so many ways.

I would like to express my sincere appreciation to my Principal Supervisor, Doctor Eduardo Pereira and Co-supervisor, Doctor Vítor Cunha, for their constant guidance and encouragement, without which this work would not have been possible. For their unwavering support. I am truly grateful.

One special thanks to PhD student João Almeida for is support, advices, guidance, valuable comments and suggestions and for help in the experimental research. Without is precious help this work would not be possible!

I want to thank to all of the companies that provided the materials used in this research: Secil, Civitest, Sika, Fibraflex and Eurocálcio – Calcários e Inertes SA.

I would like to thank my friends, and colleagues at the University of Minho for their encouragement and moral support over those five years, in particular to: Cátia Machado, Joana Machado, José Pereira, Bárbara Pereira, Ana Paula Carvalho, Ana Ribeiro, Elisabete Teixeira and Andreia Martins. We had our funny times!

Lastly, and most of all, I would like to thank my family, who has been a source of encouragement and inspiration to me throughout my life.

ABSTRACT

Marine environment is one of the most challenging environments for concrete structures. Structural concrete exposed to marine environment deserves special attention as the sea salts chemically react with the cement matrix which results in loss of strength, cracking, spalling etc.

In the present work, the behaviour of two different composites were study: Engineered Cementitious Composites (ECC) and another one based on an Alternative Binder System. A series of experiments, including compressive testing and uniaxial tension were carried out to characterize the mechanical properties of both types of materials. The single crack tension test was performed in the ECC compositions to assess the influence of the type of water used in the composition, at the micromechanical level. The most important characteristic of ECC, multi-cracking behaviour at increasing tensile strains when subject to direct tension, was confirmed in all mixtures and in all types of cures. Self-healing ability was studyed in ECC mixtures and the results showed that is possible verify that the specimens subjected to lower preloading levels and cured in the same water used to prepare the mixtures have almost fully recovered their initial mechanical characteristics. In the metakaolin based geopolymer, as an alternative binder system, the strain hardening behaviour was reached with one mixture.

The geopolymer material is a more sustainable option due to the utilization of by-products and / or wastes materials when compared to the cementitious matrix composite.

Keywords: Durability, Engineered Cementitious Composites, Strain Hardening Behaviour, Self-healing, Geopolymer

RESUMO

O ambiente marítimo é um dos mais desafiadores para as estruturas de betão. Betão armado exposto, ao ambiente marítimo, merece especial atenção devido á presença de sais do mar que reagem com matriz de cimento o que resulta em perda de resistência, fendas, fragmentação, entre outros problemas.

Este trabalho consiste no estudo do comportamento mecânico de dois compósitos diferentes: um compósito de matriz cimentícia com endurecimento em tração e um material alternativo de matriz não cimentícia. Os testes de compressão e tensão uniaxial foram realizados de modo a avaliar as propriedades mecânicas dos dois compósitos. Os resultados demonstraram que é possível o aparecimento de múltiplas fendas com o aumento da carga de tração em todas as misturas e em todos os tipos de curas. A capacidade de *self-healing* de materiais compósitos com endurecimento em tração foi estudado nos compósitos de matriz comentícia e os resultados mostraram que é possível concluir que as amostras submetidas a baixos níveis de pré-carga, curadas na mesma água utilizada para preparar as misturas, tenham recuperado quase totalmente as suas características mecânicas iniciais. O endurecimento à tração também foi obtido por uma mistura de geopolímero que é um material alternativo ao cimento Portland.

O geopolímero é uma opção mais sustentável devido à utilização de sub-produtos e/ou resíduos quando comparado com o compósito de matriz cimentícia

Palavras-chave: Durabilidade, Compósito de Matriz Cimentícia; Endurecimento em Tração, Geopolímero,

Table of Contents

\

List of Figures

Chapter 2

Chapter 3

Chapter 4

Chapter 5

List of Tables

Chapter 3

Chapter 4

Chapter 5

CHAPTER 1

Introduction

1.1 Foreword

In the twentieth century concrete has emerged as the most used construction material in numerous types of environments. Its utilization is due to good mechanical properties, its versatility and low maintenance [1]. However, the use of concrete has disadvantages such as low tensile strength, low ductility and its susceptibility to cracking.

The maritime environment is highly inhospitable to building materials. Sea water contains many salts as well as organisms which are aggressive for building materials. Extreme temperatures, wave action and hydrostatic pressures are responsible for accelerating the deterioration process of concrete, which is often observed in the coastal structures [2] [3].

The challenges of Civil Engineering, especially within the structures in extreme environments, have huge expectations with regards to the development of fibre reinforced materials for the development of more resistant and durable solutions. Therefore, it is necessary to understand the deterioration mechanism of concrete structures in marine environment in order to obtain a resilient material to such demanding actions.

The fibre reinforced composites have numerous advantages over conventional materials. These materials are the result of a combination of high strength fibres in a matrix, which may be cementitious or not. Thus, the matrix and the fibres retain their physical and chemical identities but produce a combination of mechanical properties which cannot be achieved with any of the constituents functioning separately [4]. The existence of fibres, at the microstructural level, allows better mechanical performance and durability.

1.2 Motivation

Modern structures are being exposed to severe environments and the lack of durability is one of the most serious problems in concrete infrastructures. Concrete is known to be a tension-weak material, with a tensile strength much lower than the compressive strength and very

limited tensile strain capacity resulting multiple cracks during the lifetime of concrete structures.

Engineered Cementitious Composite (ECC), is class of ultra-ductile fibre reinforced composite, with a strain capacity more than 300 times that concrete. The formation of a large number of microcracks as the load increases allows the material to have high deformability.

The existence of fibres, at microstructural level, in the composite allows better mechanical performance and durability. This study will assess the behaviour of different mixtures of fibres and matrices in order to obtain a composite that is economically viable and innovative for later use in coastal and offshore structures. To reduce the environmental impact and improve the sustainable aspect of ECC materials seawater and salted water were used in the compositions.

Alternative binder systems without ordinary Portland cement, such as geopolymers, are recently new in the Civil Engineered world. However, they have some advantages when applied in severe environments. In this this work a sustainable and consistent alternative to structural systems currently used is searched. In particular, the study will focus on the most negative aspects of actions and their effects on structures in the marine environment, and will address the deterioration mechanisms of the mechanical properties of the composites under study in this environment.

1.3 Scope and objectives

This thesis aims to:

- Understand the deterioration mechanisms of concrete structures in marine environment;
- Develop and characterize three different mixtures of Engineered Cementitious Composition using tap water, seawater and salted water in the composition;
- Assess of mechanical behaviour of fiber reinforced composites in four different types of curing environments;
- Characterize the self-healing behaviour in Engineered Cementitious Composites in different curing environments;
- Develop a composite based on an alternative binder system which does not contain ordinary Portland cement.

1.4 Structure of the dissertation

In general, information obtained from the experimental program carried out is restricted to the characterization of the initial time evolution of compressive and tensile behaviours.

The thesis is divided into six chapters presented in the following sequence:

Chapter 1: In this chapter a brief introduction to marine environment and to fibre reinforced cementitious composites is done; additionally the motivation to the research, scopes and objectives are presented.

Chapter 2: Dedicated to the state of the art, in this chapter special attention is given to the durability of concrete structures in the marine environment. In the first section, a general description of the main problems of marine environment is presented. In the second section the new materials that are investigated for using in the marine environment are approached, considering the need to improve resilience of concrete structures in the marine environment.

Chapter 3: A description of the experimental programme carried out to characterize the behaviour of Engineered Cementitious Composites is presented. In the first section the mechanical behaviour of the three different mixtures studied is presented. In the second section the influence of the mix composition while curing in the different environments is presented.

Chapter 4: This chapter is dedicated to the experimental programme carried out to characterize self-healing behaviour of two Engineered Cementitious Composites mixtures. The direct tensile test results are presented in the first section. In the second section the cracking processes are characterized by using digital image analysis and processing.

Chapter 5: This chapter was dedicated to the development and characterization of the compressive and tensile performance of fiber reinforced metakoalin based geopolymer, as well as to the use of steel fibres for the development of innovative fibre reinforced cementitious composites aimed at resilient marine structures.

Chapter 6: This last chapter is dedicated to the conclusions of developed work and to the identification of further research needs regarding the topic of investigation of this dissertation.

CHAPTER 2

State Of Art

In this chapter a brief description of the state of the art is presented, giving particular attention to the characterization of the new materials. The chapter is divided in sub-sections for a better understanding of the evolution of the knowledge and of the scientific work.

In the first section, a general description of the main problems of marine environment is presented. In the second the new materials that are investigated for using in the marine environment are approached, considering the need to improve resilience of concrete structures in the marine environment.

2.1 The oceans

The oceans are the dominant features of the planet Earth. They cover almost 70 percent of the Earth's surface. Since before recorded history, oceans have been used for transport, for food, for conquest and unfortunately for waste disposal. They are a barrier and a conduit over which people and goods have been moved with relative culture while garnering Earth's remote resources [2].

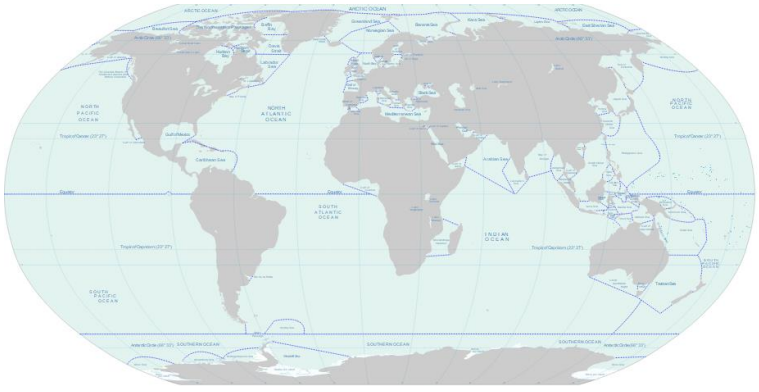

Figure 2. 1- Map of the world [5].

For thousands of years, populations have depended on the ocean for route, for trade and exploration. Nowadays, people continue to travel on the ocean and rely on the resources that de seawater contains. Most recently scientists and other experts hope that the ocean will be used

more widely as a source of renewable energy. Some countries have already harnessed the energy of ocean waves, temperature, currents, or tides to power turbines and generate electricity [3].

Marine and offshore structure were designed to improve the quality of the population by protecting the land from the severe action of the sea, and to allow the exploitation of seawater resources.

2.1.1 Marine and offshore structures in the context of Climate Change

Marine and offshore structures play a crucial role in the economic, social and political development of most countries. They support diverse and productive ecosystems that provide valuable goods and services.

Sea level rise is caused primarily by two factors related to global warming: the added water from melting land ice and the expansion of sea water as it warms. Over the past century, the burning of fossil fuels and other human and natural activities has released enormous amounts of heat-trapping gases into the atmosphere. These emissions have caused the Earth's surface temperature to rise, and the oceans absorb about 80 percent of this additional heat [6].

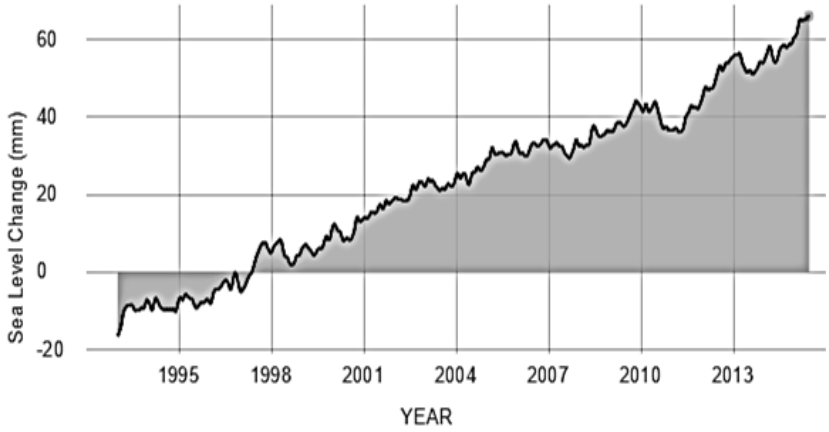

Figure 2.2- Sea-level rise over the years [7].

As seawater reaches farther inland, it can cause destructive erosion, flooding of wetlands, contamination of aquifers and agricultural soils, and destroy habitats for fish, birds, and plants. When large storms hit land, higher sea levels mean bigger, more powerful storm surges that can strip away everything in their path. In addition, hundreds of millions of people live in areas that will become progressively vulnerable to flooding. Higher sea levels would force them to abandon their homes and relocate and low-lying islands could be submerged completely. Marine structures are seen as one of the options as response to this problem [8].

There are numerous types of marine structures with different functions, such as protection of the territory and population, and support of commercial activities. As an example, Ports and harbours are a vehicle for goods and enclose four important functions:

- Administrative (ensuring that the legal, socio-political and economic interests of the state and international maritime authorities are protected);
- Development (ports are major promoters and instigators of a country's or wider regional economy);
- Industrial (major industries process the goods imported or exported in a Port);
- Commercial (Ports are international trade junction points where various modes of transport interchange; loading, discharging, transit of goods).

Figure 2.3- The largest Port in the world located in China [10].

Coastal defence structures have a strong influence on the configuration of the shoreline. They have as main function the protection of the population and the land from the sea-level rise. Artificial structures can influence sediment transport, reduce the ability of the shoreline to

respond to natural forcing factors and fragment the coastal space [4]. This can result in loss of habitats and lead to noise and visual disturbance of birds. On the positive side, coastal defence structures can increase shipping and tourism and increase or restore natural habitats in certain cases. To protect the land and populations from the sea there are several techniques that can be used as breakwaters, dikes, gabions and seawalls Figure 2.4.

Figure 2.4- Breakwaters in front of a public beach [11].

In the last decades, the offshore structures have developed rapidly to meet the need to exploit deeper waters as a result of depletion of shallow water easy-to reach resources. This need for deep-water developments and a desire to continue to exploit depleting shallow water reserves has spawned new forms of offshore structures for production [12]. One example is the Sakhalin-1 Consortium, which consists of the world's biggest oil platform and involves the production in particularly harsh conditions localized in Russia (Figure 2.5).

Figure 2.5- The Sakhalin-1 Consortium - the biggest oil rig in the world [12].

In Portugal

The sea represents a unique advantage for Portugal. The favourable location of the border of Portugal in Western Europe, where maritime traffic converges from worldwide, its long coast line and the size of its Exclusive Economic Zone are unique competitive advantages for this country [5].

The national marine activity has been losing dimension as a productive activity, not having kept pace with the competition created by the sector's liberalization. This decrease was accompanied by a decline of the shipbuilding sector, materialized in the closure of many yards and reducing the capacity of many others.

The port of Lisbon receives every year around 500 000 tourists, and the capital city hosts the major port of the country in terms cruise landings and the third port in terms of cargo transport. The “Grande Lisboa” region also concentrates the national shipbuilding and repair industry, and is the fourth region in terms of fishery activities.

The sector of commercial ports has required a significant economic development, accompanied by diversification and provision of infrastructure and port services, associated to an increase in the availability and expertise capabilities to meet traffic requirements with significant impact, such as import/export and containerized cargo transhipment or petroleum products, natural gas and coal.

The port of Sines (Figure 2.6) is one of the few deep-water ports at European level and has a very important role in the Portuguese economy. This port is the national leader for cargo handled and is critical in the energy supply of the country.

Figure 2.6- Port of Sines [14].

2.1.2 The marine environment

The ocean combines a few of the most aggressive environments in the world for engineering structures. Seawater and sea environments combine unique characteristics that create a challenge to civil engineering such as:

- Chemical composition;
- Marine Organisms;
- Temperature;
- Hydrostatic pressure;
- Storm waves;
- Fog and spray;
- Ice impact and ice abrasion.

Therefore, oceans are one the most difficult environments to concrete structures due physical and chemical factors.

Seawater contains salts and ions such as chlorine, sodium, sulfur, magnesium, calcium and potassium. These can affect the freezing point and the alkalinity of the water. Seawater also contains small amounts of dissolved gases. Many of these gases are dissolved into seawater by the atmosphere through the constant stirring of the sea surface by wind and waves [2]. The concentration of gases that can be dissolved into seawater from the atmosphere is determined by temperature and salinity of the water. The increasing of the temperature or the salinity leads to the reduction the amount of gas that ocean water can dissolve.

The temperature of seawater varies widely with the depth and climate zone. In addition to that, the temperature affects the growth of marine organisms and determines the rate of chemical and electrochemical reactions in concrete [2]. Temperature and density share an inverse relationship. As temperature increases, the space between water molecules increases—also known as density, which therefore decreases. If the temperature of water decreases its density increases, but only to a point. Salinity and density share a positive relationship. As density increases, the amount of salts in the water increases. Various actions can contribute to changes in the density of seawater [6].

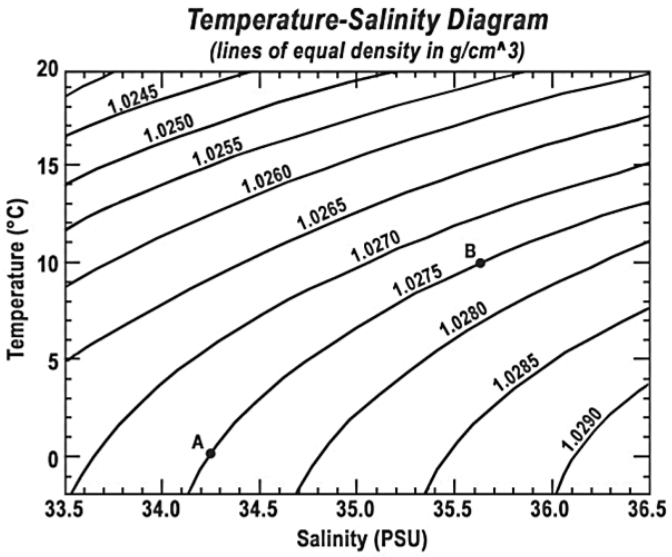

Figure 2.7- Relation between temperature-salinity-density [16].

The currents and the tidal action are the two most important aspects of the sea affecting the durability of the materials that are used in marine construction. Tides are caused by the gravitational interaction between the Earth and the Moon. The gravitational attraction of the moon causes the oceans to bulge out in the direction of the moon. Twice a day the oceans experience a natural event that moves massive amounts of water [2].

Currents, that are essential for maintaining the existing balance of life on Earth, are driven by several factors such as:

- The rise and fall of the tides, that create a current in the oceans, near the shore, as well as in bays and estuaries along the coast;
- Winds, mostly the ones that blow along the shoreline;
- Thermohaline circulation, that is a process driven by differences in the water due temperature and salinity in different parts of the ocean [7].

Figure 2.8- Storm wave caused by hurricane winds. [18].

2.1.3 Durability of concrete structures in the marine environment

Reinforced concrete is the most commonly used construction material in the world [8]. With the exponential growth of human population and industrialization, concrete is now used not only for buildings but also for highways, bridges, underground mass transit facilities, water treatment systems and marine structures [2]. Because the modern structures are being exposed to severe environments the lack of durability is one of the most serious problems in concrete infrastructures.

The durability of a structure represents its ability to serve its intended purposes for a sufficiently long period of time. A durable structure is expected to serve without deterioration to the extent that major repair is required before expiry of its design life [9].

In marine environment, the structures are exposed to a serious number of physical and chemical interactions that affect the strength and stiffness of the concrete causing crack, leading to other types of concrete deterioration such as corrosion, alkali-silica reaction and sulphate attack, resulting in further cracking and disintegration [10].

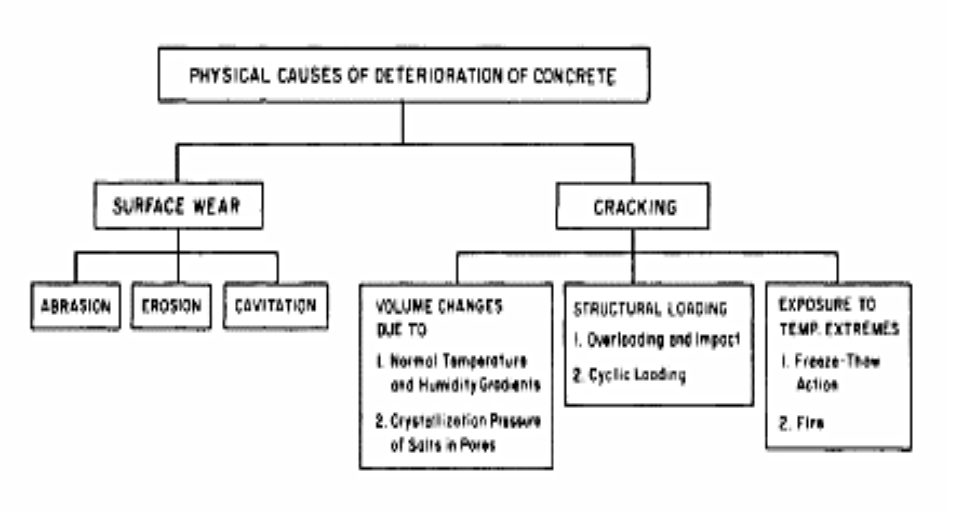

Figure 2. 9- Physical causes of deterioration of concrete [2].

The deterioration processes depend on the exposure conditions. These can be classified into three different exposure zones depending upon the nature and effect on the exposed structure.

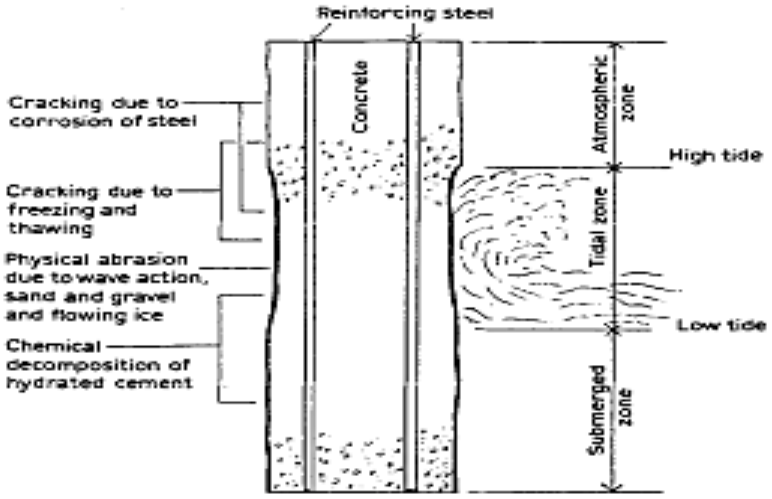

Figure 2. 10- Possible degradation mechanisms acting on concrete exposed seawater [21].

The structures located in the tidal and atmospheric zone are more vulnerable to the aggressive action of seawater than those which are continuously and fully submerged in the water as offshore structures [1].

Corrosion of reinforcement occasionally takes place in the submerged parts of the structure due to the lack of oxygen [10]. In tidal/splash zone, concrete is repeatedly wetted by seawater with

alternate periods of drying during which pure water evaporates. The dissolved salts are left behind in the form of crystals, mainly sulphates. This area is also subjected to damage due to salt crystallization, as well as freezing and thawing in a cold climate.

The atmospheric zone is that part of the structure above the splash zone and the damage is similar to that in the splash zone but in a lesser degree.

The deterioration process results from the combined effects of chemical action of seawater constituents on cement hydration products, crystallization of salts within concrete, alkali-aggregate expansive reactions, corrosion reinforced bars, freezing and thawing in a cold climate, and physical erosion due the wave action and floating objects. As soon as the concrete is attacked by any of these processes, the permeability tends to increase and consequently it is more susceptible to further attack by various other processes [10].

Corrosion of embedded steel is, generally, the major cause for concrete deterioration in reinforced and prestressed concrete structures exposed to seawater, although in low-permeability concrete this does not appear to be the first cause of cracking.

The main causes for insufficient watertightness are [11]:

- Poorly proportioned concrete mixtures;
- Absence of properly entrained air if the structure is located in a cold climate;
- Insufficient consolidation and curing;
- Lack of concrete cover on embedded steel;
- Badly designed or constructed joints;
- Microcracking in hardened concrete due to the lack of control of loading conditions and other factors, such as thermal shrinkage, drying shrinkage, and alkali aggregate expansive reactions.

In Figure 2.11 shows one example of corrosion of reinforced concrete

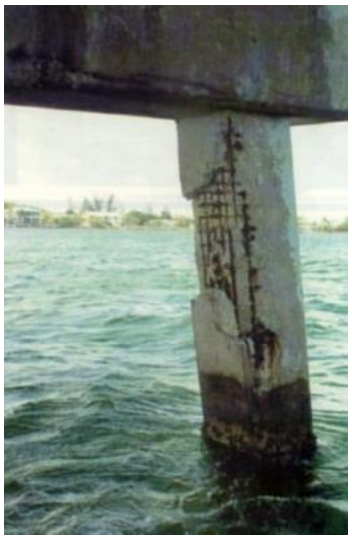

Figure 2. 11- Example of corrosion of reinforced concrete structures [24].

Physical attack

Frost-thaw damage

This type of damage represents a durability problem to concrete structures [12]. The most frequent cause for cracking and spalling, in cold climates, is frost action [2]. Disintegration is caused by the freezing of water inside the pores of the concrete, since the water expands by 9% on freezing and creates disruptive internal pressures. If the induced stress is higher than the strength of the hardened cement paste, cracking will happen. The damage to the paste increases with the number of freezing and thawing cycles. Freeze-thaw damage to the aggregate depends largely on the size, number and continuity of its pores. Aggregates with low permeability and high strength are more resistant to freeze-thaw action [10]. A permeable, weakened concrete, then falls an easy victim to other physical and chemical agents [2].

Figure 2. 12- Frost action damage in a reinforced concrete structure [26].

Erosion/abrasion

Erosion can occur for prolonged exposure of the concrete to continued attrition by stones and shingle carried by water, as may occur in hydraulic structures or in seawater. Good dense concrete will normally resist a high-velocity flow of water, provided the flow is smooth and streamlined. Concrete will abrade where exposed to the forces of cavitation, as occurs in those portions of hydraulic structures designed to dissipate energy by incorporating obstructions to the free flow of water. The cavities collapse with impact and sudden changes in direction, resulting in pressures which may cause wearing (pitting) of the concrete surface [10].

Chemical attack

Chloride attack

Chloride attack is one of the most important aspects considering the durability of concrete. Chloride ions enter the concrete from cement, water, aggregate, admixtures and by diffusion from the ambient environment and causes the corrosion of the reinforcement [1].

The ingress of chloride by capillary action via airborne salt spray and/or the wetting and drying with seawater is the major contribution to chloride driven corrosion in marine concrete structures. If there are chloride ions in the pore water adjacent to the reinforcing steel above a certain concentration, the passive iron oxide film in the steel reinforcement breaks down. Chloride contents from 0.1 to 0.4% or more may initiate corrosion.

The corrosion products, being of greater volume than the parent metal, exert pressure and thus cause the concrete to crack and eventually spall. Common types of visual deterioration damage are rust staining, spalling, exposed rebar and delamination [10].

Figure 2. 13- Example of chloride attack in marine structures [24].

Sulfate Attack

Concrete is vulnerable to attack by sulphate, causing cracking and spalling due to expansion.

Where sulphates are present in water or soils, the permeability of concrete and the presence of water allows sulphate ions to diffuse into the concrete and create an expansive reaction causing spalling and deterioration. A similar effect is caused by alkali aggregate reaction whereby the presence of water in concrete permits a reaction between silica in certain aggregates and the alkalis in cement.

The main sulphate of interest in sea-water is magnesium sulphate that reacts with calcium aluminates, silicates and lime in cement forming magnesium hydroxide, calcium sulphate (gypsum) and calcium sulphoaluminate (ettringite).

Ettringite is finally decomposed and gypsum precipitated, leaving a soft concrete. An appreciable loss of strength can occur, particularly when leaching conditions are present. Magnesium and ammonium sulphates are the most damaging to concrete. The type of sulphate and the concentration present can influence the nature and rate of decomposition [21],

Figure 2. 14- Example of sulfate attack in a concrete structure near the sea. [25].

2.1.4 Strategies to improve the durability of reinforced concrete

Concrete structures are designed considering that they will require no maintenance during their service life. However, the marine environment causes countless damages to concrete structures. In this condition chloride penetration and chloride induced reinforcement corrosion rates can be very high, often leading to a reduced service life.

Any method of protection and repair, to be successful in the long term, must restore passivity by removing the causes of corrosion or prevent corrosion through cathodic protection or anodic control [13].

Traditional repair methods involve the removal of chloride contaminated concrete and cleaning of the corrosion present in the steel. The cleaned steel surface is next coated with an insulating coating to ensure that any chlorides remaining in the old concrete will not reach the steel again. Many layers of coating, mostly epoxy products, are used to cover defects and the last layer needs to be sanded to provide better adhesion to the repair mortar. Before applying the repair mortar it is necessary to apply an insulating adhesive as a primer. After, the selected repair mortar is installed to a predetermined cover thickness [2].

There are many ways to decrease the corrosion process, however cathodic protection is the only technology that has proven to stop corrosion in existing reinforced concrete structures, regardless of the chloride content in the concrete. Cathodic protection is defined as the reduction or elimination of corrosion by making the metal a cathode via an impressed direct current or by connecting it to a sacrificial or galvanic anode. In the last decades, this method of repair has

been successfully used to protect underground pipelines, ship hulls, offshore oil platforms, underground storage tanks, and many other structures exposed to corrosive environments [14].

The Kyle of Tongue Bridge (Figure 15) in Sutherland, Northern Scotland opened in 1970, and was patch repaired in 1989 due to chloride induced corrosion. However, inspections from 1999 onwards reported on-going corrosion and structural deterioration. A refurbishment contract was let in 2011 to extend the service life of the structure for a 30 year period by providing corrosion arrest and prevention [31].

Figure 2. 15- Cathodic protection used in Kyle of Tongue Bridge [28]

2.2 Alternative Materials

Concrete, that is the most elementary construction material, is known to be a tension-weak material, with a tensile strength much lower than the compressive strength (typically 10%) and very limited tensile strain capacity [2]. However, the durability, the capacity to take multiple shapes and low maintenance makes the concrete the most used material in marine and offshore construction.

Cracks and internal flaws exist even prior to loading, and the mechanical behaviour of concrete under distinct loading conditions is mostly governed by the influence of these initial flaws and weak regions on the initiation and propagation of cracks. Also, the great difference between the nature and mechanical properties of aggregates and the cementitious materials in the concrete matrix induce important stress gradients at the transition regions between the different phases.

Synthetic composite materials are a recent addition. These materials must perform in harsh environments, subjected to the various corrosive and erosive actions of the sea, under dynamic cyclic and impact conditions over a wide range of temperatures.

2.3 Engineered Cementitious Composites (ECC)

Engineered Cementitious Composites (ECC) is a class of cement-based materials typically reinforced with Polyvinyl Alcohol (PVA) fibres developed for applications in the large material volume usage. One of its first predecessors was developed in 1960 by Romauldi and co-workers, that used short steel fibres in concrete to reduce the brittleness [15]. In 1980 began the interest in fibre reinforced concrete materials with tensile ductility. Ductility is a measure of tensile deformation (strain) capacity typically associated with ductility in steel.

Krenchel and Stang in 1989 demonstrated that the ductility behaviour of concrete could be increased by hundreds of times with the presence of continuous aligned fibres in the cement matrix [15].

In 1993, the first ECC material was developed at the University of Michigan by Professor Li and his co-workers with a typical moderate tensile strength of 4-6 MPa and higher ductility of 3-5 % [16].

This material can be regarded as a family of materials with a range of tensile strengths and ductilities that can be adjusted depending on the demands of a particular structure.

Pseudo-strain hardening behaviour in tension exhibited by ECC is the consequence of the development of multiple cracks under tensile loading. ECCs display significantly higher ductility and more reliable crack width control than reinforced concrete does [17]. The fact that this material shows multiple cracking behaviour represents a dual advantage in engineering applications: while more cracks develop at the same tensile deformation, the individual crack openings are significantly smaller [18].

Extensive research has shown that the most fundamental property of a fibre reinforced cementitious material is the fibre bridging property across a matrix crack.

The result of this multiple cracking behaviour is enhanced durability and improved preservation of functional properties at the structural level. In addition, high energy dissipation ability exists at the level of a single crack, which is amplified by the large number of cracks typically developed [18]

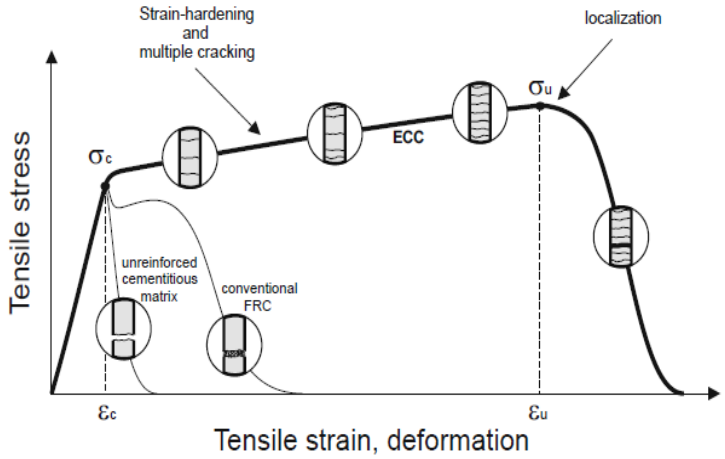

Figure 2. 16- Typical tensile-stress-strain diagram of ECC [18].

The mechanical behaviour in tension of ECC is the result of a delicate balance of multiple factors such as: the interfacial bonding and fibre pull-out properties, the mechanical characteristics of the fibres and of the matrix, the distribution of flaw sizes in the matrix, the fibre orientation and their dispersion in the matrix. This factors play an important role in the resulting composite mechanical behaviour [18].

Cement, fly ash, water, sand, super plasticizer and fibres are the common materials used to produce the ECC material. Normally, this composite contains 2 % of fibres in volume, which represents the critical fiber content that allows the strain-hardening response.

2.3.1 Tensile Strain Hardening Behaviour

The most important characteristic of ECC is the high tensile ductility represented by a uniaxial tensile stress-strain curve with strain capacity as high as 5% or more. This composite shows elastic behaviour (similar to concrete) until the “yield point” is reached, when the first micro cracks appear in the specimen or the structure. Final failure occurs when one of the multiple cracks forms a fracture plane. The high tensile ductility is of great value in improving the structural ultimate limit state in terms of structural load and deformation capacity, as well as energy absorption [15].

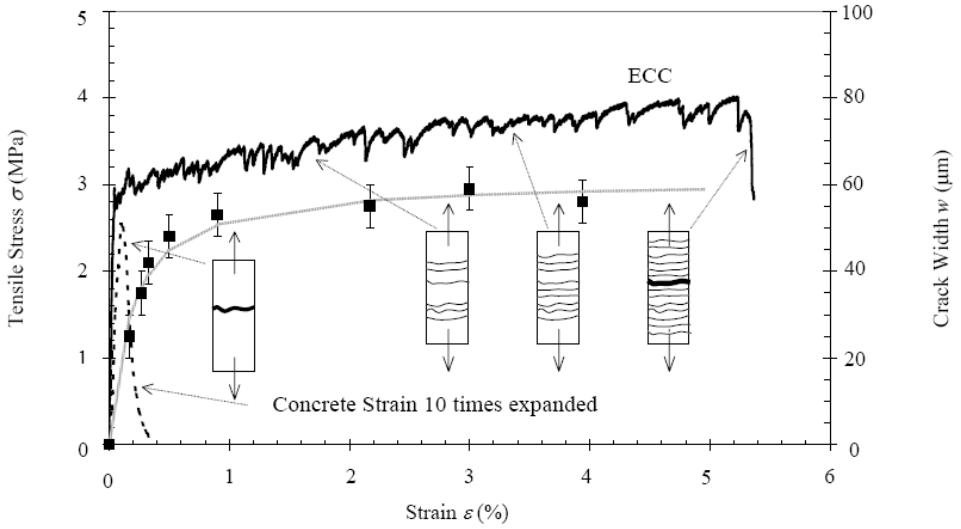

Figure 2. 17- Typical tensile behaviour of ECC and concrete [36]

Tensile strengths between 4 MPa and 14 MPa can be obtained, depending on the mixture composition.

Closely associated with the strain-hardening and multiple cracking behaviours is the small steady state crack width. Even at a strain of 4-5%, crack widths of ECC remain below 100 μm. Such small crack widths imply a significant improvement in structural durability [18]

2.3.2 Compressive Behaviour

ECC materials are designed to exhibit high toughness and significant tolerance to damage in tension. Compared with concrete ECC has a similar compressive strength (between 40 MPa and 80 MPa) and ultimate compression strain around 0,45-0,65%. However, the post peak behaviour of ECC tends to descend more gently that concrete [15]. The elastic modulus of this material ranges between 20–30 GPa. The utilization of ECC was demonstrated to significantly improve the mechanical performance of structures when compared with conventional concrete, by considerably delaying the loss of structural integrity due to excessive deformation and preventing brittle failure. The influence of fiber reinforcement on the composite compressive strength is commonly assumed as negligible, although it contributes to increase the post-cracking energy dissipation ability. [7]

2.3.3 Self-healing

Durability of reinforced concrete structures can be caused by a wide variety of reasons. Cracking is one of the major flaw or damages in any stage of concrete structure. They are many reasons for cracks appearance as loading, volumetric change due the high temperatures, creep, plastic settlement, shrinkage, or deterioration mechanisms such as alkali-silicate reaction and freezing/thawing cycles [19]

If micro-cracks grow and reach the reinforcement, gases and liquids can penetrate, not only the concrete itself may be attacked, but also the reinforcement will be corroded when it is exposed to water and oxygen, and possibly carbon dioxide and chlorides.
In the last decades, there is growing interest in the phenomenon of mechanical properties recovery in self healed concrete materials, commonly known as autogenous healing. [19]

Experimental investigation and practical experience have demonstrated that healing of cracks in cementitious materials leads to a gradual reduction of permeability over time for water flowing under a hydraulic gradient. In extreme cases, cracks can be sealed completely and that can improve durability, permeability and potentially mechanical properties.
Self-healing behaviour depends of the crack width, smaller cracks heal faster and more efficient that larger cracks. The healing process involves chemical and physical mechanism. There is a various number of healing process but the main is precipitation of calcium carbonate crystals.

2.4 Geopolymers

Portland cement concrete is the most used building material in the world; however, its manufacture is energy-intensive. Generating approximately one ton of CO_2 for each ton of Portland cement produced, this binder is one of the primary causes of global warning. The manufacture of this building material also requires significant over-exploitation of natural resources as limestone quarries (it's necessary over 3.0 billion tonnes of raw material to produce 2.0 billion tonnes of Portland cement). [20]. For these reasons, the necessity of development of a friendly environmental material that consumes less energy is crucial.
Geopolymer materials are inorganic polymers synthesised by the reaction of an alkaline silicate solution and an aluminosilicate source at near-ambient temperature, which was first tried in 1978 by Davidovits [21]. This environmentally sustainable material uses waste products in the

compositions and has a significantly lower CO_2 footprint when compared with Portland cement. [22]. In 1994, Glukhovsky proposed a general mechanism for the activation reaction of geopolymer material, consisting in three stages [42]:

1º) Destruction-coagulation;

2º) Coagulation-condensation;

3º) Condensation-crystallisation.

Figure 2.18 presents a highly simplified reaction mechanism for geopolymerization of metakaolin based geopolymers.

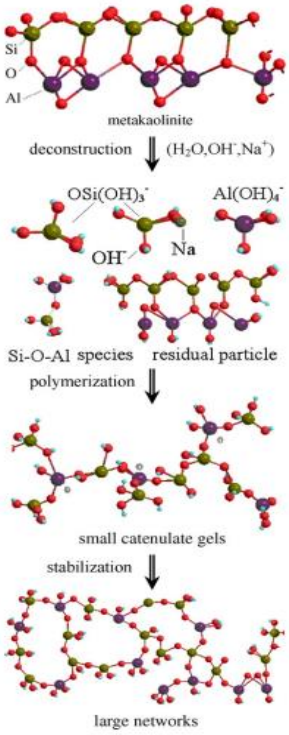

Figure 2. 18- Geopolymerization process, including the deconstruction of MK by the activation of alkaline solution, the polymerization of generated alumina/silica-hydroxy species and the stabilization of fresh formed structures. **[43]**

The dissolution of metakaolinite in alkaline solution is exothermic and in this process, the Si–O and Al–O bonds on particle surfaces are broken down. The deconstruction products in alkali–MK system will polymerize into gels as their concentrations grows up. The polymerization is exothermic and becomes the main contribution of heat evolution. After, approximately 4500 min, the process goes into a thermally steady stage, during which the fresh formed small gels are probably transformed into larger networks by local reorganization. [43]

In 1989, the first residential building made of alkali-activated cement concrete was built.

Figure 2. 19- The first residential building made of alkali-activated cement concrete without any OPC. (20-storey residential building, Lipetsk, Russian Federation, 1987–1989) [44].

The low energy process results in a fast-setting material that exhibits exceptional hardness and strength that can be comparable to the ones obtained with cement binders. Depending on the material that is used to produce the geopolymer can display different ranges of properties and characteristics different. There is a wide variety of raw materials that can be used to manufacture the alkali-activated cement such as fly ash, metakoalin, silica fume, blast furnace slag and red mud. When the geopolymeric materials are derived from coal ash the mechanical and chemical properties can by higher than that obtained with common cement. [23]

2.4.1 Advantages and applications of geopolymer

Geopolymer binders have similar behaviour to Portland cement. Geopolymeric material have advantages when compared to Portland cement, such as: [20]

- Abundant raw materials resources: geopolymeric materials use mostly waste materials as raw materials with any pozzolanic or alumino-silicate compounds;
- Energy saving and environmentally friendly: thermal processing of natural alumino-silicates at relative low temperatures (600° to 800°) provides suitable geopolymeric raw materials;
- Simple preparation technique: geopolymers can be produced by mixing alumino-silicate reactive materials and alkaline solutions, then curing at room temperature.
- Good volume stability: geopolymers have 4/5 lower shrinkage than Portland cement.

- Reasonable strength gain in a short time: it can set and harden at a room temperature and can gain reasonable strength in a short period.
- Ultra-excellent durability: geopolymer concrete can withstand thousands of years of weathering attack without too much function loss.
- High fire resistance and low thermal conductivity: geopolymers can withstand 1000° to 1200° without losing functions.

The described characteristics can be used in many fields, not only in civil engineering but also in automotive and aerospace industries, plastics industries, waste management, art and decoration, retrofit of buildings, etc. [20]. However, workability is one of the disadvantages of geopolymeric materials. This materials has quick setting times, which make its use very difficult in some fields. [24]

The University of Queensland's Global Change Institute, designed by Hassell, has become the first building in the world to use cement free for suspended construction. Geopolymer concrete has been used and named the new material Earth Friendly Concrete (EFC). Comprising sand, aggregate and a binder that contains ground granulated blast furnace slag (a waste product from steel production) and fly ash (a waste product from coal fired power generation), EFC contained no Portland cement.

Figure 2. 20- The Global Change Institute - First building using geopolymer as structural material. **[47]**

2.4.2 Mechanical Properties

Depending on the raw material selection and processing conditions, geopolymers can exhibit a wide variety of properties and characteristics, including high compressive strength, low shrinkage, fast or slow setting, acid resistance, fire resistance and low thermal conductivity.

Temperature, relative humidity, curing time and the alkali activation process are factors that affect the compressive strength and other mechanical properties of the geopolymer. [25]. The presence of silicate ions in the alkaline solution substantially improves the mechanical strength and modulus of elasticity values but it has a slightly adverse effect on the otherwise very strong matrix/aggregate and matrix/steel bond. [26].

The availability of aluminium for the reaction can influence the geopolymer strength. Fly-ash based geopolymer and metakoalin based geopolymer have different behaviours after exposure to elevated temperatures. According with Kong et al, metakoalin geopolymer suffers compressive strength loss after temperature exposure. However, for fly-ash based geopolymer the compressive strength increases. Compressive strength in metakoalin geopolymer can decrease in about 17 % after elevated temperature exposure. With regards to the evolution of strength with time, Chatterjee et al, in 2003 showed that alkali activated slag has shown progressive gain of strength from 21 MPa in 3 days to 36 MPa in 1 year [46].

2.4.3 Fibre reinforced alkali-activated binder

The fibre reinforced alkali-activated binders are still unknown subjected in the scientific world.

Geopolymeric materials are inherently brittle. Despite the high brittleness of the AAS (Alkali-Activated Slag) mortar, strain hardening and high tensile ductility in polyvinyl alcohol (PVA) fibre reinforced ASS mortar was achieved by Lee et al [46]. They conduct a series of mechanical tests (compressive strength, uniaxial tensile performance and flexural performance) in three different of mixtures cured in water for 28 days. PVA fiber (2 vol%) was used as reinforcement in all three mixes. From the test results they conclude that was possible to obtain, it tensile strain hardening behaviour and ductility as high as 4.7%. The compressive strength ranges between 15 and 35 MPa.

In Figure 2.21 the cracking pattern of fiber reinforced ASS mortar, achieved by Lee et al, is showed.

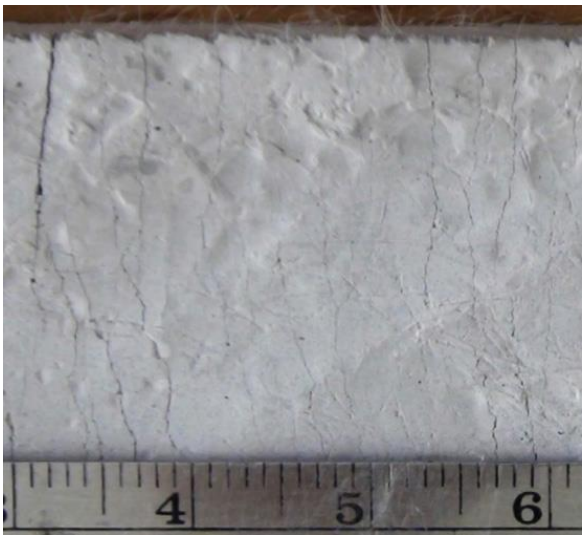

Figure 2. 21- Multiple micro-crack obtained dureing the unixial tensile test of geopolymer specimens.

By inducing fibre reinforcement, such as short fibres or unidirectional long fibres into alkali-activated binder the mechanical properties can be improved. The percentage and type of fibres that are added to the binder is fundamental to have specific mechanical properties. [26]

In 2014, Ohno and Li [50] achieved strain hardening behaviour with fly ash based geopolymers with tensile ductility over 4%. They concluded that the temperature curing improves both strength and ductility properties.

CHAPTER 3

Mechanical Characterization

In this chapter the experimental work conducted using Engineered Cementitious Materials is presented. The materials and compositions, as well as the mechanical characterization of all the different mixtures developed and tested, is presented and discussed. This research was conducted considering mostly the potential applications of these materials in the context of maritime constructions.

Given that the present chapter is long, and for the sake of clarity, the structure of the chapter is described briefly. Considering that this research is dedicated to the assessment of the effect of using seawater, or curing under seawater, on the tensile and compressive properties of Strain Hardening Cementitious Composites, this chapter addresses this topic by carrying out three types of mechanical tests: the compression tests for assessing the deformability and compressive strength, the single crack tension test to assess the influence of the seawater at the micromechanical level, and the direct tension tests to assess the tensile behaviour and multiple crack formation potential of the mixtures. Because salted water is frequently used to represent the seawater in laboratorial experiments on structures, the salted water is also considered both as a mixture ingredient and as a curing environment.

The chapter starts in section 3.1 with the brief description of the methods and procedures used to produce and test the mixtures investigated. After that, the compressive, single crack tensile and direct tension tests are carried out for characterizing the mechanical behaviour of mixture A in section 3.2 (made with tap water), mixture B in section 3.3 (made with seawater) and mixture C in section 3.4 (made with salted water). All mixtures are characterized considering four different curing environments, which will be further detailed in section 3.1: air, tap water, seawater and salted water. Finally, in section 3.5 the average results obtained in terms of compression, single crack and direct tension tests are compared considering each curing environment, trying to evaluate the influence of the composition and of the curing time. At last, section 3.6 summarizes the main conclusions of this section.

3.1 Materials and Compositions

3.1.1 Compositions

Within the scope of this thesis, three different compositions have been developed. The materials which are common to all mixtures are: cement 42.5N type I, fly ash, water, viscosity modifying agent (VMA), sand, limestone filler, super-plasticizer (SP) and PVA fibres.

Three types of water were used: tap water, seawater and salted water. Seawater was collected in Vila do Conde with salinity that ranges between 3.1-3.5%. Salted water was used to represent the seawater with 3% of salt dissolved by volume.

Super plasticizer *Sika ViscoConcrete 3002 HE* was used in the mixtures in order to reduce the water ratio in the mortar. The density of this material is 1.06 kg/dm^3.

In this research work, silica sand with a maximum grain size below 500 μm and a specific gravity of 2630 kg/m^3 was used. Limestone filler have 2.70 Mg/m^3 of density.

The density of fly ash used in the compositions is 2420 kg/m^3. The mechanical characterization of fly ash were conducted by Rui Reis et al [51].

The dimensions of PVA fibres are 8 mm in length and 40 μm in diameter. The tensile strength of the fibre is 1600 MPa, the Young's modulus is 41 GPa and the density is 1300 kg/m^3.

Figure 3.1- Image of PVA fibres.

In the Mixture A, normal water was used in the composition. Mixture C has the same composition of Mixture A but the water added in the mortar mix was salted. In Mixture B seawater was used in the composition. In this particular case, in order to obtain good distribution

of PVA fibres in the mixture it was necessary to increase the amount of super-plasticizer from 1% to 3%.

Table 3. 1- Mixtures Composition for 2 L

	Ma	***Mb***	***Mc***
Materials	g	g	g
Cement	836,9	829,8	836,9
Fly Ash	1653,7	1639,7	1653,7
Sand	292,9	290,4	292,9
Filler	292,9	290,4	292,9
Tap Water	657,9		657,9
Seawater		589,9	
SP 3002	31,6	93,9	31,6
VMA	2,5	2,5	2,5
PVA Fibre	52	52	52
Salt (NaCl)			19,7

3.1.2 Mixing Procedure

A mortar blender with 3L capacity was used to prepare all the ECC mixtures (Figure 20). Firstly all the materials were collected and weighted. Solid ingredients, including cement, fly ash, sand, limestone filler and VMA were put in the bowl and mixed for one minute in slow speed.

Figure 3.2- Mixer, spoon and bowl used to mix the materials.

Water and super-plasticizer were then added into the bowl while mixing and mixed for 5 minutes. After that, the mixer was stopped in order to obtain the fresh properties of the mortar.

The mixer was restarted and all the fibres were added into the mortar and mixed until the fibres are well distributed (about 2 minutes). Then the fresh properties were tested, before casting.
The specimens were cast in different moulds and then vibrated in the shaking table, in order to reduce the air entrapped in the mixture. After one day in the mould the specimens were demoulded and moved into the climatic chamber. The temperature and humidity in the climatic chamber are, respectively, 20ºC and 60%. The same mixing procedure was adopted in all mixtures in order to obtain constant experimental results.

3.1.3 Fresh Properties

The fresh properties were studied before and after the PVA fibres were added to the mortar. This test was performed according with EN 1015-3. The mini-slump time and the mini-slump final spread were measured. To execute the mini-slump test it is necessary to prepare the flow table, the cone, the Plexiglas surface and the measuring tape (Figure 3.3). The mini-slump time consists in measuring the time taken by the mixture to reach a 20 cm diameter drawn in the Plexiglass surface after lifting the cone. The mini-slump final spread was measured by registering the dimensions of two perpendicular diameters of the final spread mixture.

Figure 3.3- Setup used to perform the mini-slump test.

Table 3.2- Fresh behaviour of the mixtures assessed using the mini-slump test.

	MA	***MB***	***Mc***
t20 (s)	no data	n.d	n.d
dxd (cm)	19x19	18x19	18x18
t20 (s) (with fibres)	n.d	n.d	n.d
dxd (cm) (with fibres)	15x17	18x15	16x17

The workability is very sensitive to the amounts of each ingredient adopted in each mixture.

The mini-slump was used to study the influence that the quantity of water and the viscosity modifying agent have in the mortar fresh behaviour. As show in table 2, the compositions are more fluid without the fibres. After adding the fibres the mixtures exhibit a more viscous behaviour and require more time to spread in the Plexiglas. As an example, Figure 3.4 shows the appearance obtained while evaluating fresh properties of Mixture A before and after adding the fibres.

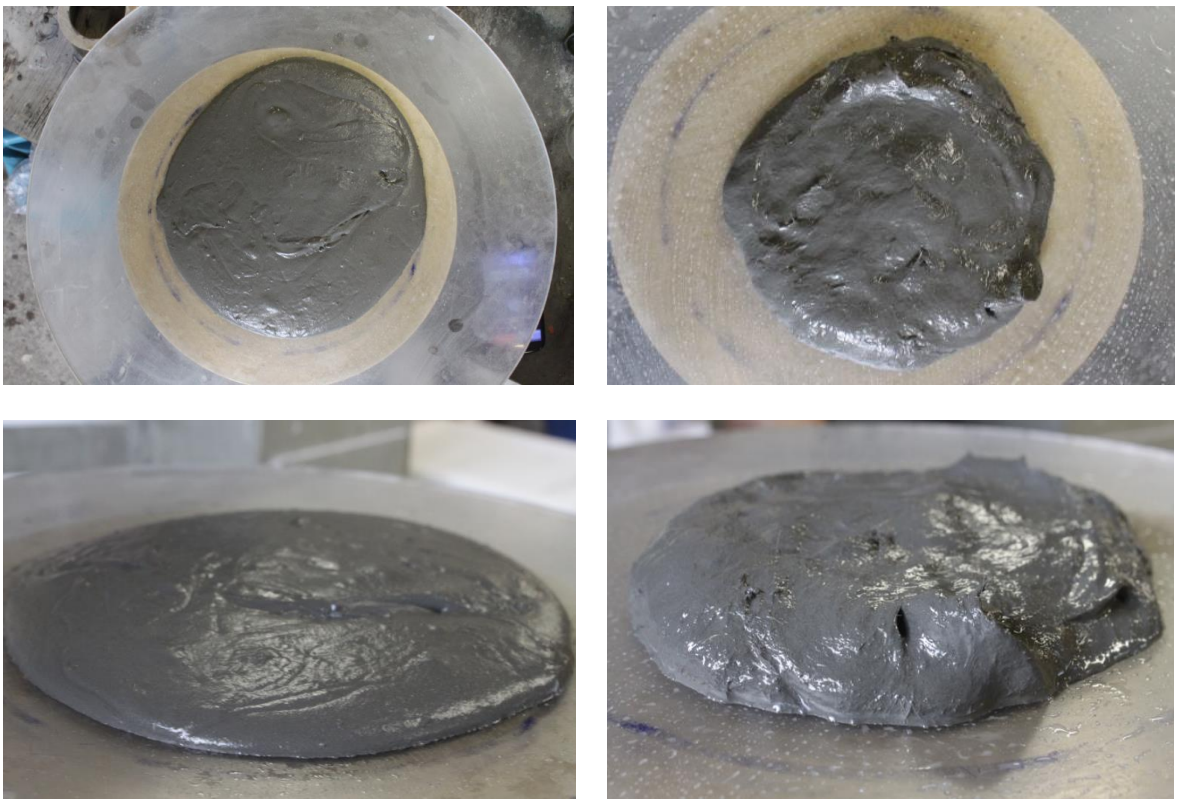

Figure 3.4- Images showing the fresh behaviour of Mixture A with and without fibres.

3.1.4 Specimens

Compressive tests were carried out using cubes measuring 50 x 50 x 50 mm^3.

Figure 3.5-.Moulds used to cast the specimens for compression testing.

The specimens for direct tension testing and for characterizing the tensile stress-strain responses were cast using dogbone-shaped moulds. These moulds were 20 mm thick, 370 mm long and 100 mm wide (the straight central part was 50 mm wide and 110 mm long).

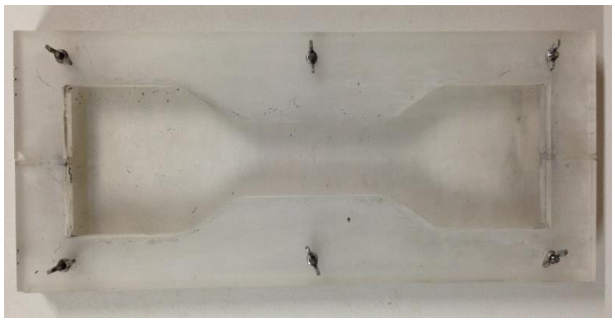

Figure 3.6- Moulds used to cast the specimens for direct tension testing.

In addition to the tensile behaviour in terms of the stress-strain response, in order to study the responses in terms of tensile stress versus the crack mouth opening displacement, notched coupon specimens were used. To prepare these specimens one acrylic mould 1000 mm long, 150 mm wide and 15 mm thick was used. One week after casting the large plates were demoulded, and were cut afterwards in order to obtain individual coupon specimens 15 mm thick, 200 mm long and 60 mm wide.

Figure 3.7- Moulds used to cast the plates for coupon specimens.

3.1.5 Curing environments

All the specimens prepared in this work were cured in 4 types of environments: air (20ºC of temperature and 60% of humidity) or immersed in tap water, salted water and seawater. The average temperature of tap water, salted water and seawater is 18ºC.

Tensile and compressive tests were carried out for each mixture at the curing ages of 14 and 28 days.

3.2 Mixture A

The Mixture A was prepared with tap water, as previously mentioned. Compression, single crack tension and direct tension tests were performed in order to characterize the main mechanical properties of the mixture.

3.2.1 Compressive behaviour

In concrete, compression strength is the most important mechanical characteristic. In general ECC shows similar behaviour to the one found in regular concrete. In this study, one actuator with 200 kN load cell and one LVDT (Linear Variable Differential Transformer) were used. The compressive tests were carried out at a constant displacement increment of 0,02 mm/sec. This procedure was based on EN 196-1:1995.

Figure 3.8- Setup used for the compression tests.

The values of the compression stress and the compression strain were calculated using the following equations:

$$\sigma = \frac{F}{A}$$

$$\varepsilon = \frac{\delta}{h}$$

Where:

- F is the applied load;
- σ is the compression stress;
- A is the area of the cross-section of the specimen;
- Ɛ is the compressive strain;
- δ is the displacement measured by the LVDT;
- h is the height of the specimen.

The displacement used to calculate the strain in all specimens tested overestimates the real compressive strain. This occurred because it was not possible measure the displacement between the top and the bottom surface of the specimen. However, in order to exclude the effect of the reaction frame deformation, the load-displacement response between the two testing plates when using a steel cube between them was measured. This response is elastic and was subtracted from all the experimental responses obtained.

In this study, the compressive strength was tested for two different ages. Three cubes were tested for all different types of cure.

One example of the specimen used in this experimental programme is shown in Figure 3.9.

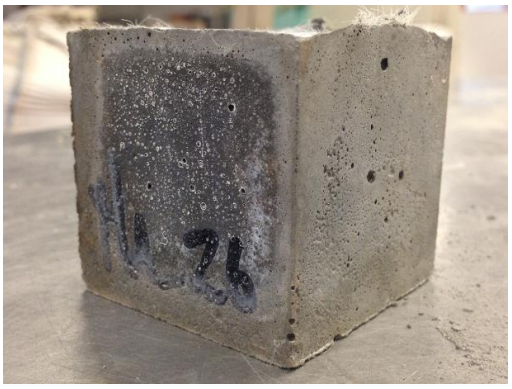

Figure 3.9- Example of cubic specimen of Mixture A before testing.

14 days

The results obtained from the 3 specimens tested for each different curing environment are represented in Figure 3.10.

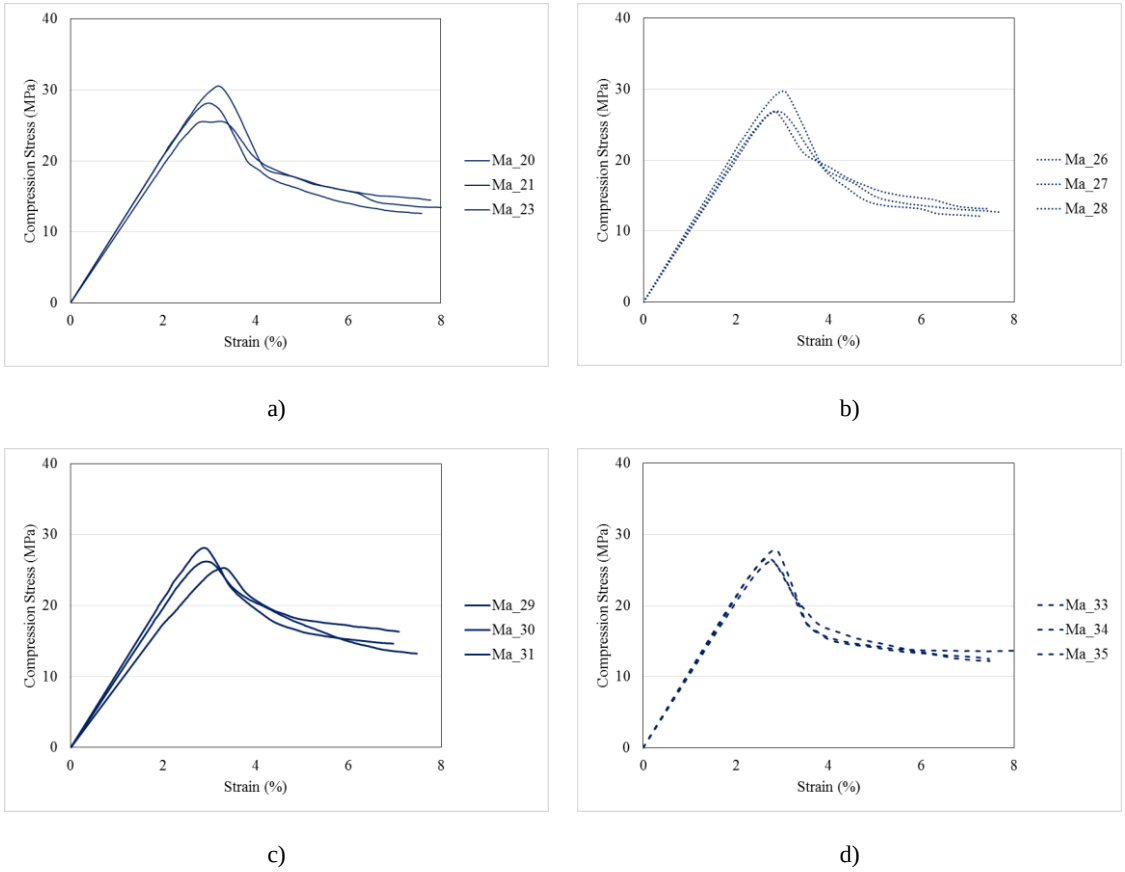

Figure 3.10- Compressive test results of Mixture A at 14 days for different curing environments: a) air: b) seawater; c) tap water; d) salted water.

All the 3 specimens, for each environment, showed a similar behaviour. The post-peak behaviour, for all specimens tested, tends to show a more gentle decrease (when compared with concrete). The peak strains obtained are quite consistent, with an average of about 3%.

Figure 3.11 shows one specimen after testing. The specimens tested exhibited multiple cracks that started to appear before the maximum compressive stress was reached.

Figure 3. 11- Example of a cubic specimen after testing.

In order to compare the results obtained in the different environments it was necessary calculate the average curve of the 3 specimens tested for each type of curing environment.

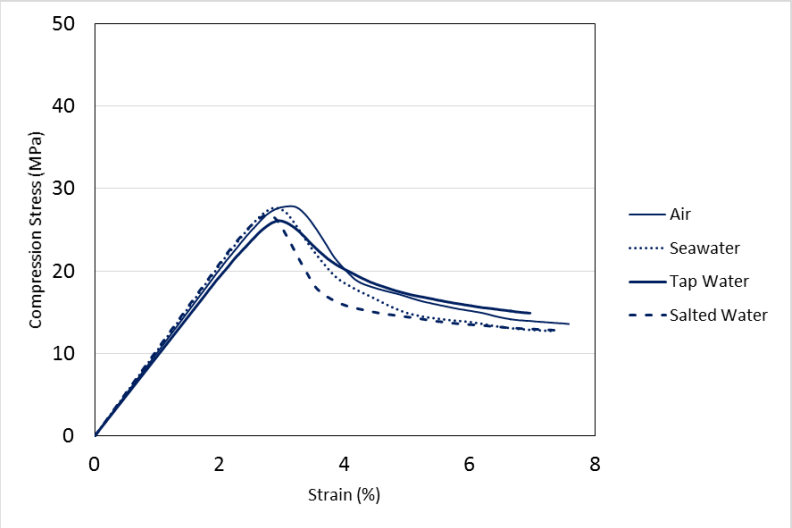

Figure 3.12- Compressive test results of Mixture A at 14 days for all types of curing.

As demonstrated in Figure 3.12 the type of curing environment does not influence significantly the compressive behaviour of Mixture A. The high compressive strain shows that this material is very deformable. In Table 3.3 it is possible to verify the ultimate stress results obtained in each specimen tested. These values are typical for ECC materials [16].

Table 3.3- Maximum compressive stresses obtained for Mixture A in all curing environments at 14 days.

Cure	Specimen	Compressive strength (MPa)	Average (MPa)	Standard Deviation	Coefficient of Variation
Air	Ma_20	25,56	28,07	2,03	7
	Ma_21	28,13			
	Ma_23	30,53			
Seawater	Ma_26	29,77	27,05	2,15	8
	Ma_27	26,87			
	Ma_28	24,52			
Tap Water	Ma_29	26,21	26,54	1,18	4
	Ma_30	28,13			
	Ma_31	25,30			
	Ma_33	27,82	26,86	0,68	3
	Ma_34	26,61			

Salted Water	Ma_35	26,22

Other important property is the elasticity modulus. Normally, in order to determine this mechanical property another type of specimens should be used (cylinders). However, in order to obtain an indication of value of the elasticity modulus, the compressive results shown previously were used. This nominal value of the elastic modulus was calculate using the following equation:

$$E = \frac{\sigma_{2/3} - \sigma_{1/3}}{\varepsilon_{2/3} - \varepsilon_{1/3}}$$

Where:

- E is the nominal elastic modulus;
- $\sigma_{1/3}$ is one third of the ultimate compression stress;
- $\sigma_{2/3}$ is two thirds of the ultimate compression stress;
- $\varepsilon_{1/3}$ is the strain obtained for one third of the ultimate compression stress;
- $\varepsilon_{2/3}$ is the strain obtained for two thirds of the ultimate compression stress.

In the Table 3.4 the results obtained for the nominal elasticity modulus of each specimen are presented. The nominal elasticity modulus range between 8.7 and 10.8 GPa. The lower results, when compared with the traditional cement, are explained mostly by the type of specimen used, which leads to significantly higher deformations for the same load levels. However, although this procedure does not allow the determining of the objective value of the elastic modulus, it allows the comparing of results and the discussion required in the context of this research.

Table 3. 3- Elastic modulus of Mixture A specimens (14 days)

Curing	Specimen	Nominal Elasticity Modulus (GPa)	Average (GPa)	Standard Deviation (GPa)	Coefficient of Variation
Air	Ma_20	9,70	10,13	0,30	3
	Ma_21	10,33			
	Ma_23	10,35			
Seawater	Ma_26	10,80	10,41	0,30	3
	Ma_27	10,33			
	Ma_28	10,09			
	Ma_29	9,87			

Tap Water	Ma_30	10,47	9,69	0,72	7
	Ma_31	8,73			
Salted Water	Ma_33	10,54	10,39	0,11	1
	Ma_34	10,33			
	Ma_35	10,30			

Figure 3.13 represents the average elasticity modulus obtained for each type of curing. The higher value of nominal elasticity modulus was reached by the specimen cured in seawater. However, all types of cure have very similar values [33].

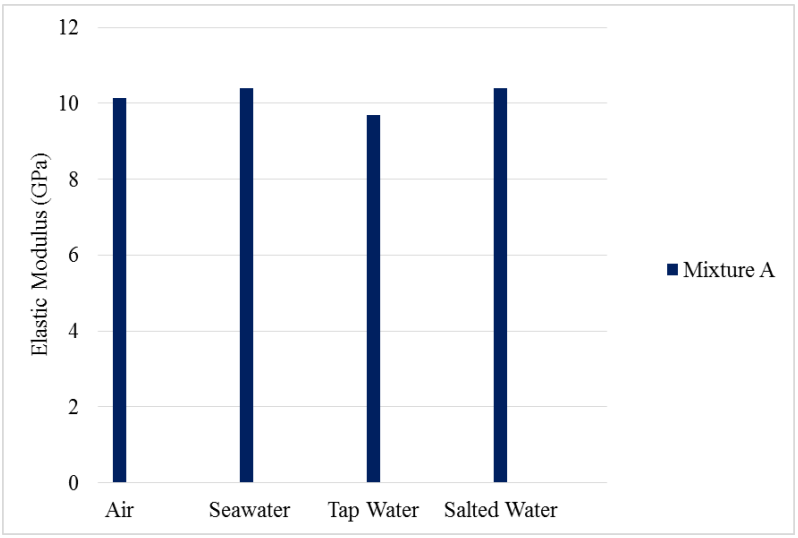

Figure 3. 13- Average of Mixture A elastic modulus (14 days)

28 days

Figure 3.14 represents the compression test results of Mixture A for each type of curing environment at 28 days.

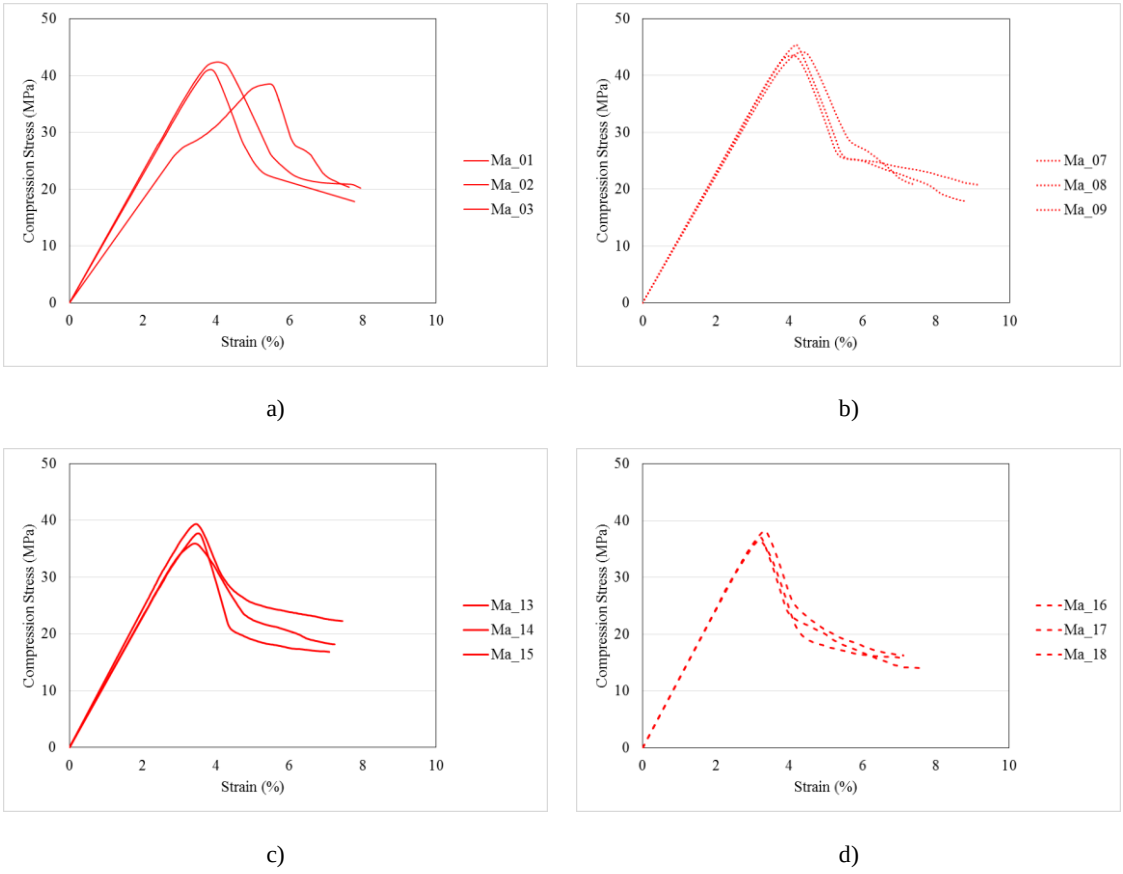

Figure 3. 14 - Compressive results of Mixture A, 28 days: a) cured in air; b) cured in seawater; c) cured in tap water; d) cured in salted water.

One of the specimens cured in air showed a different behaviour than expected, considering all the other results obtained. That difference can be justified by the fact that this specimen could have an imperfection or was not correctly prepared. For all the other types of curing the 3 specimens tested showed similar behaviours in compression.

Figure 3.15 shows one specimen after testing. The expected behaviour for ECC mixtures was obtained, the specimens did not disintegrate after rupture and showed small cracks even before the ultimate compression stress was achieved.

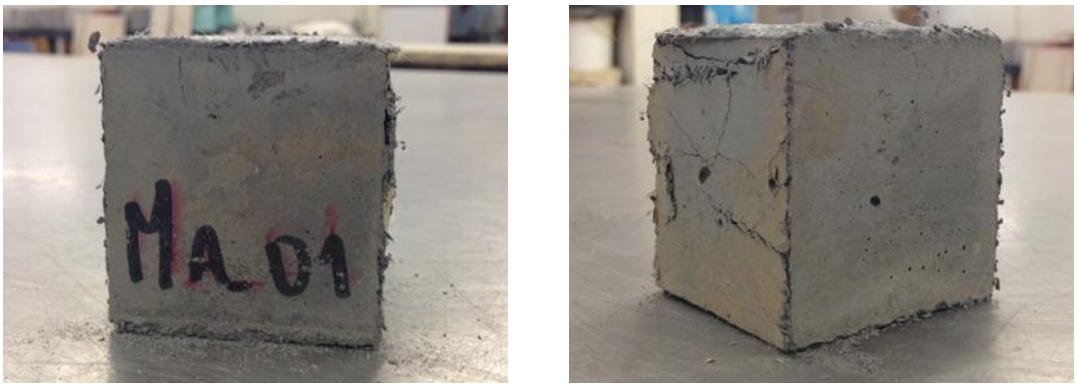

Figure 3.15- Example of Mixture A cube after the test

Figure 3.16 shows the average results obtained for each type of curing. The specimens that were cured in air and seawater showed higher compressive strength. The peak strain ranged between 3% and 4%.

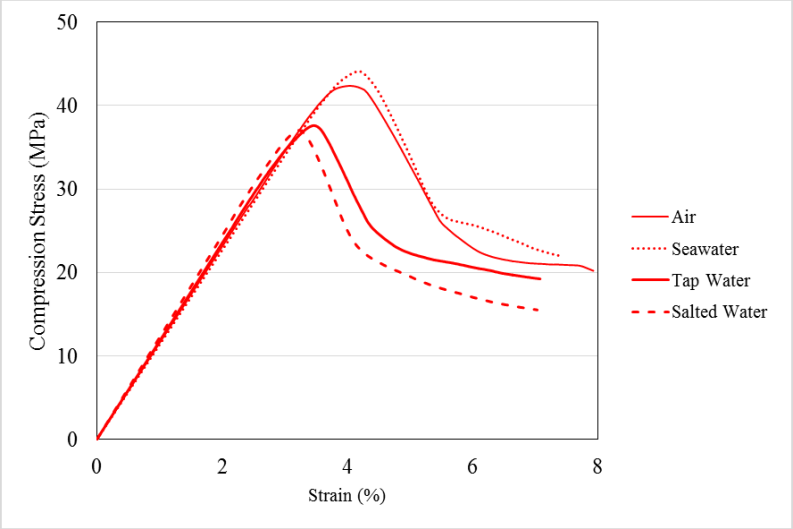

Figure 3. 16- 28 days compressive results of Mixture A in all types of cure

The results showed that the compressive strength of Mixture A was influenced by the type of curing. As shown in Table 3.5, the compressive strength ranged between 35 and 46 MPa and the coefficient of variations obtained were quite low.

Table 3. 4- Maximum compressive results of Mixture A in all environments (28 days)

Cure	Specimens	Compressive strength (MPa)	Average (MPa)	Standard Deviation	Coefficient of Variation
Air	Ma_01	38,52	40,64	1,60	4
	Ma_02	42,37			
	Ma_03	41,04			
Seawater	Ma_07	44,12	44,33	0,79	2
	Ma_08	45,39			
	Ma_09	43,50			
Tap Water	Ma_13	37,71	37,66	1,40	4
	Ma_14	39,35			
	Ma_25	35,92			
Salted Water	Ma_16	38,19	37,27	0,68	2
	Ma_17	37,08			
	Ma_18	36,56			

The nominal elasticity modulus was calculated as previously. The results in Table 3.6 show that the maximum value was reached when the specimens were cured in salted water.

Table 3.5- Elastic modulus of Mixture A specimens (28 days)

Cure	Specimen	Elasticity Modulus (GPa)	Average (GPa)	Standard Desviation	Coefficient of Variation
Air	Ma_01	9,08	10,64	1,10	10
	Ma_02	11,55			
	Ma_03	11,28			
Seawater	Ma_07	11,16	11,34	0,13	1
	Ma_08	11,48			
	Ma_09	11,37			
Water	Ma_13	11,50	11,76	0,31	3
	Ma_14	12,20			
	Ma_15	11,57			
Salted Water	Ma_16	12,16	12,19	0,03	0
	Ma_17	12,24			
	Ma_18	12,18			

Figure 3.17 represents the average of the elastic modulus value in each type of cure.

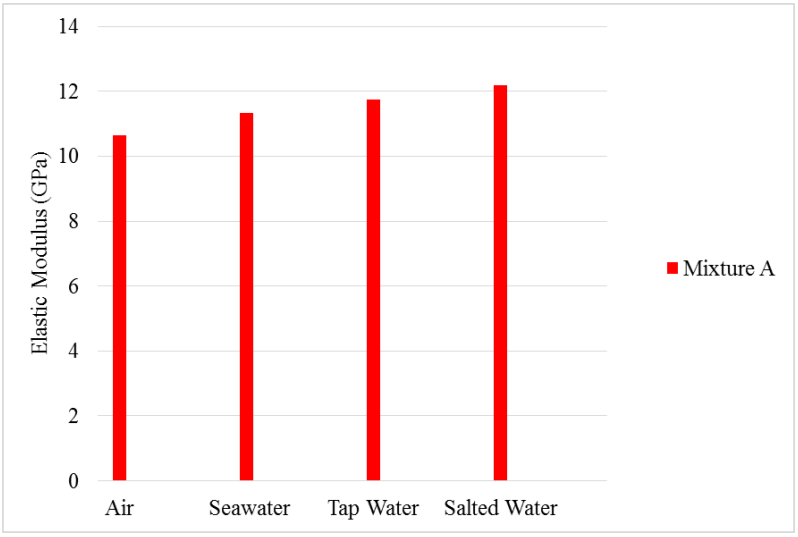

Figure 3. 17 - Elastic modulus average of Mixture A (28 days)

The seawater curing seems to have no influence in the maximum compression stress. However, higher values of the elasticity modulus were achieved when the Mixture A was cured in salted water.

14 vs 28 days

In this study, 2 different ages of each mixture were tested as previously mentioned. In Figure 3.18 the results of the two ages are compared. As expected the specimens tested at 28 days showed higher compression stress.

There is a difference between the ultimate strain at 14 days and at 28 days, which is higher in the first two types of curing (Figure 3.18.a) and Figure 3.18.b)). The difference of the results between both ages is less perceptible when the curing occurred in water or salted water.

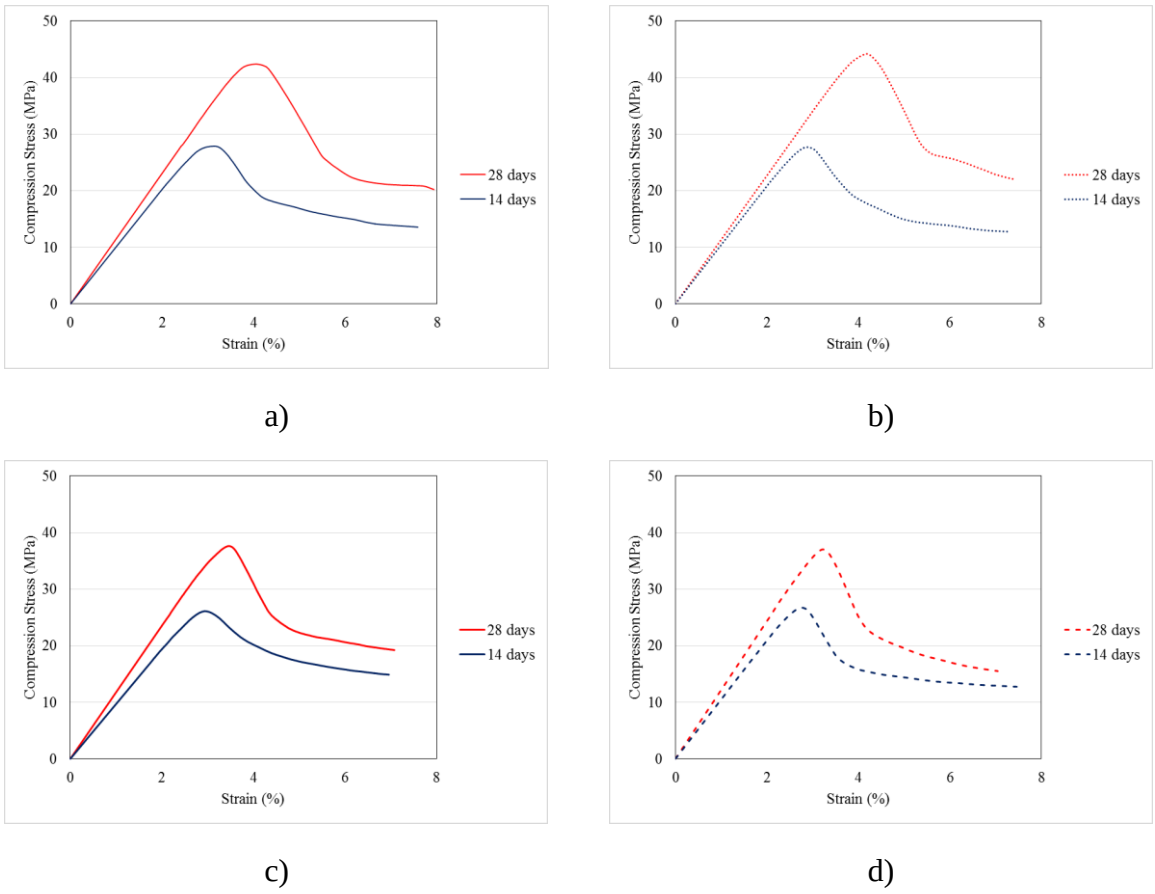

Figure 3. 18- 14 vs 28 days compressive results of Mixture A: a) cured in air; b) cured in seawater c) cured in tap water; d) cured in salted water

Figure 3.19 represents the average results of compression strength. At 14 days the results obtained, regardless of the type of curing, have been essentially similar. However, at 28 days some differences were noticeable, mainly for the specimens cured in air and seawater.

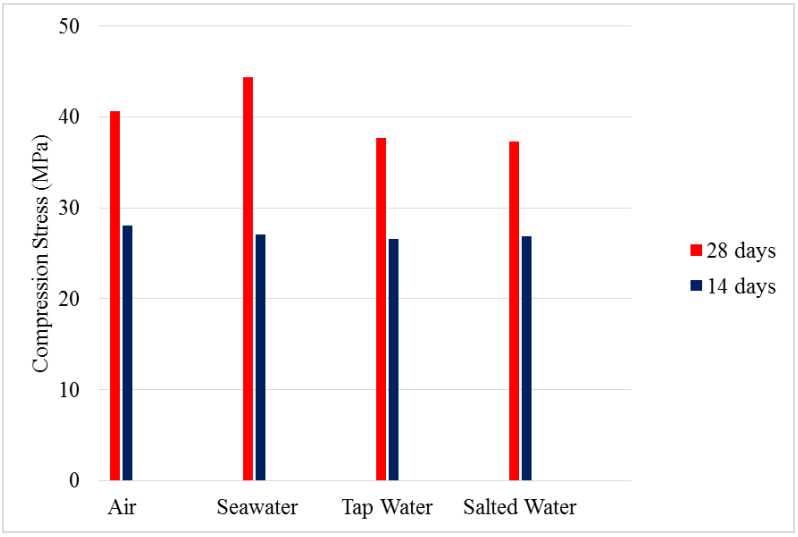

Figure 3. 19- Comparison between the compressive strength results obtain at different ages.

Figure 3.20 shows the nominal elastic modulus results obtained in both ages.

The 14 days old specimens have shown higher elasticity modulus when cured in seawater and salted water. However, the results at 28 days showed that the higher values were obtained when curing occured in tap water and salted water. The maximum compression strength is achived when curing in air and seawater.

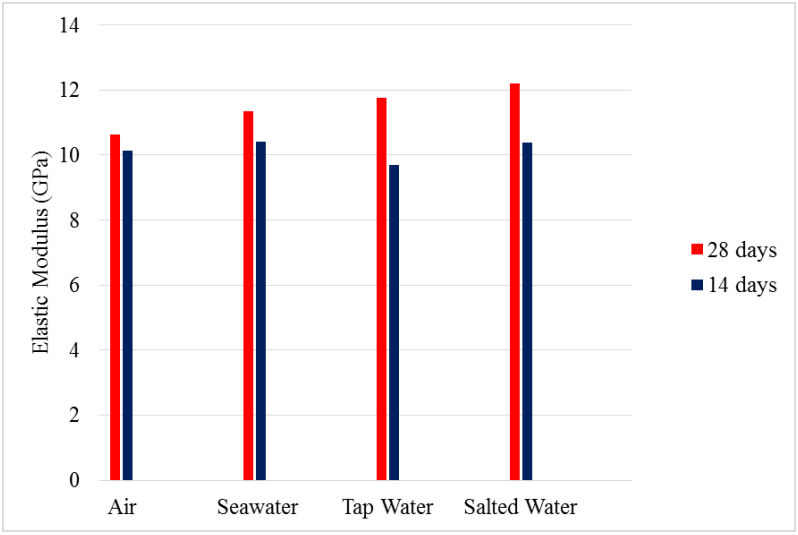

Figure 3. 20- Comparison between the elastic modulus results obtain in different ages

3.2.2 Single Crack Tension Test (SCTT)

This test has purpose of studying the tensile stress *versus* the crack opening response of fibre reinforced cementitious composites, as well as the energy that is necessary to open a single crack. [27] This information is important for supporting the design of the cementitious matrix composite, as well as the numerical simulation of its nonlinear behaviour.

The specimens used in this test are 20 mm thick, 200 mm long and 60 mm wide. One notch was made in the middle of the each specimen. The purpose of the notch is creating one single crack in the specimen. The initial section of the specimen was 60 mm by 20 mm and at the notched section it decreased to 36 mm by 13.3 mm (Figure 3.21).

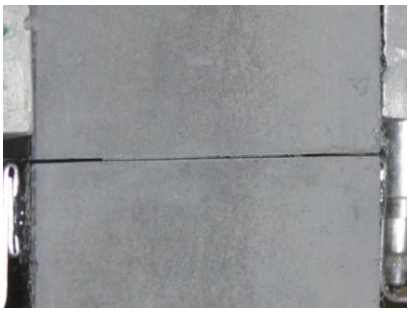

Figure 3. 21- Example of notch made in the SCTT specimens

One actuator with 200 kN load cell, two grips (one grip was connected with the actuator and the other was fixed in the reaction frame) and 3 Linear Variable Differential Transformers (LVDT's) were used in this test. The LVDT's were placed in the specimen to measuring the Crack Mouth Opening Displacement (CMOD) (Figure 3.22). The tests were carried out at a constant displacement increment of 0,01 mm/sec.

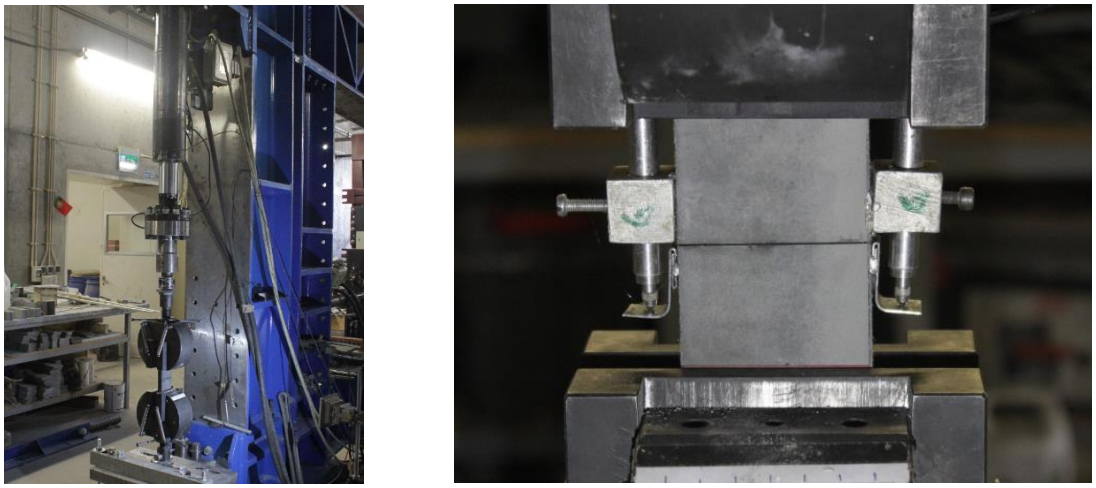

Figure 3. 22- Test setup and the method used to measure the central displacement of the specimen

The tensile stress and the CMOD were calculate using the following equations:

$$\sigma = \frac{F}{A}$$

$$CMOD = \frac{\delta_1 + \delta_2}{2}$$

Where:

- F is the applied load;
- σ is the tensile stress;
- A is the area of the notch in the specimen;
- δ_1 is the displacement measured by the LVDT;
- δ_2 is the displacement measured by the second LVDT;

The crack mouth opening displacements (CMOD) were obtained by averaging the displacements measured in the LVDT's, although these were later verified to be practically similar.

Tests were carried out at 2 different curing ages. For each type of cure 3 specimens were tested.

14 days

The results of Single Crack Tension Test (SCTT) for 14 days specimens are represented in Figure 3.23.

The specimens have different behaviours depending of the type of curing used. They show different types of stress-CMOD responses: the specimens cured in air show responses that don't have peaks like in the other cases. These peaks are most likely representing the formation of cracks. This test is more useful when only one crack is formed, but that doesn't seem to have been the case in some of the specimens. These unexpected cracks can occur for various reasons: the section of the notch should have been smaller, the matrix was not mature enough or the mortar was not correctly spread in the mould.

The typical behaviour should show, at the onset, a higher stiffness phase until the crack starts to open. After that stage the decrease of tensile stress should occur until the PVA fibres start to "work". Afterwards the crack opens until the maximum tensile stress is reached.
The specimens cured in seawater showed the lowest values of CMOD.

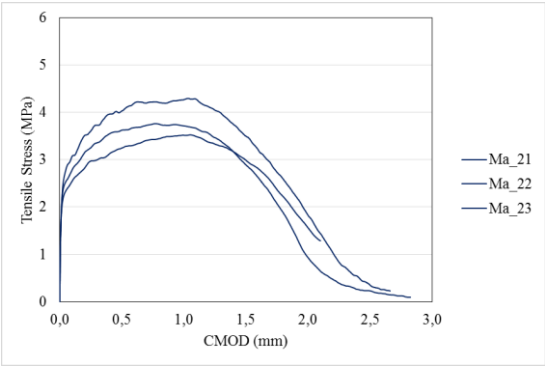

a)

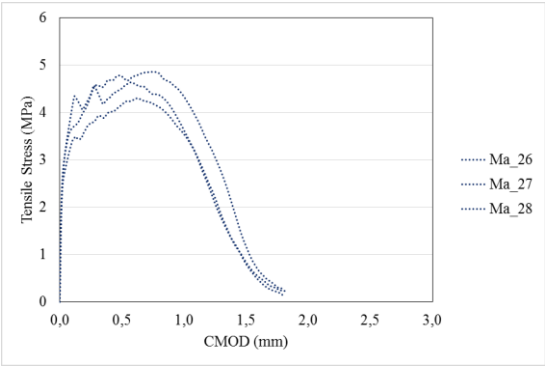

b)

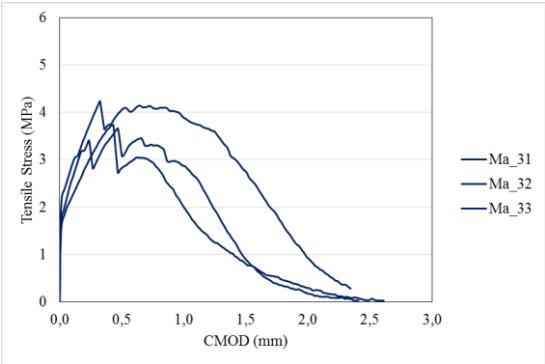

c)

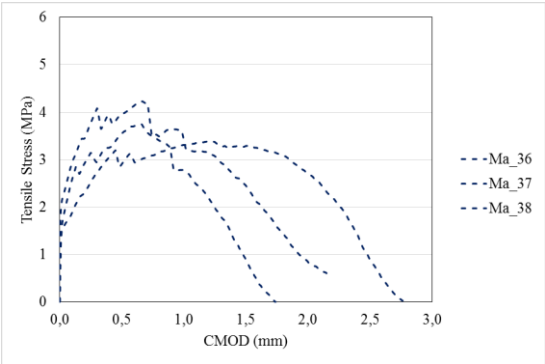

d)

Figure 3. 23- SCTT results of Mixture A, 14 days: a) cured in air; b) cured in seawater; c) cured in tap water; d) cured in salted water

Figure 3.24 represents the average responses for each environment. These responses were obtained from the average stresses measured for 3 specimens at each CMOD.

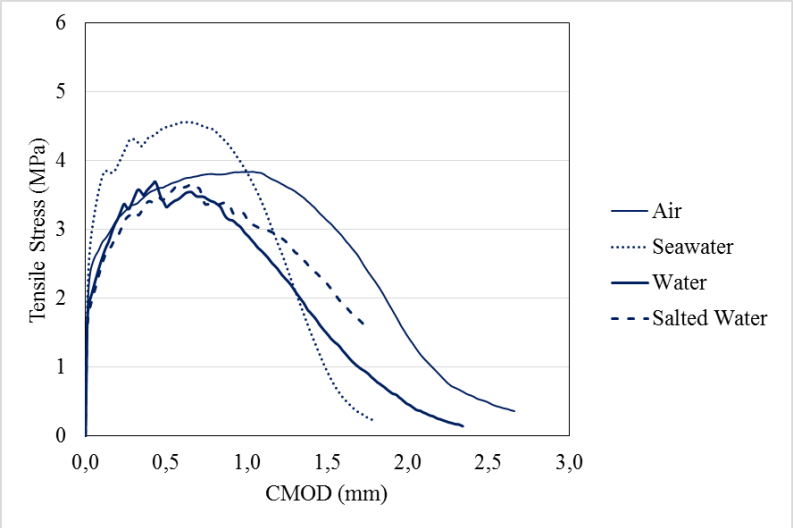

Figure 3. 24- SCTT results of Mixture A (14 days)

The look of the specimens after testing is shown in Figure 3.27. This figure shows the notched sections of the specimens from two distinct angles.

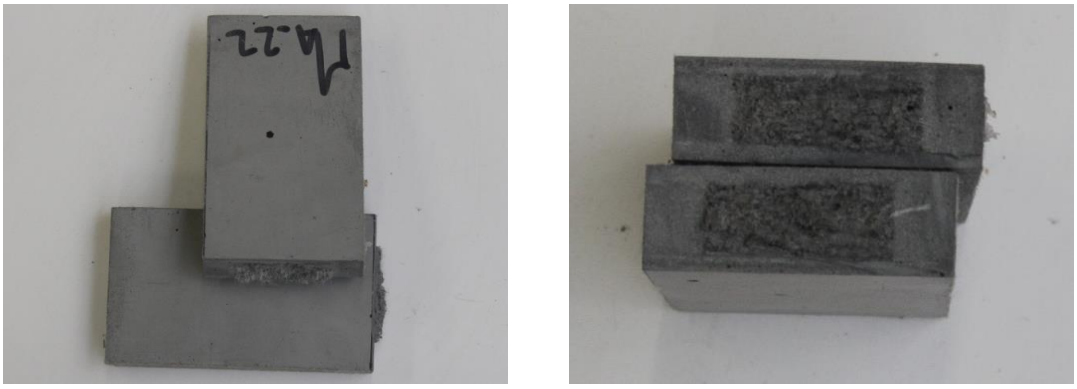

Figure 3. 25- Example of Mixture A specimen used in this test

28 days

The results of Single Crack Tension Test (SCTT) for specimens after 28 days of curing are represented in Figure 3.26. As shown, the specimens cured in air and seawater reached higher tensile stresses at lower crack mouth open displacements. All responses for all types of curing show multiple peaks.

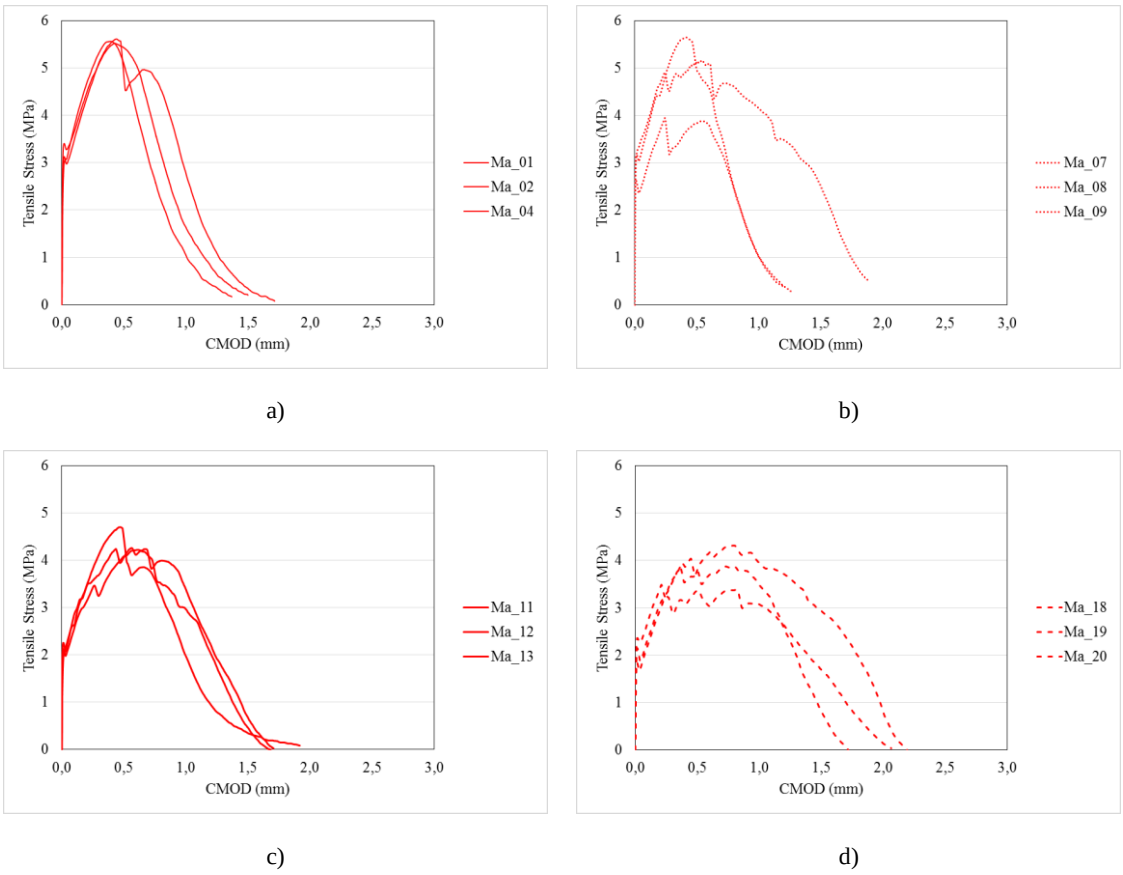

Figure 3. 26- SCTT results of Mixture A, 28 days: a) cured in air; b) cured in seawater; c) cured in water; d) cured in salted water.

As previously, the average curves were computed for all types of curing. Figure 3.27 shows that the specimens that were cured in air reach higher tensile stress and the specimens that were cured in salted water the lowest.

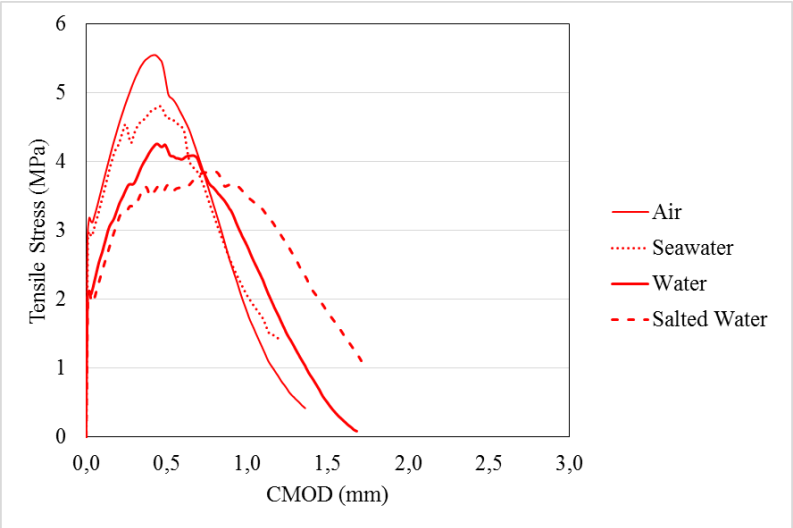

Figure 3. 27- SCTT results of Mixture A (28 days)

Figure 3.28 shows the cross-section of one specimen of Mixture A cured for 28 days after testing.

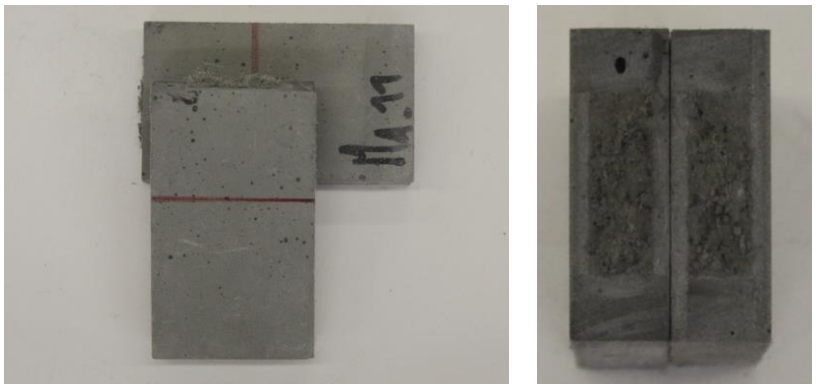

Figure 3. 28 – Example of a 28 days specimen of Mixture

14 vs 28 days

In this study, 2 different ages of each mixture were tested. Figure 3.31 shows the behaviour of Mixture A for all curing environments. The curves represented are the average of Mixture A for each age.

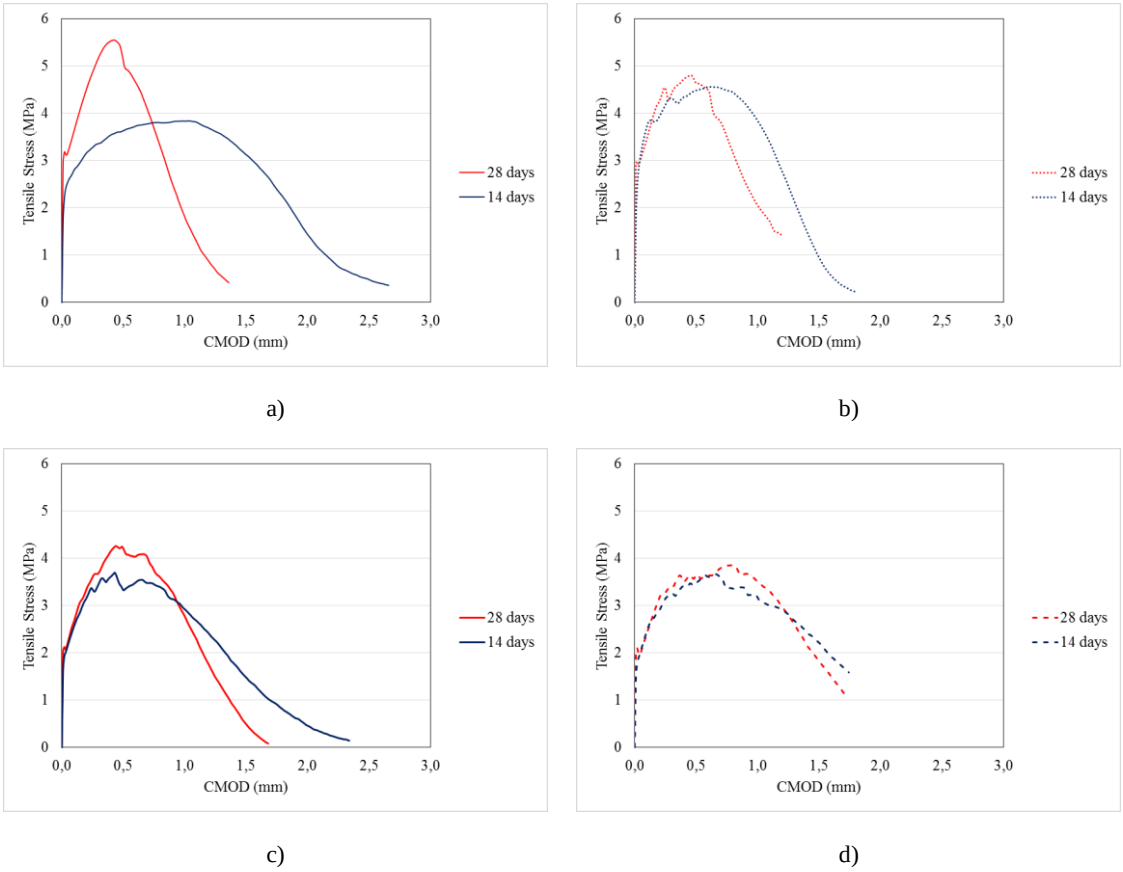

Figure 3. 29 - 14 vs 28 days SCTT results of Mixture A: a) cured in air; b) cured in seawater; c) cured in tap water; d) cured in salted water.

The specimens that were cured in air show the greatest change in the behaviour observed: the 28 days specimens reach higher tensile stresses at lower crack opening displacements. That happens because the matrix is more mature at 28 days old, therefore higher tensile force is necessary open the initial crack. The same trend was observed in the cases of seawater and tap water curing, but less evident.

3.2.3 Tensile Stress-Strain Behaviour

The most important characteristic of Engineering Cementitious Composites is revealed by their tensile behaviour. For characterising this behaviour dogbone specimens were used. Before testing all specimens were rectified to improve the adherence with the surface of the grips and to avoid the slip of the specimens during the test.

One actuator with a 200 kN load cell, two grips (one grip was connected with the actuator and the other was fixed in the reaction frame) and 3 Linear Variable Differential Transformers (LVDT's) were used in this test. (Figure 3.30)

Figure 3. 30- Test setup used for the tensile tests

During testing the specimens were subjected to an imposed increasing tensile displacement at a constant rate of 0,010 mm/s. To measure the specimen displacement in the central area, two LVDT´s were used. These LVDT´S were fixed between two points in the specimen at a 10 cm distance.

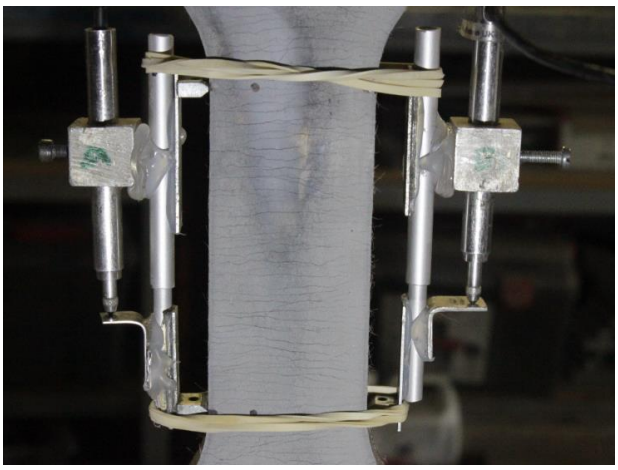

Figure 3. 31- Method used to measure the central displacement of the specimen

The tensile stress and the tensile strain were calculated according to the following equations:

$$\sigma = {}^{F}/_{A}$$

$$\varepsilon = {}^{(\delta_1 + \delta_2)}/_{\Delta L} \times 100$$

Where:

- σ is the tensile stress;
- F is the applied force;
- A is the area of the cross-section of the specimen;
- ε is the tensile strain;
- δ_1 and δ_2 are the displacements measured in the LVDT's;
- ΔL is the distance between the two fixed points at which the LVDT's are placed.

The central displacement was obtained by averaging the displacements measured in the two opposite LVDT's, although these were later verified to be practically similar. Tensile tests have been carried out at two different curing ages, 14 days and 28 days.

14 days

Three specimens for each type of curing were tested. The stress-strain results of all specimens of Mixture A are represented in Figure 3.34. The specimens tested showed the typical tensile behaviour that characterizes ECC.

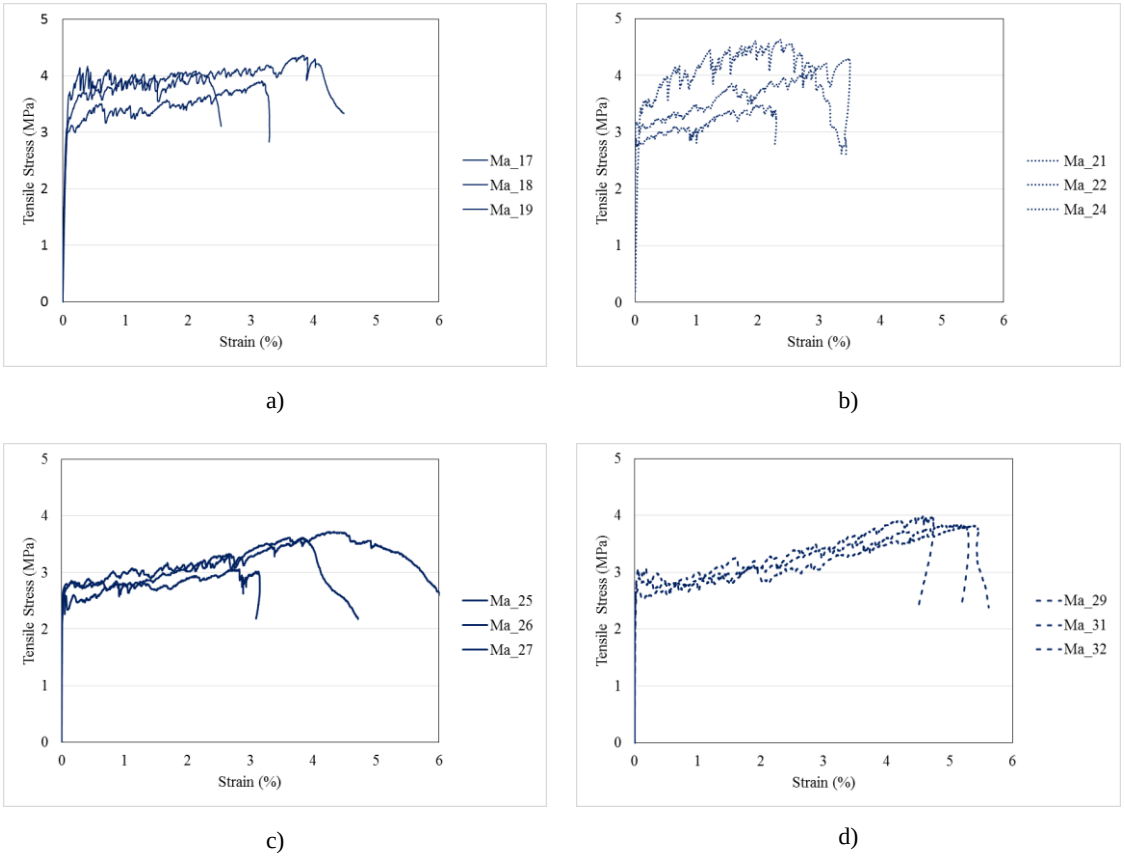

Figure 3. 32- Tensile results of Mixture A, 14 days: a) cured in air; b) cured in seawater; c) cured in tap water; d) cured in salted water.

The responses represented in Figure 3.32 show high stiffness before the formation of the first crack at about 0.03-0.33% of tensile strain. After the first crack formation, all the specimens exhibited the appearance of several micro-cracks at increasing tensile stresses, reaching high values that range between 3 and 4.6 MPa. The specimens tested reached an ultimate tensile strain between 2 and 5.5 %.

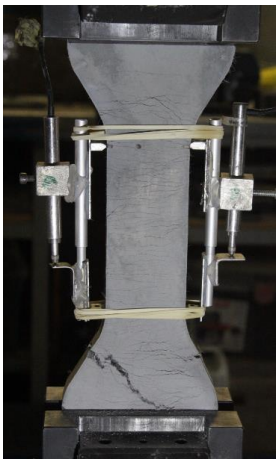

Figure 3. 33-Example of a 28 days specimen of Mixture A during testing.

Table 3.7 represents the main results obtained from each tensile response: the first crack stress σc, the strain at first crack Ɛc, the ultimate tensile stress σm and the ultimate tensile strain Ɛm.

Table 3. 6– Properties of tensile curves of Mixture A in all environments (14 days)

Cure	Specimen	σc (Mpa)	Ɛc (%)	σm (Mpa)	Ɛm (%)
Air	Ma_17	3,07	0,06	3,91	3,17
	Ma_18	3,70	0,33	4,37	3,82
	Ma_19	3,71	0,11	4,17	0,39
Seawater	Ma_21	2,92	0,24	3,49	1,98
	Ma_22	3,18	0,03	4,30	3,49
	Ma_24	3,42	0,09	4,63	2,38
Tap Water	Ma_25	2,74	0,04	3,05	2,75
	Ma_26	2,83	0,22	3,71	4,34
	Ma_27	2,85	0,16	3,61	3,63
Salted Water	Ma_29	2,89	0,08	3,82	5,13
	Ma_31	2,71	0,05	3,82	5,41
	Ma_32	3,05	0,06	3,99	4,59

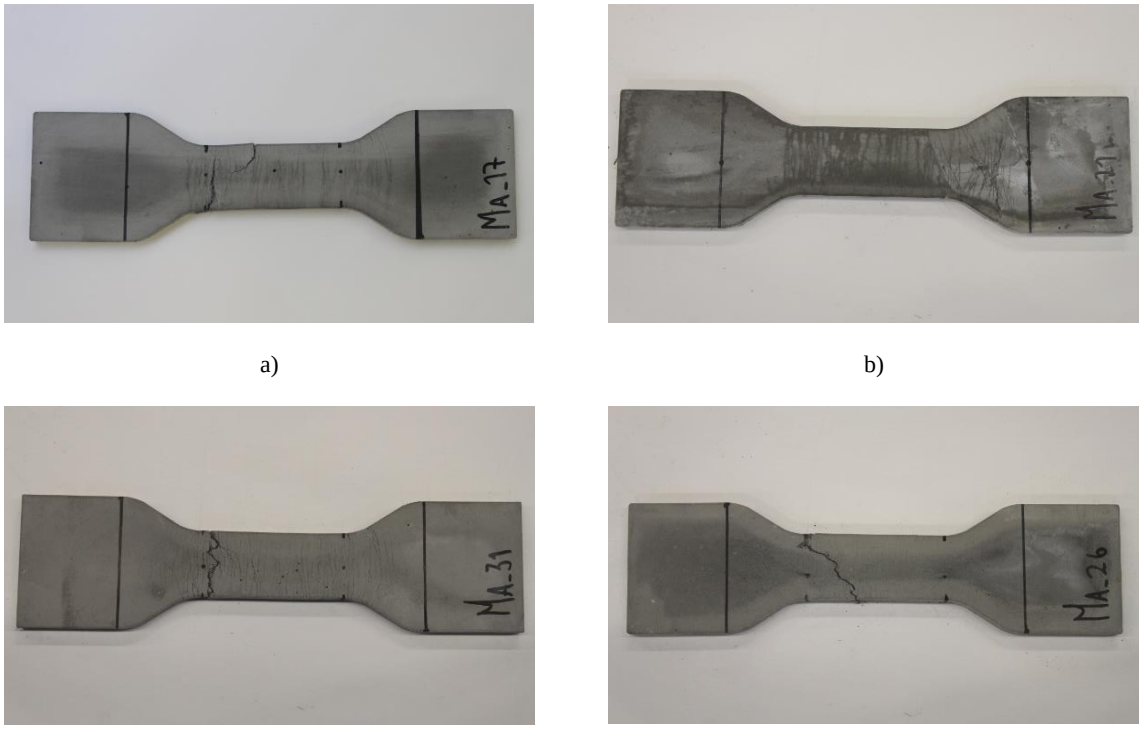

a) b)

c) d)

Figure 3. 34- Mixture A dogbone specimens tested after 14 days of curing: a) in air; b) in seawater; c) in tap water; d) in salted water.

Figure 3.34 shows one example of the specimens of each type of curing environment after testing.

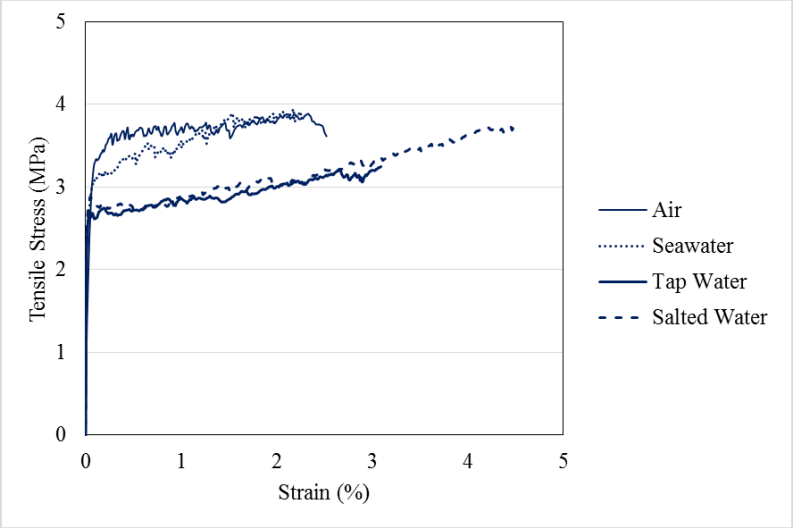

Figure 3. 35- Average tensile test results for Mixture A in all environments (14 days).

Figure 3.35 shows the average curves obtained for each type of curing. Each curve was calculated using the tensile stress-strain results of the 3 specimens tested; the maximum value of strain in the average curve corresponds to the minimum strain value reached by the three specimens tested.

The type of environment in which the specimens were cured has a significant influence in the tensile responses obtained for Mixture A. The specimens that were cured in air and seawater reached higher tensile strengths but lower ultimate tensile strains.

28 days

Three specimens were tested for each curing environment. The tensile stress-strain results for 28 days specimens are represented in Figure 3.37. All the specimens showed the typical strain hardening behaviour of ECC materials. The specimens cured in tap water showed higher peaks in the strain hardening phase resulting cracks with larger width.

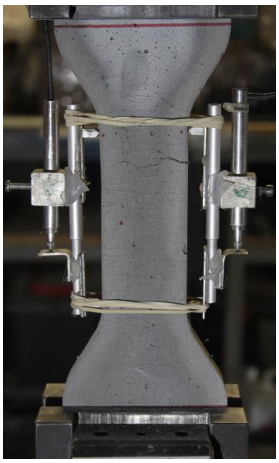

Figure 3. 36- Example of a 28 days specimen of Mixture A during the test

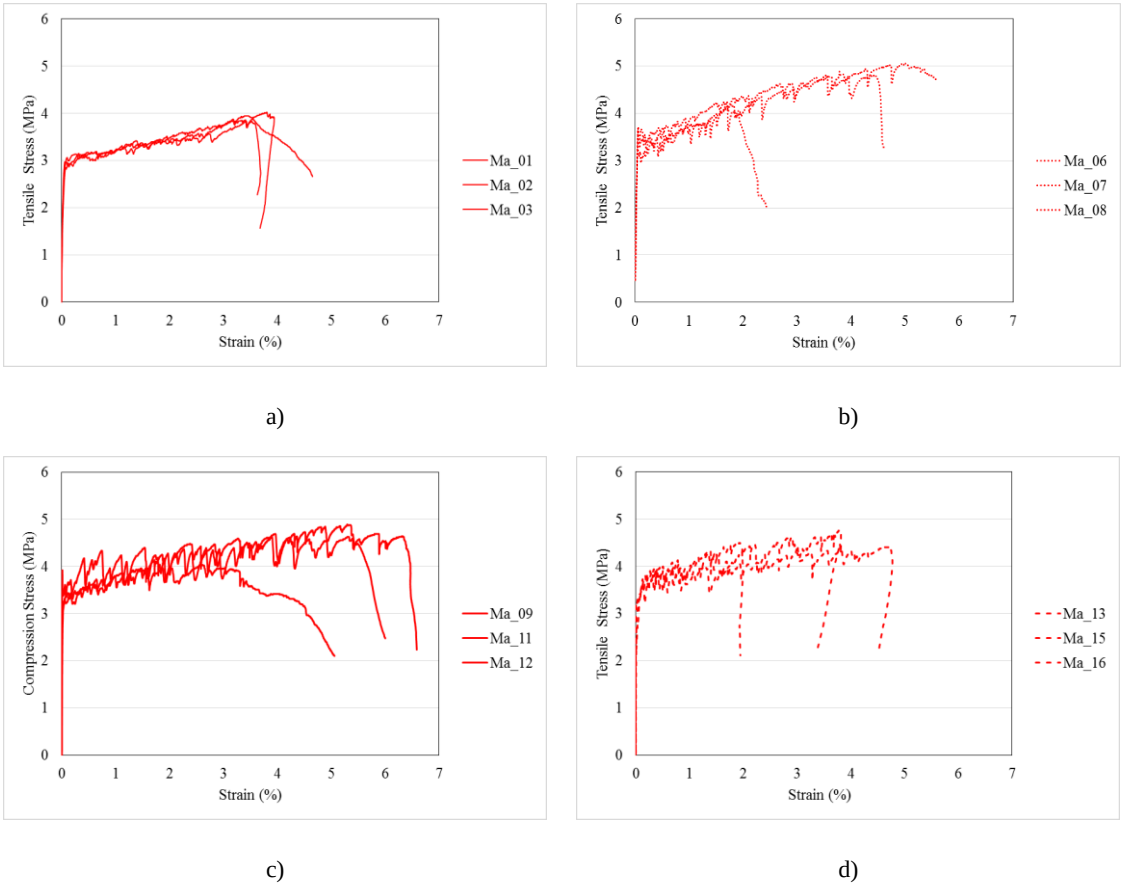

Figure 3. 37 - Tensile test results for Mixture A after 28 days of curing: a) in air; b) in seawater; c) in tap water; d) in salted water.

The first crack tensile stress ranges between 3 and 4 MPa. In table 3.8 are represented the main properties of each specimen. The specimens cured in air showed the lower tensile stress.

Table 3. 7- Properties of tensile curves of Mixture A in all environments (28 days

Cure	Specimen	σc (Mpa)	Ɛc (%)	σm (Mpa)	Ɛm (%)
Air	Ma_01	3,06	0,10	3,94	3,47
	Ma_02	3,15	0,32	3,83	3,53
	Ma_03	2,97	0,06	4,02	3,81
Seawater	Ma_06	3,69	0,05	4,89	3,78
	Ma_07	3,19	0,09	4,13	1,71
	Ma_08	3,71	0,06	5,05	5,00
Tap Water	Ma_09	3,92	0,01	4,03	2,60
	Ma_11	3,42	0,13	4,69	5,88
	Ma_12	3,32	0,06	4,89	5,30

Salted Water	Ma_13	3,31	0,06	4,40	4,69
	Ma_15	3,73	0,13	4,50	1,94
	Ma_16	3,21	0,01	4,77	3,82

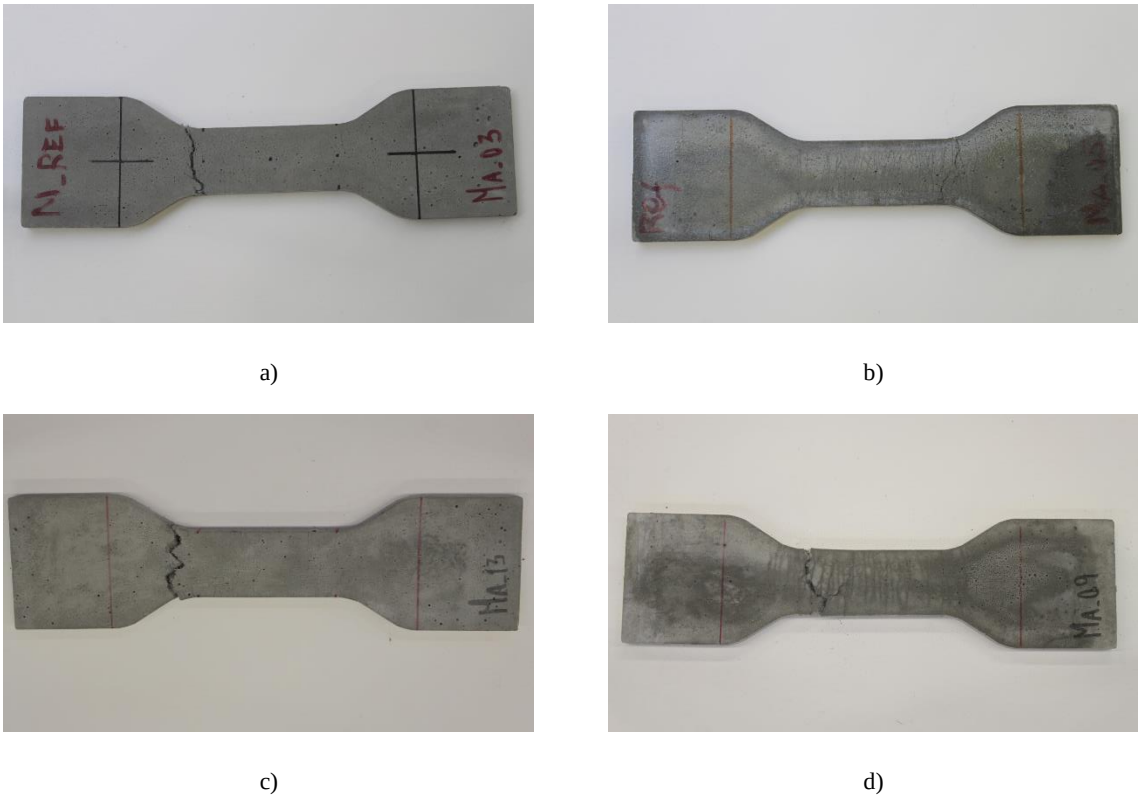

a) b)

c) d)

Figure 3. 38- 28 days Mixture A dogbone specimens after the test: a) cured in air; b) cured in seawater; c) cured in tap water; d) cured in salted water.

The average results obtained for each type of environment were calculated using the tensile stress-strain responses of the three specimens. These results are presented in Figure 3.39.

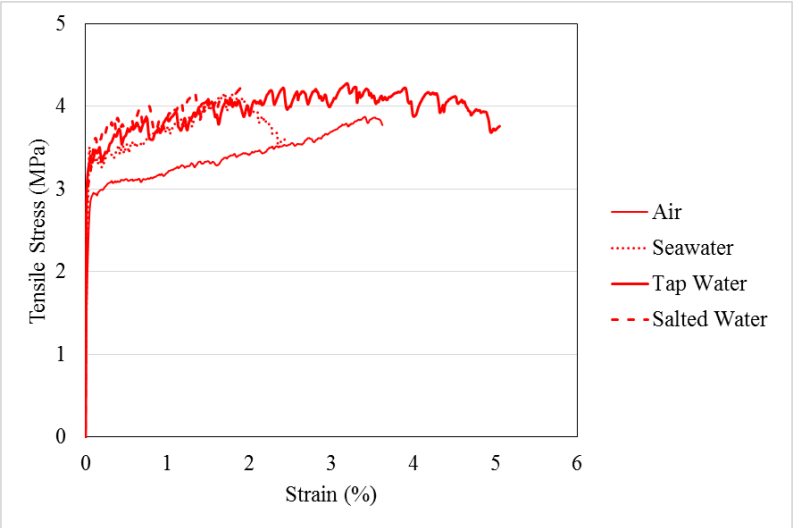

Figure 3. 39- Average tensile responses obtained for Mixture A cured in all environments (28 days).

The specimens cured in tap water showed higher ultimate strain values. During the strain hardening phase of the stress-strain response, all the cures show a different behaviour. That difference is explained when the crack pattern is analysed. The more pronounced "peaks" of tensile stress-strain response correspond to the formation of cracks with larger crack width.

14 vs 28 days

In this study, 2 different ages of each mixture were tested. In general, the 28 days old specimens reached higher tensile stress values. This increase is the result of a more mature matrix. The comparison between the results obtained at the two curing ages is presented in Figure 3.40.

The results obtained for the specimens cured in air were different than the expected. These showed higher tensile stress values when tested at 14 days of curing, in contrast to what was observed for all the other curing environments.

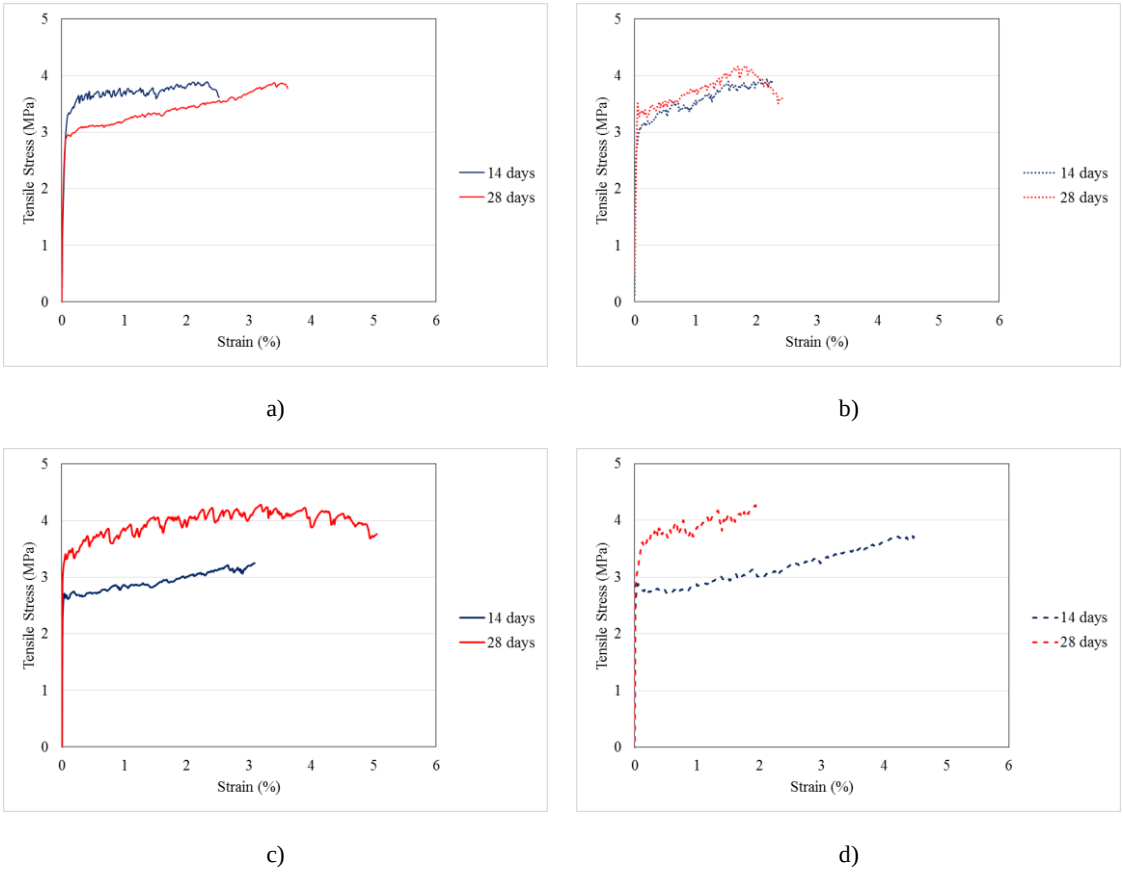

Figure 3. 40- 14 days versus 28 days tensile test results of Mixture A: a) cured in air; b) cured in seawater; c) cured in tap water; d) cured in salted water.

3.3 Mixture B

The Mixture B was prepared using seawater, as previously mentioned. The compression test, the single crack tension test and the direct tension test were carried out as previously in order to characterize the mechanical behaviour of mixture B when cured in the different environments previously described.

3.3.1 Compressive behaviour

The setup and procedure used to test the Mixture B was the same explained in section 3.2.1.

14 days

The results obtained for all 3 specimens tested for each different environment are represented in Figure 3.41. In general, the 3 specimens for each environment showed similar responses in

compression. The post-peak load descend appeared more gentle than the one typically obtained for concrete. The minimum peak strain was 2% and the maximum 4%.

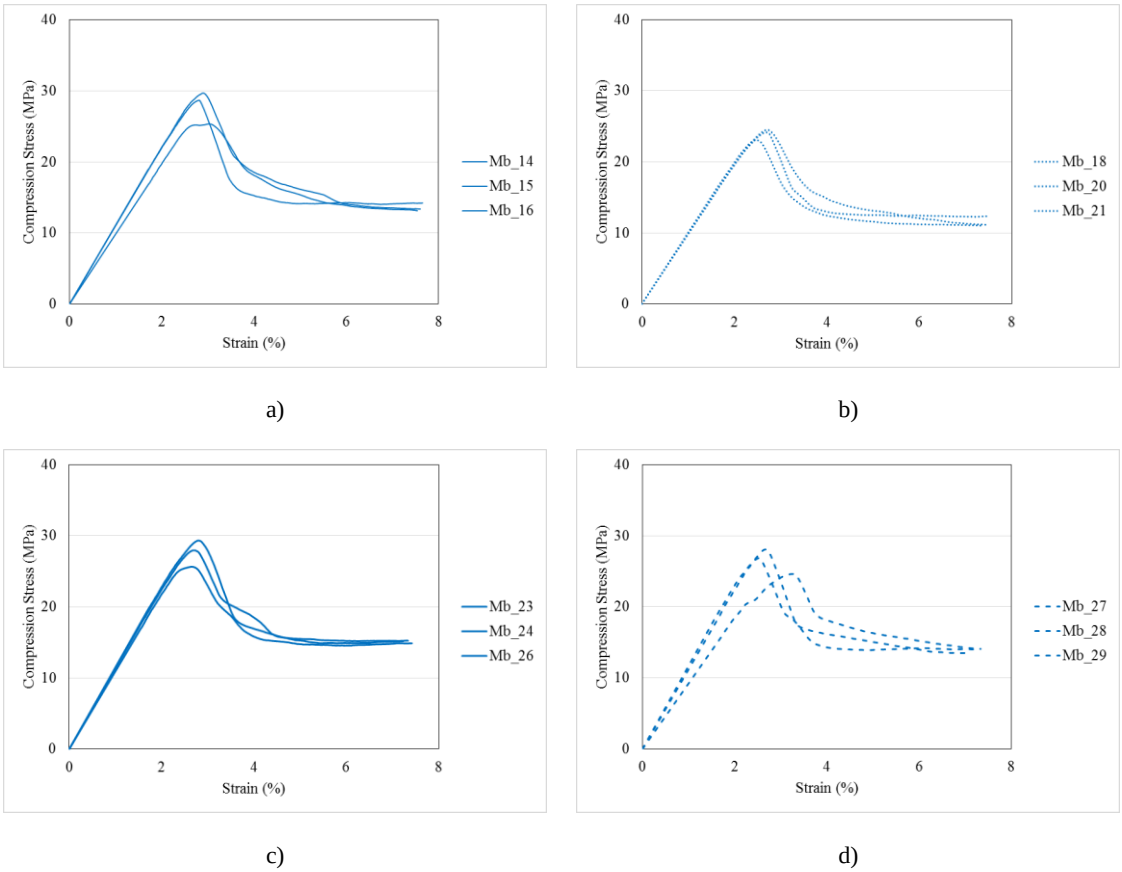

Figure 3. 41- Compression test results for Mixture B at 14 days: a) cured in air; b) cured in seawater; c) cured in tap water; d) cured in salted water

Figure 3.42 shows one specimen after testing. In general the specimens exhibited multiple cracks, which started to be visible before the maximum compressive stress was reached.

Figure 3. 42- Example of a cubic specimen after the test

Mixture B compressive tests resulted in essentially similar behaviours for all types of curing. The average results for each type of curing are represented in Figure 3.43. The average curve was calculated as explained in section 3.2.1.

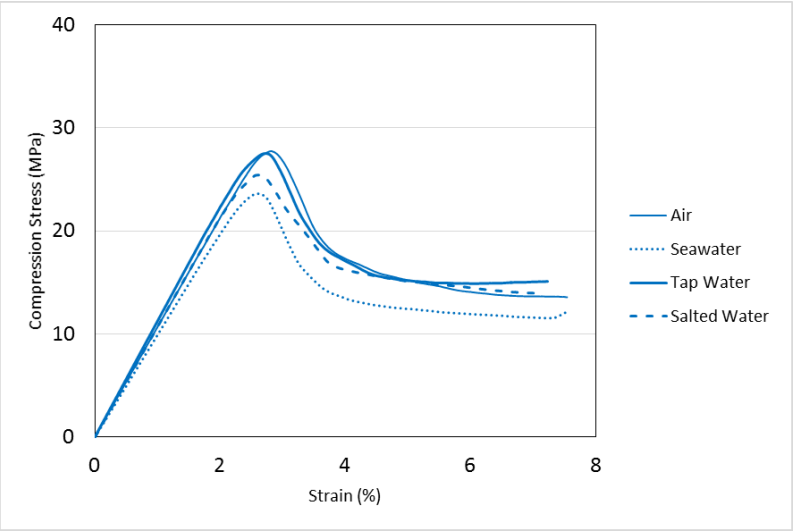

Figure 3. 43- 14 days compressive results of Mixture B in all types of cure

The compressive strength obtained for all specimens was below 30 MPa, as presented in Table 3.9. The specimens cured in air showed the maximum compressive stress, and the minimum was achieved with the specimens cured in seawater.

Table 3. 8- Compressive strengths of Mixture B for all curing environments at 14 days.

Cure	Specimen	Compressive strength (MPa)	Average (MPa)	Standard Deviation	Coefficient of Variation
Air	Mb_14	25,34	27,90	1,86	7
	Mb_15	29,69			
	Mb_16	28,68			
Seawater	Mb_18	24,14	23,90	0,62	3
	Mb_20	23,05			
	Mb_21	24,52			
Tap Water	Mb_23	29,31	27,63	1,52	5
	Mb_24	25,63			
	Mb_26	27,94			
Salted Water	Mb_27	24,66	26,56	1,43	5
	Mb_28	28,11			
	Mb_29	26,90			

The nominal elastic modulus was calculated using the same procedure explained in section 3.2.1. The lower value of elastic modulus was obtained when Mixture B was cured in seawater.

Table 3. 9 - Elastic modulus of Mixture B specimens (14 days)

Cure	Specimem	Elasticity Modulus (GPa)	Average (GPa)	Standard Desviation	Coefficient of Variation
Air	Mb_14	9,86	10,68	0,58	5
	Mb_15	11,05			
	Mb_16	11,13			
Seawater	Mb_18	9,89	9,92	0,10	1
	Mb_20	10,07			
	Mb_21	9,82			
Tap Water	Mb_23	11,50	11,25	0,24	2
	Mb_24	10,93			
	Mb_26	11,32			
Salted Water	Mb_27	9,24	10,73	1,08	10
	Mb_28	11,22			
	Mb_29	11,73			

28 days

Figure 3.48 represents the compression test results obtained for Mixture B considering each type of curing 28 days after casting.

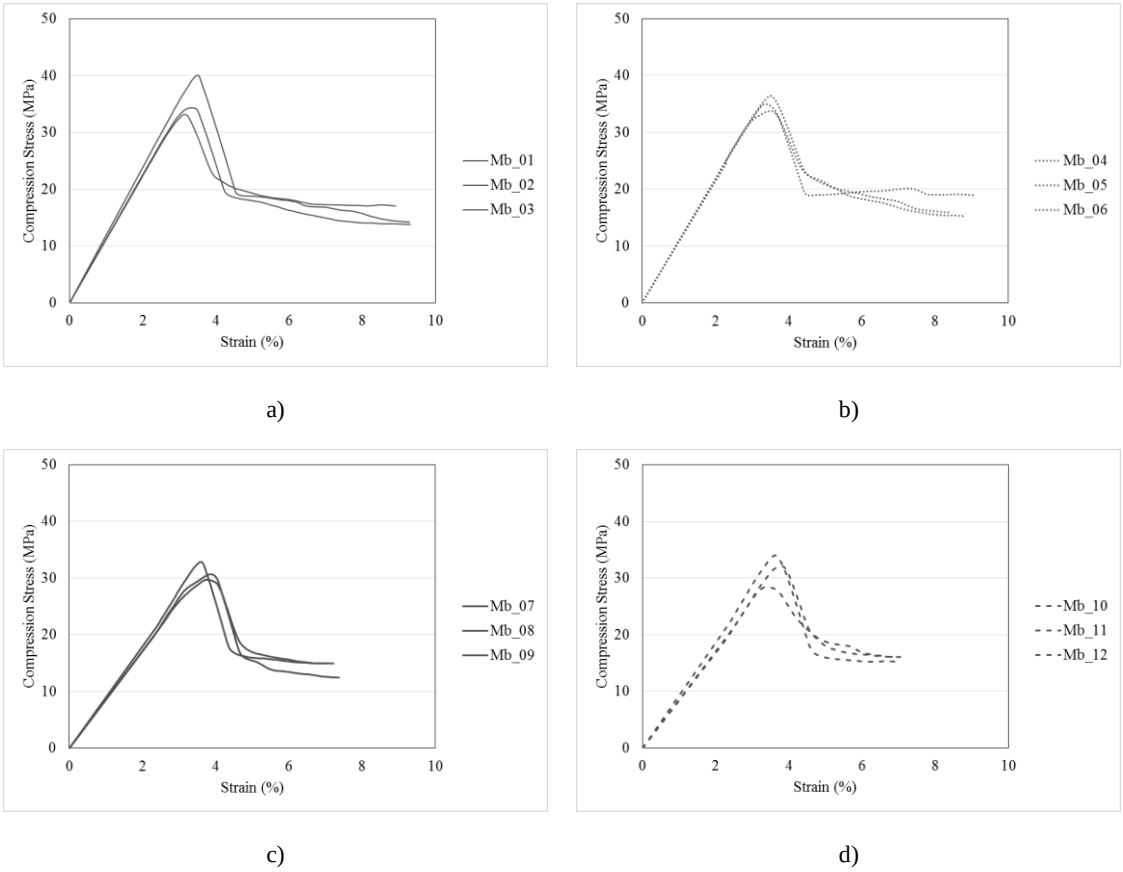

Figure 3. 44- Compressive results of Mixture B, 28 days: a) cured in air; b) cured in seawater; c) cured in tap water; d) cured in salted water.

The compressive response of Mixture B is slightly different depending on the type of curing considered. The elastic phase of the response, in some cases, show different inclinations, as observed in Figure 3.45.

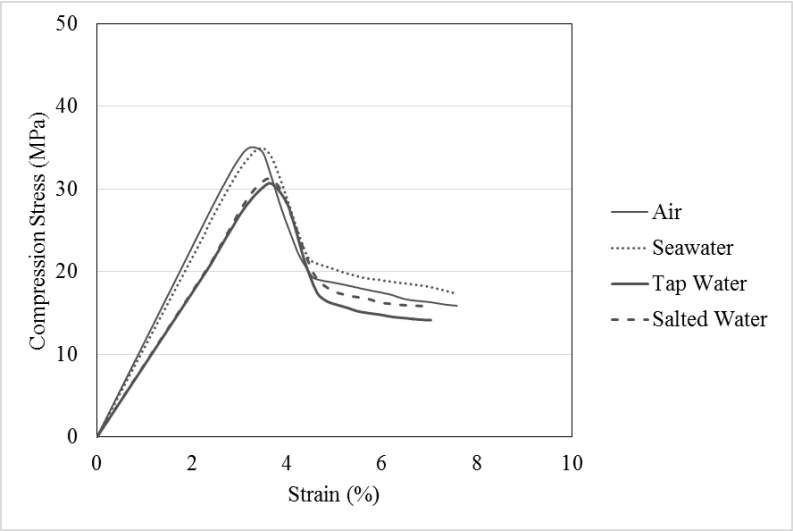

Figure 3. 45- 28 days compressive test results of Mixture B for all types of curing.

The compressive strengths obtained are shown in Table 3.11, ranging between 30 and 40 MPa, and the strains at peak compressive stress varied between 3 % and 4 %. The specimens cured in water and salted water showed the lowest compressive strengths.

Table 3. 10- Compressive strengths of Mixture B for all curing environments at 28 days.

Cure	Specimen	Compressive strength (MPa)	Average (MPa)	Standard Deviation	Coefficient of Variation
Air	Mb_01	40,04	35,85	3,00	8
	Mb_02	33,17			
	Mb_03	34,33			
Seawater	Mb_04	33,77	35,54	1,25	4
	Mb_05	36,43			
	Mb_06	36,43			
Tap Water	Mb_07	29,68	31,06	1,32	4
	Mb_08	30,66			
	Mb_09	32,84			
Salted Water	Mb_10	28,41	31,50	2,33	7
	Mb_11	34,05			
	Mb_12	32,02			

The values of the nominal elastic modulus were calculated for all specimens tested and are presented in Table 3.12.

Table 3. 11- Elastic modulus of Mixture B specimens (28 days)

Cure	Specimen	Elasticity Modulus (GPa)	Average (GPa)	Standard Desviation	Coefficient of Variation
Air	Mb_01	11,93	11,46	0,34	3
	Mb_02	11,16			
	Mb_03	11,29			
Seawater	Mb_04	10,89	10,82	0,10	1
	Mb_05	10,68			
	Mb_06	10,91			
Tap Water	Mb_07	8,55	8,71	0,20	2
	Mb_08	8,58			
	Mb_09	8,99			
Salted Water	Mb_10	8,42	8,76	0,40	5
	Mb_11	9,32			
	Mb_12	8,53			

14 vs 28 days

Figure 3.46 shows the comparison between the compression test results obtained for the different curing ages.

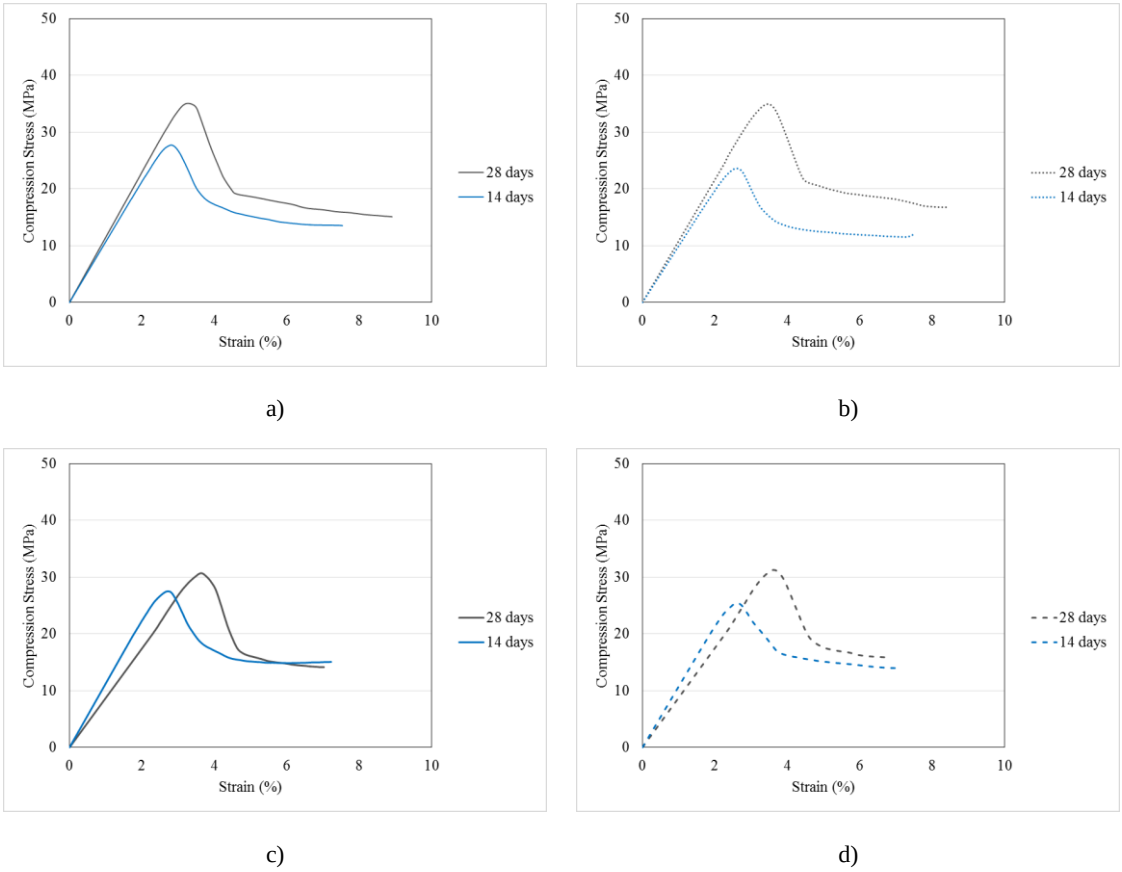

Figure 3. 46 – 14 days versus 28 days compression test results for Mixture B: a) cured in air; b) cured in seawater; c) cured in tap water; d) cured in salted water.

As expected, the 28 days results showed higher compression strengths when compared with the 14 days results. However they have different behaviours. The specimens cured in air and seawater showed a significant increase in compression strength, which was not so evident for the other types of curing.

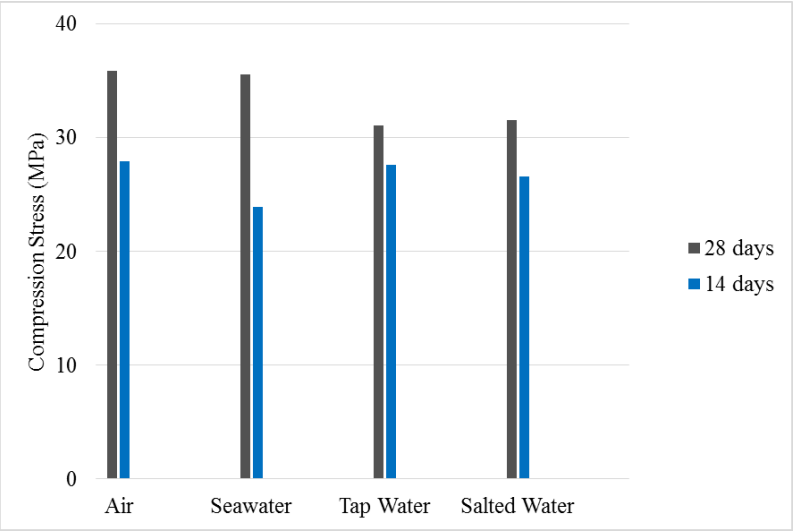

Figure 3. 47- Compressive strength results obtained at different curing ages.

Unexpectedly, the specimens cured in tap water and salted water showed a reduction in the nominal elasticity modulus at 28 days, as shown in Figure 3.48.

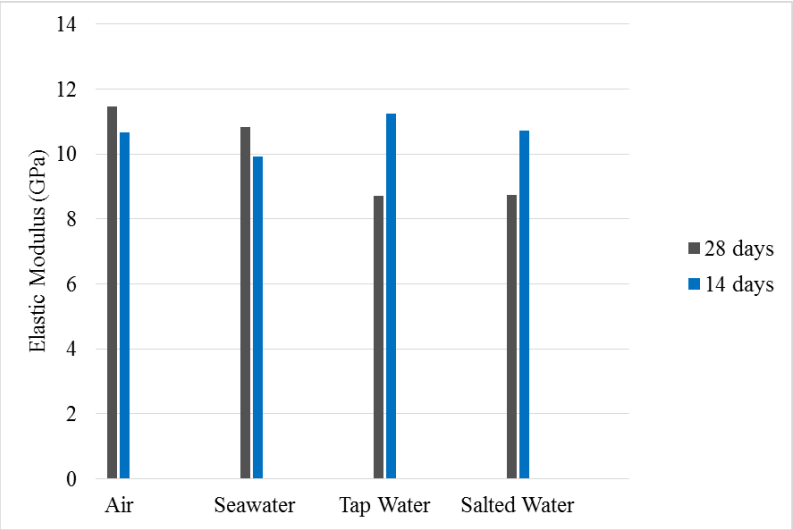

Figure 3. 48- Comparison between the elasticity modulus obtained at different curing ages.

When the mixture is tested at 14 days old, the specimens cured in air and tap water show higher results. The 28 days old specimens showed higher compression stress when cured in air and seawater.

3.3.2 The Single Crack Tension Test (SCTT)

The setup and procedures used to test the Mixture B were the same as explained in section 3.2.2.

14 days

The results of Single Crack Tension Test (SCTT) for specimens 14 days old are represented in Figure 3.49. The 3 specimens that were cured in air showed different tensile results. However those specimens were the ones reaching the lowest crack mouth opening displacements.

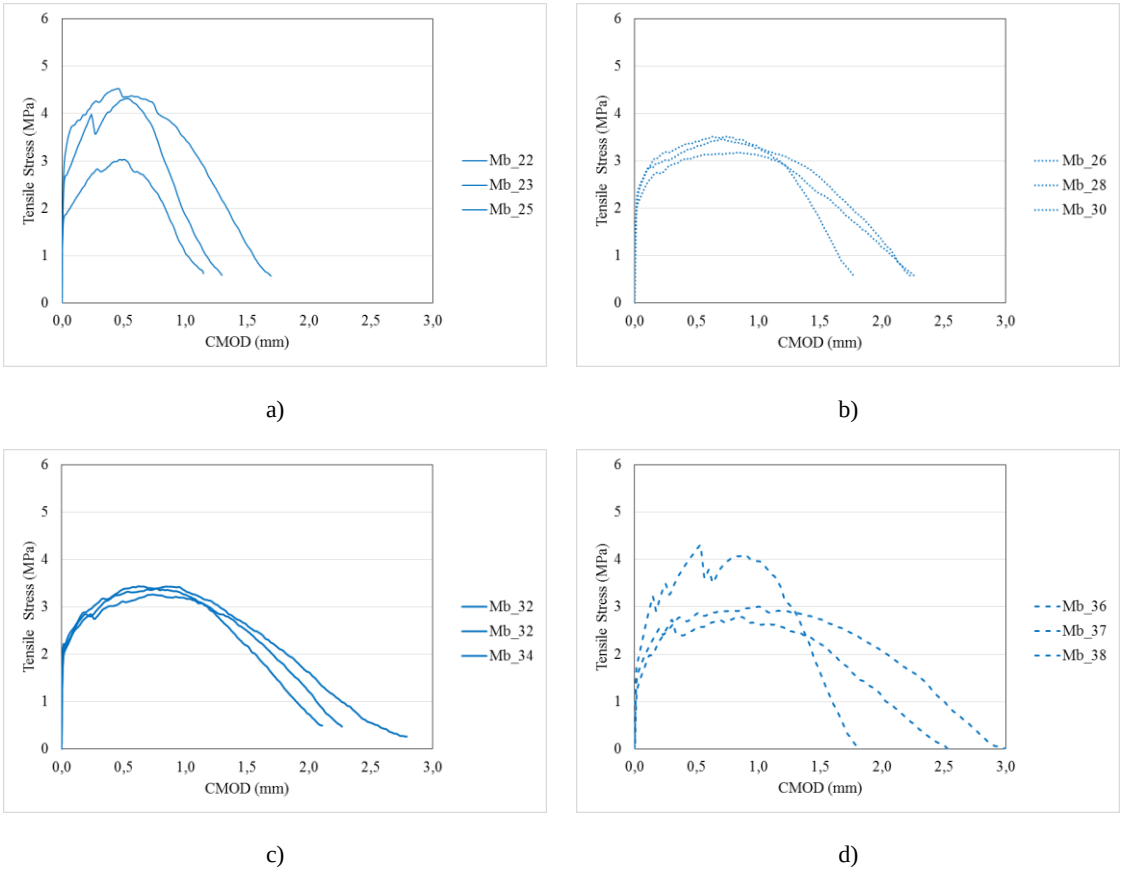

Figure 3. 49- SCTT results of Mixture B after 14 days of curing: a) in air; b) in seawater; c) in tap water; d) in salted water.

Figure 3.50 shows the average curves for all curing environments. The procedure used to calculate the average curve was explained in section 3.2.2.

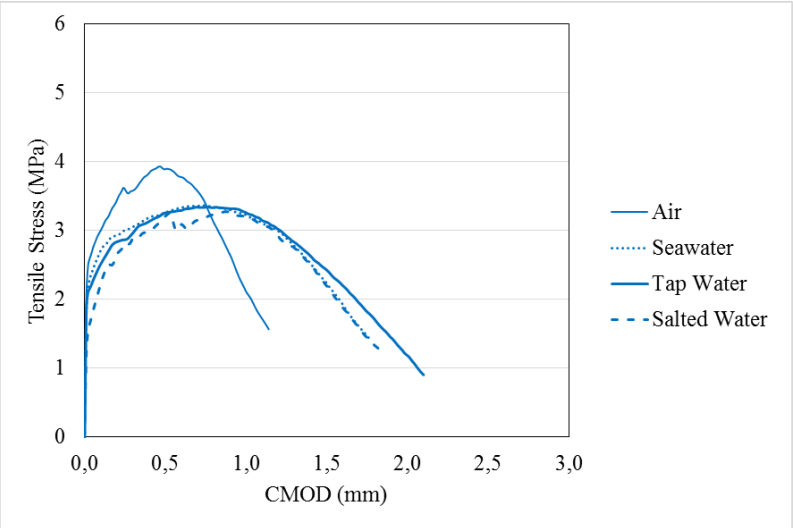

Figure 3. 50- SCTT results of Mixture B (14 days)

The specimens that reached higher tensile stresses were the ones cured in air. The other types of curing resulted in similar tensile responses.

28 days

The results obtained for the specimens cured for 28 days are represented in Figure 3.51.

As before, all specimens tested showed a high stiffness phase until the crack opens. The tensile stress that causes the matrix to reach is maximum tensile stress ranged between approximately 2 MPa and 3 MPa.

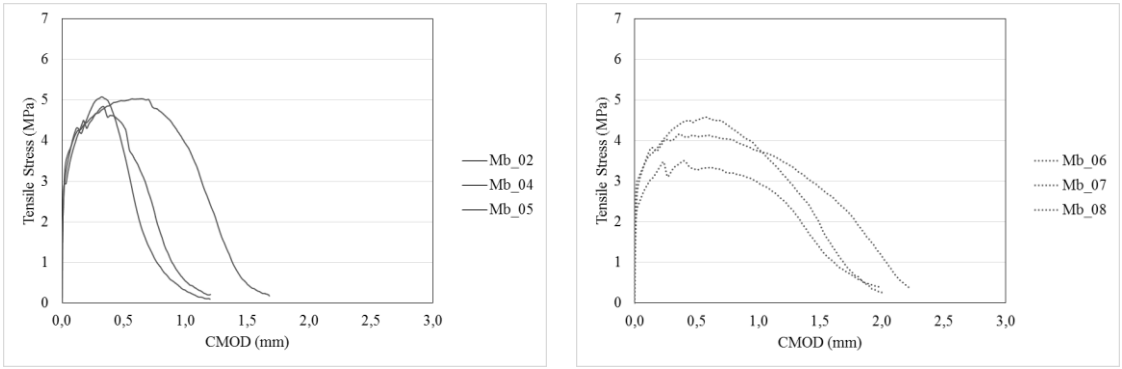

a) b)

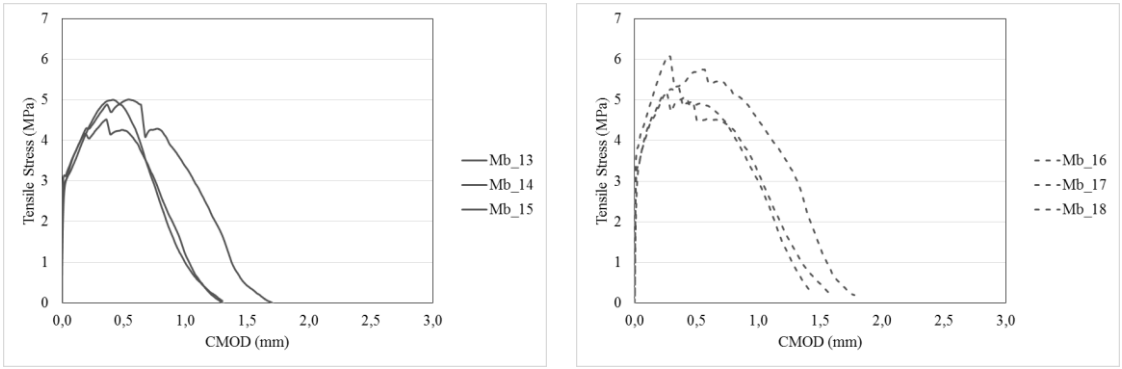

c) d)

Figure 3. 51- SCTT results for Mixture B after 28 days of curing: a) in air; b) in seawater; c) in tap water; d) in salted water.

The average curves obtained for all types of curing are represented in Figure3.58.

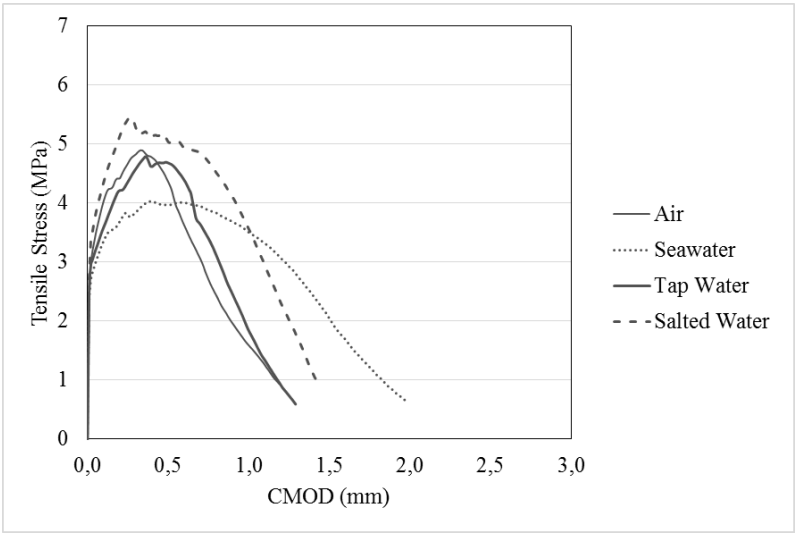

Figure 3. 52- SCTT results of Mixture B (28 days)

14 vs 28 days

The SCTT test results obtained for both curing ages are compared in Figure 3.53.

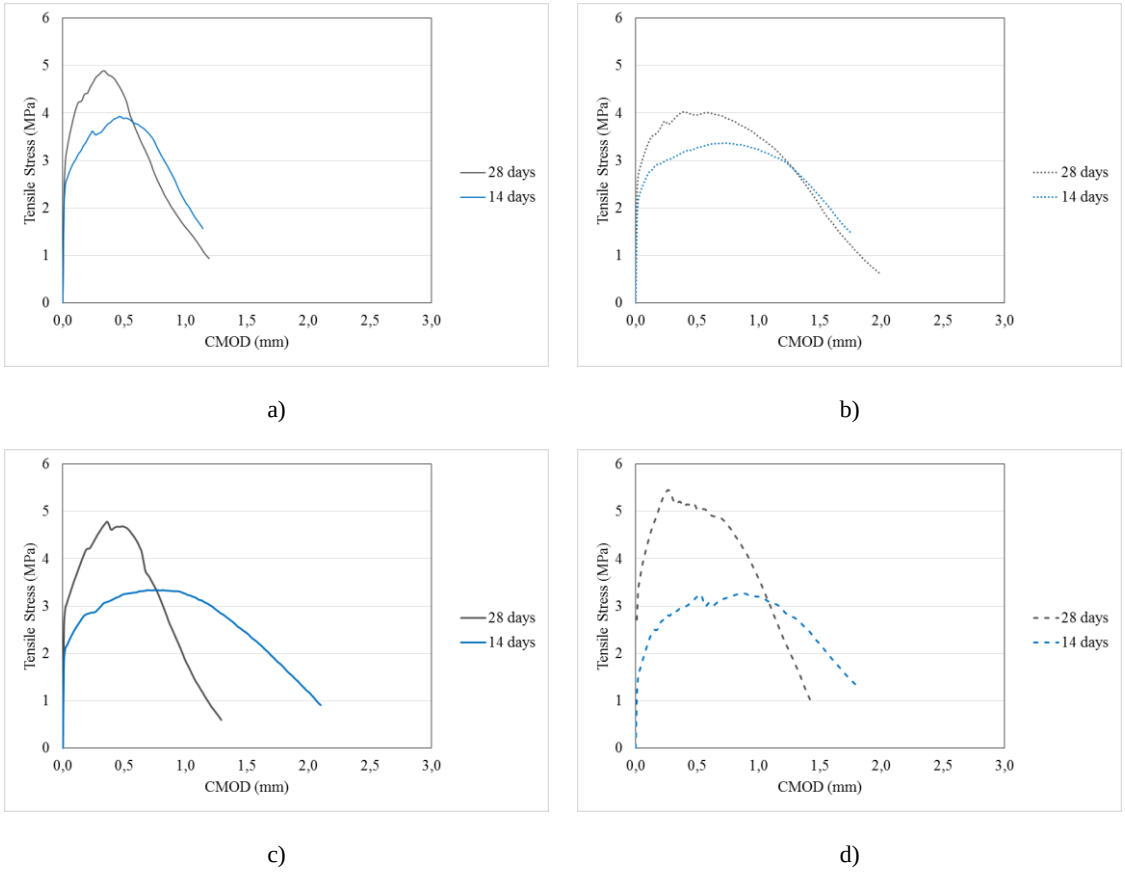

Figure 3. 53- 14 days versus 28 days SCTT test results of Mixture B: s) cured in air; b) cured in seawater; c) cured in tap water; d) cured in salted water.

The single crack tension test results revealed that higher tensile stresses were reached when testing occurred after 28 days of curing. With the increase of the peak tensile stresses reached the CMOD decreases. That fact occurs because, after 28 days of curing, the matrices are more mature.

3.3.3 Tensile Stress-Strain Behaviour

The procedure and methods used to perform this test was explained in section 3.2.2.

14 days

Three specimens were tested for each type of curing. The results obtained after 14 days of curing are presented in Figure 3.54.

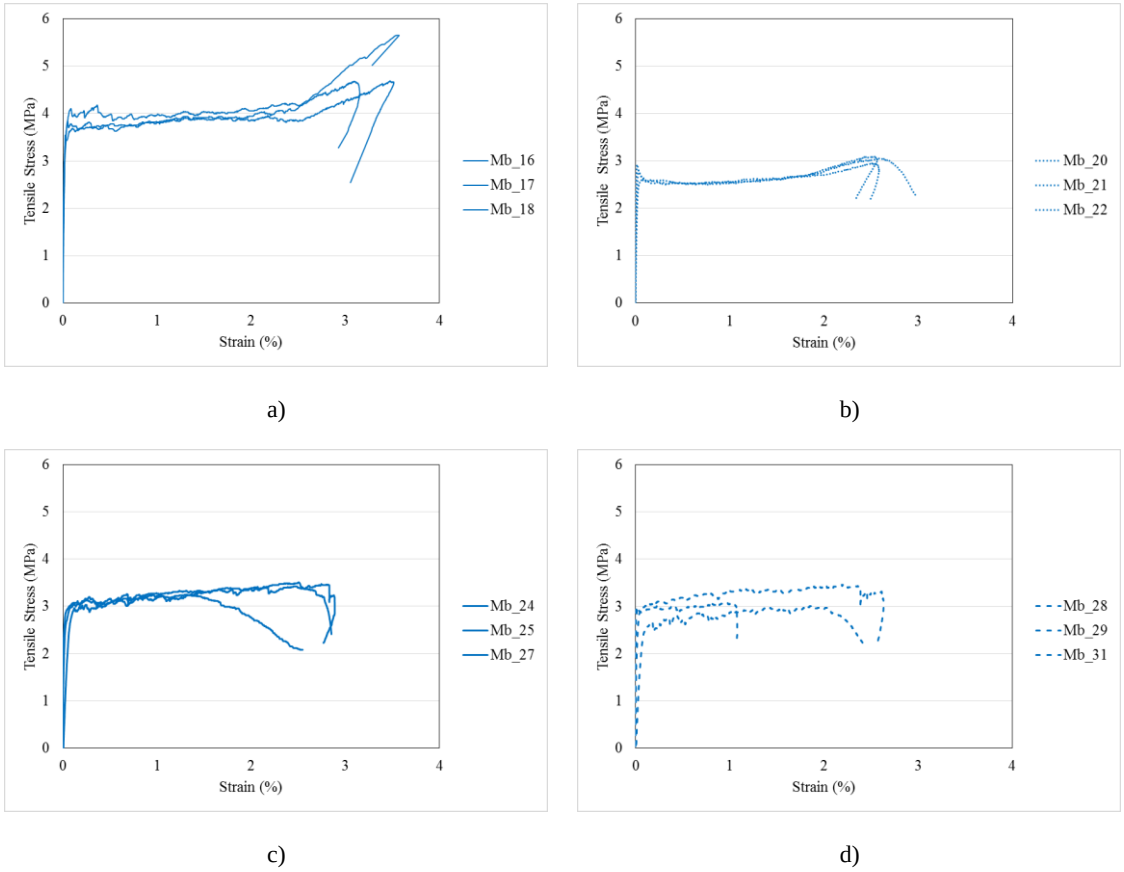

Figure 3. 54- Tensile results of Mixture B, 14 days: a) cured in air; b) cured in seawater; c) cured in water; d) cured in salted water.

As before, mixture B shows the typical tensile stress-strain behaviour of ECC materials. The main results obtained for each specimen are presented in Table 3.13. The first cracking strain ranged between 0.03-0.16%. In this mixture, the strain hardening phase shows less stress local peaks, which means that the cracks formed are very tight. The specimens that were cured in air have reached very high tensile stresses before failure.

Table 3. 12- Tensile results of Mixture B for all curing environments at 14 days.

Curing	Specimen	σc (Mpa)	Ɛc (%)	σm (Mpa)	Ɛm (%)
Air	Mb_16	3,69	0,10	5,65	3,57
	Mb_17	3,85	0,05	4,69	3,47
	Mb_18	4,08	0,08	4,68	3,10
Seawater	Mb_20	2,92	0,02	2,94	2,50
	Mb_21	2,60	0,08	3,08	2,45
	Mb_22	2,80	0,03	3,05	2,59
Tap Water	Mb_24	3,08	0,11	3,51	2,51
	Mb_25	3,11	0,16	3,28	0,99
	Mb_27	2,96	0,12	3,42	2,49
Salted Water	Mb_28	2,96	0,01	3,07	0,98
	Mb_29	3,05	0,13	3,45	2,20
	Mb_31	2,60	0,14	3,00	1,86

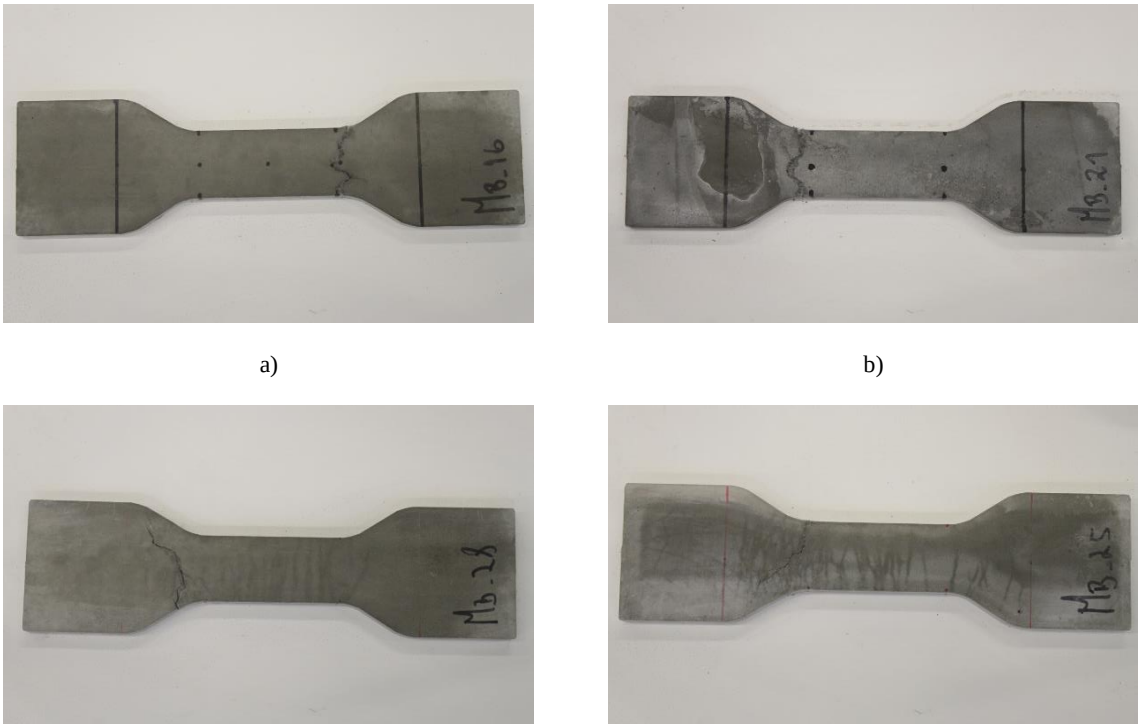

a) b)

c) d)

Figure 3. 55- Mixture B dogbone specimens tested after 14 days of curing: a) in air; b) in seawater; c) in tap water; d) in salted water.

The average curves for each type of curing are represented in Figure 3.56. The average curve was calculate with the same procedure explained in section 3.2.3. As shown, the curing environment significantly influenced the tensile responses obtained.

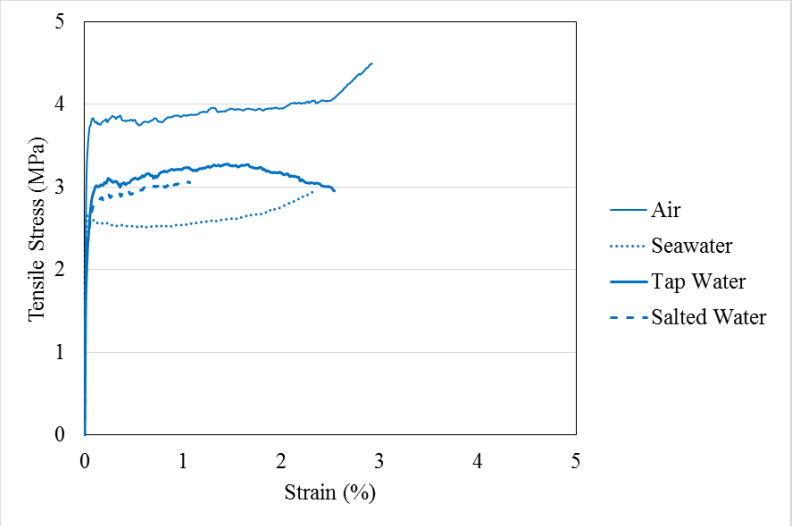

Figure 3. 56- Average tensile results of Mixture B in all environments (14 days)

The specimens cured in air reached the highest tensile stresses, in contrast with the specimens cured in seawater that reached the lowest tensile stresses. The salted water curing led to the lowest ultimate strains.

28 days

As before, three specimens were tested for each type of curing. The results obtained after 28 days of curing are represented in Figure 3.57.

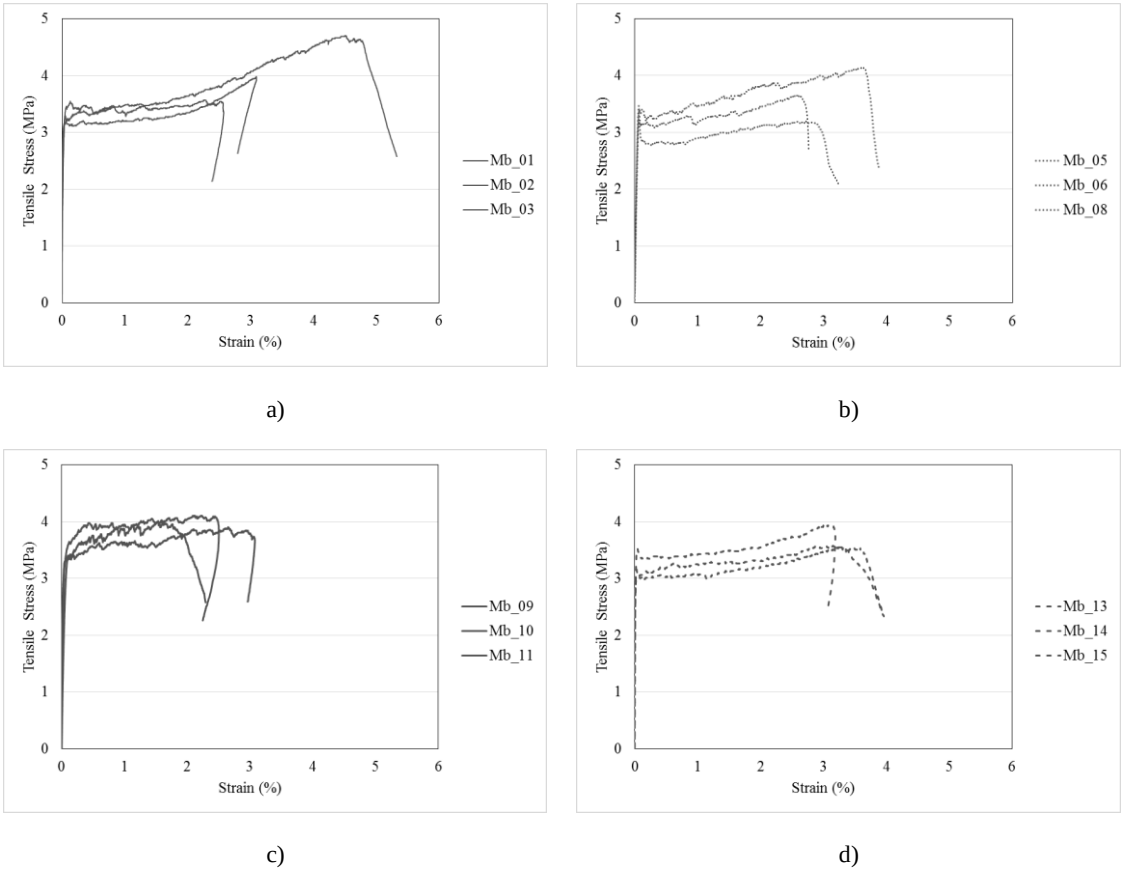

Figure 3. 57- Tensile test results for Mixture B after 28 days of curing: a) in air; b) in seawater; c) in tap water; d) in salted water.

All the specimens showed the typical tensile stress-strain behaviour of ECC. The maximum tensile stress ranged, for all types of curing, between 3 and 4 MPa. The specimens cured in air reached higher ultimate strains. The main results are presented in Table 3.14.

Table 3. 13 – Tensile results of Mixture B for all curing environments at 28 days.

Curing	Specimen	σc (Mpa)	Ɛc (%)	σm (Mpa)	Ɛm (%)
Air	Mb_01	3,16	0,03	3,57	2,29
	Mb_02	3,43	0,06	4,70	4,52
	Mb_03	3,29	0,06	3,98	3,09
Seawater	Mb_05	3,22	0,06	3,22	0,06
	Mb_06	3,46	0,07	3,65	2,60
	Mb_08	3,40	0,07	4,13	3,64
Tap Water	Mb_09	3,58	0,10	4,10	2,24
	Mb_10	3,27	0,04	3,91	2,65
	Mb_11	3,36	0,10	3,99	1,53
Salted Water	Mb_13	3,16	0,03	3,54	3,22
	Mb_14	3,50	0,05	3,93	3,11
	Mb_15	3,12	0,22	3,58	3,19

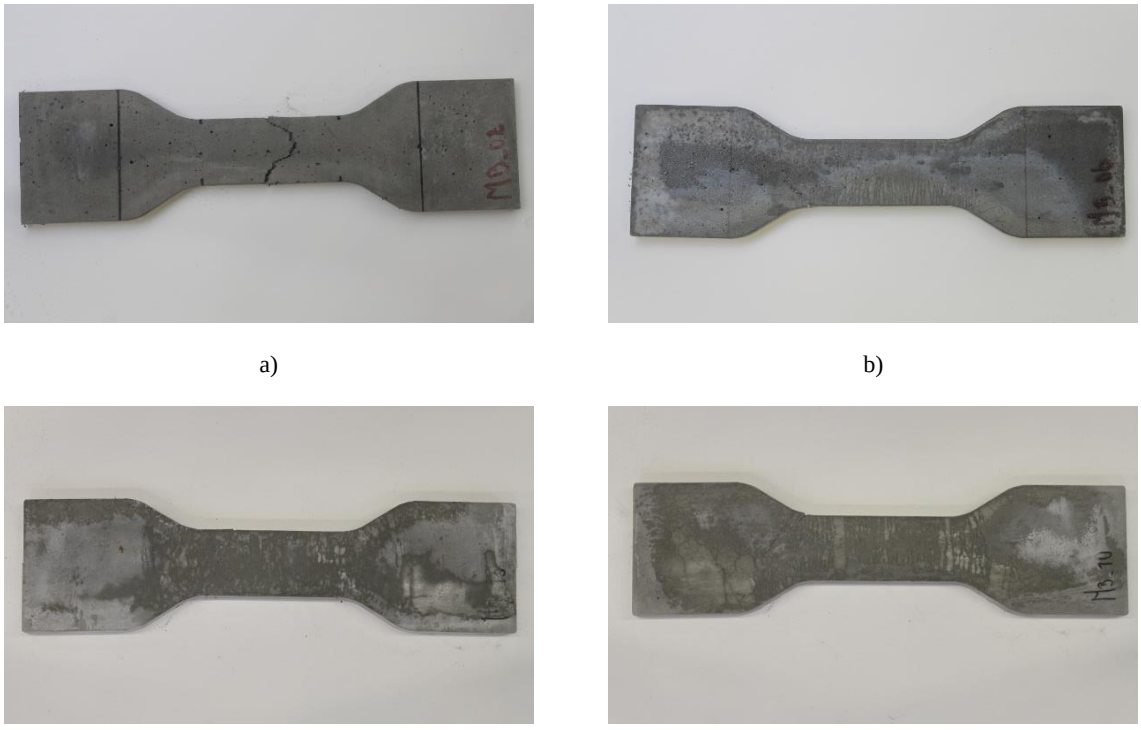

a) b)

c) d)

Figure 3. 58- 28 days Mixture B dogbone specimens after the test: a) cured in air; b) cured in seawater; c) cured in water; d) cured in salted water

Figure 3.59 represents the average tensile stress-strain curves for all types of curing environments. The average curves were calculated following the same procedure explained in section 3.2.3. The higher tensile stress is achieved by the specimens that were cured in water.

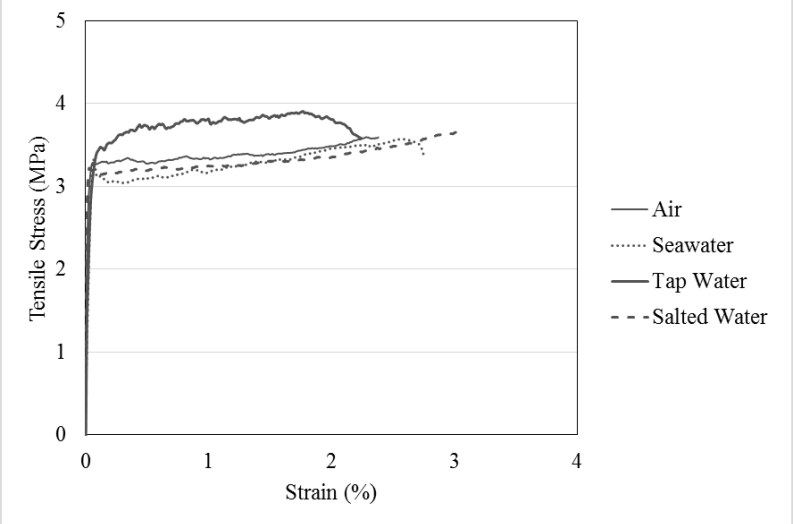

Figure 3. 59- Average tensile results of Mixture B in all environments (28 days)

For all the types of curing, the tensile responses start with high stiffness until the strain reaches approximately 0.07 %. Then, after the formation of the first crack, the tensile stress continues to increase until the failure is achieved.

14 vs 28 days

In this study, 2 different curing ages of each mixture were tested. The comparison between the results obtained for the two distinct ages are presented in Figure 3.60.

In Figure 3.60 (a) it is possible to confirm that the specimens tested at 14 days old reach higher tensile stresses. In contrast, for all the other types of curing the opposite occurs. The expected result would be a consistent increase of the tensile stresses reached with the increase of the curing age.

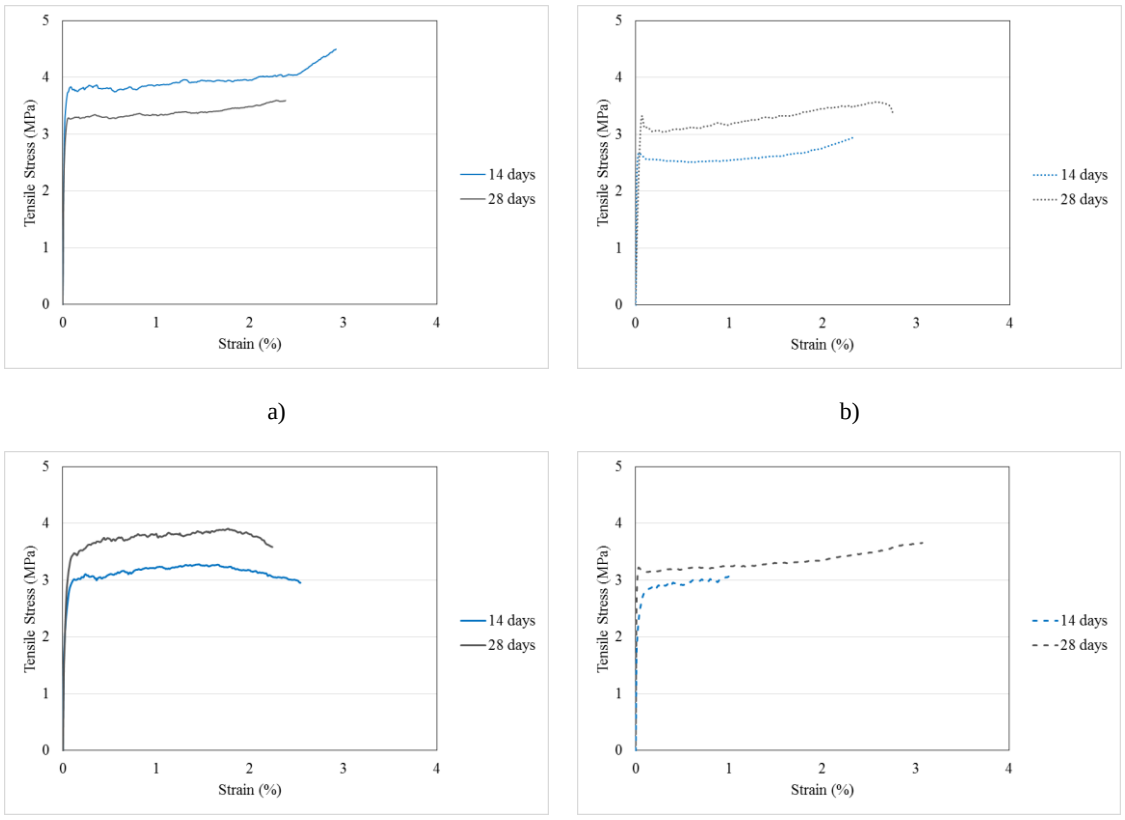

Figure 3. 60- 14days versus 28 days tensile test results for Mixture B: a) cured in air; b) cured in seawater; c) cured in tap water; d) cured in salted water.

This mixture, which is made with seawater, has one particularity: the cracks that appear in the strain hardening phase have a width that is significantly smaller than usual, almost invisible until failure is reached.

3.4 Mixture C

The Mixture C was prepared using salted water, as previously mentioned. Compression, single crack tension and direct tension tests were carried out to characterize the mixture mechanical behaviour.

3.4.1 Compressive behaviour

The setup and procedure used to test the Mixture C was the same explained in section 3.2.1.

14 days

The results obtain in the 3 specimens tested for each different environment are represented in Figure 3.61. The peak strain varied between a minimum of 3% and a maximum of 4%.

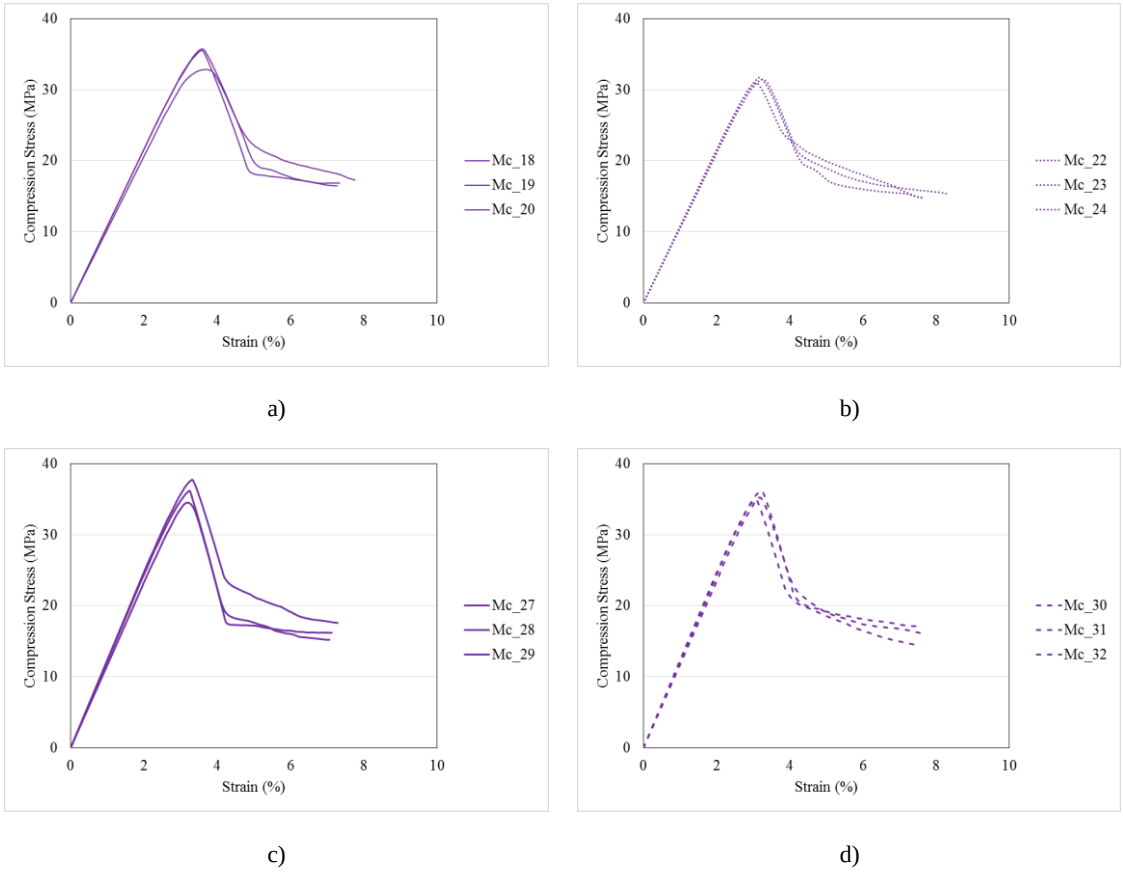

Figure 3. 61- Compressive results of Mixture C, 14 days: a) cured in air; b) cured in seawater; c) cured in tap water; d) cured in salted water.

The maximum compression stress, in all cures, range between 30 and 40 MPa. All the specimens exhibited multiple cracks that started to appear before the maximum compressive stress was reached. To compare the results obtained from curing in the different environments it was necessary calculate the average curve of the 3 specimens tested for each type of curing. The average curves were calculates using the same procedure explained in section 3.2.1. Figure 3.62 shows the average results for each type of curing.

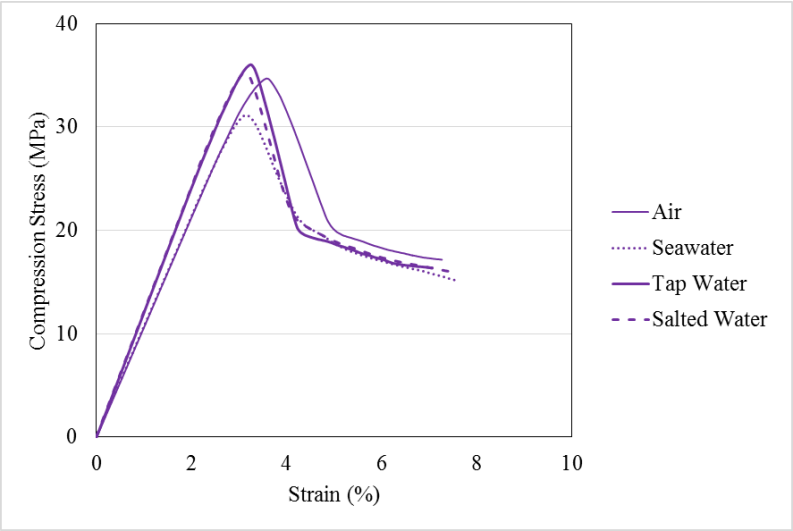

Figure 3. 62- 14 days compressive results of Mixture C in all types of cure

The peak strain ranges between 3% and 4%. The main results obtained are presented in Table 3.15. The dispersion of results among each type of curing was low.

Table 3. 14- Compressive strengths of Mixture C for all curing environments at 14 days.

Cure	Specimen	Compressive strength (MPa)	Average (MPa)	Standard Deviation	Coefficient of Variation
Air	Mc_18	35,56	34,72	1,32	4
	Mc_19	32,86			
	Mc_20	35,74			
Seawater	Mc_22	31,41	31,35	0,31	1
	Mc_23	30,95			
	Mc_24	31,69			
Tap Water	Mc_27	36,21	36,17	1,32	4
	Mc_28	37,77			
	Mc_29	34,54			
Salted Water	Mc_30	35,26	35,48	0,50	1
	Mc_31	36,17			
	Mc_32	35,00			

The lowest compression strengths of Mixture C specimens were obtained when the specimens were cured in seawater.

The nominal elastic modulus was calculated as explained earlier for Mixture A. The results are presented in Table 3.16.

Table 3. 15- Elastic modulus of Mixture C specimens at 14 days.

Cure	Specimen	Elasticity Modulus (GPa)	Average (GPa)	Standard Desviation	Coefficient of Variation
Air	Mc_18	10,81	10,65	0,23	2
	Mc_19	10,32			
	Mc_20	10,81			
Seawater	Mc_22	10,51	10,68	0,13	1
	Mc_23	10,73			
	Mc_24	10,82			
Water	Mc_27	12,23	12,08	0,32	3
	Mc_28	12,38			
	Mc_29	11,63			
Salted Water	Mc_30	11,74	12,08	0,26	2
	Mc_31	12,12			
	Mc_32	12,37			

The nominal elastic modulus ranged between 10 and 12 MPa. This property is related with the elastic phase of the compression response. The curing environments that have led to the highest values of compressive stress, which were tap water and salted water, also led to the higher values of elastic modulus.

28 days

Three specimens for each type of curing environment were tested. The results obtained are represented in Figure 3.63.

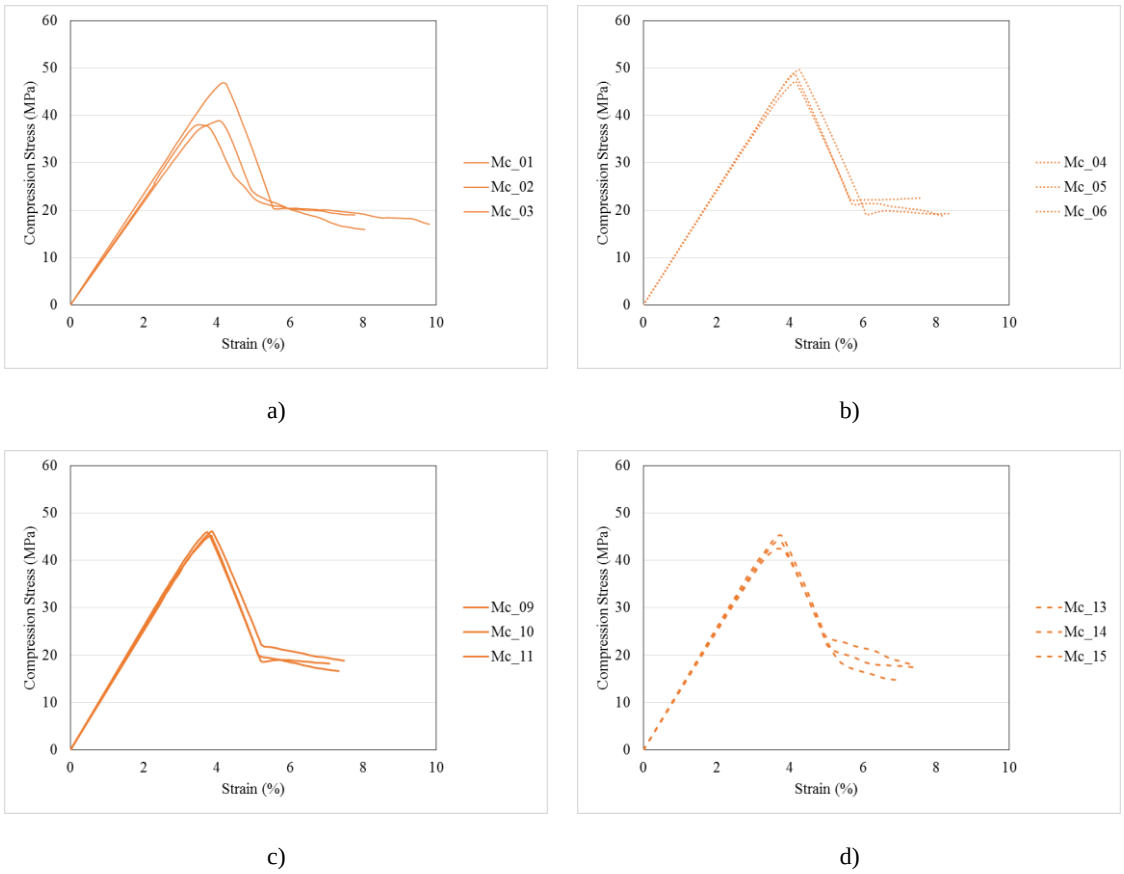

Figure 3. 63- Compressive results of Mixture C, 24 days: a) cured in air; b) cured in seawater; c) cured in water; d) cured in salted water.

Figure 3.64 shows the average results of each type of curing. The elastic phase is mostly similar for all types of curing. The peak strain ranged between 3 and 4 %.

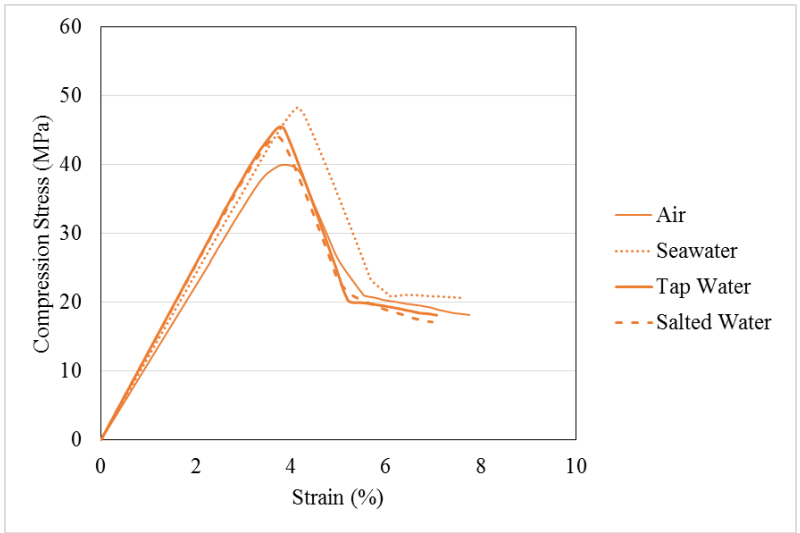

Figure 3. 64- 28 days compressive results of Mixture C in all types of cure

The results obtained are summarized in Table 3.17:

Table 3. 16- Compressive strengths obtained for Mixture C in all curing environments at 28 days.

Cure	Specimen	Compressive strength (MPa)	Average (MPa)	Standard Deviation	Coefficient of Variation
Air	Mc_18	38,90	41,28	3,99	10
	Mc_19	46,90			
	Mc_20	38,05			
Seawater	Mc_22	48,78	48,51	1,01	2
	Mc_23	49,59			
	Mc_24	47,16			
Tap Water	Mc_27	45,30	45,82	0,37	1
	Mc_28	46,17			
	Mc_29	45,99			
Salted Water	Mc_30	45,38	43,97	1,17	3
	Mc_31	44,01			
	Mc_32	42,52			

The type of curing has influenced the compression test results and the seawater curing has led to the highest compressive strength.

The elasticity modulus was calculated as explained earlier for Mixture A. The results obtained are presented in Table 3.18.

Table 3. 17- Elasticity modulus of Mixture C specimens at 28 days.

Cure	Specimen	Elasticity Modulus (GPa)	Average (GPa)	Standard Desviation	Coefficient of Variation
Air	Mc_18	10,84	11,21	0,36	3
	Mc_19	11,70			
	Mc_20	11,09			
Seawater	Mc_22	12,20	12,12	0,08	1
	Mc_23	12,15			
	Mc_24	12,00			
Tap Water	Mc_27	12,75	12,79	0,20	2
	Mc_28	12,57			
	Mc_29	13,05			

Salted Water	Mc_30	12,91	12,71	0,17	1
	Mc_31	12,71			
	Mc_32	12,51			

The maximum elasticity modulus was reached when the specimens were cured in water and the minimum was achieved when the specimens were cured in air.

14 vs 28 days

Figure 3.65 shows the comparison between the compression test results obtained for different curing ages. As expected, the 28 days specimens reached higher compression strengths than the 14 days ones. However, this effect is more pronounced in some cases, such as in the case of seawater curing.

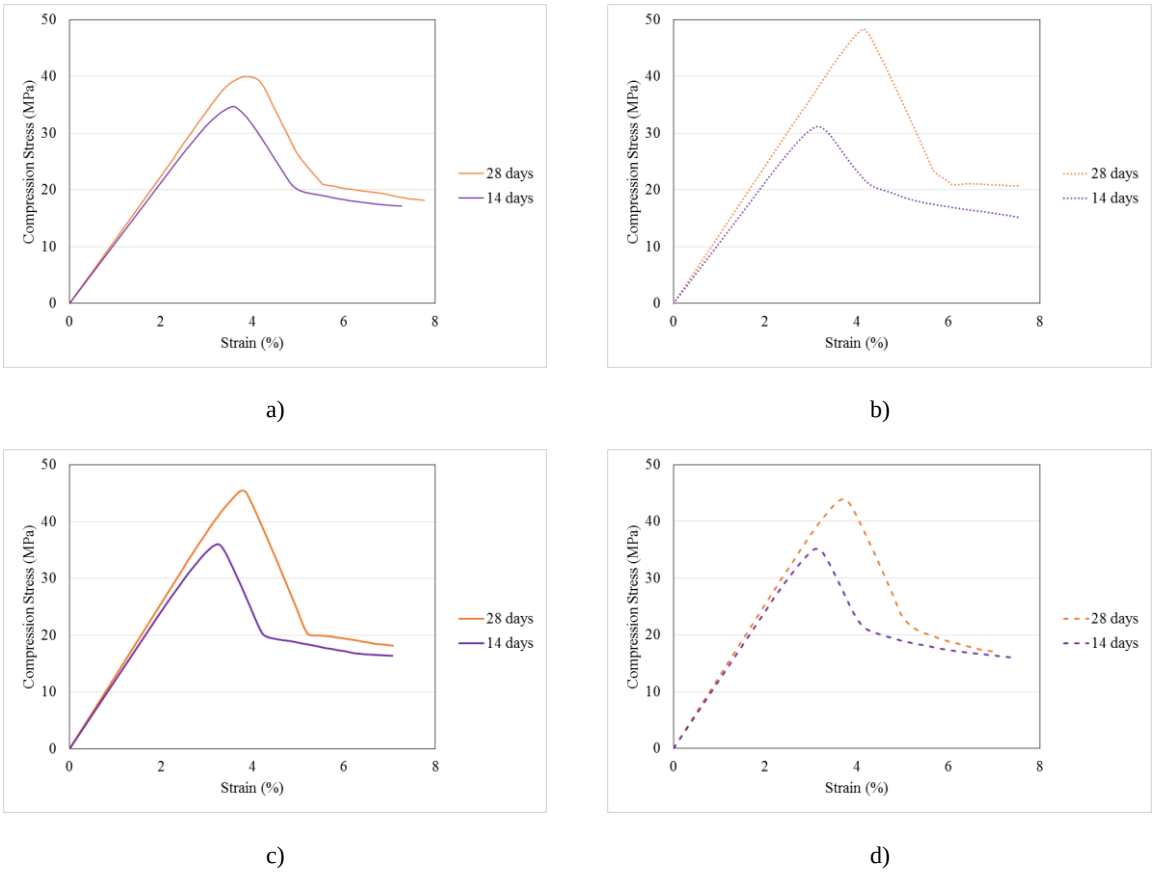

Figure 3. 65- 14 days versus 28 days compression test results for Mixture C: a) cured in air; b) cured in seawater; c) cured in tap water; d) cured in salted water.

Mixture C has shown, for all types of curing, higher compressive strengths at 28 days. The compressive responses are, for both ages and for each curing environment, very similar.

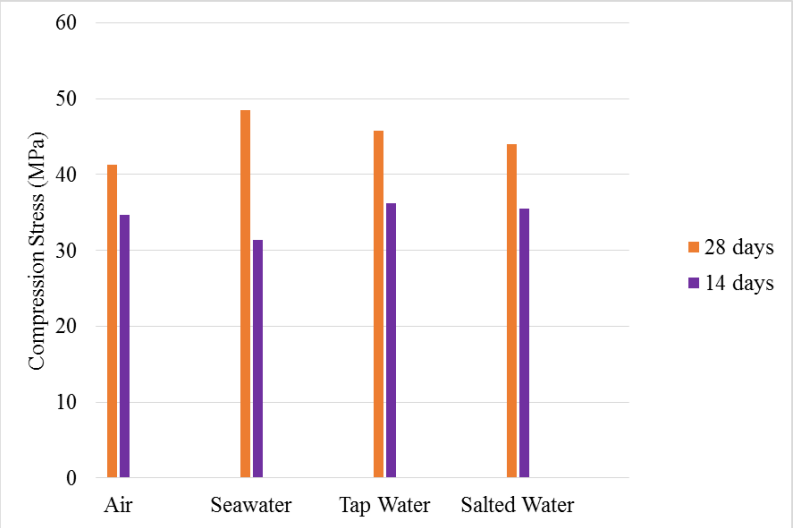

Figure 3. 66- Comparison compressive strength results obtained at different curing ages.

Figure 3.66 compares the compressive strengths obtained for the two curing ages at the four different curing environments. As expected, the compression strength increased when the curing time increased. The seawater curing resulted in the higher increase of compressive strength between curing ages, having also reached the highest results.

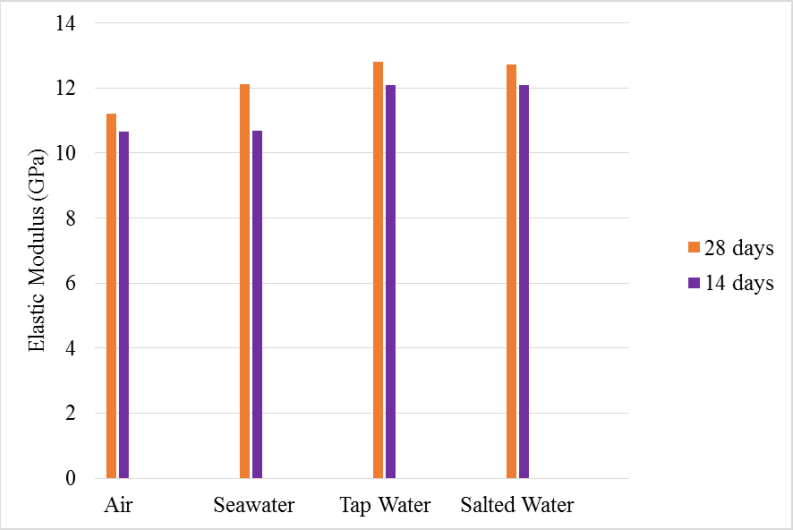

Figure 3. 67- Comparison between the elasticity modulus obtained at different curing ages.

The elasticity modulus results show the same behaviour in both ages. In this case the maximum values, in both ages, were obtained when the specimens were cured in water.

3.4.2 Single Crack Tension Test (SCTT)

The procedure and methods used to perform this test were explained in section 3.2.2.

14 days

The results of the Single Crack Tension Test (SCTT) for specimens with 14 days old are represented in Figure 3.68. Three specimens for each type of curing environment were tested.

The three specimens cured in salted water reached the lowest tensile stresses among all specimens tested.

All the specimens showed a high stiffness phase in the beginning of the testing sequence. After reaching the tensile strength of the matrix, the formation of new cracks was revealed by several drops and pickups of the tensile stress until the peak stress was reached. Since the purpose of this test is to characterise the mechanical tensile response of a single crack, these results mean that the potential of the material to develop multiple cracks is very high and a greater reduction of the effective section at the notch would be necessary.

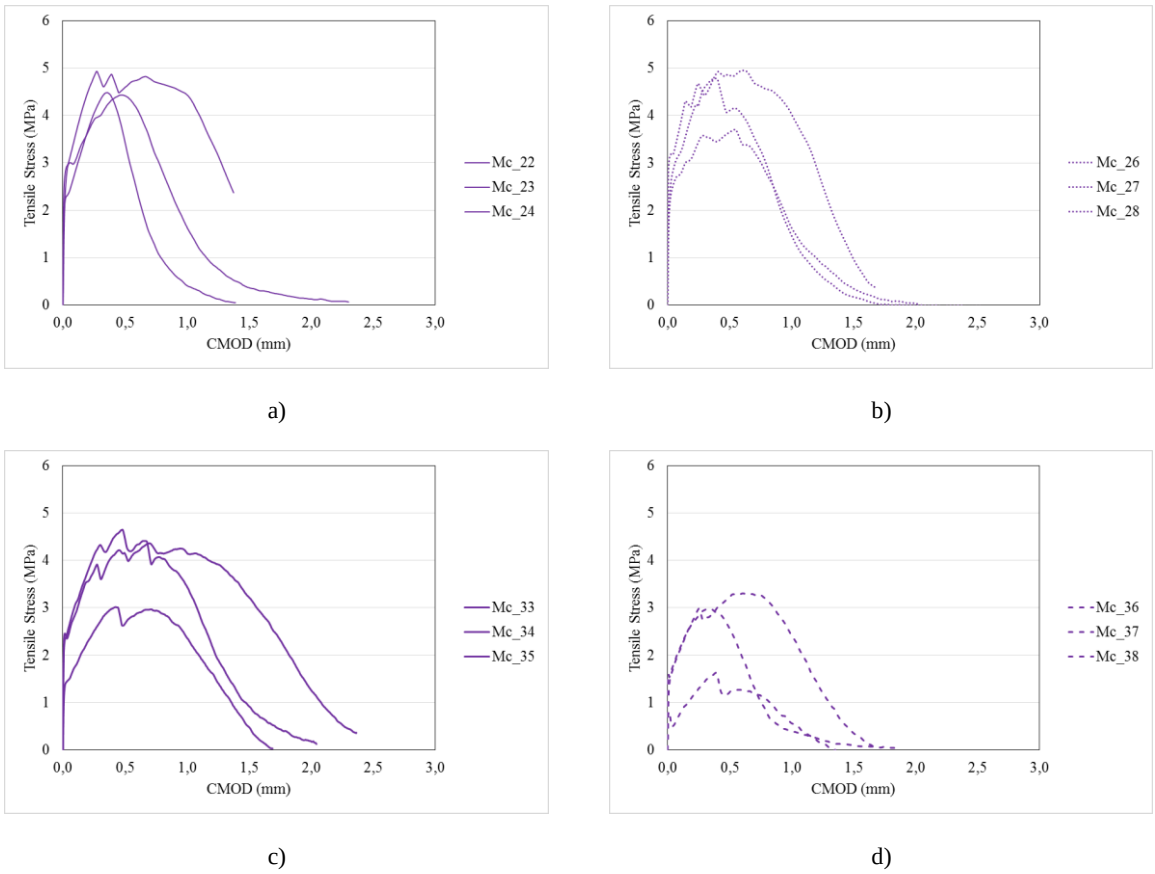

Figure 3.68- SCTT results for Mixture C after 14 days of curing: a) in air; b) in seawater; c) in tap water; d) in salted water.

Figure 3.69 shows the average curve obtained for all curing environments. The procedure used to calculate the average curve was explained in section 3.2.2.

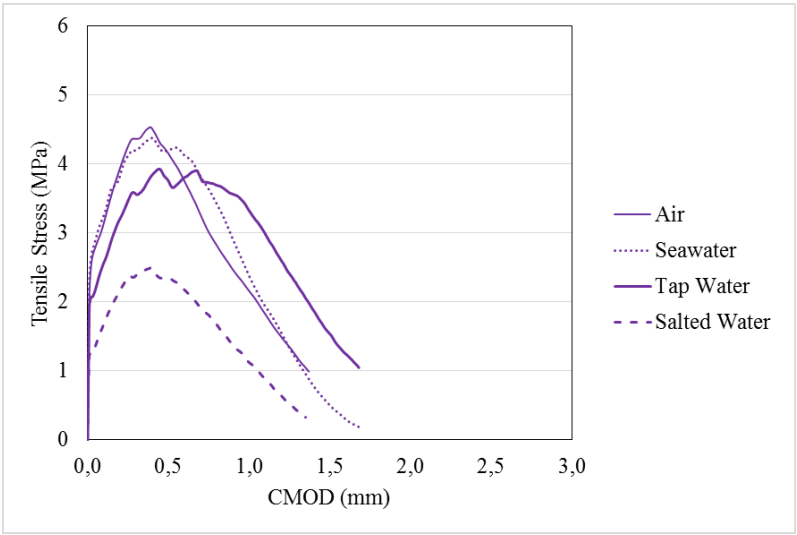

Figure 3. 69- SCTT results of Mixture C (14 days)

In general it becomes evident that the curing in salted water resulted in clearly lower tensile stresses for all crack openings.

28 days

The results of Single Crack Tension Test (SCTT) for specimens 28 days old are represented in Figure 3.70. In all the specimens tested, the results revealed the appearance of more than one crack, according to what has been discussed previously.

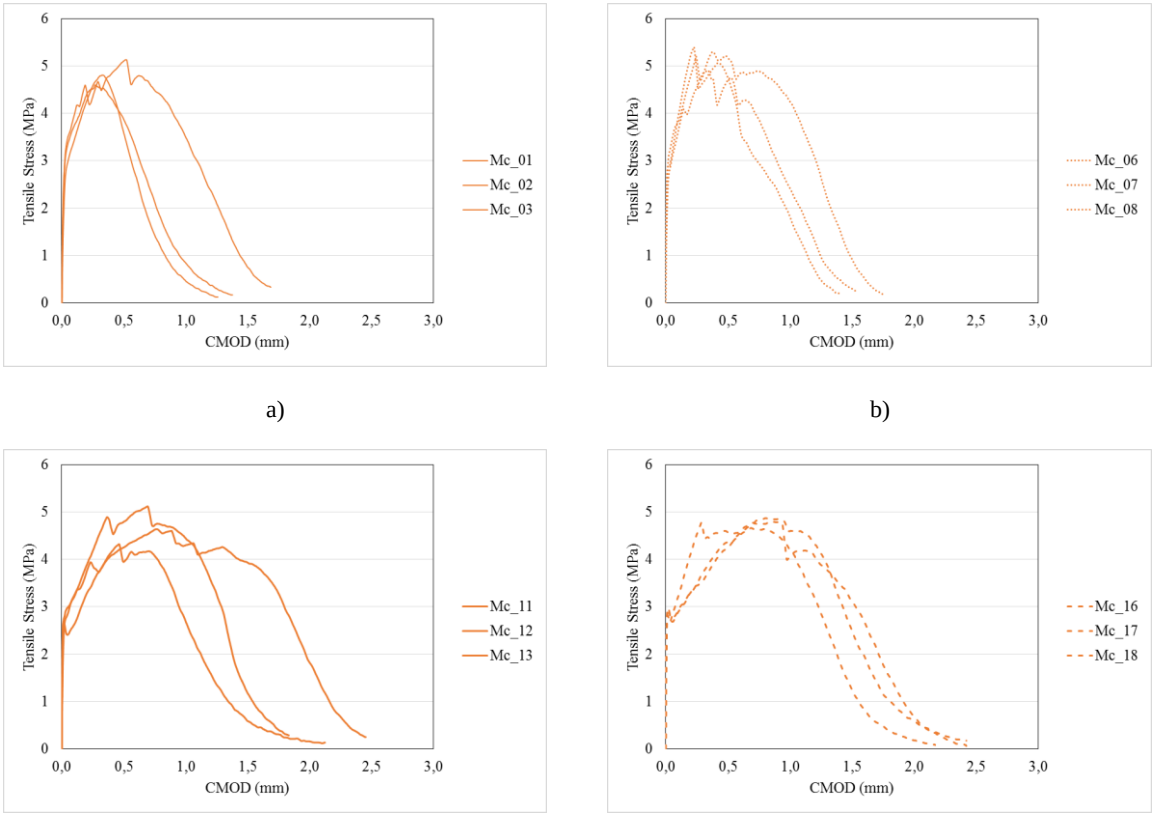

Figure 3. 70- SCTT results of Mixture C, 28 days: a) cured in air; b) cured in water; d) cured in salted water.

The tensile stress – CMOD responses obtained are very similar in the specimens cured in tap water and salted water. The tensile stress that causes the matrix to crack ranged between 2 to 3 MPa.

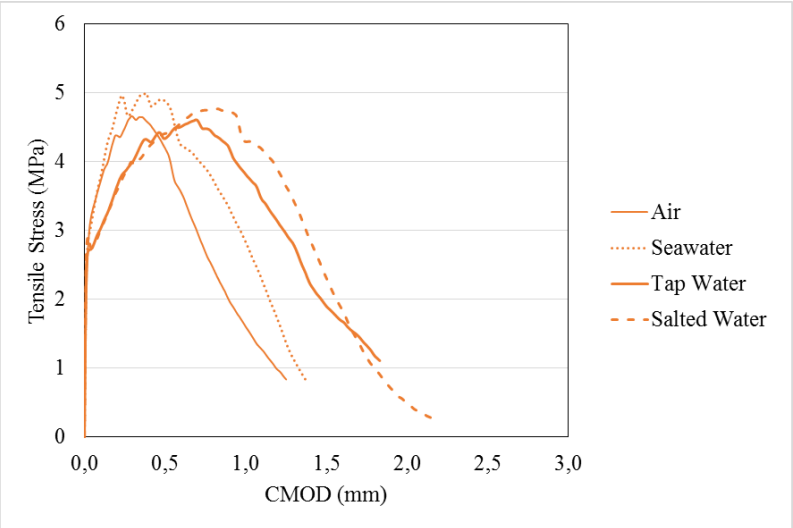

Figure 3. 71- SCTT results of Mixture C (28 days)

Figure 3.71 shows the average results for all types of curing. The procedure used to calculate the average curve was explained in section 3.2.2. The maximum tensile stresses reached for all curing environments ranged between 4 MPa and 5 MPa.

14 vs 28 days

The results obtained for both ages were compared in Figure 3.72. In general the specimens showed similar behaviour for both ages. However, the specimens cured in salted water show a great difference between both ages.

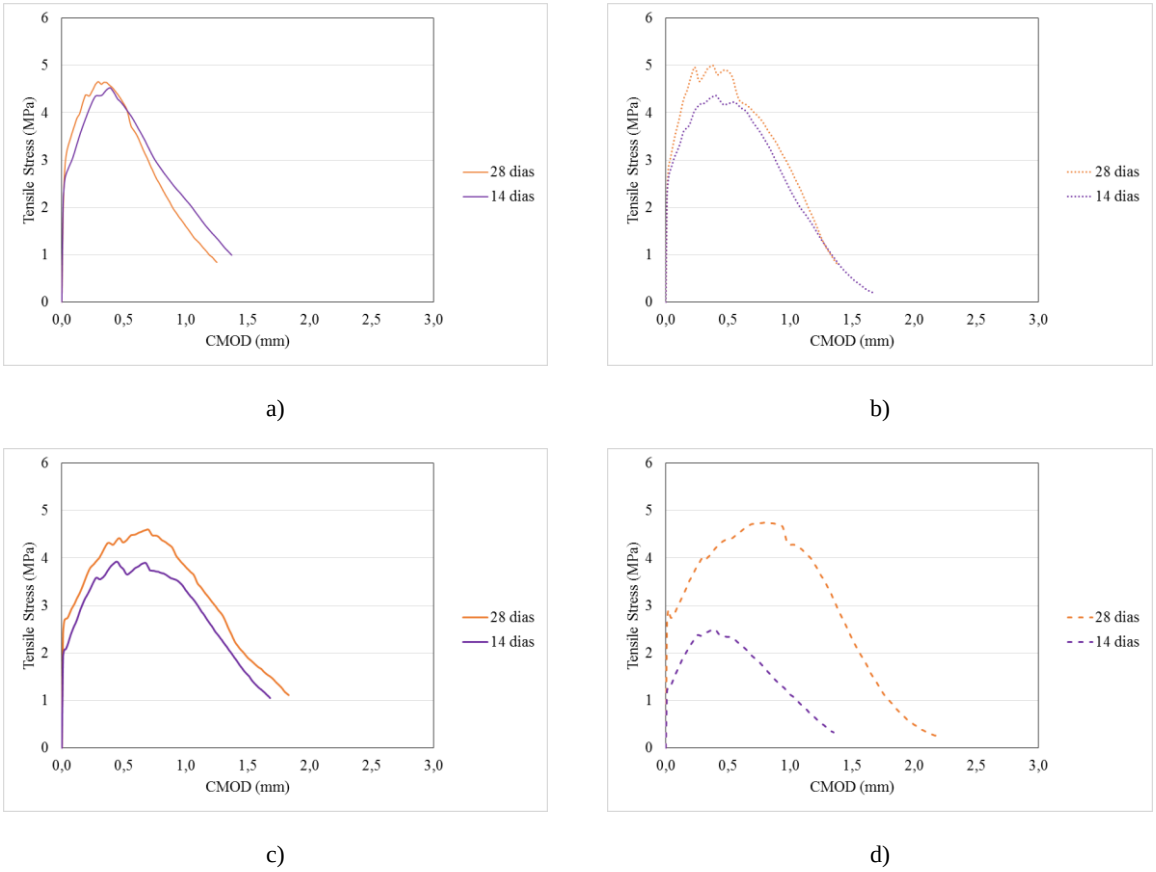

Figure 3. 72- 14 days versus 28 days SCTT results for Mixture C: a) cured in air; b) cured in seawater; c) cured in tap water; d) cured in salted water.

Although the results obtained approximate the expected behaviours, in some cases the specimens still reveal the formation of more than one crack.

3.4.3 Tensile Stress-Strain Behaviour

The procedure and methods used to perform this test were explained in section 3.2.3.

14 days

Three specimens were tested for each type of curing environment. The results obtained are presented in Figure 3.73.

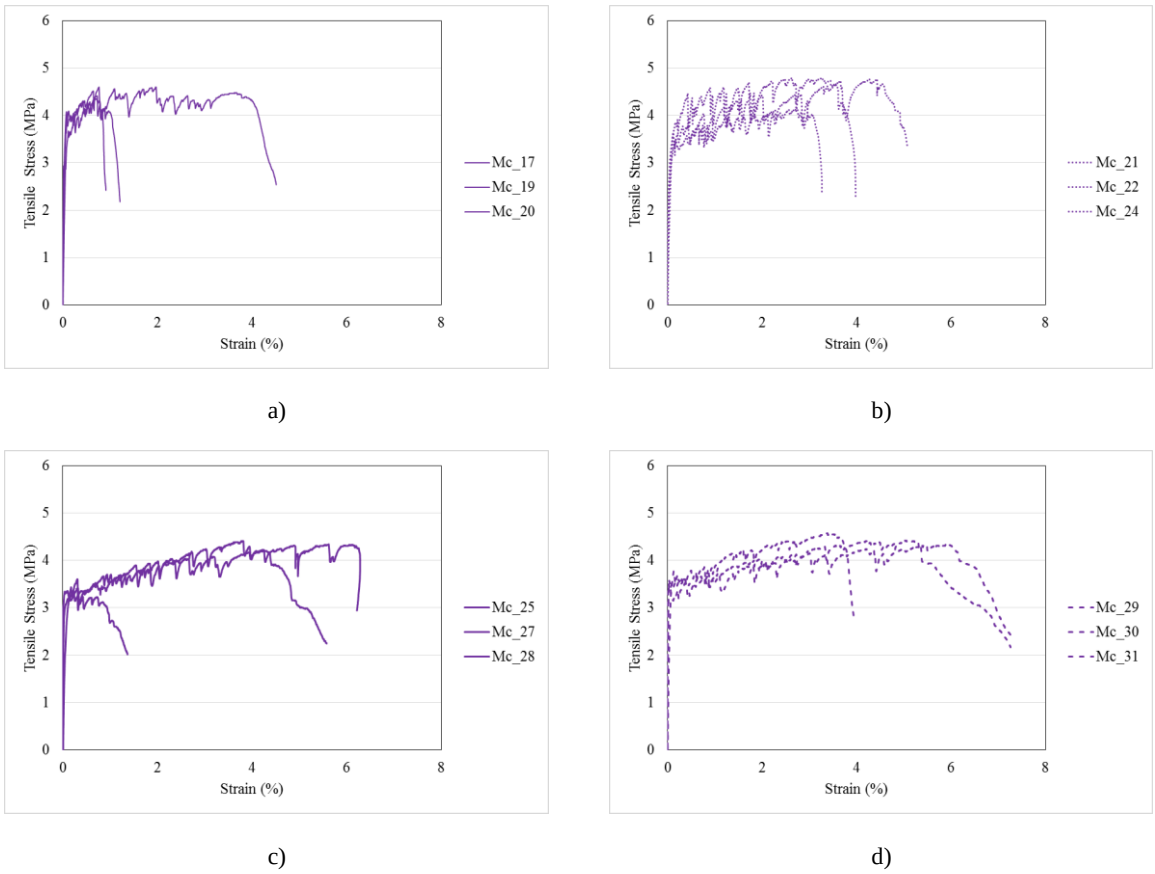

Figure 3. 73- Tensile results of Mixture C 14 days after curing: a) in air; b) in seawater; c) in tap water; d) in salted water.

The strain hardening behaviour was achieved in all specimens tested. All sudden stress peaks that appear in the strain hardening phase represent the formation of new cracks. In Table 3.19 the main properties, such as the tensile stress and strain reached when the first crack is formed and the maximum tensile stress strain for each specimen are presented.

Table 3. 18- Tensile stress-strain results of Mixture C for all curing environments at 14 days.

Cure	Specimen	σc (Mpa)	Ɛc (%)	σm (Mpa)	Ɛm (%)
Air	Mc_17	3,95	0,07	4,35	0,72
	Mc_19	4,08	0,08	4,60	1,97
	Mc_20	3,67	0,12	4,41	0,72
Seawater	Mc_21	3,44	0,15	4,13	2,74
	Mc_22	3,63	0,12	4,77	4,28
	Mc_24	3,83	0,19	4,80	2,62
Tap Water	Mc_25	3,20	0,12	4,34	5,62
	Mc_27	3,34	0,04	4,41	3,82
	Mc_28	3,43	0,17	3,60	0,31
	Mc_29	3,58	0,04	4,44	4,24

Salted Water	Mc_30	3,50	0,02	4,35	5,93
	Mc_31	3,78	0,14	4,57	3,39

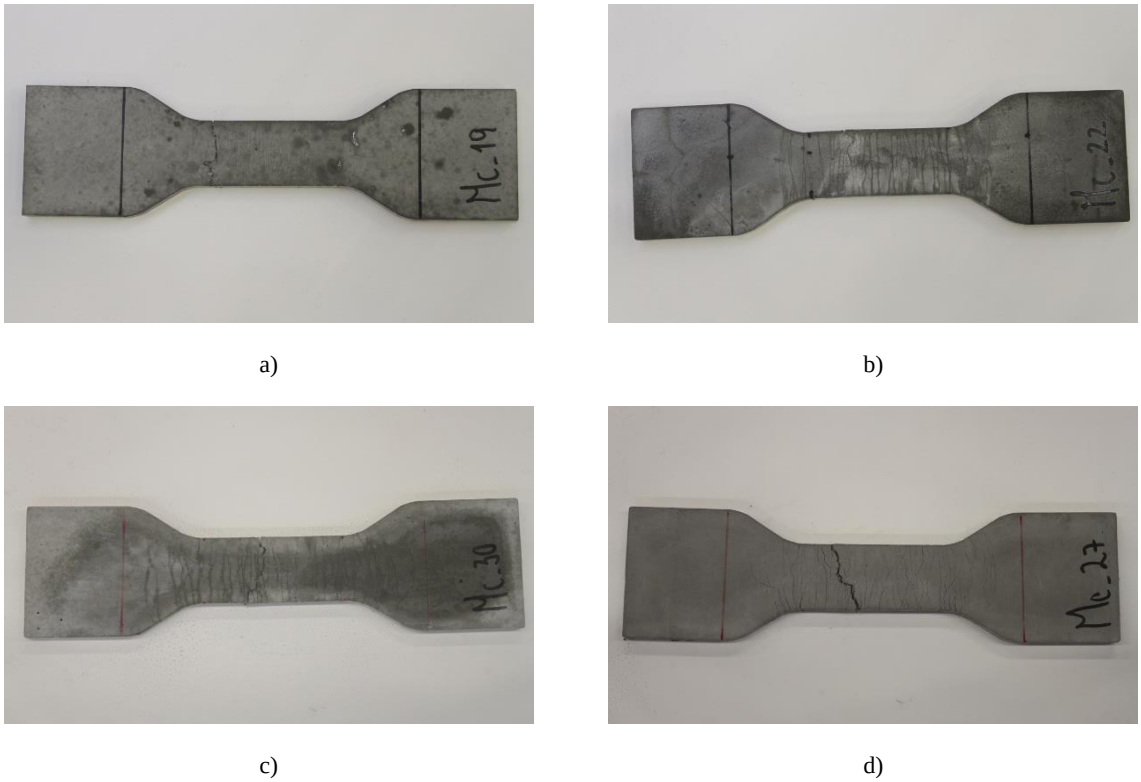

a) b)

c) d)

Figure 3. 74- Mixture C dogbone specimens tested after 14 days of curing: a) in air; b) in seawater; c) in tap water; d) in salted water.

The first cracking stress ranged between 3 MPa and 4 MPa. The average results for each type of curing environment are represented in Figure 3.75.

The specimens cured in salted water and seawater reached the highest ultimate strains.

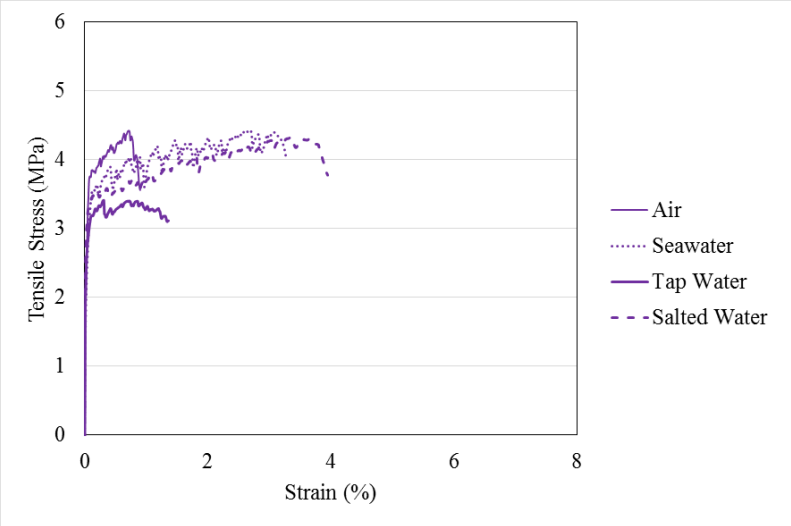

Figure 3. 75- Average tensile results of Mixture C in all environments (14 days)

28 days

Three specimens were tested for each type of curing environment.

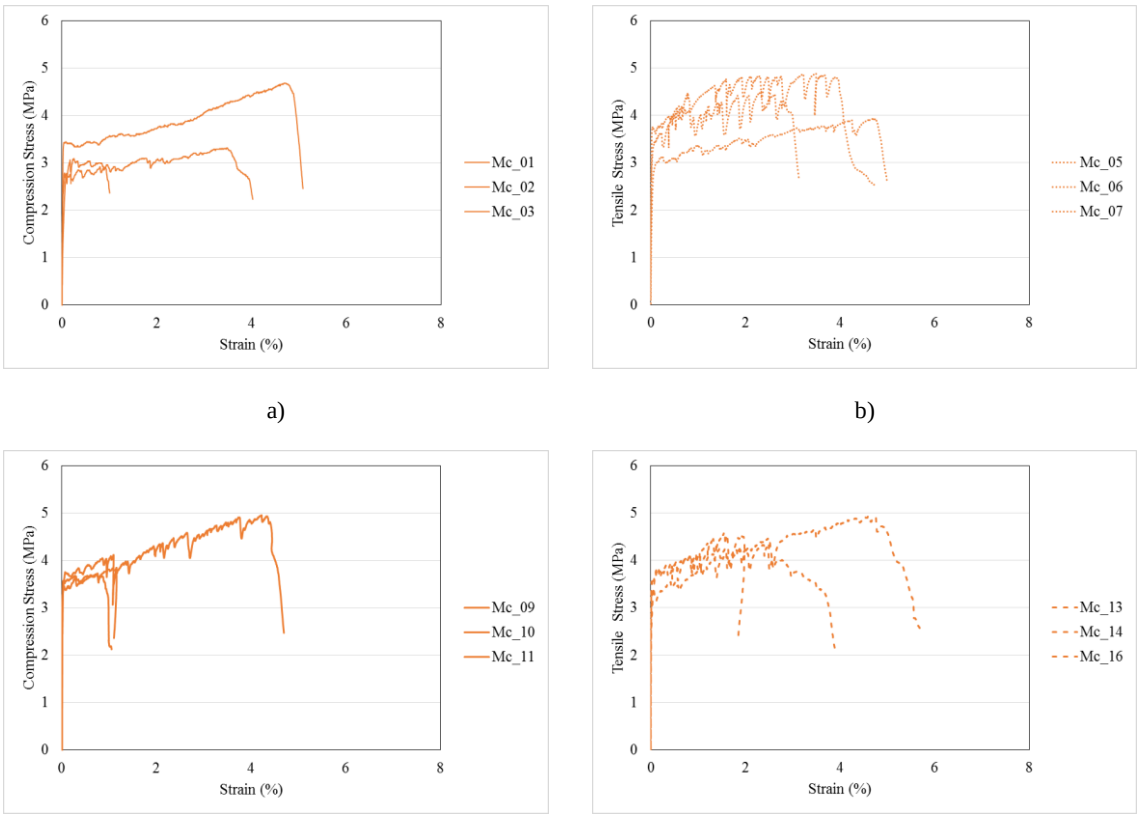

Figure 3. 76- Tensile test results for Mixture C 28 days after curing: a) in air; b) in seawater; c) in tap water; d) in salted water.

The results obtained are presented in Figure 3.76.

The specimens have different behaviours. Even when comparing the specimens within the same type of curing, different behaviours have been obtained.

However, all specimens showed the typical stress-strain behaviour of the ECC, with the formation of multiple microcracks at increasing tensile stresses. The specimens cured in seawater have reached the maximum tensile stress. The results obtained are summarized in Table 3.20.

Table 3. 19- Tensile test results of Mixture C for all curing environments at 28 days.

Cure	Specimen	σc (Mpa)	Ɛc (%)	σm (Mpa)	Ɛm (%)
Air	Mc_01	2,78	0,10	3,31	3,49
	Mc_02	2,78	0,05	3,09	0,30
	Mc_03	3,43	0,04	4,68	4,76
Seawater	Mc_05	3,01	0,15	3,92	4,70
	Mc_06	3,75	0,05	4,88	3,50
	Mc_07	3,14	0,03	4,51	2,34
Tap Water	Mc_09	3,57	0,03	3,73	0,75
	Mc_10	3,46	0,04	4,95	4,22
	Mc_11	3,75	0,07	4,11	1,09
Salted Water	Mc_13	3,41	0,06	4,33	2,39
	Mc_14	3,37	0,01	4,58	1,56
	Mc_16	3,81	0,13	4,94	4,60

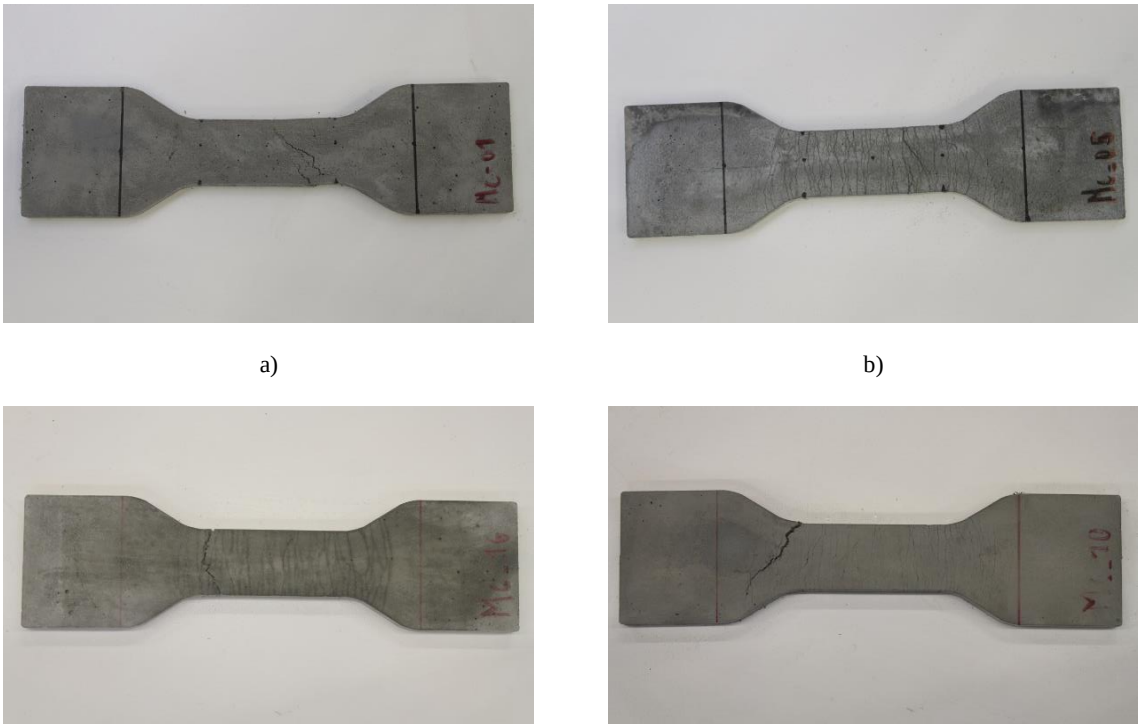

a) b)

c) d)

Figure 3. 77- Mixture C dogbone specimens tested 28 days after curing: a) in air; b) in seawater; c) in tap water; d) in salted water.

The average curves for all curing environments are represented in Figure 3.78.

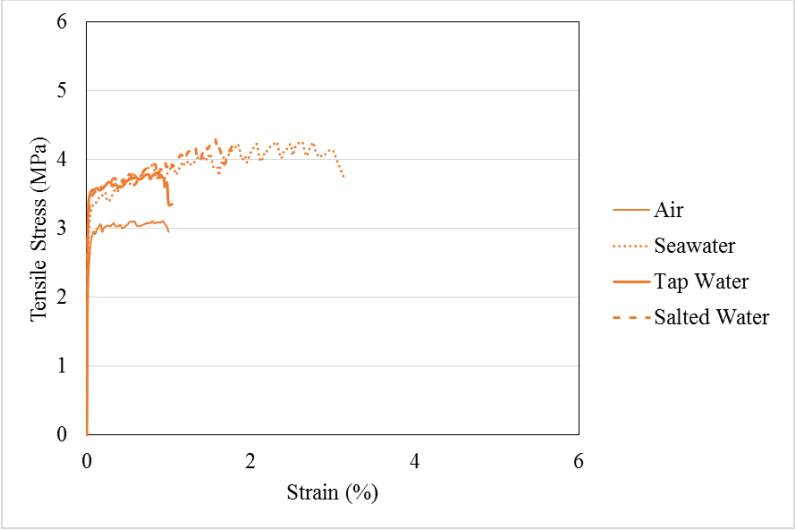

Figure 3. 78- Average tensile results of Mixture C in all environments (28 days)

The specimens cured in salted water reached the higher ultimate strain.

14 vs 28 days

In this study, 2 different ages of each mixture were tested. The comparison between the two ages is presented in Figure 3.79.

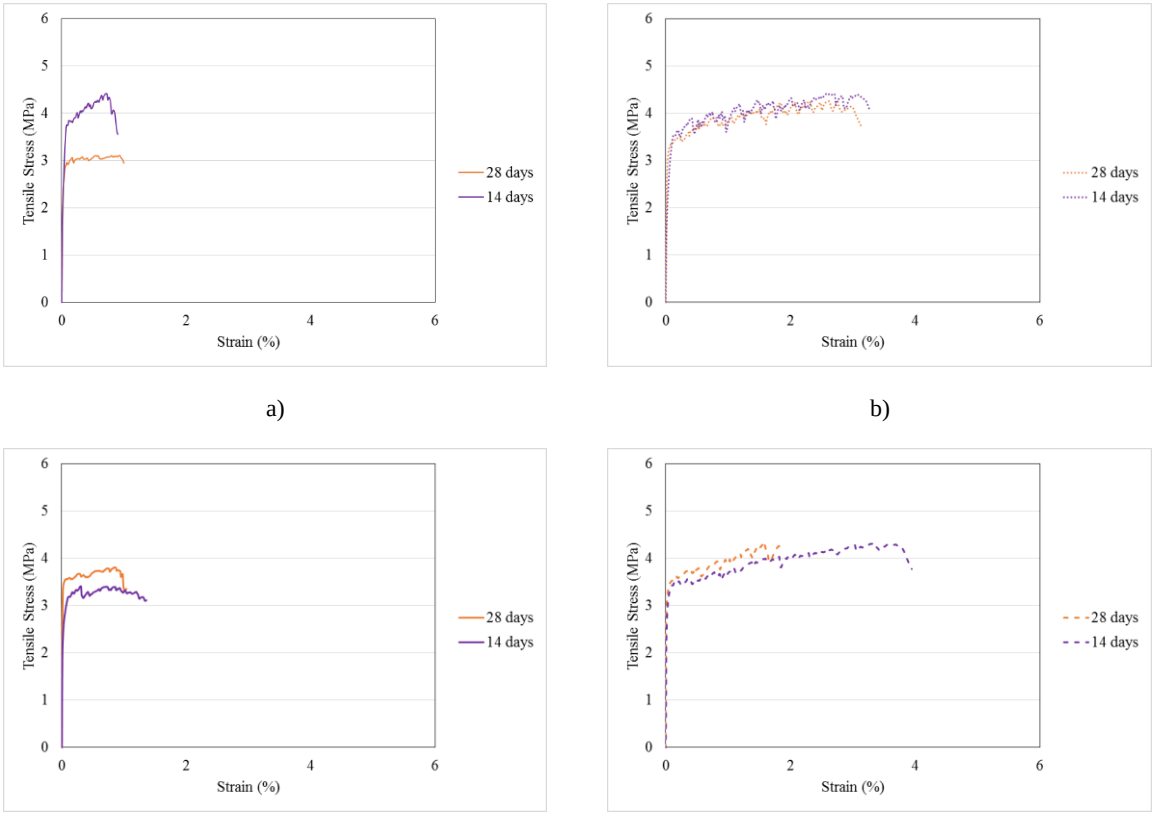

Figure 3. 79- 14 days versus 28 days tensile test results of Mixture C: a) cured in air; b) cured in seawater; c) cured in tap water; d) cured in salted water.

In Figure 3.79 (a) is possible to confirm that the specimens cured in air and tested 14 days after casting have reached higher tensile stresses than the ones tested 28 days after casting. Normally, when the curing time increases the tensile stresses reached tend to be higher, as observed in the other three curing environments. Therefore, the results obtained for the specimens cured in air were not expected.

3.5 Influence of the mix composition

In this section, all the results obtained for all mixtures will be compared from the perspective of the mixture composition, in order to evaluate the influence of the different types of water used in the mixtures on the compressive, single crack tensile and direct tension testing when curing in the four different environments.

3.5.1 Air curing

3.5.1.1 Compressive behaviour

14 days

In Figure 3.80 the average responses of the compression tests of each mixture cured in air are represented. Mixture C, which was made with salted water, has reached the highest compressive strengths.

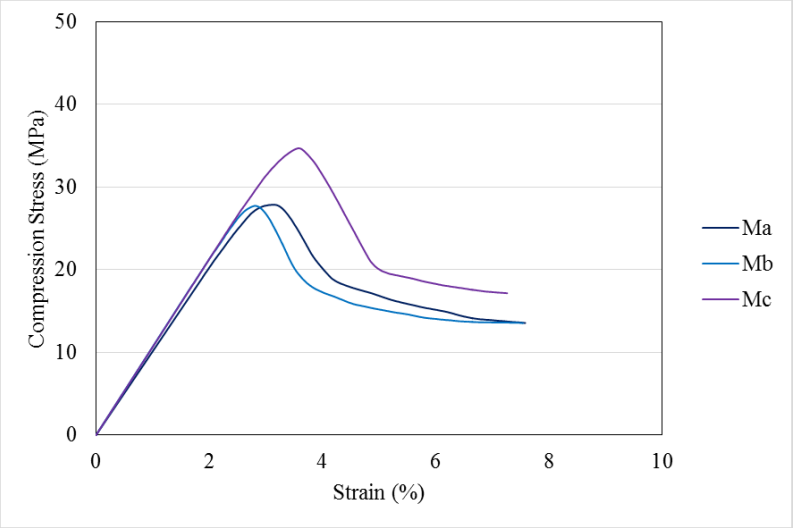

Figure 3. 80- Average compressive responses obtained for all mixtures 14 days after curing in air.

At 14 days all mixtures have reached compressive strengths between 20-30 MPa.

It is possible to conclude that the use of seawater and salted water in the ECC mixtures compositions does not lead to a decrease of the compression strength when cured in air. Actually the addition of salted water resulted in greater compressive strengths than expected.

The average compression strengths and elasticity modulus obtained for all mixtures are represented in Figure 3.81.

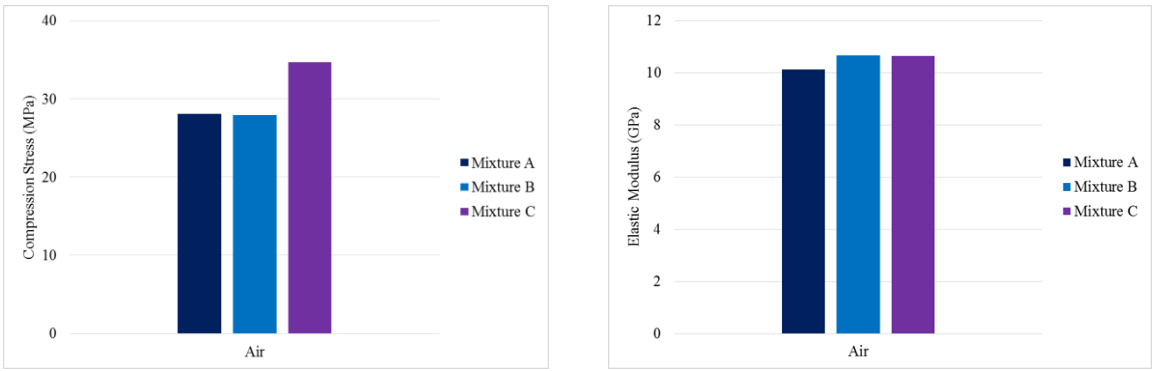

Figure 3.81- Maximum compressive stress and elastic modulus of different mixtures cured in air (14 days)

The elasticity modulus have similar values in Mixtures B and C. They showed higher results when compared with the traditional ECC mixture (Mixture A).

28 days

In Figure 3.82 the average responses of the compression tests at 28 days are shown. The mixture that reached highest compressive strengths was Mixture A, and the lowest by Mixture B.

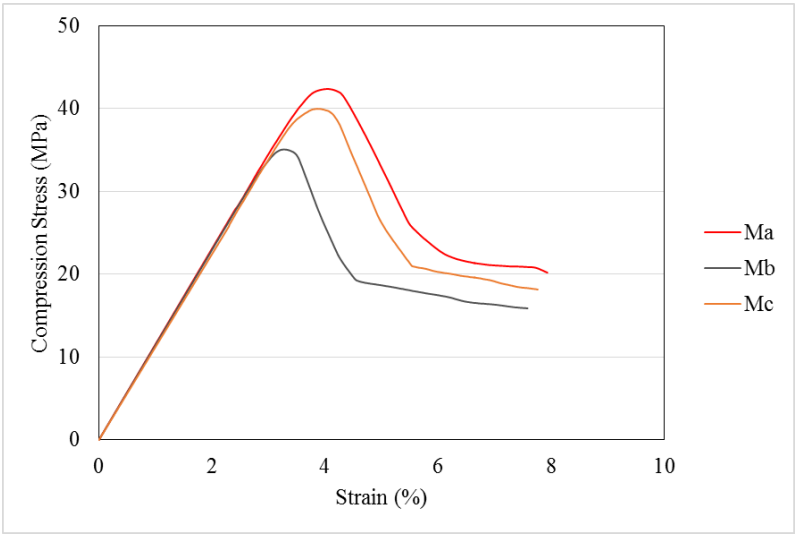

Figure 3. 82- Compressive behaviour results of different mixtures cured in air (28 days)

In contrast to the results obtained at 14 days, the results obtained at 28 days show that the use of seawater and salted water resulted in a decrease of the compression strengths at 28 days. However, the three mixtures showed the typical compressive behaviour normally associated to Engineered Cementitious Composites, with a smooth load decay after reaching the peak stress.

Figure 3.83 represents the average results for the compressive strength and elastic modulus obtained in all mixtures.

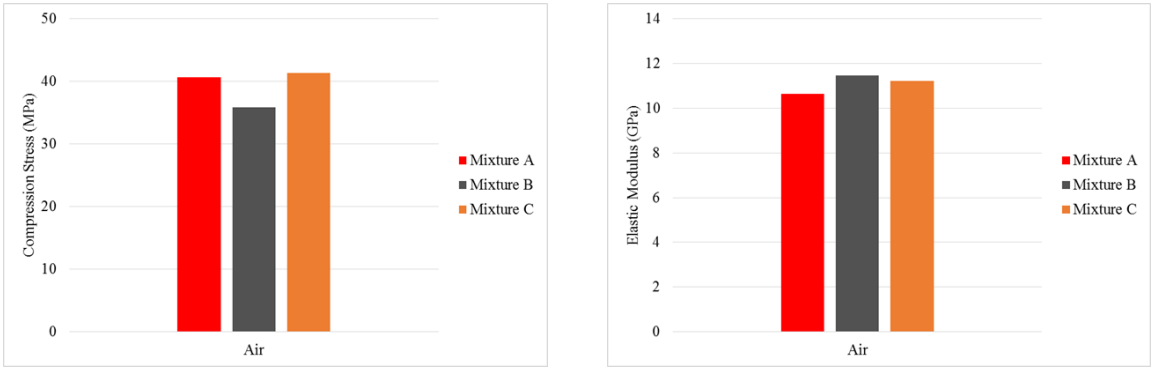

Figure 3. 83- Maximum compressive stress and elastic modulus of different mixtures cured in air (28 days)

Mixture B has reached the highest values of elastic modulus the lowest compressive strength when compared with the other two mixtures. The nominal elastic moduli ranged between 10 to 12 GPa.

14 vs 28 days

Figure 3.84 represents the compression test results of all mixtures cured in air at both ages. All mixtures showed higher compressive strengths after 28 days of curing.

Mixture C reached the highest compressive strength when tested at 14 days and Mixture A at 28 days. Mixture B showed the lowest compressive stresses at both ages.

It is possible to conclude that the seawater used in the composition contains some substances, probably of organic nature, that led to the lowest compression results. Sodium chloride is frequently added to water to represent the maritime curing conditions, however these results have confirmed that this procedure does not assure good representativeness, since Mixture C (salted water) has reached the highest compressive strengths. The only difference between these two compositions was that Mixture B used water from the sea and Mixture C used water with dissolved NaCl in the composition.

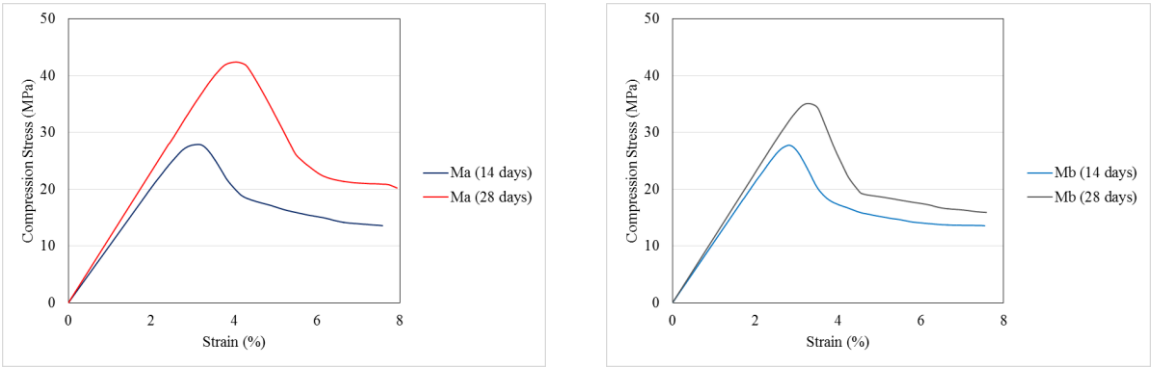

a) b)

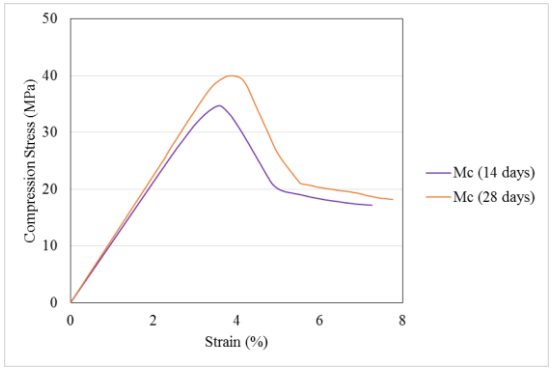

c)

Figure 3. 84- 14 days versus 28 days compression test results of specimens cured in air: a) Mixture A; b) Mixture B; c) Mixture C.

3.5.1.2 The Single Crack Tension Test (SCTT)

14 days

Figure 3.85 shows the average single crack tension test results of each mixture after curing in air.

The mixtures tested showed different behaviours. Mixture A developed higher crack mouth opening displacements. Mixtures B and C have reached higher tensile stresses for lower CMODs

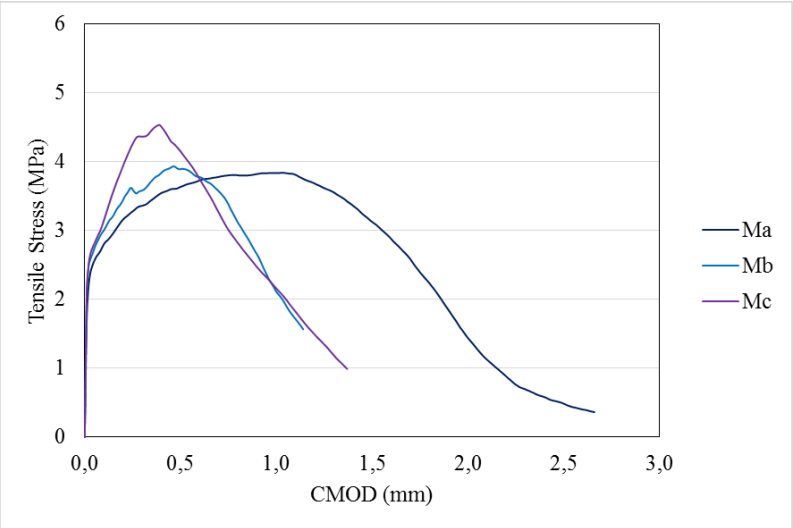

Figure 3. 85- SCTT test results obtained after 14 days of curing in air.

It is possible to conclude that the use of seawater and salted water affects the single crack behaviour of ECC mixtures, probably by altering the matrix tensile strength or stiffness, and therefore promoting the formation of additional cracks. The interface between the fibre and the matrix is also very likely affected.

28 days

Figure 3.86 shows the single crack tension results of each mixtures tested, at 28 days, cured in air. At this age, the results of each mixture are very similar.

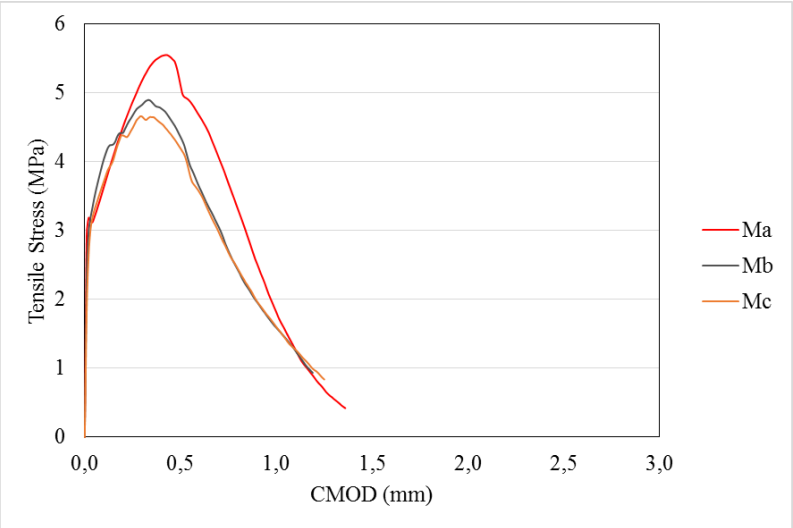

Figure 3. 86- 28 days SCTT results obtained in all mixtures cured in air

The effect of the use of seawater and salted water in the composition becomes less evident at 28 days. The maximum tensile stress reached ranged between 4.5 MPa and 6 MPa, but the mixtures containing seawater and salted water reached lower tensile stresses than the one with tap water.

14 vs 28 days

The SCTT test results obtained at both ages are compared in Figure 3.87.

Mixture A shows a clearly different behaviour in both ages. The results at 14 days show the development of larger crack mouth opening displacement at lower tensile stresses. In opposition, when the specimens are tested at 28 days, the response shows less deformability at higher tensile stresses. That difference may be explained by the fact that the specimens at 28 days have reached high compressive strengths, revealing a much more mature matrix, therefore the test results show that higher loads must be reached to start opening the initial crack.

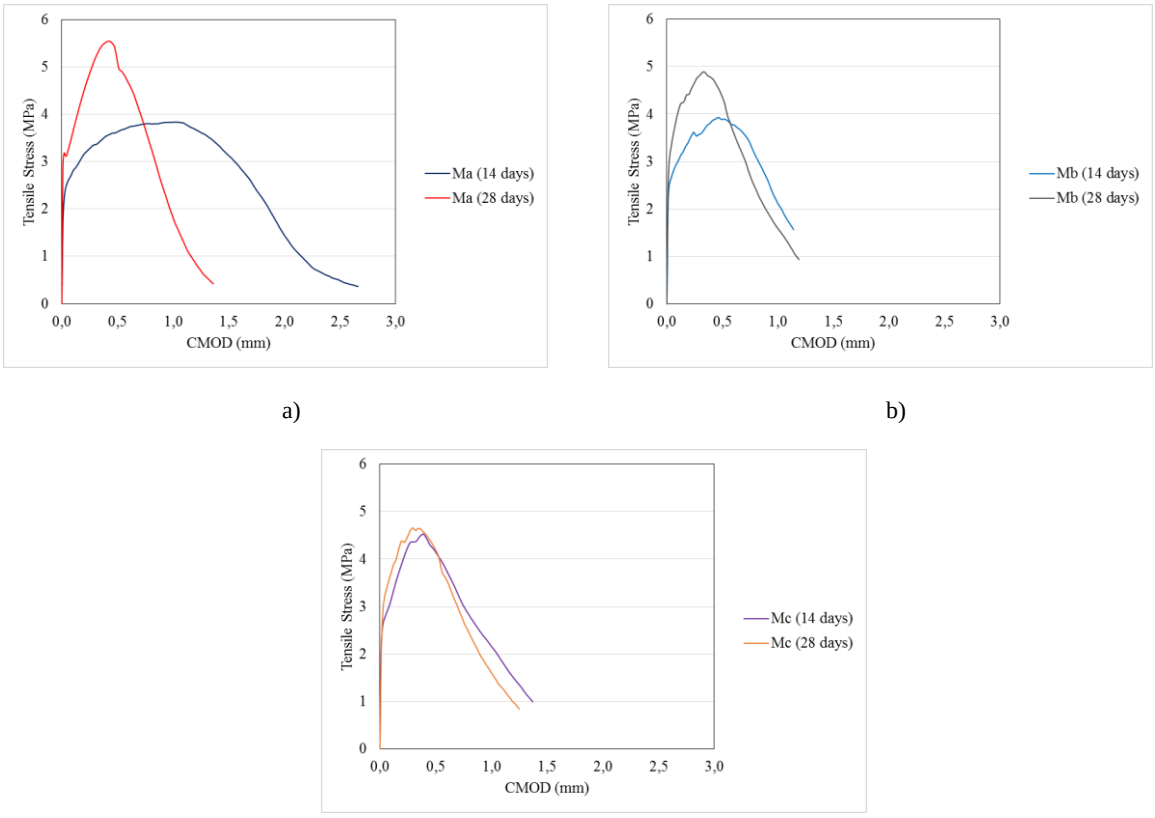

Figure 3. 87- 14 days versus 28 days SCTT test results of specimens cured in air: a) Mixture A; b) Mixture B; Mixture C.

The Mixture B and Mixture C show similar behaviours in both ages.

It is possible to conclude that the use of seawater and salted water in the ECC composition affects the single crack behaviour, and that the effect that the seawater or the tap water may have on the matrix properties or the fibre-matrix interface fade away in time.

3.5.1.3 Tensile Stress-Strain Behaviour

14 days

The average direct tension test results of all mixtures tested at 14 days are represented in Figure 3.88. As shown, Mixture A showed the typical response of ECC materials, with the development of an initial high stiffness phase until the tensile strength of the matrix reached. After that, the strain hardening behaviour with the formation of multi-cracking occurs. Mixture B exhibited a similar behaviour but the crack openings observed were much smaller. Mixture C has reached lower strain values when compared with the other mixtures but achieved the highest tensile stress values.

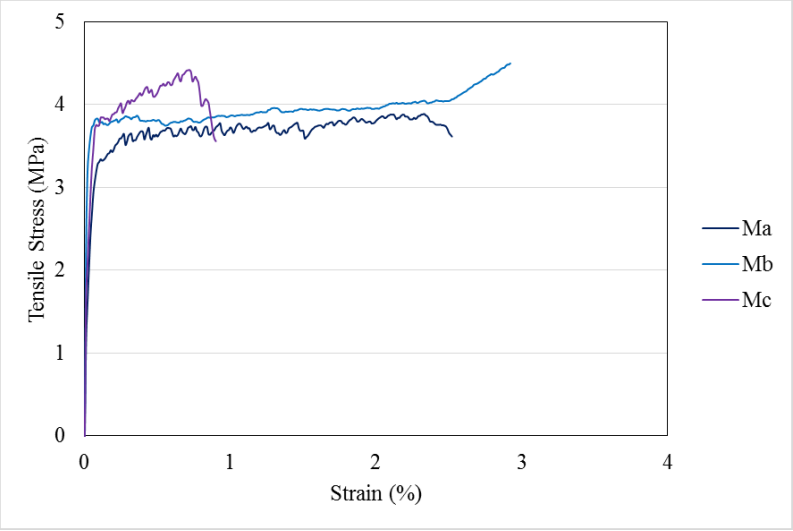

Figure 3. 88- 14 days tensile results obtained in all mixtures cured in air

The use of seawater has resulted in the development of cracks with a much smaller width. In fact, the cracks developed only became visible at a much later stage when compared with the other specimens, almost before reaching the ultimate tensile stress.

28 days

Figure 3.89 shows the tensile results of all mixtures when cured in air after 28 days of curing. The mixture that achieved highest strains was Mixture A and the lowest strains were achieved by Mixture C.

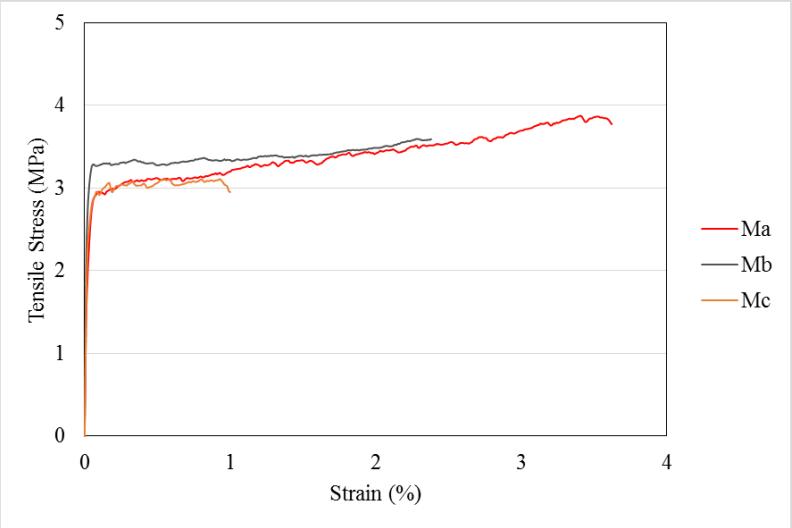

Figure 3. 89- 28 days tensile results obtained in all mixtures cured in air

The use of salted water in the composition of the mixture seemed to have resulted in poorer ability to develop multiple cracks and decrease the strain capacity of the ECC mixtures.

14 vs 28 days

Figure 3.90 shows the direct tension test results for both ages when air cured.

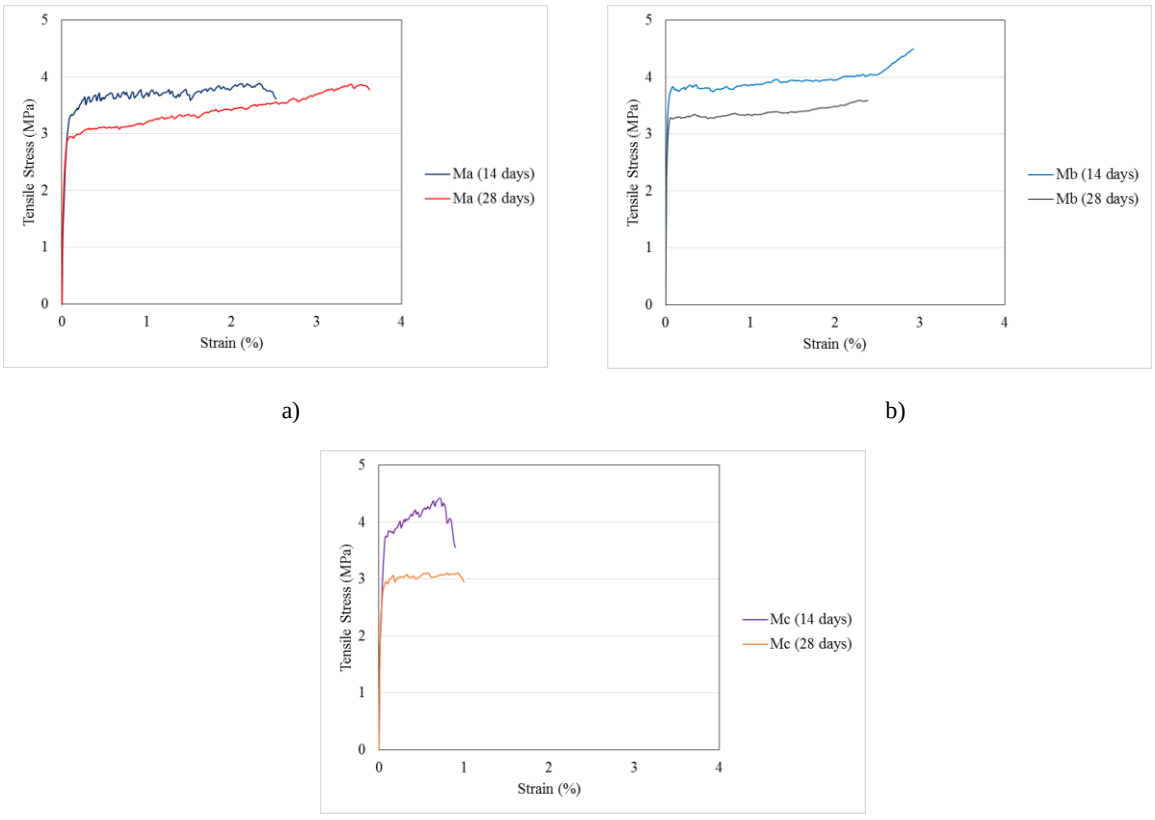

Figure 3. 90 – 14 days vs 28 days tensile test results when cured in air: a) Mixture A; b) Mixture B; c) Mixture C.

3.5.2 Seawater curing

3.5.2.1 Compressive behaviour

Figure 3.91 shows the average compression test results of the three mixtures when cured in seawater. Mixture C has reached the highest compressive strengths.

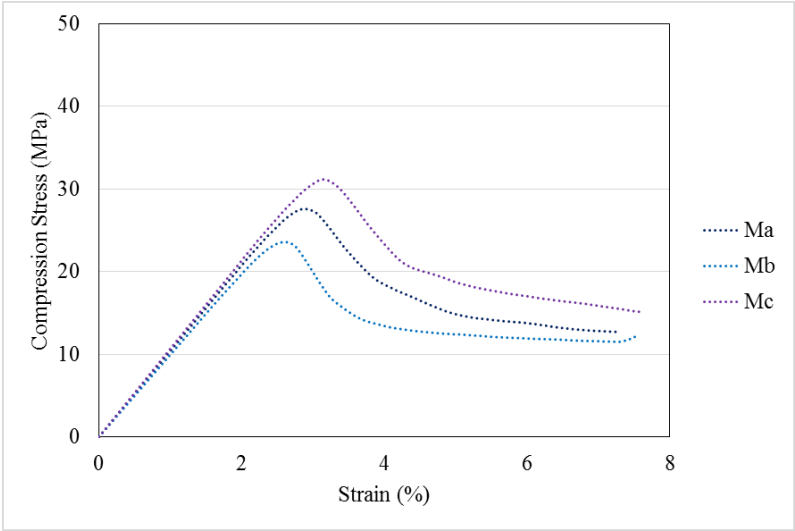

Figure 3. 91- Compression test results of the three mixtures cured in seawater 14 days after casting.

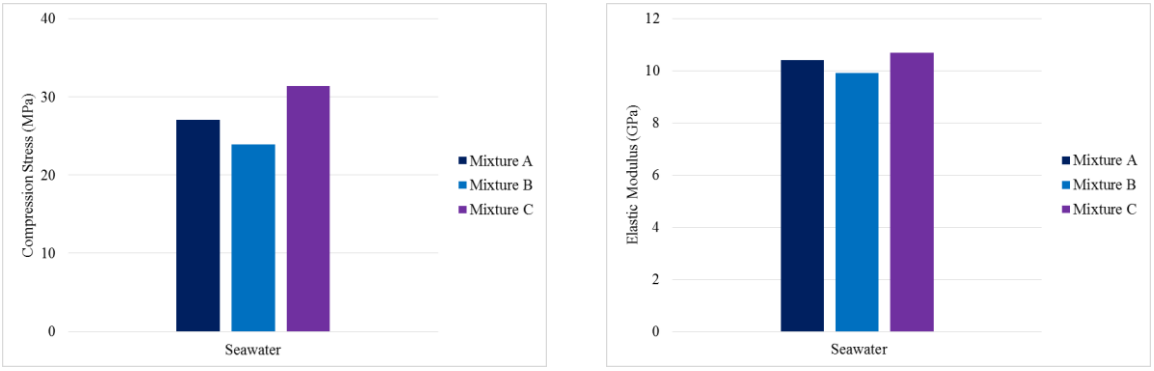

Figure 3. 92- Compressive strength and elastic modulus obtained 14 days after curing in seawater.

The use of seawater in the composition seems to have decreased the compressive strength when comparing the results of mixtures A and B. However, the use of salted water in mixture C has resulted in the opposite effect.

28 days

Figure 3.93 shows the average compression test results of the three mixtures when curing in seawater. The compressive strengths obtained ranged between 30 MPa and 50 MPa. The lowest strengths were obtained with Mixture B.

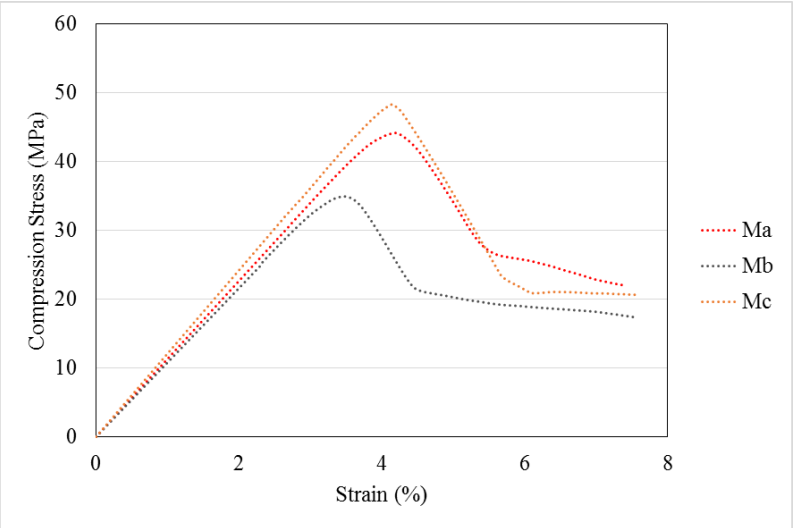

Figure 3. 93- Compressive behaviour results of different mixtures cured in seawater (28 days)

The highest compressive strength and elastic modulus were achieved by Mixture C, as shown in Figure 3.94.

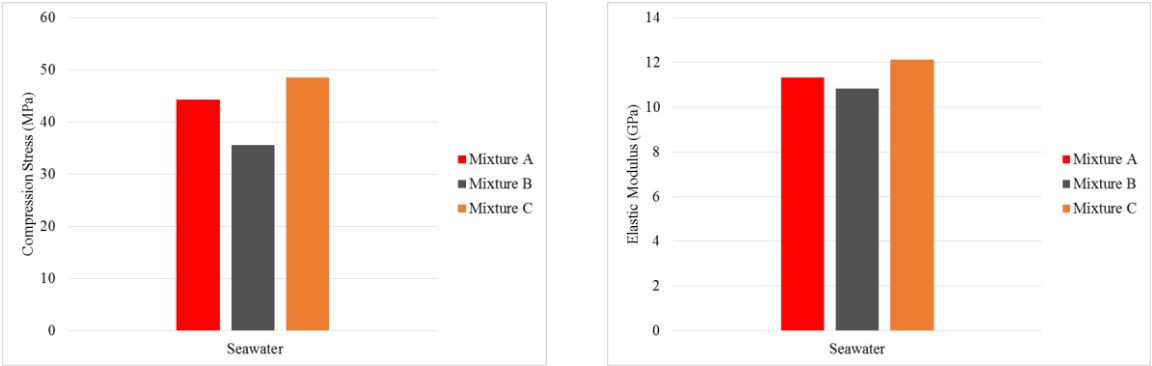

Figure 3. 94- Maximum compressive stress and elastic modulus of different mixtures cured in seawater (28 days)

14 vs 28 days

Figure 3.95 summarizes the compression test results obtained for all mixtures cured in seawater. All mixtures showed higher compressive strengths when tested at 28 days old. Mixture C has reached the highest compressive strength in both ages. In contrast Mixture B, which is made with seawater, has reached the lowest compressive strength.

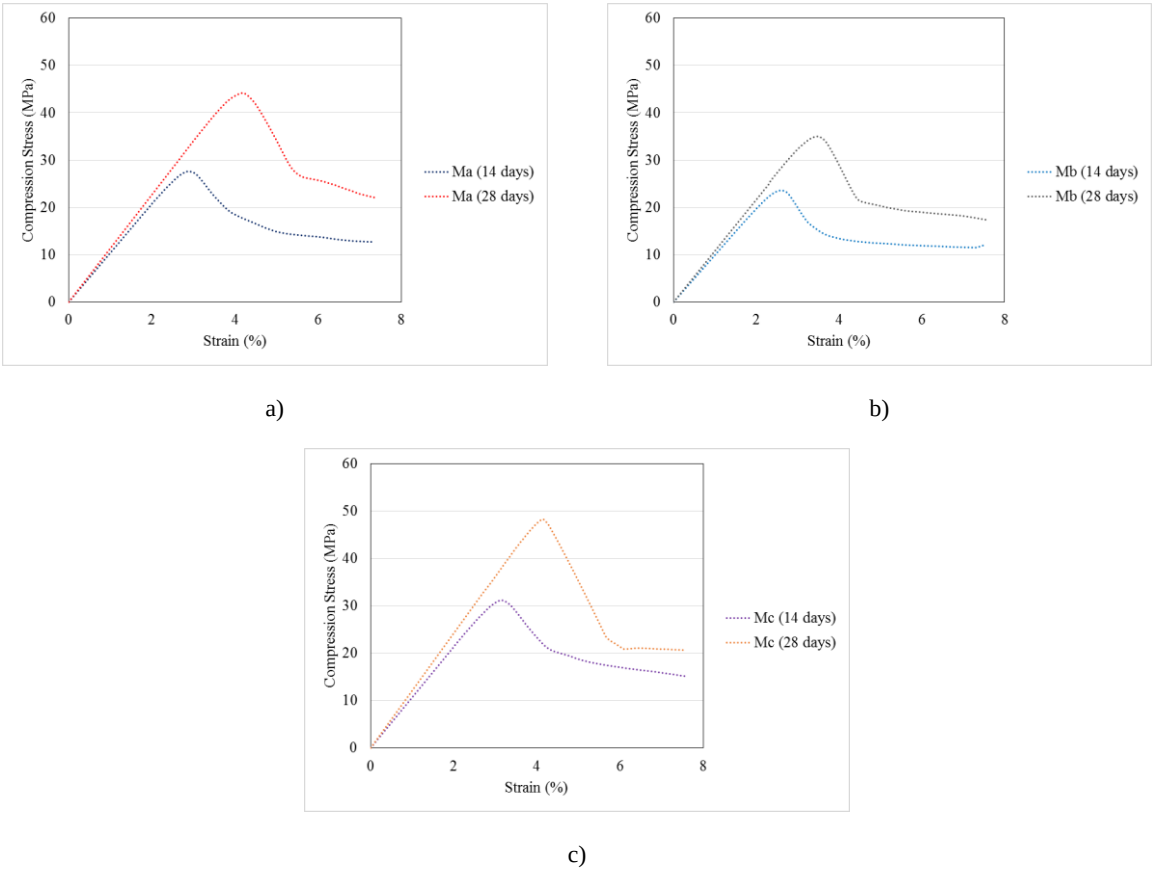

a) b)

c)

Figure 3. 95- 14 vs 28 days compression results cured in seawater: a) of Mixture A; b) of Mixture B; c) of Mixture C

Mixture A showed the expected behaviour, therefore the seawater curing did not affect the mechanical behaviour of the classical mixture containing tap water.

3.5.2.2 Single Crack Tension Test (SCTT)

14 days

Figure 3.96 shows the average SCTT results of each mixture when cured in seawater for 14 days. The responses obtained are quite different. Mixture B has reached the lowest tensile stresses for higher CMODs.

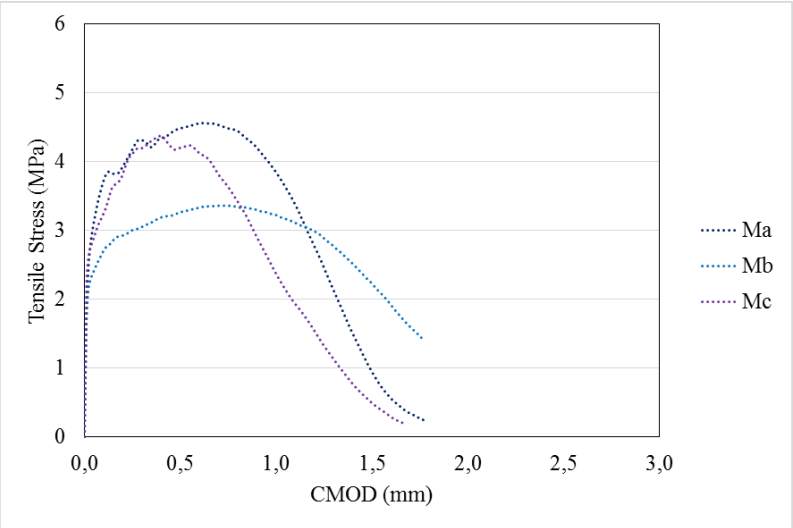

Figure 3. 96- 14 days SCTT results obtained in all mixtures cured in seawater

The CMODs ranged between 1.5-2 mm and the maximum tensile stress varies from 3 to 5 MPa.

28 days

Figure 3.97 shows the SCTT test results obtained when curing the three mixtures in seawater. Mixture B has shown a slightly different behaviour relatively to the other two mixtures. Mixtures A and C exhibited more abrupt stress peaks.

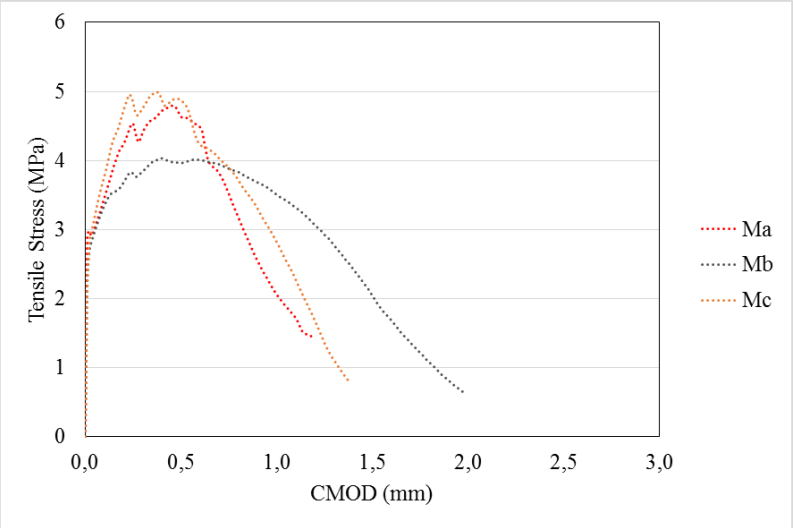

Figure 3. 97- 28 days SCTT test results obtained for all mixtures cured in seawater for 28 days.

14 vs 28 days

The SCTT results of the 3 mixtures tested when cured in seawater are presented in Figure 3.98. Both ages tested show approximately similar behaviours. It's possible to confirm that the lowest tensile stresses were reached by Mixture B.

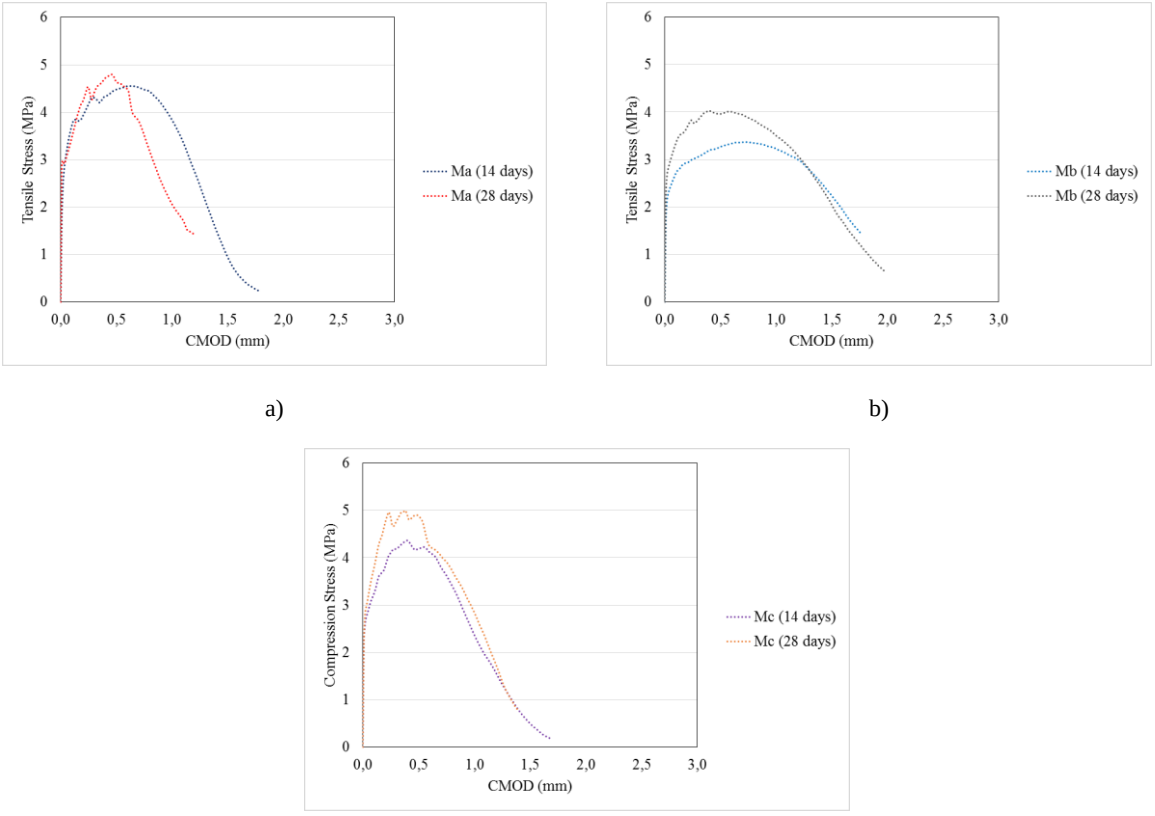

Figure 3. 98- 14 days vs 28 days SCTT results of specimens cured in seawater: a) Mixture A; b) Mixture B; Mixture C.

The use of seawater seems to have resulted in the development of lower tensile stresses. However, since the CMODs reached were clearly larger, this may be an indication of the formation of significantly more microcracks at the notched section.

3.5.2.3 Tensile Stress-Strain Behaviour

14 days

Figure 3.99 shows the average direct tension test results of all mixtures cured in seawater. Mixture B has revealed a distinctive behaviour. The Mixtures A and C, in the strain hardening

phase, showed sudden stress peaks that represent the formation of new cracks. However, Mixture B doesn't show the same behaviour. That difference is explained by the fact that the cracks formed in Mixture B develop very small widths, resulting in a smoother cracking process.

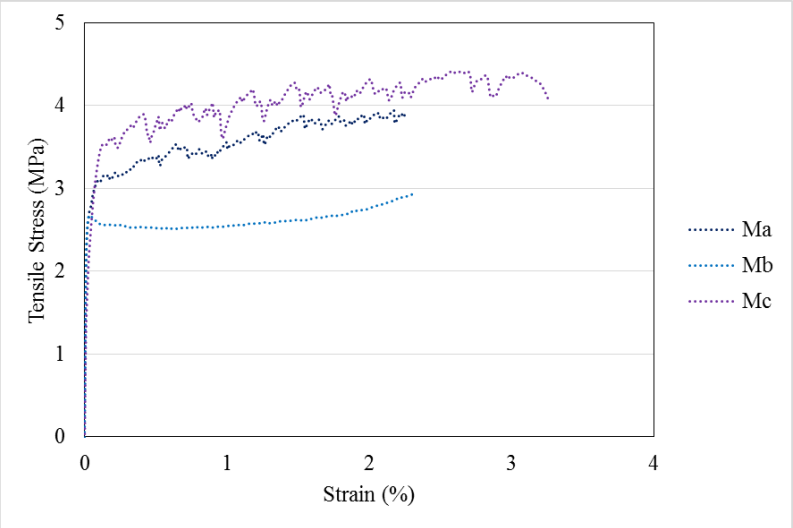

Figure 3. 99- 14 days tensile test results obtained for all mixtures after curing in in seawater for 14 days.

28 days

Figure 3.100 shows the average tensile test results obtained for all mixtures cured in seawater. All mixtures have reached very close ultimate strains. That confirms that the use of seawater and salted water in the ECC composition does not compromise the strain hardening potential at 28 days.

Tensile strengths ranged between 3.5 MPa and 4.5 MPa.

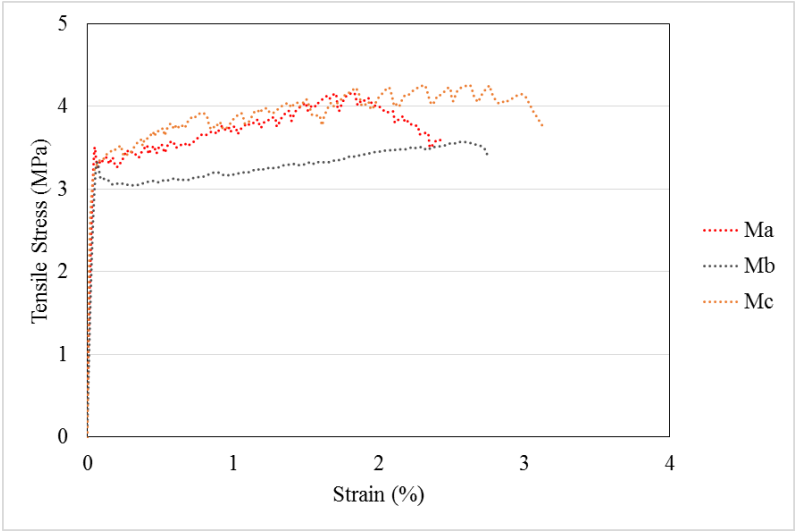

Figure 3. 100- 28 days tensile test results obtained for all mixtures after curing in seawater for 28 days.

14 vs 28 days

In Figure 3.101, the comparison between the two ages results is made.

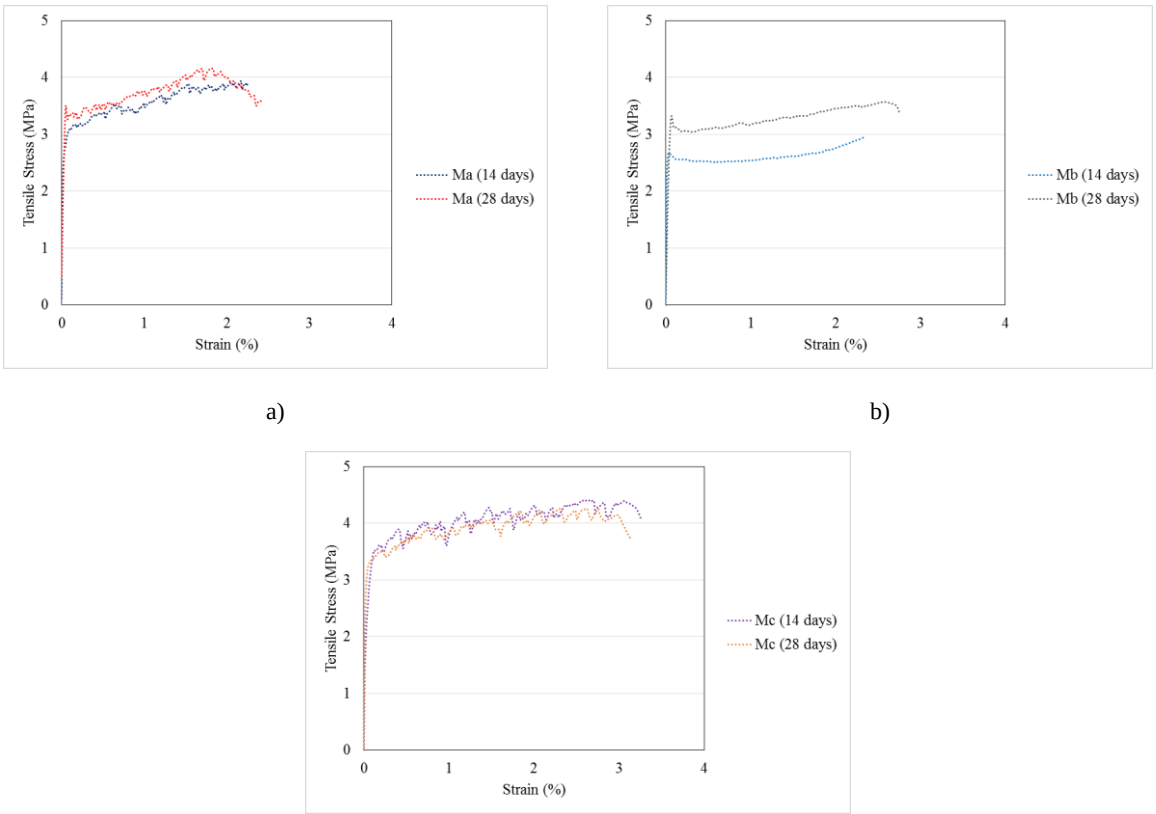

a) b)

c)

Figure 3. 101- 14days vs 28 days tensile test results of specimens cured in seawater: a) Mixture A; b) Mixture B; c) Mixture C.

The seawater cure doesn't influence the behaviour of ECC mixture. Both ages tested achieved similar behaviour, when compared between mixtures. The specimens tested with 28 days achieved higher results, except Mixture C that have similar results in both ages.

3.5.3 Tap water curing

3.5.3.1 Compressive behaviour

14 days

The compression test results of all mixtures cured in tap water are represented in Figure 3.102. The compressive strengths ranged between 25 MPa and 35 MPa. These results are typical of ECC mixtures. The use of salted water in the composition increased the compressive strength.

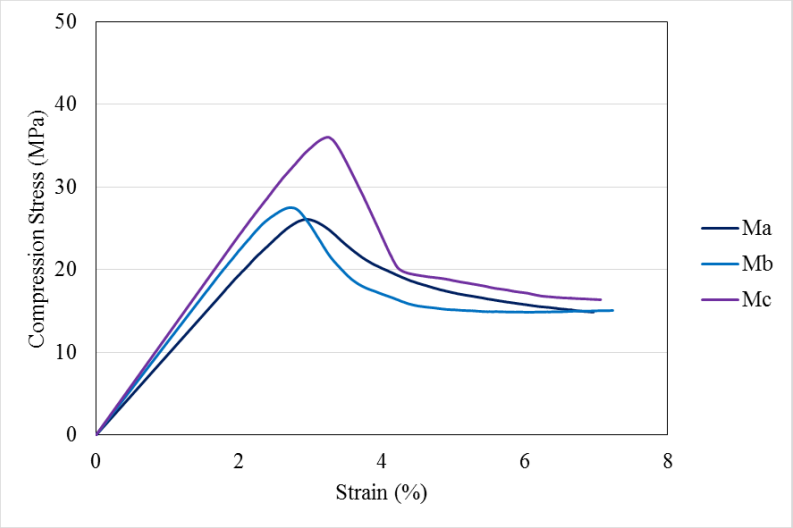

Figure 3.102- Compression test results for all mixtures cured in tap water for 14 days.

In Figure 3.103 it is possible to confirm that the Mixture C has reached the highest compressive strength and elasticity modulus. The elasticity modulus for all mixtures ranged between 10 and 12 GPa.

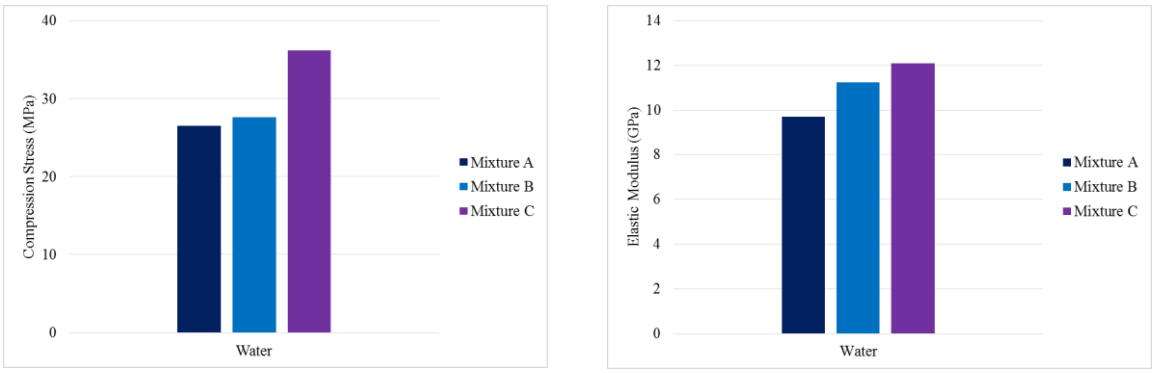

Figure 3. 103- Compressive strength and elastic modulus for specimens cured in tap water for 14 days.

28 days

The 28 days results are represented in Figure 3.104. Mixture C have reached the highest compressive strength.

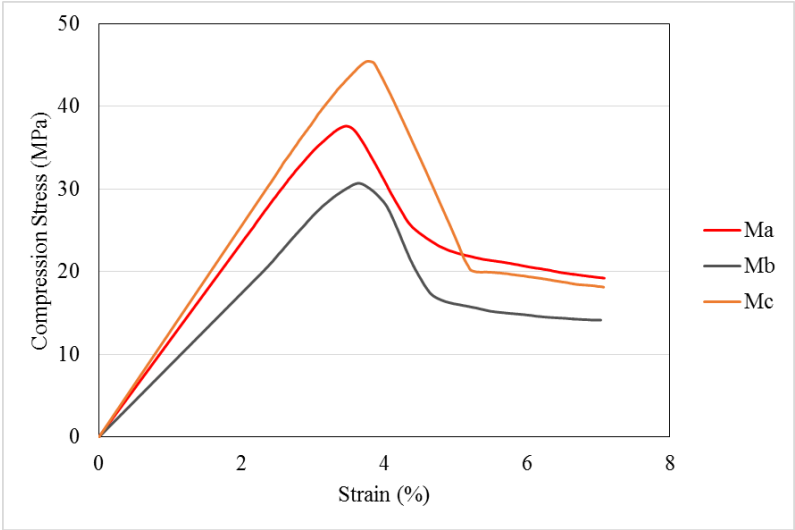

Figure 3. 104- Compression test results for specimens cured in tap water for 28 days.

Mixture B has reached the lowest compressive strength and elastic modulus. The average elastic modulus and compressive strengths obtained are represented in Figure 3.105.

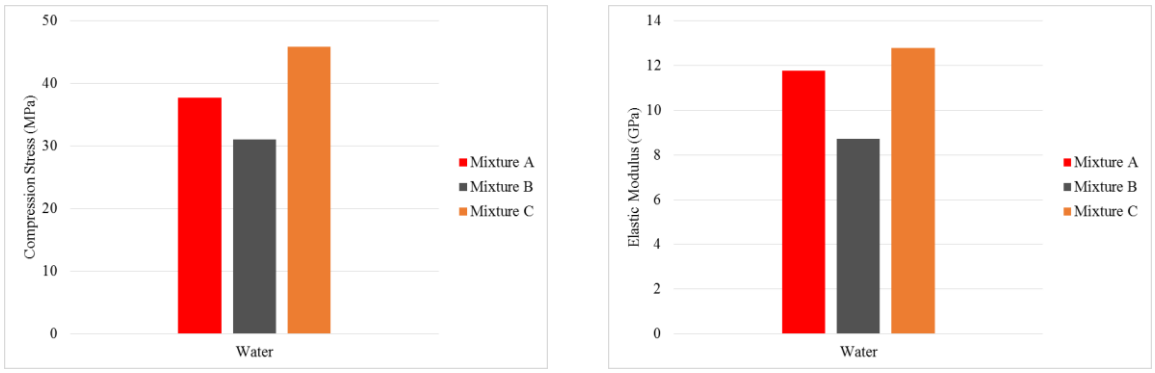

Figure 3. 105- Compressive strength and elastic modulus for specimens cured in tap water for 28 days.

As in the previous sections, the mixture containing seawater has again reached the lowest compressive strength and elasticity modulus among all mixtures.

14 vs 28 days

Figure 3.106 represents the compression test results of all mixtures cured in water at both ages. All mixtures showed higher compressive strengths when tested at 28 days. Mixture C showed the highest compressive strengths in both ages, reaching almost 50 MPa.

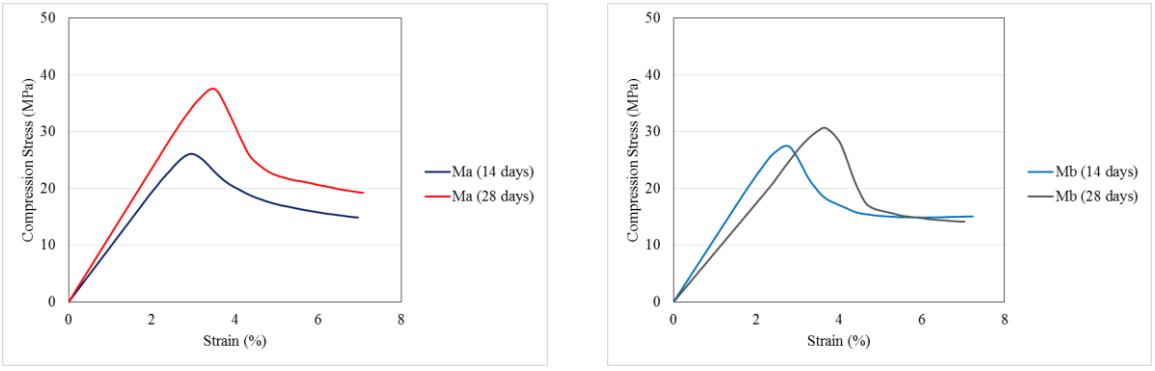

a) b)

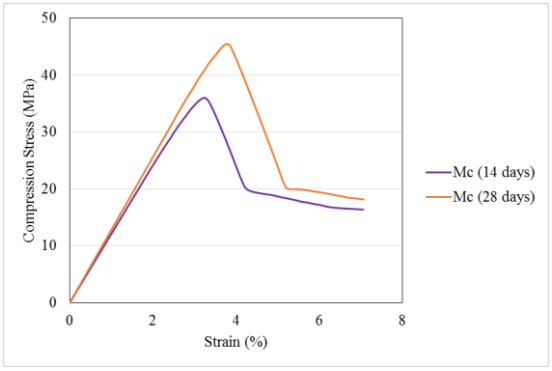

c)

Figure 3. 106- 14 days versus 28 days compression test results of specimens cured in water: a) Mixture A; b) Mixture B; c) Mixture C

3.5.3.2 Single Crack Tension Test (SCTT)

14 days

Figure 3.107 shows the 14 days results of each mixture when cured in tap water. The Mixture A and C showed similar behaviours: both maximum tensile stress and CMODs have almost the same values. In both mixtures, the specimens evidenced the probable formation of more than one crack.

In contrast, Mixture B has shown a different behaviour, with a much smoother response.

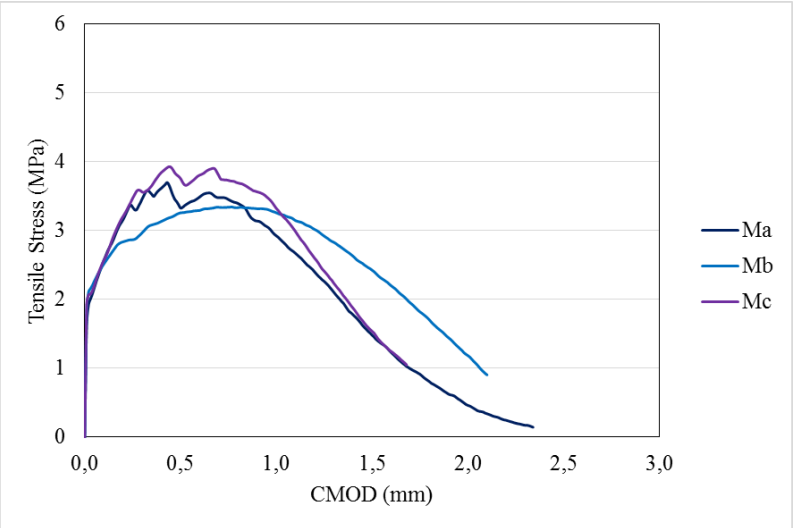

Figure 3. 107- 14 days SCTT results obtained in all mixtures cured in water

28 days

Figure 3.108 shows the SCTT test results after 28 days of curing in tap water. All the specimens showed a similar behaviour. The CMOD ranged between 1.20 and 2 mm. In all mixtures, the specimens showed more than one crack.

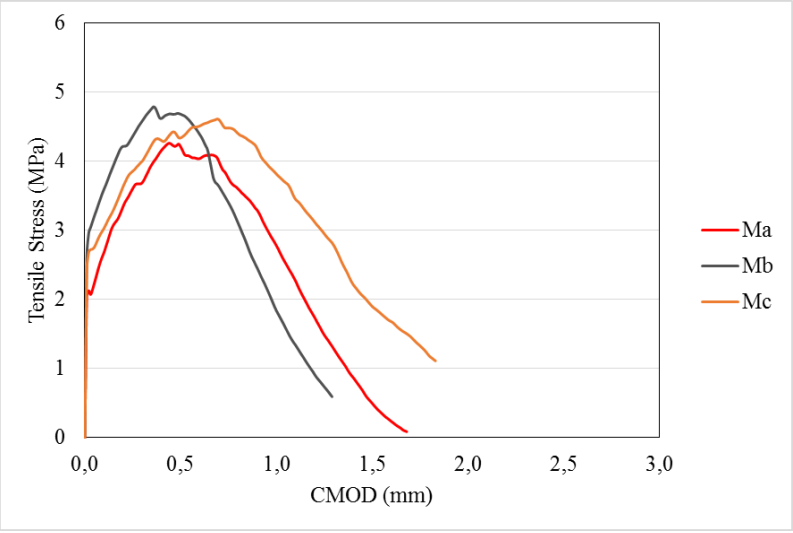

Figure 3. 108- 28 days SCTT results obtained in all mixtures cured in tap water

14 vs 28 days

The SCTT results of the three mixtures when cured in water are presented in Figure 3.109. The specimens tested after 28 days showed higher tensile strengths. In Mixture B the tensile

response also seems to have suffered a significant alteration of shape, translating to a less ductile and more resistant response with the age, which may indicate the formation of less microcraks and a result that is closer to the one searched in this type of test.

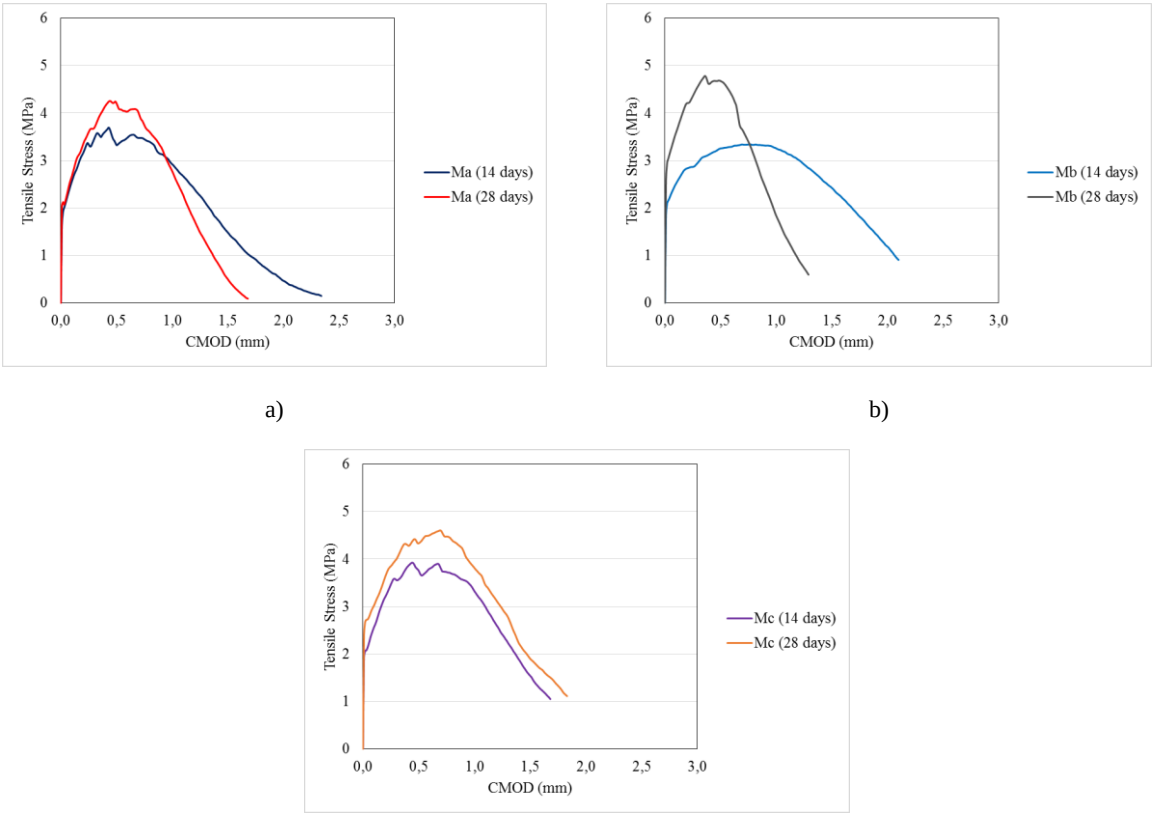

Figure 3. 109- 14 vs 28 days SCTT results cured in water: a) of Mixture A; b) of Mixture B; of Mixture C.

3.5.3.3 Tensile Stress-Strain Behaviour

14 days

The direct tension test results of all mixtures cured in tap water are represented in Figure 3.110.

Mixture C has reached lower tensile strains. However all mixtures cured in tap water reached the minimum requirements for a typical strain-hardening material.

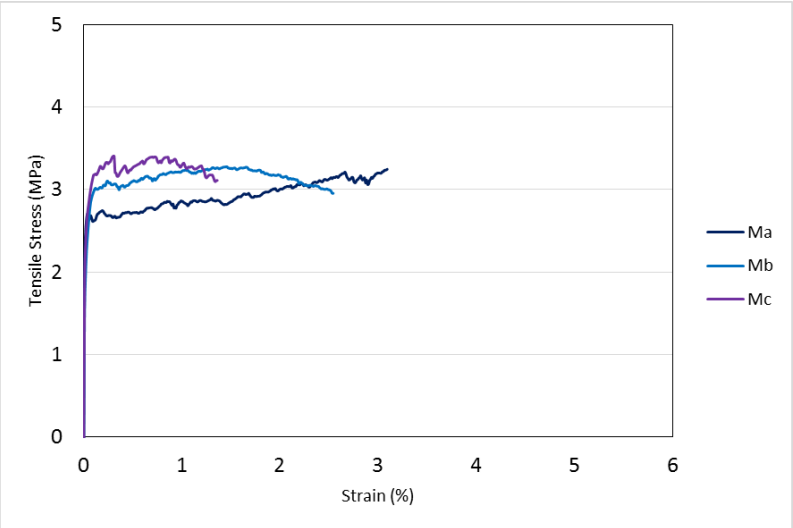

Figure 3.110- Direct tension test results obtained in all mixtures cured in water for 14 days.

Tensile strengths ranged between 3 MPa and 3.5 MPa.

28 days

Figure 3.111 represents the average direct tension test results of all mixtures cured in water. Tensile strengths ranged between 3 MPa and 4.5 MPa.

Mixture A, made with tap water, exhibited the highest strain capacity and reached the highest tensile stress.

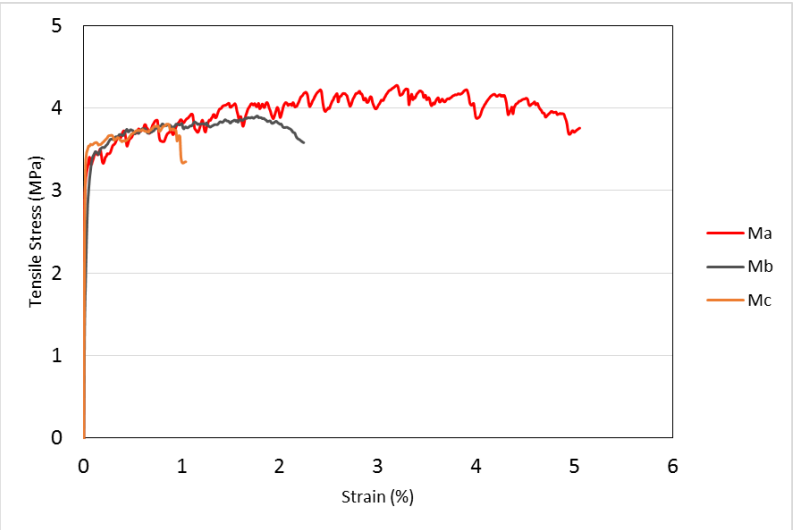

Figure 3. 111- Direct tension test results obtained for all mixtures cured in water for 28 days.

All specimens tested have shown the multiple cracking behaviour.

14 vs 28 days

The comparison between the average results of each mixture after 14 days and 28 days of curing in tap water is shown in Figure 3.112.

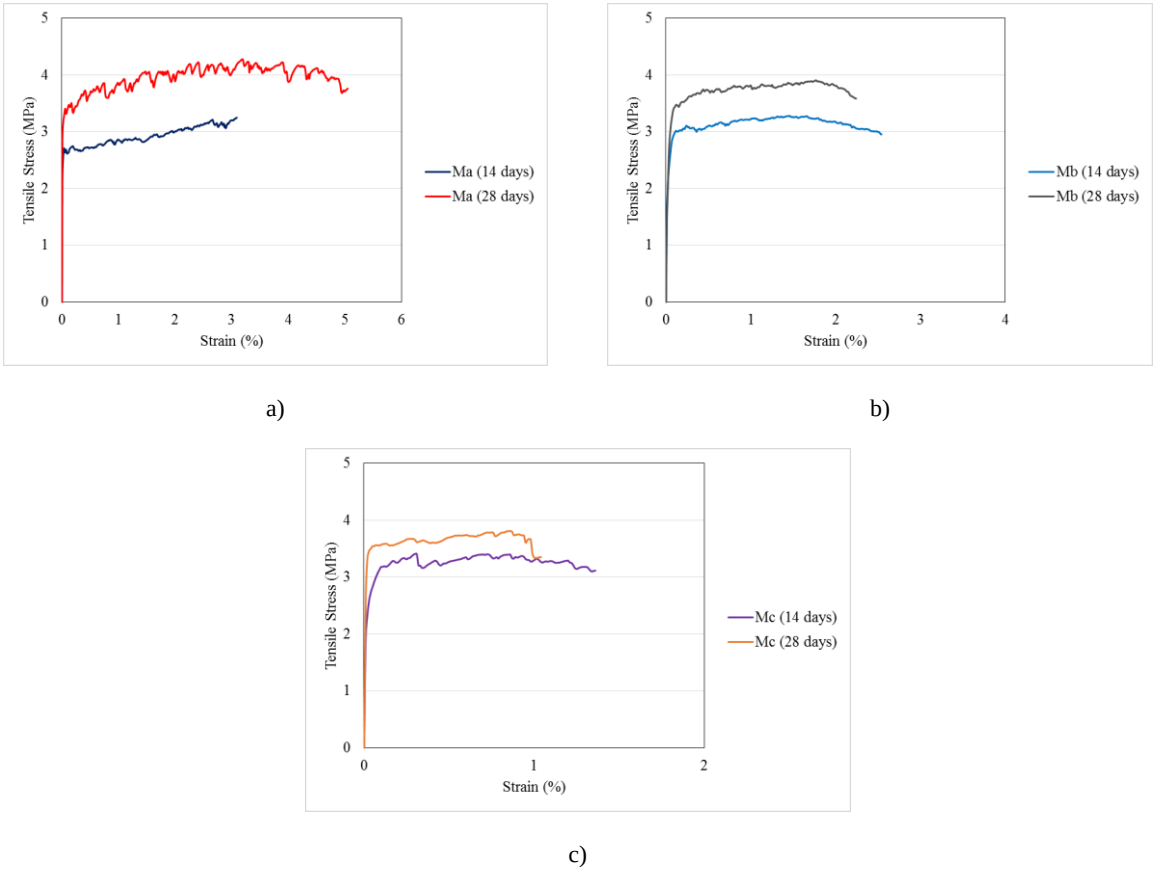

Figure 3. 112- 14 days vs 28 days direct tension test results of specimens cured in water: a) Mixture A; b) Mixture B; c) Mixture C.

The highest tensile stresses were reached at 28 days, with the exception of Mixture A which showed visible sudden stress peaks during the tensile hardening multiple-cracking stage and higher stresses at 14 days.

The water curing may have had a negative influence on the tensile behaviour of Mixture A because with the increase of curing time the tensile capacity and multiple cracking potential reduced. For the other mixtures the curves observed were very similar, although the tensile stresses increased with the age.

3.5.4 Salted water curing

3.5.4.1 Compressive behaviour

14 days

Figure 3.113 shows the average compression test results obtained in all mixtures after 14 days of curing.

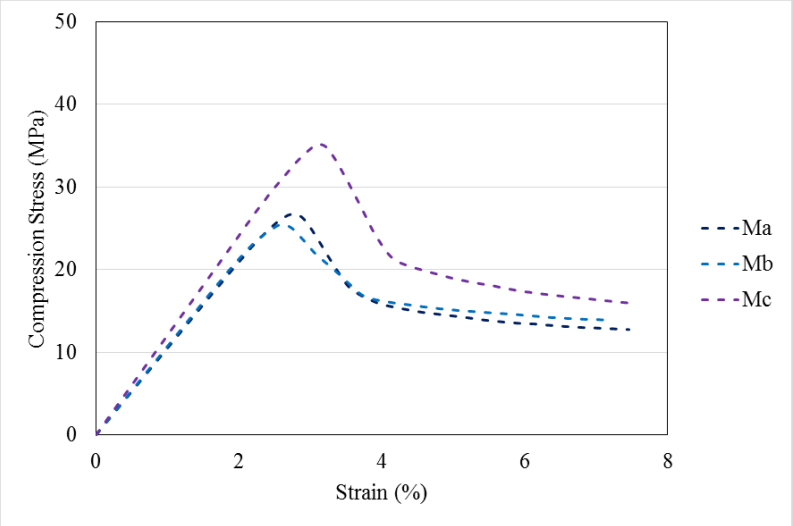

Figure 3. 113- Compression test results of different mixtures cured in salted water for 14 days.

Mixture C has reached the highest compressive strength among all mixtures. The other mixtures have shown essentially similar behaviours. The compressive strengths obtained ranged between 25 MPa and 35 MPa.

The compressive strength and the elasticity modulus of the different mixtures cured in salted water are represented in Figure 3.114. The mixture made with salted water has reached both the highest compressive strength and the highest elasticity modulus.

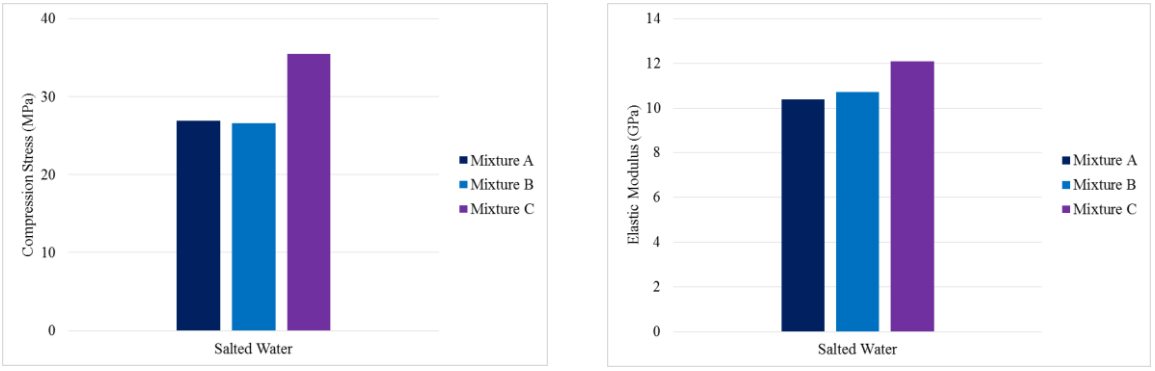

Figure 3. 114- Compressive strength and elasticity modulus of different mixtures cured in salted water for 14 days.

28 days

Figure 3.115 represents the average results of the compression tests of all mixtures cured in salted water.

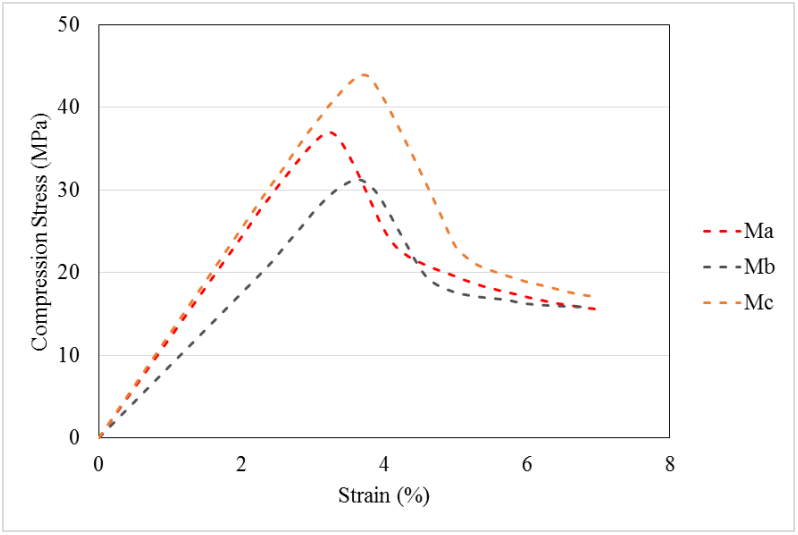

Figure 3. 115- Compression test results of all mixtures cured in salted water for 28 days.

Mixture C as reached both the highest compressive strength and highest elasticity modulus.

Both the average values of compressive strength and of the nominal elasticity modulus of all mixtures are represented in Figure 3.116.

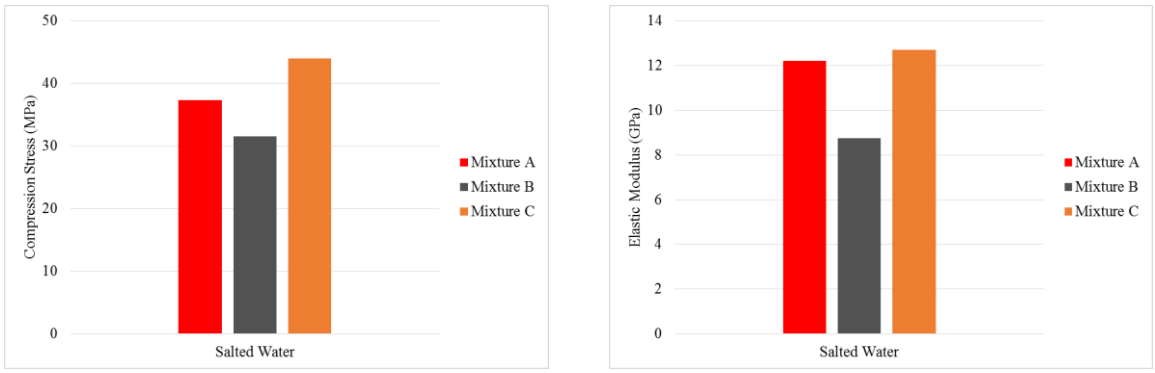

Figure 3. 116- Maximum compressive stress and elasticity modulus of different mixtures cured in salted water (28 days)

14 vs 28 days

Figure 3.117 represents the average compression test results of all mixtures cured in salted water at both ages. The results obtained at 28 days reached higher compressive strengths when compared with the 14 days results.

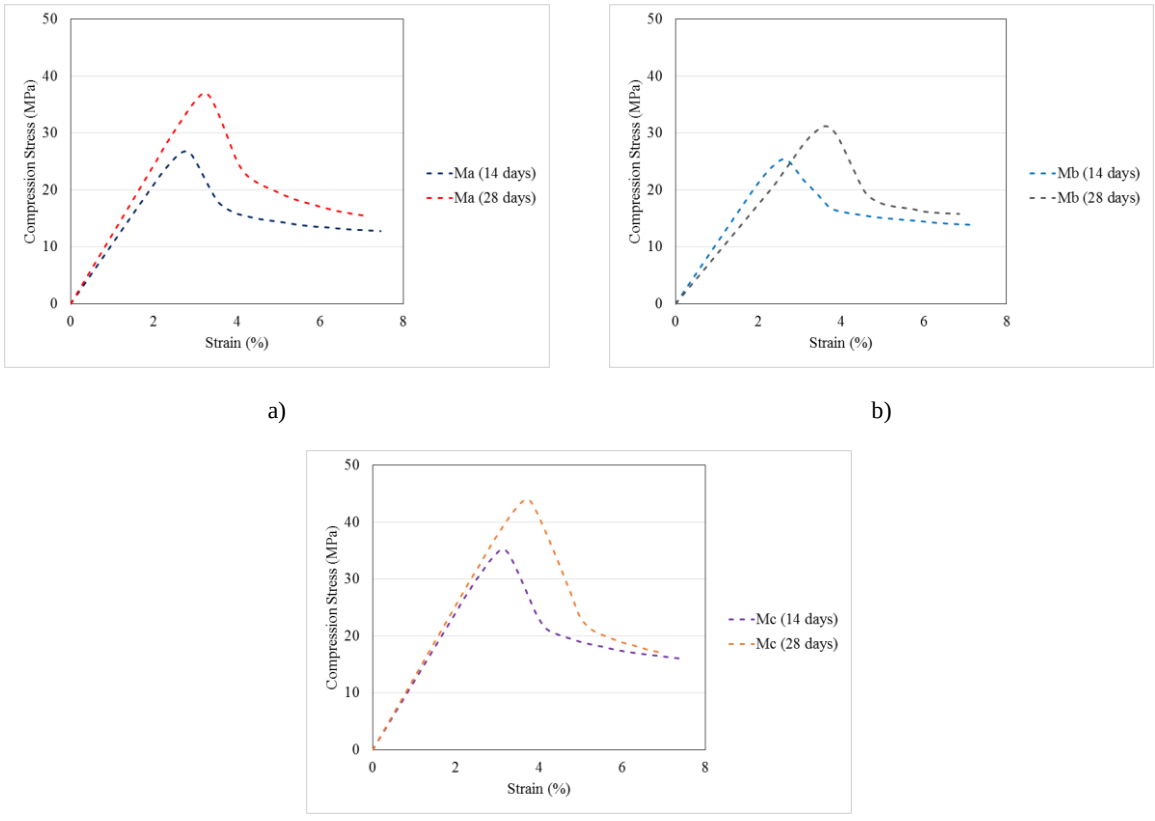

a) b)

c)

Figure 3. 117- 14 days versus 28 days compression test results of specimens cured in salted water: a) Mixture A; b) Mixture B; c) Mixture C

Mixture C showed higher compressive strengths at both ages, when cured in salted water. The opposite happens with Mixture B.

3.5.4.2 Single Crack Tension Test (SCTT)

14 days

Figure 3.118 shows the average SCTT results for all mixtures cured in salted water.

Mixture C has reached the lowest tensile stress values, for also lower CMODs.

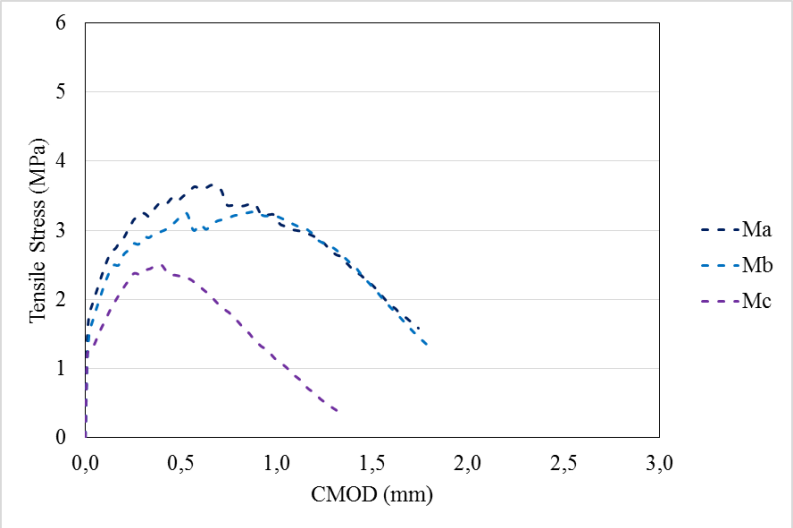

Figure 3. 118- SCTT results obtained in all mixtures cured in salted water for 14 days.

The tensile strength of the matrix ranged between 1 MPa and 2 MPa. Mixture A and B seem to have led to the development of more than one crack before failure.

28 days

The average SCTT results of all mixtures cured in salted water are represented in Figure 3.119. The maximum tensile strength was reached by Mixture B All mixtures have resulted in tensile responses which indicate the formation of more than one crack.

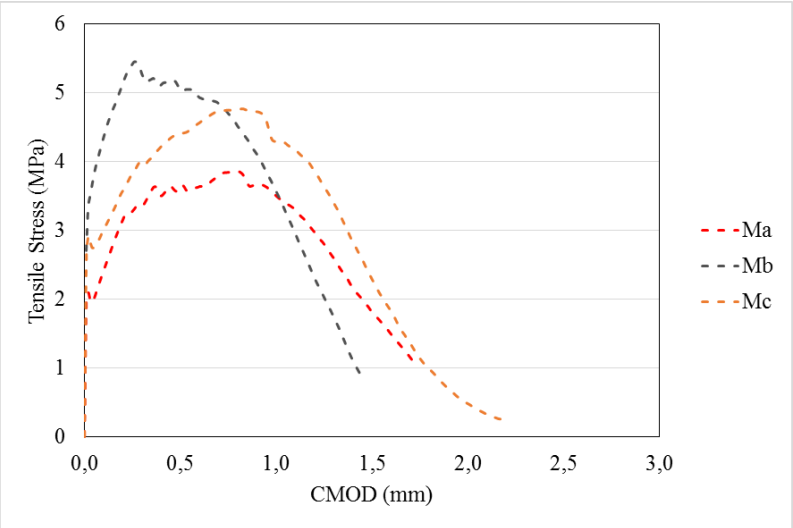

Figure 3.119- SCTT results obtained for all mixtures cured in salted water for 28 days.

14 vs 28 days

Figure 3.120 shows the average SCTT for both ages. At 28 days all specimens developed higher tensile stresses at lower crack mouth opening displacements. This happens because the matrix is more mature. In the case of Mixture C the specimens tested developed not only higher tensile stress but also for higher CMODs at 28 days when compared with 14 days results.

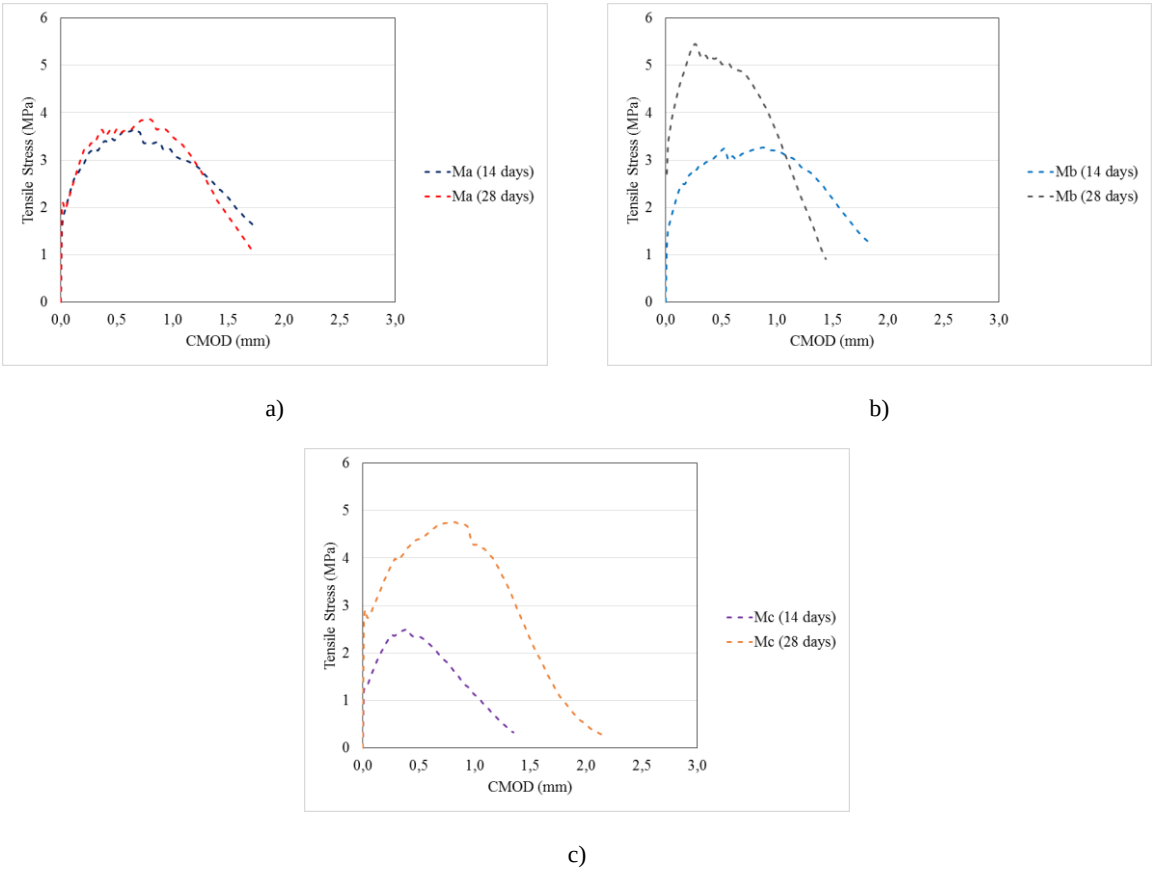

Figure 3. 120- 14 days vs 28 days SCTT results of specimens cured in salted water: a) Mixture A; b) Mixture B; Mixture C.

3.5.4.3 Tensile Stress-Strain Behaviour

14 days

The average direct tension test results of all mixtures cured in salted water are represented in Figure 3.121. Mixture B showed lower strain capacity. Mixture C has reached the highest tensile stress when compared with the other mixtures.

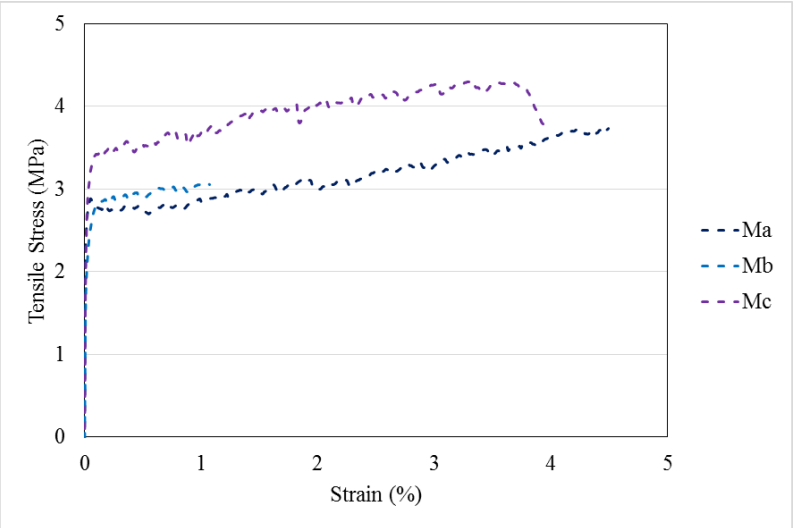

Figure 3. 121- Direct tension test results obtained for all mixtures cured in salted water for 14 days.

28 days

Figure 3.122 shows the average direct tension test results of all mixtures tested at 28 days. Mixture B reached the highest tensile strain capacity. Mixture A and C have shown essentially similar tensile stress-strain responses.

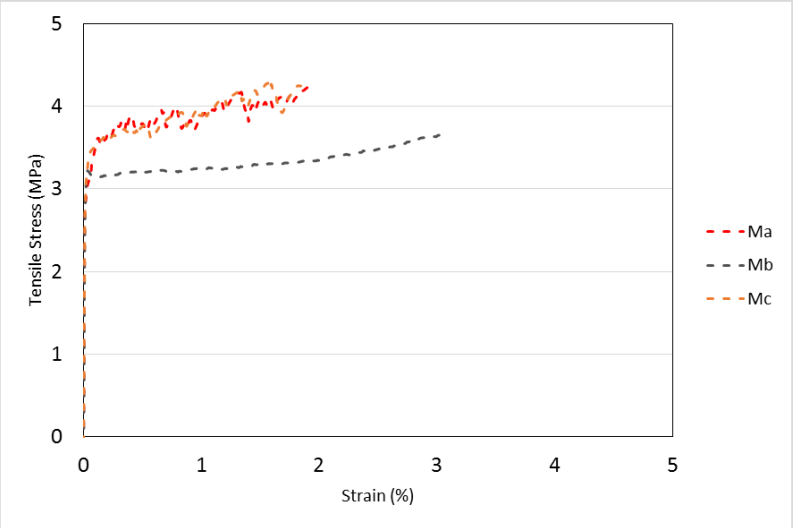

Figure 3.122- Direct tension test results obtained in all mixtures cured in salted water for 28 days.

14 vs 28 days

The comparison between the average direct tension test results at both ages is shown in Figure 3.123. The specimens tested at 28 days have reached, in general, higher tensile stress values. In Mixture B the maximum strain capacity is reached in the 28 days specimens, in contrast to the other mixtures.

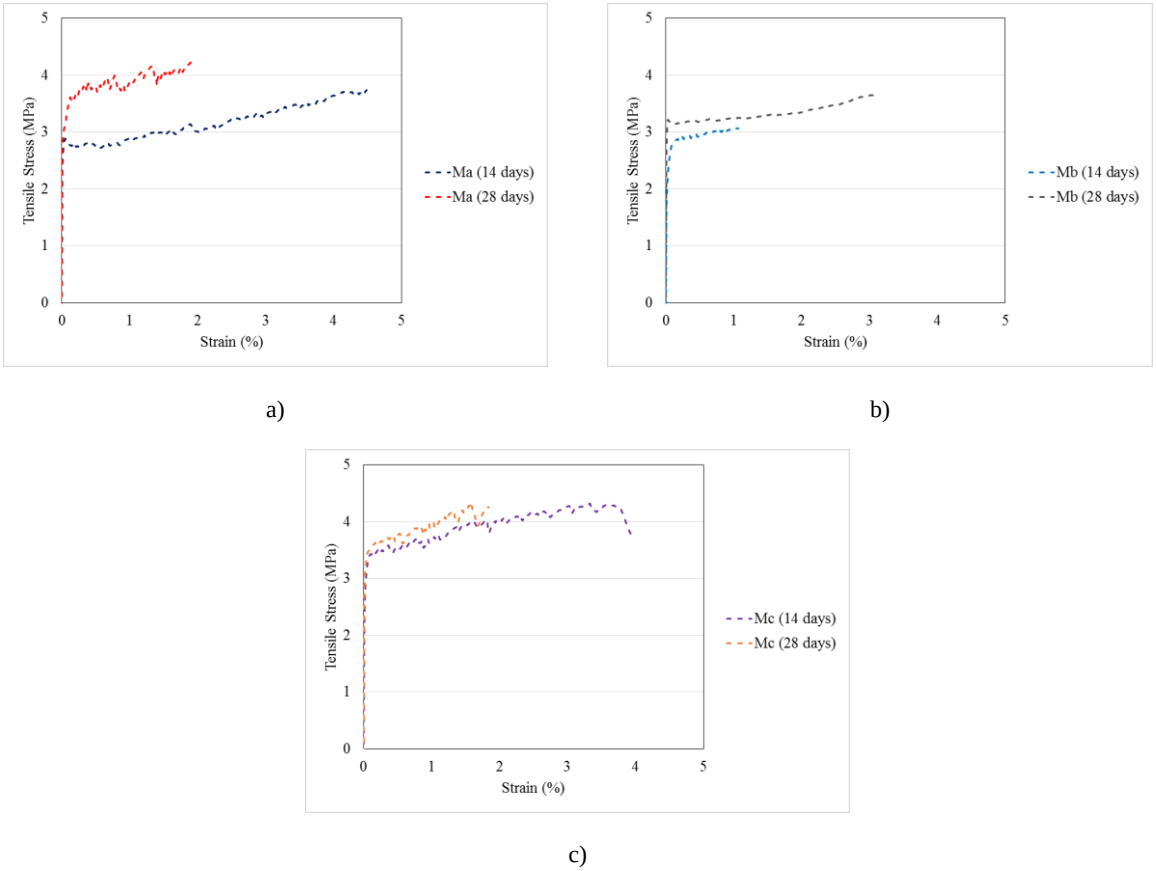

Figure 3.123- 14 days versus 28 days direct tension test results of specimens cured in salted water: a) Mixture A; b) Mixture B; c) Mixture C.

3.6 Conclusions

In this chapter it was confirmed that is possible to replace the water used in ECC materials by seawater and salted water without substantially compromising the typical strain hardening behaviour of ECC materials. However the mechanical behaviour is visibly altered for some types of environment.

The most important characteristic of ECC, multi-cracking behaviour at increasing tensile strains when subject to direct tension, was confirmed in all types of mixtures. In fact, Mixture B

developed tighter crack patterns when subjected to tensile deformations. This can result in the improvement of the durability of structures when ECC materials are used in the in marine environment, due to the ability of the material to control crack opening below extremely low values, well below the 100 μm.

The highest values of compressive strength were achieved by Mixture C (made with salted water). It was shown also that the salted water does not represent well the effect of seawater on ECC mechanical characteristics, since in all perspectives the responses obtained when seawater or salted water were considered have been quite different.

CHAPTER 4

Self-healing

The ability of cementitious materials to self-heal is a characteristic that has been motivating significant research in the recent past. Cementitious material may exhibit different forms of self-healing ability, but in general the underlying process is based on the formation of calcium carbonate precipitates. The process resembles the healing processes observed in living organisms or even humans, for example the one observed in bones when fracture occurs. These processes have inspired, more recently, a few attempts to promote bio mineralization in cementitious composites.

In more conventional concretes, reinforced with fibres or not, spontaneous self-healing may occur mostly when concrete compositions are rich in cement and the concrete elements are immersed in water. However the process assumes a very small scale, mostly because cracks formed easily exceed the scale of tens of micrometers and therefore do not favour the process. In contrast, strain hardening cementitious composites have the ability to control crack widths below these limits during the cracking process. In addition, the traction stresses generated between the opposite cracks planes tend to close the cracks once the loading level is reduced. These and other factors seem combine and create the apparently optimal conditions to promote the spontaneous self-healing at a much larger scale.

In this chapter, considering the need to increase durability and resilience of maritime structures through the microstructural innovation, the capacity of strain hardening cementitious composites to self-heal will be evaluated considering the compositions characterized in the previous chapter. For that purpose, the cracking processes occurring in specimens subjected to uniaxial tension test will be documented using digital imaging analysis. After 14 days of curing an initial procedure for pre-cracking the specimens is carried out, after which the specimens are taken back to the curing environment. After 28 additional days of curing the specimens are tested again using the uniaxial tension test procedure and, by analysing the tensile responses and comparing it before and after the second stage of curing, it is possible to distinguish mechanical effects of the self-healing process such as the recovery of stiffness up to certain tensile stress levels.

4.1 Materials and Compositions

In this study, two different mixtures were used. The materials and quantities used in this work are presented in Table 4.1:

Table 4. 1- Mixtures compositions

	Mb	***Mc***
Materials	g	g
Cement	829,8	836,9
Fly Ash	1639,7	1653,7
Sand	290,4	292,9
Filler	290,4	292,9
Tap Water		657,9
Seawater	589,9	
SP 3002	93,9	31,6
VMA	2,5	2,5
PVA Fibre	52	52
Salt (NaCl)		19,7

These mixtures are similar to the ones used in the previous chapter. The mixing procedure and their fresh behaviour were explained in sections 3.1.2 and 3.1.3 of Chapter 3.

4.2 Specimens and curing environments

The specimens used for direct tension testing were cast using the dogbone-shaped moulds. This moulds are 20 mm thick, 370 mm long and 100 mm wide (the central part is 50 mm wide and 110 mm long), as shown in the previous chapter.

Air, seawater and salted water were used as curing environments for the different specimens, according to the procedures described in the previous chapter. Mixture B specimens were cured in air and seawater and the Mixture C specimens were cured in air and salted water.

4.3 Compressive behaviour of Mixtures B and C

In the previous chapter the characterization of the compressive behaviour of Mixtures B and C were already carried out. Table 4.2 summarizes the compressive strengths obtained at 14 days.

Table 4. 2-Compressive strength of Mixtures B and C after 14 days of curing.

	Cure	Specimen	Compressive Stress (MPa)	Average (MPa)
Mixture B	Air	Mb_14	25,34	27,90
		Mb_15	29,69	
		Mb_16	28,68	
	Seawater	Mb_18	24,14	23,90
		Mb_20	23,05	
		Mb_21	24,52	
Mixture C	Air	Mc_18	35,56	34,72
		Mc_19	32,86	
		Mc_20	35,74	
	Salted Water	Mc_30	35,26	35,48
		Mc_31	36,17	
		Mc_32	35,00	

In order to assess the self-healing processes, in this chapter the specimens were first tested in direct tension at 14 days and then at 42 days, which means 30 days after the pre-damage, as described in the subsequent sections. Therefore, with the aim of knowing the compressive behaviour of the mixtures studied in this chapter also at 42 days, cubic specimens of both mixtures were prepared and tested. Six specimens of each mixture were prepared. The procedure adopted for the compression test was explained in section 3.2.1.

In Figure 4.1 the compression test results of Mixture B are represented. For each type of curing three specimens were tested.

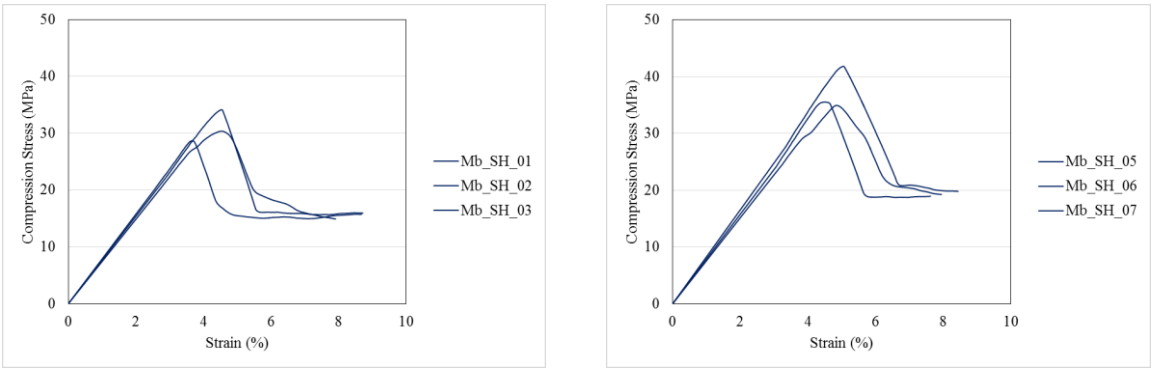

a) b)

Figure 4. 1- Compression test results at 42 days of Mixture B: a) cured in air; b) cured in seawater.

Figure 4.2 are represented the compressive results of Mixture C. For each type of cure, air or salted water, three specimens were tested.

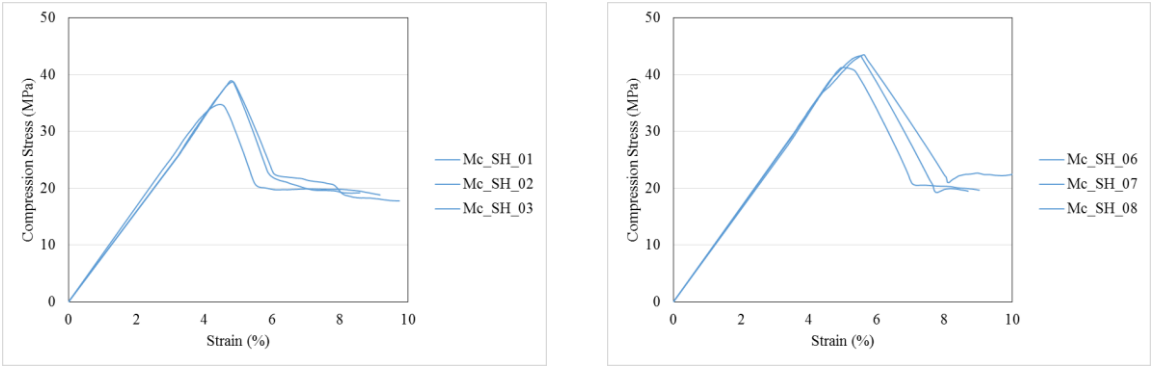

Figure 4. 2- Compression results at 42 days of Mixture C: a) cured in air; b) cured in salted water

All specimens showed the typical compression behaviour of this type of materials: the post-peak behaviour tends to descend more gently when compared with concrete, due to the effect of crack restraining provided by the fibre reinforcement.

Table 4. 3- Maximum compression stress of each specimen tested

	Cure	Specimen	Stress (Mpa)	Average (Gpa)	Standard Desviation	Coefficient Variation
Mixture B	Air	Mb_SH_01	34,14	31,06	2,28	7
		Mb_SH_02	28,68			
		Mb_SH_03	30,36			
	Seawater	Mb_SH_04	41,81	37,43	3,11	8
		Mb_SH_05	34,94			
		Mb_SH_06	35,53			
Mixture C	Air	Mc_SH_01	38,75	37,47	1,93	5
		Mc_SH_02	34,75			
		Mc_SH_03	38,92			
	Salted Water	Mc_SH_06	43,32	42,69	1,02	2
		Mc_SH_07	41,25			
		Mc_SH_08	43,50			

The highest compressive stress was reached by Mixture C, in both ages, when cured in salted water.

4.4 Tensile behaviour of Mixture B

Mixture B was prepared using seawater, as previously mentioned. The specimens were demoulded after 24 h and then 6 specimens were cured in air (inside of a climatic chamber) and the other 6 specimens were cured in seawater. After 14 days of curing the specimens were divided into two groups and each group was subjected to a different stage of pre-loading. After pre-loading, the specimens were placed back in the respective curing environments for 28 days more. The uniaxial tensile test was then used to assess the process of self-healing and the magnitude of recovery of the initial mechanical properties. The procedure used to perform the uniaxial tension test was explained in section 3.2.3.

4.4.1 Pre-loading up to 0.75% of tensile strain

As explained before, two different stages of pre-loading were used. In this section, all the specimens were pre-load until the central part of the specimens reached 0.75% of tensile strain. For measuring the displacement of the specimens and computing tensile strain of the central part, two LVDT's were used during testing. Three specimens were tested for each type of curing environment.

Specimens cured in Air

In this section the specimens were air cured for a total period of 42 days. Figure 4.3 represents the entire tensile response obtained. During the pre-loading phase the responses showed the typical behaviour of ECC materials: the development of an initial stage of high tensile stiffness until the formation of the first crack, and after that the initiation of the multiple cracking stage, during which the moderate tensile hardening occurs with the formation of multiple cracks.

After the pre-loading up to a tensile strain of 0.75%, the specimens were cured for 28 days more in the climatic chamber. During that time, the cracks that exist from the pre-loading stage partially close and the specimen recovers some of its initial high stiffness. That process is called self-healing. When the specimens are subjected to tensile loading again the response shows initially the total recovery of the previous tensile stiffness. Subsequently, while the tensile stress increases, at a certain level of stress the cracks that, during the 28 days of cure, were fully repaired, start to open again and the recovered stiffness is lost. At a later stage new cracks start

to form in regions of the matrix that were left intact in the previous stage, and a strain-hardening response is obtained again until failure.

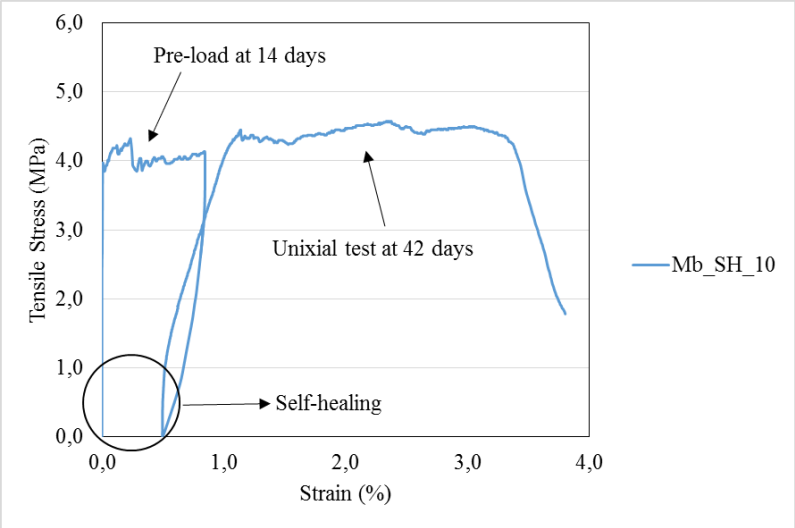

Figure 4. 3- Uniaxial tensile results of one specimen cured in air

All the specimens tested have shown the ability to regenerate, recovering the initial stiffness until a tensile stress of 0.7 MPa was again reached during the second loading cycle.

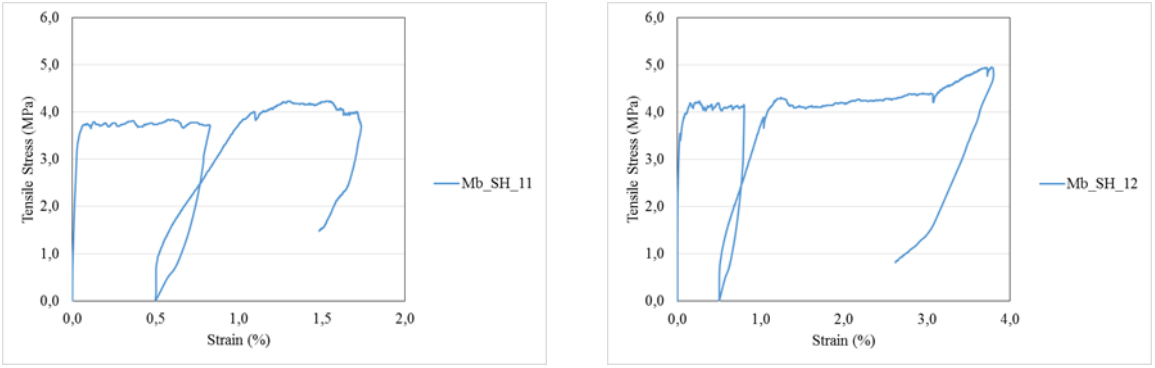

Figure 4. 4- Tensile results of the other two specimens tested

The first crack stress (σc), the maximum stress (σm) and the maximum tensile strain (εm) of each specimen tested are presented in Table 4.4.

Table 4. 4- Main characteristics of all specimens tested cured in air

Specimen	σc (MPa)	σm (MPa)	εm (%)
Mb_SH_10	3,97	4,57	3,80
Mb_SH_11	3,73	4,23	1,74
Mb_SH_12	3,55	4,95	3,80

Specimens cured in seawater

The specimens cured in seawater were pre-loaded until reaching 0.75% of tensile strain is achieved, after 14 days of curing. Subsequently, the specimens were submerged in seawater for 28 days more. The uniaxial tensile test showed that the specimens tested has practically fully healed, recovering the initial stiffness up to tensile stress levels very close to the maximum previously experienced. In Figure 4.5 it is possible to confirm that the specimen recovered the initial stiffness until 2.30 MPa of tensile stress was again reached.

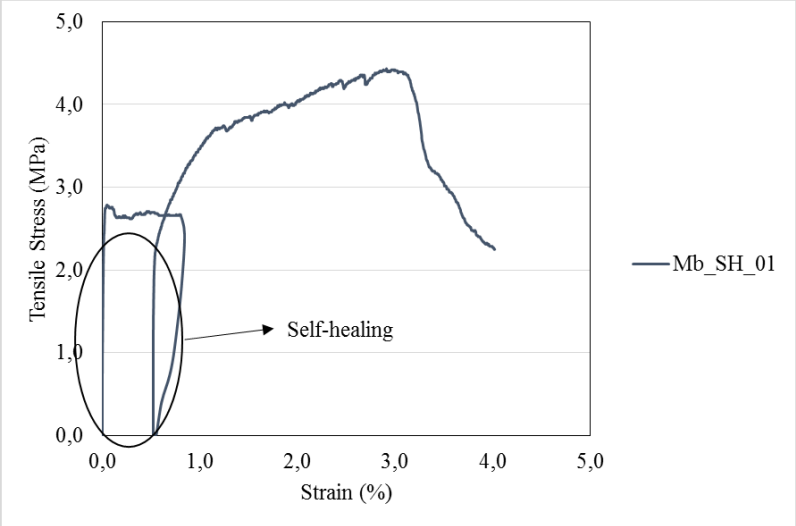

Figure 4. 5- Uniaxial tensile test results of one of the specimens cured in seawater.

All the specimens showed a practically similar behaviour. After the initial recovery of stiffness, the specimens showed the steady increase of tensile stress until the maximum tensile strain was reached. Additionally, it seems that after the additional 28 days of curing the specimens have established a new strain hardening plateau, at tensile stresses significantly higher (about 1 MPa more).

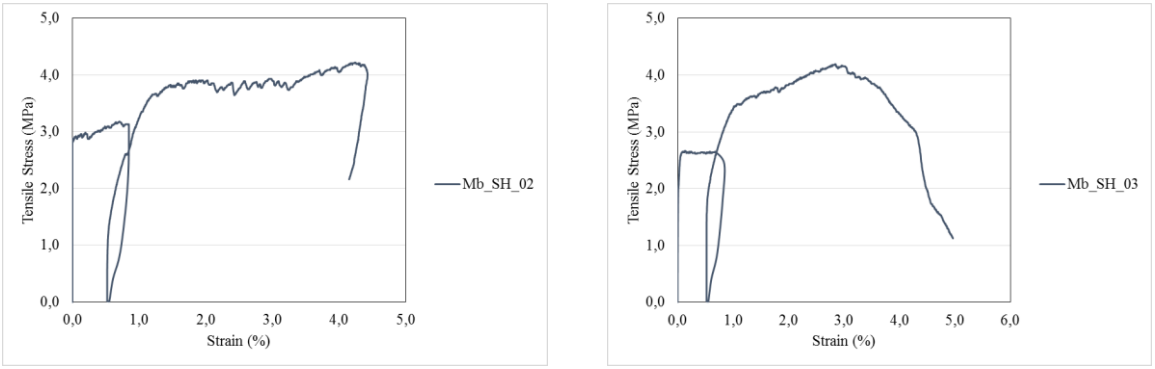

Figure 4. 6- Uniaxial tensile test results of the other two specimens cured in seawater.

The first cracking stress (σc), the maximum stress (σm) and the maximum tensile strain (εm) of the specimens cured in seawater are presented in Table 4.5.

Table 4. 5- Main tensile characteristics of all specimens cured in seawater.

Specimen	σc (MPa)	σm (MPa)	εm (%)
Mb_SH_01	2,79	4,43	4,02
Mb_SH_02	2,89	4,22	4,43
Mb_SH_03	2,65	4,19	4,96

4.4.2 Pre-loading up to 1.5 % of tensile strain

Specimens of the same compositions were also subjected to a preloading procedure that reached 1.5% of imposed tensile strain. Three specimens were tested for each type of curing environment.

Specimens cured in air

Figure 4.7 is represented the tensile behaviour obtained for the first specimen tested. The pre-loading phase, which has occurred after 14 days of curing, has shown as before an initial elastic behaviour until the formation of first crack. After that, the specimen developed multiple cracks until the 1.5% of strain is reached. When the specimen was tested up to failure, after 28 more days of curing, exhibited self-healing behaviour by recovering the initial stiffness up to a tensile stress of 0.65 MPa. After that, the previously formed and healed cracks start to reopen, and when the tensile stress of 4.3 MPa is reached new cracks start to form, until failure is reached.

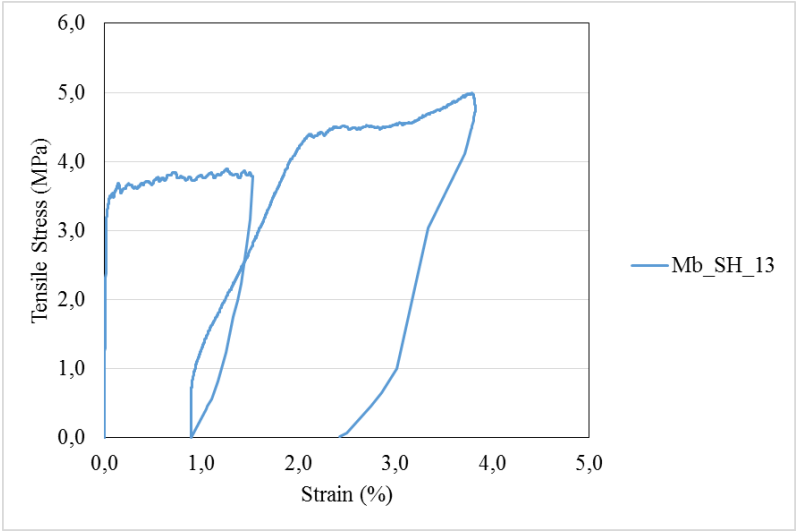

Figure 4. 7- Tensile results of one specimen tested cured in air

The tensile results of the other two specimens are represented in Figure 4.8. In these two cases the full recovery of the initial stiffness was maintained up to a tensile stress level of 0.7 MPa.

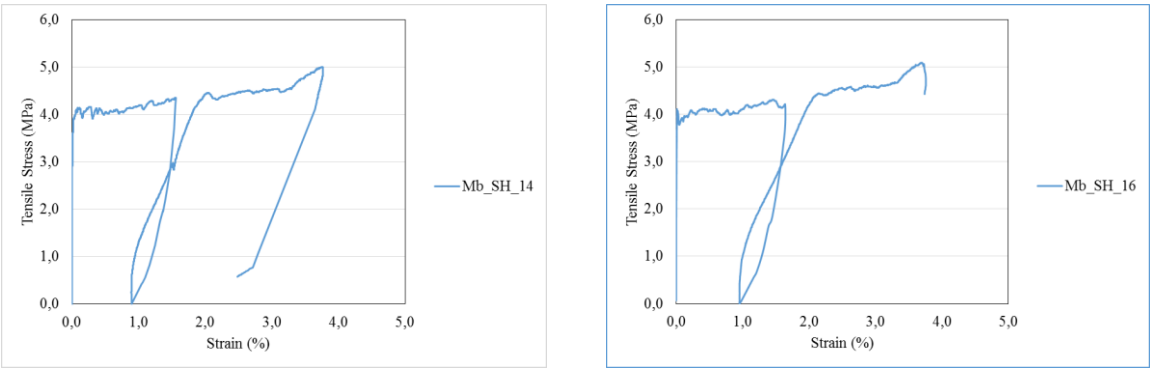

Figure 4. 8- Tensile results of the other two specimens tested cured in air

In Table 4.6 the main tensile results are summarized.

Specimen	σc (MPa)	σm (MPa)	εm (%)
Mb_SH_13	3,48	5,00	3,83
Mb_SH_14	3,91	5,00	3,77
Mb_SH_16	4,11	5,09	3,76

Table 4. 6- Main tensile characteristics of all specimens cured in air.

Specimens cured in seawater

Following the same procedure of pre-loading the specimens the 1.5% of tensile strain was reached, the specimens cured in sweater were also tested. After the pre-loading procedure after 14 days of curing, as before the specimens were submerged in seawater for 28 days more. The uniaxial tensile results showed that the recovered initial stiffness was preserved in the second loading cycle until the tensile stress of 1.5 MPa was reached. Figure 4.9 shows the behaviour of the first of three specimens cured in seawater.

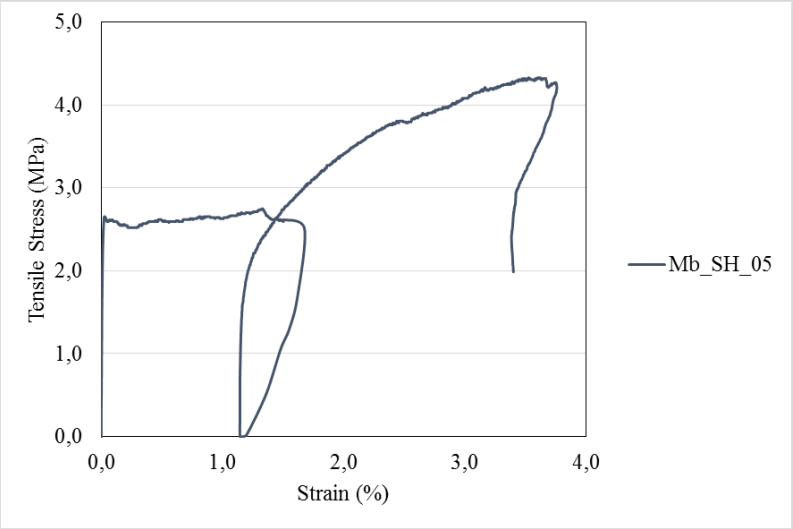

Figure 4. 9- Uniaxial tensile test results of one of the specimens cured in seawater.

The other two specimens tested have shown similar behaviours and sustained the self-healed properties until reaching 1.3 MPa of tensile stress. The tensile results of the other two specimens are represented in Figure 4.10.

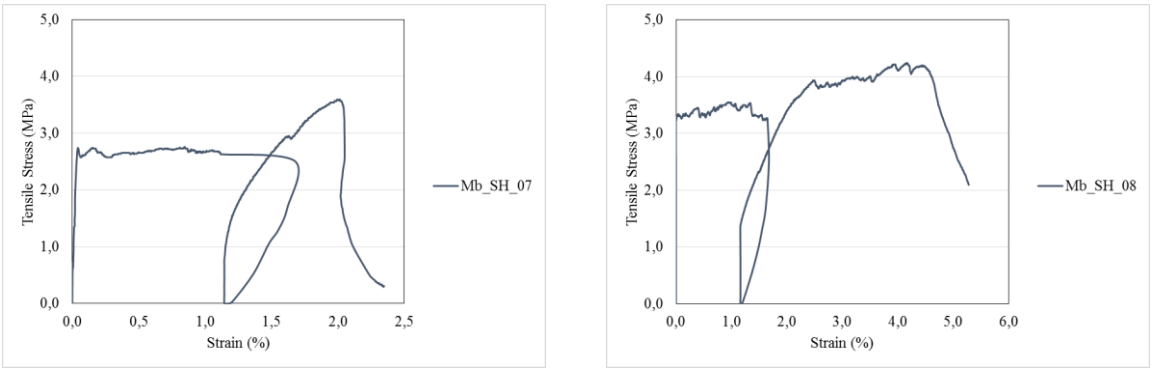

Figure 4. 10- Uniaxial tensile test results of the other two specimens cured in seawater.

In Table 4.7 the main tensile results are summarized.

Table 4. 7- Main tensile characteristics of all specimens cured in seawater.

Specimen	σc (MPa)	σm (MPa)	εm (%)
Mb_SH_05	2,65	4,33	3,76
Mb_SH_07	2,73	3,59	2,35
Mb_SH_08	3,18	4,24	5,29

4.5 Tensile behaviour of Mixture C

Mixture C was prepared using salted water in the composition. The six specimens were demoulded 24 h after casting and then cured in air (inside of a climate chamber at 20º of temperature and 60% of relative humidity), as before. Six other specimens were cured in salted water. After 14 days of curing, the two groups of specimens were subjected to two different pre-loading procedures reaching 0.75% and 1.5% of tensile strain respectively, as explained in the previous section. After pre-loading, the specimens were placed back in the respective curing environments for 28 days more. The uniaxial tensile test was carried out in all specimens after a total of 42 days of curing. The testing procedure used was explained in section 3.2.3.

4.5.1 Pre-loading up to 0.75% of tensile strain

In this section, all the specimens were pre-loaded until the specimen reached 0.75% of tensile strain. Three specimens were tested for each type of curing.

Specimens cured in air

The specimens were air cured for 42 days. At 14 days, all the specimens were pre-loaded until a tensile strain of 0.75% was reached. Figures 4.11 and 4.12 show the tensile responses obtained. The pre-loading phase shows the typical initial high stiffness stage with a rapid increase of tensile stress until the formation of the first crack, and after that the strain hardening behaviour with the formation of multiple cracks is obtained. At 42 days, all the specimens were tested until failure was achieved. In Figure 4.11 it is possible to confirm that the cracks formed during the pre-loading stage undergo a self-healing process and the specimen recovers some of

the initial high stiffness. The specimen retained the recovered stiffness until a tensile stress of 0.7 MPa was again reached.

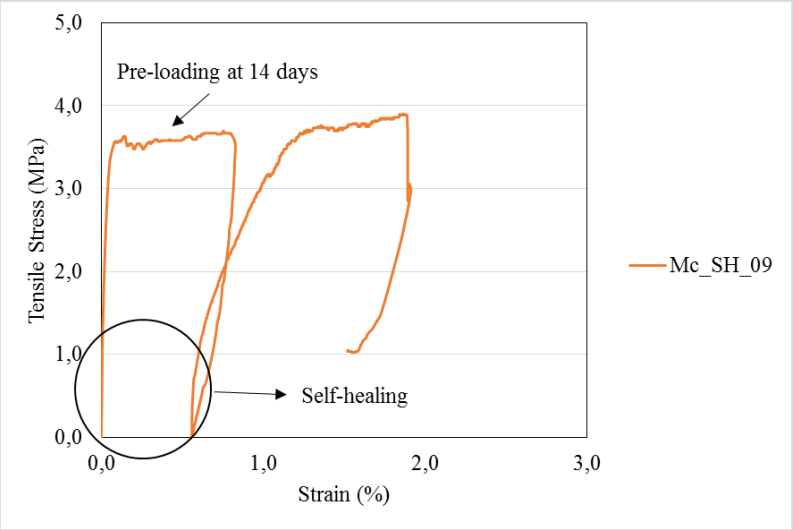

Figure 4. 11- Uniaxial tensile test results of one of the specimens cured in air.

The other two specimens tested have shown essentially similar tensile responses and preserved the recovered initial stiffness until 0.6 MPa of tensile stress was again reached. The tensile results of the other two specimens are represented in Figure 4.12.

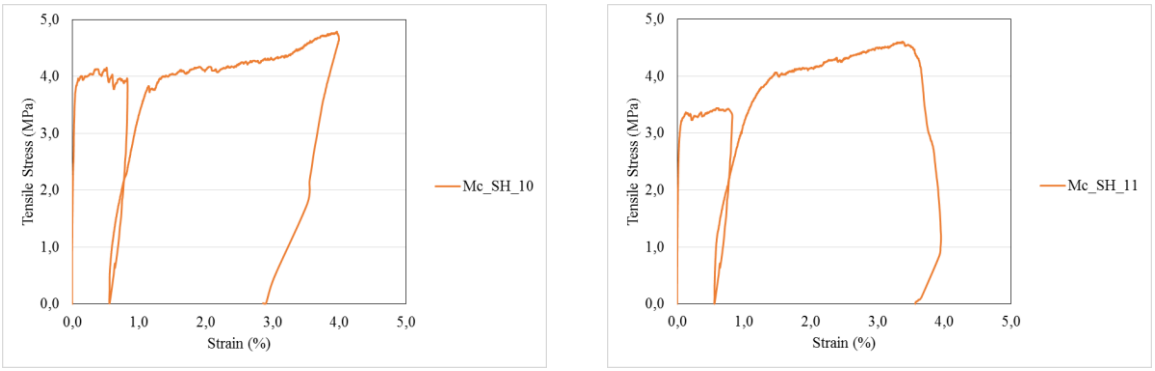

Figure 4. 12- Uniaxial tensile test results of the two other specimens cured in seawater.

The main tensile results obtained are presented in Table 4.8.

Table 4. 8- Main tensile characteristics of all specimens cured in air.

Specimen	σc (MPa)	σm (MPa)	εm
Mc_SH_09	3,57	3,90	1,91
Mc_SH_10	3,96	4,79	4,00
Mc_SH_11	3,22	4,61	3,95

Specimens cured in salted water

The specimens cured in salted water were pre-loaded until a tensile strain of 0.75% was reached, after 14 days of curing. Subsequently, the specimens were submerged in salted water for 28 days more. The uniaxial tensile test responses obtained showed that the specimens tested have recovered the initial stiffness until 1.3 MPa of tensile stress was again reached.

Figure 4.13 shows the tensile response obtained for the first specimen tested.

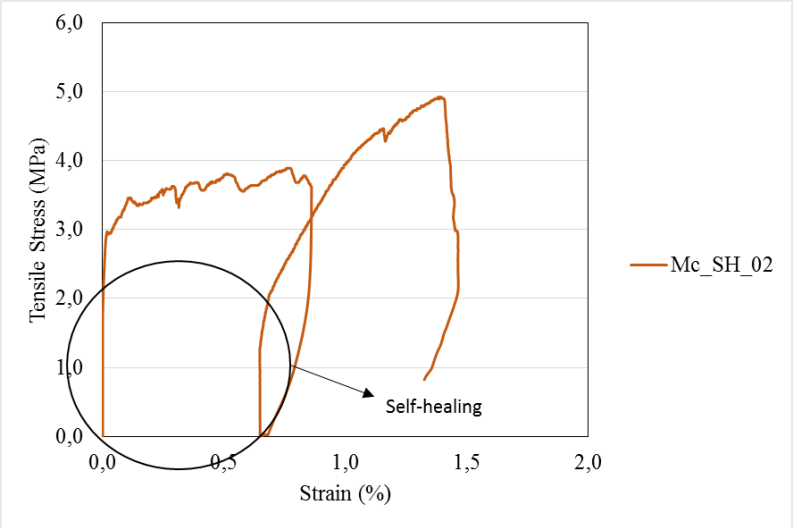

Figure 4. 13- Uniaxial tensile test results of one of the specimens cured in salted water..

The specimen Mc_SH_03 recovered the initial stiffness and preserved it until the tensile stress of 1 MPa was again reached, and after that has showed higher tensile stress values between the reopening of the old cracks and the formation of new cracks. This increase can be explained by the fact that the matrix has become more mature. However, specimen Mc_SH_04 has shown a different behaviour. The specimen preserved the recovered initial stiffness until a tensile stress of 1.2 MPa was again reached and, after that, the old cracks started to reopen. The tensile results of these two specimens are represented in Figure 4.14.

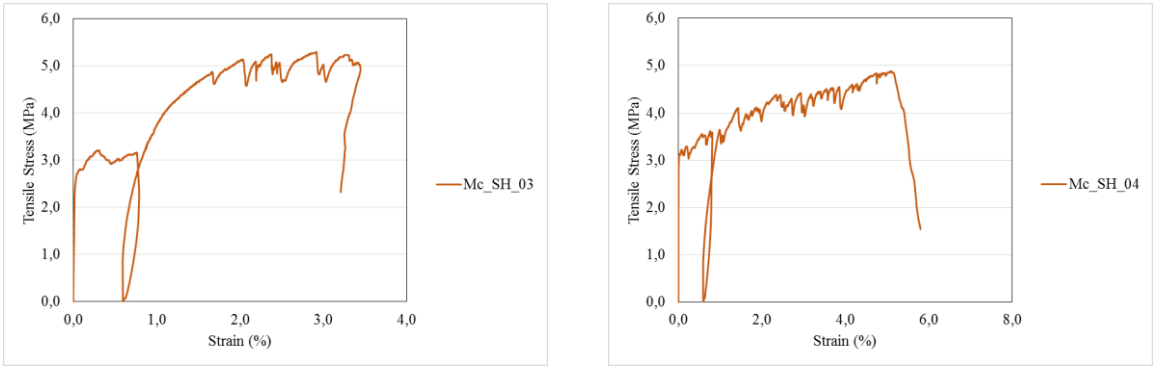

Figure 4. 14- Tensile results of the other two specimens tested

In Table 4.9 other important properties are presented, such as the first cracking stress, the maximum tensile stress and the maximum tensile strain.

Table 4. 9- Main tensile characteristics of all specimens cured in salted water.

Specimen	σc (MPa)	σm (MPa)	εm (%)
Mc_SH_02	2,97	4,93	1,47
Mc_SH_03	2,81	5,29	3,45
Mc_SH_04	3,13	4,88	5,80

4.5.2 Pre-loading up to 1.5% of tensile strain

In this section all the specimens were pre-load until the specimen reached 1.5% of tensile strain, instead of 0.75% as previously.

Specimens cured in air

Figure 4.15 represents the tensile behaviour of one specimens tested. In this case, when the specimen was tested 28 days after the additional curing, the old cracks started to reopen at 0.3 MPa of tensile stress. When the tensile stress reached 4.1 MPa new cracks started to appear until the maximum tensile stress was achieved.

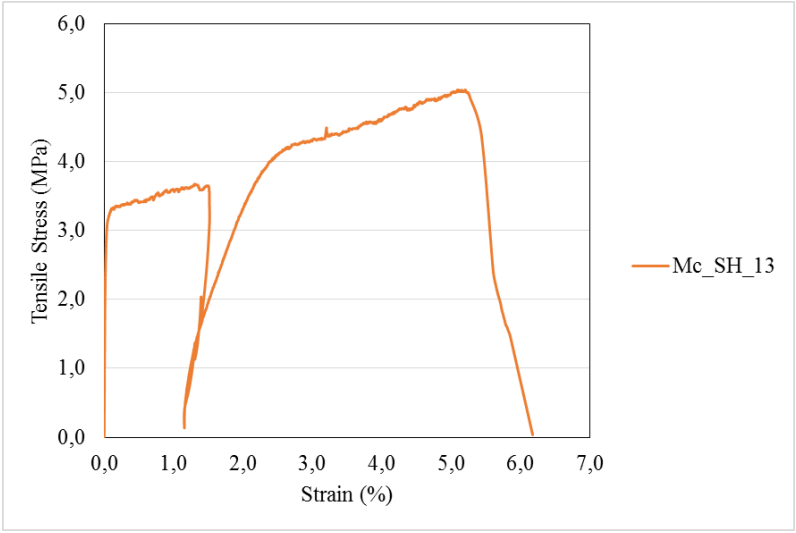

Figure 4. 15- Uniaxial tensile test results of one of the specimens cured in air.

The other two specimens tested showed higher tensile stresses at which the recovered stiffness is lost. Both specimens recovered the initial high stiffness until a tensile stress of 0.8 MPa was again reached. The tensile results of both specimens are represented in Figure 4.16.

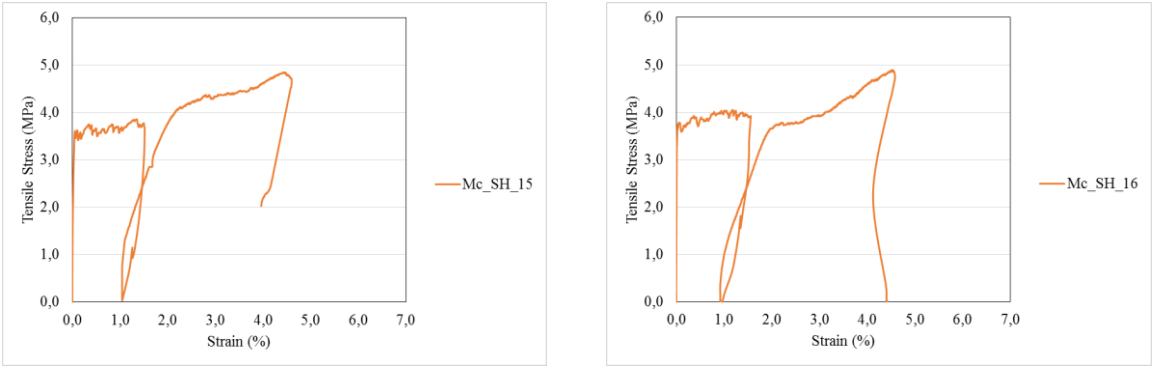

Figure 4. 16- Uniaxial tensile test results of the other two specimens cured in air.

The first cracking stress, the maximum tensile stress and the maximum tensile strain of all specimens are presented in Table 4.10.

Table 4. 10- Main tensile characteristics of all specimens cured in air.

Specimen	σc (MPa)	σm (MPa)	εm (%)
Mc_SH_13	3,32	5,04	6,17
Mc_SH_15	3,61	4,84	4,60
Mc_SH_16	3,63	4,89	4,58

Specimens cured in salted water

As previously, Mixture C specimens were pre-loaded until a tensile strain of 1.5% was reached. After pre-loading, the specimens were submerged in salted water for 28 days more. Figure 4.17 shows the tensile response of Mc_SH_05 specimen, which was cured in salted water. The uniaxial tensile response showed the ability to retain the recovered initial stiffness until a tensile stress of 1.3 MPa was again reached.

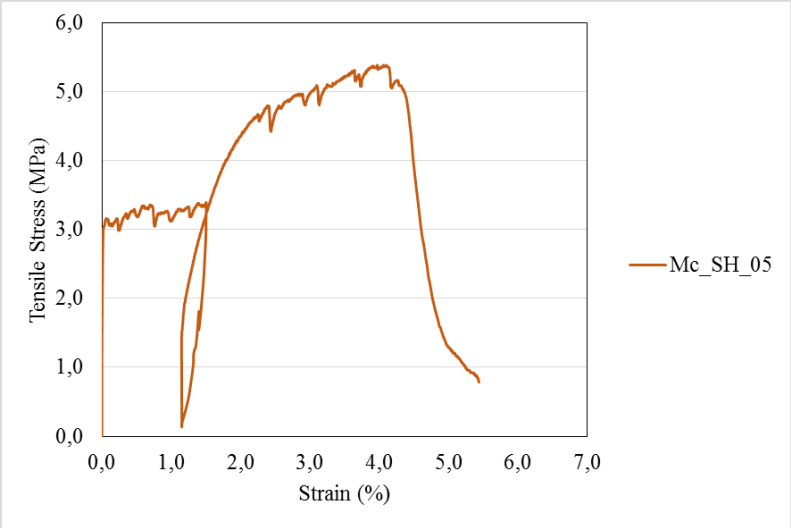

Figure 4. 17- Uniaxial tensile test results of one of the specimens cured in salted water.

The other two specimens tested showed self-healing behaviour until 1.5 MPa as it is possible to confirm in Figure 4.18.

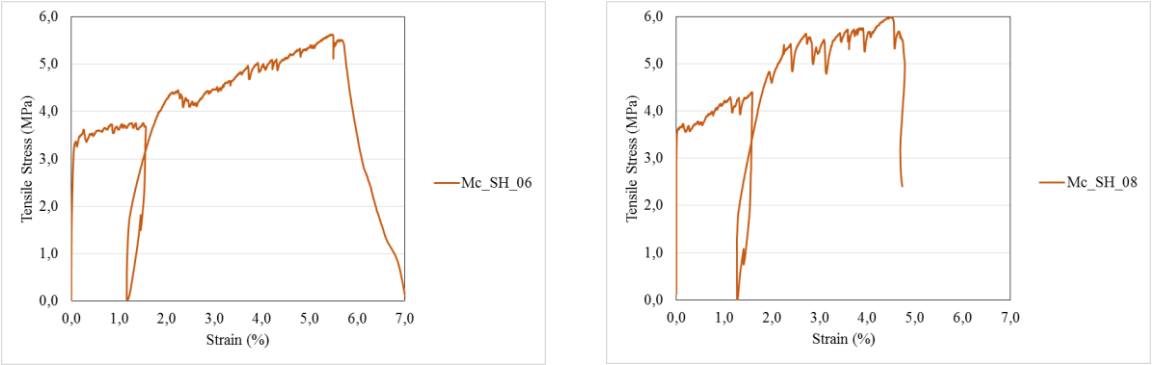

Figure 4. 18- Uniaxial tensile test results of the other two specimens cured in salted.

Table 4.11 summarizes the main tensile results obtained.

Table 4. 11 Main tensile characteristics of all specimens cured in salted water.

Specimen	σc (MPa)	σm (MPa)	εm (%)
Mc_SH_05	3,14	5,39	5,44
Mc_SH_06	3,36	5,62	7,09
Mc_SH_08	3,64	5,99	4,79

4.6 Digital image analysis and documentation of the cracking processes

Independently of the tensile stress levels and the overall deformations reached, the cracking processes established in each of the composites tested may be influenced by both the curing environment and the type of water used in its composition. Cracking processes are even more sensitive to these and other parameters, therefore their thorough characterization is essential for the full understanding of the effect of seawater or salted water on the tensile behaviour of strain hardening cementitious composites.

In this section the crack patterns developed during the tensile tests conducted to assess the self-healing response are characterized using digital image analysis. As previously shown, two different types of pre-loading schemes and two different types of curing were studied. The digital image analysis was conducted using Digital Image Correlation (DIC) algorythms. DIC is a non-contact measurement method to analyse surface displacement within an area of interest of an object. Digital images during pre-loading (at 14 days) and during the final failure testing (at 42 days) were captured and compared in terms of the grey level of each pixel. The two major purposes of using DIC analysis in the present study were to obtain visual images of multiple cracking pattern development, and to compute crack width distributions.

Mixture B

Figure 4. 19 shows the results obtained for one of the specimens cured in air and pre-loaded at 0.75% of strain. The main stages of the entire loading sequence are identified and numbered over the tensile response.

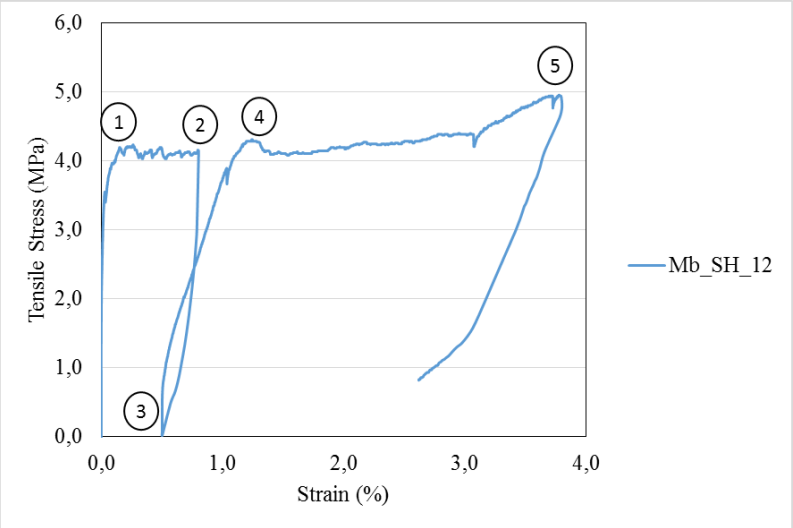

Figure 4. 19- Self-healing behaviour of one specimen cured in air and pre-loaded at 0.75%

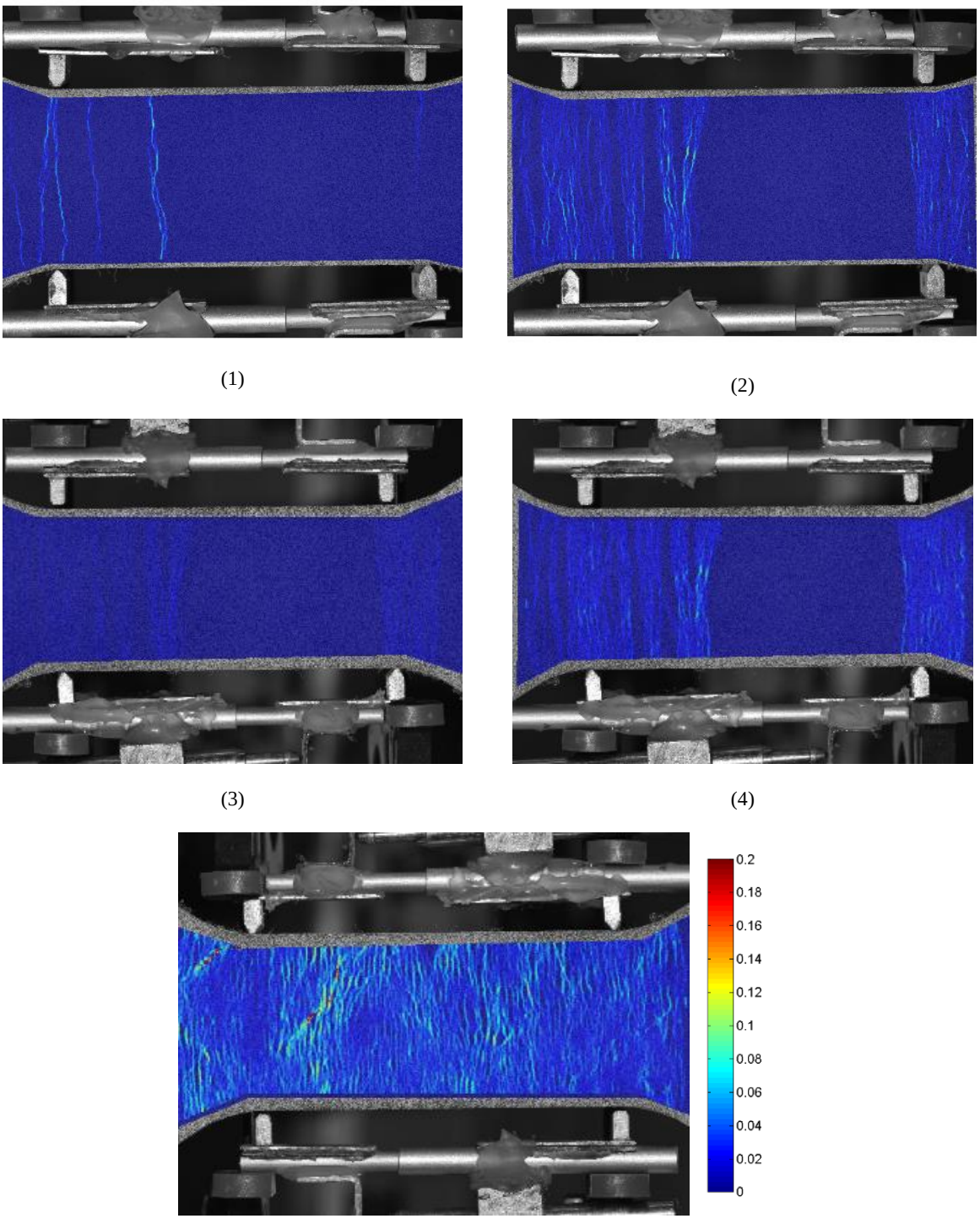

(1) (2)

(3) (4)

(5)

Figure 4. 20- Crack patterns obtained at stages 1 to 5 of Mixture B specimen cured in air and pre-load at 0.75%.

In Figure 4. 20 the first principal strain fields obtained for all stages of the tensile response identified are presented. Comparing Figure 4. 20 (2) and Figure 4. 20 (3) it is possible to visualize that most of the cracks were forced to close at the end of the pre-loading procedure due to the strong traction stresses generated at the opposite crack faces by the fibre reinforcement.

It is also possible to visualize that, between stages 3 and 4, only the previously generated cracks which underwent self-healing open again. Only from stage 4 onwards new cracks start to form, until failure is reached when crack saturation occurs. Before the failure is achieved, the specimen showed a diffuse crack pattern formed by multiple cracks that have a small width and good distribution in the central part of the specimen, as can be visualized in Figure 4. 20 (5).

The specimen represented in Figure 4. 21 was cured in seawater and pre-load until the tensile strain of 0.75% was reached.

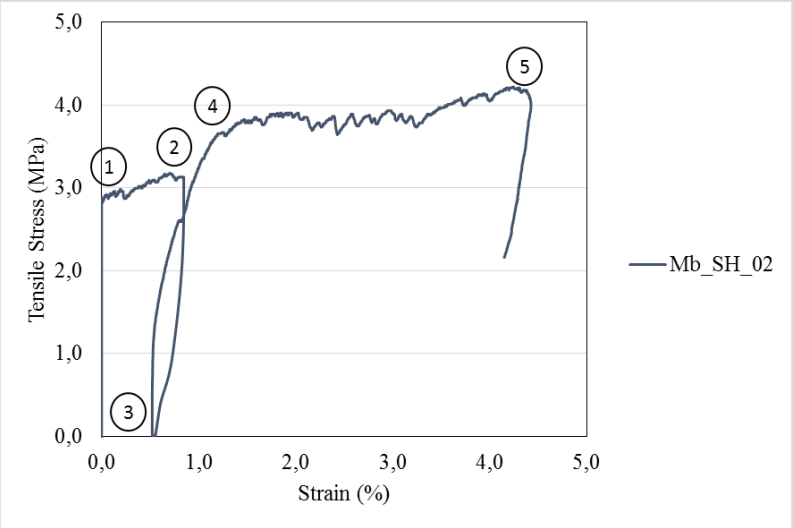

Figure 4. 21- Self-healing behaviour of one specimen cured in salted water and pre-loaded at 0.75%

The cracks obtained during the pre-loading stage are not so evenly distributed (Figure 4. 22 (2)). However, the Digital Image Correlation analysis showed that the specimen also underwent a very effective self-healing process after 28 days submerged in seawater.

After the initial stage of high recovered stiffness, the cracks start to reopen until new ones start to form. The cracks, before the failure, show small widths, but not as small as the ones obtained with the Mixture B specimen cured in air, as previously shown.

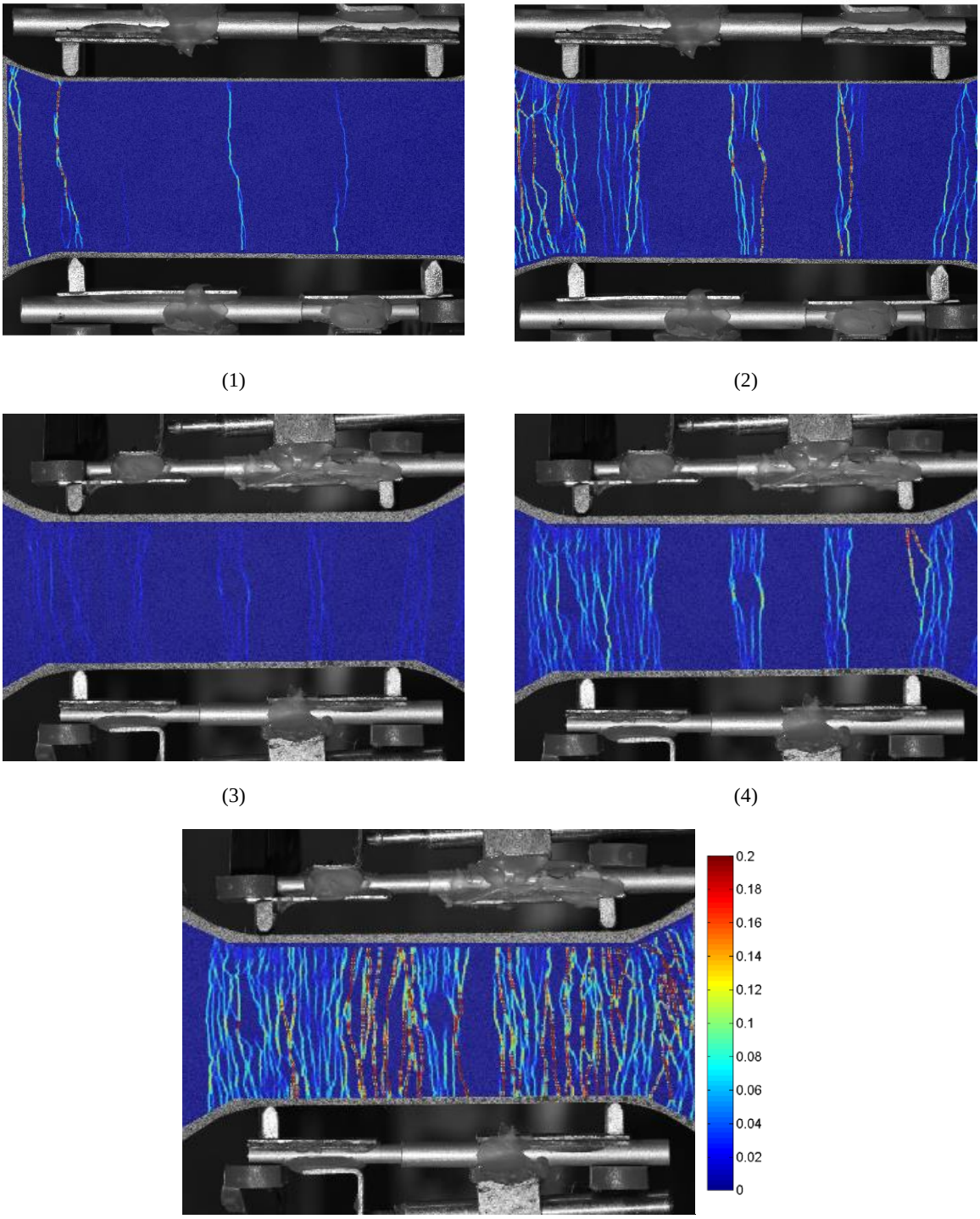

Figure 4. 22- Crack patterns obtained at stages 1 to 5 of Mixture B specimen cured in seawater and pre-load at 0.75%.

Figure 4. 23 represents the tensile response obtained for one Mixture B specimen cured in air and pre-loaded up to 1.5% of tensile strain at 14 days.

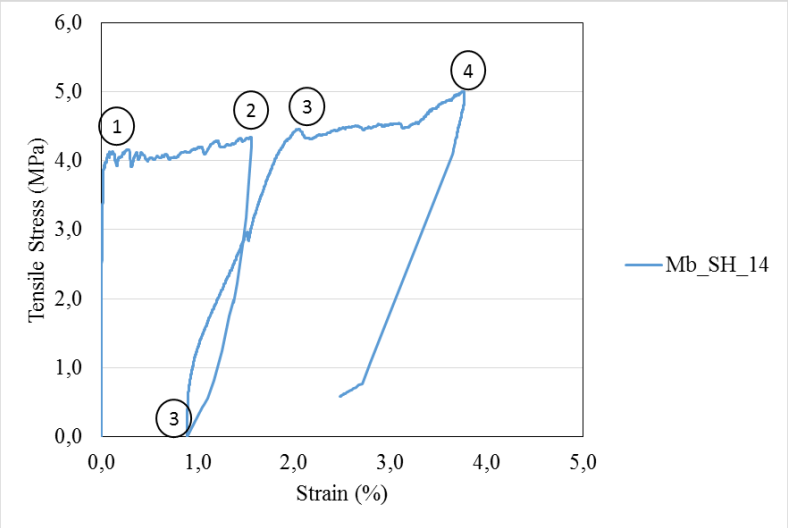

Figure 4. 23- Self-healing behaviour of one specimen cured in air and pre-loaded at 1.5%.

As shown, after the additional 28 days of curing, the cracks that appeared during the pre-loading stage were repaired and the initial stiffness was recovered until a tensile stress of about 0.6 MPa was again attained. From this point onwards, the previously closed cracks start to reopen until new cracks star to for in the second stage of tensile hardening and multiple crack formation.

In the end of the test, the specimen showed a distributed crack pattern across the entire surface with very small crack widths, as can be confirmed in Figure 4. 24.

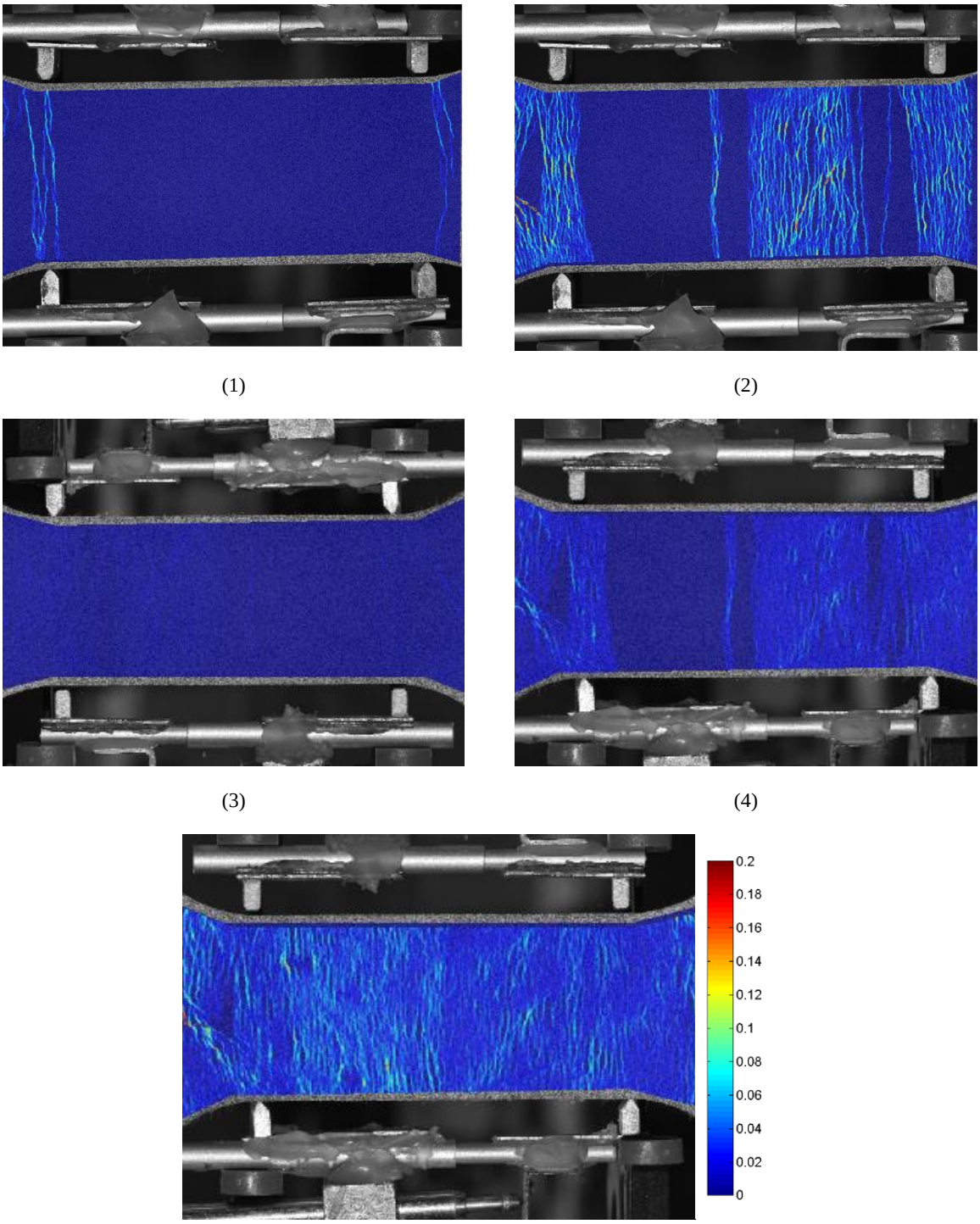

(1) (2)

(3) (4)

(5)

Figure 4. 24- Crack pattern of Mixture B specimen cured in air and pre-load at 1.5%

Figure 4. 25 represents the tensile response of a specimen cured in seawater and pre-loaded with 1.5% of tensile strain.

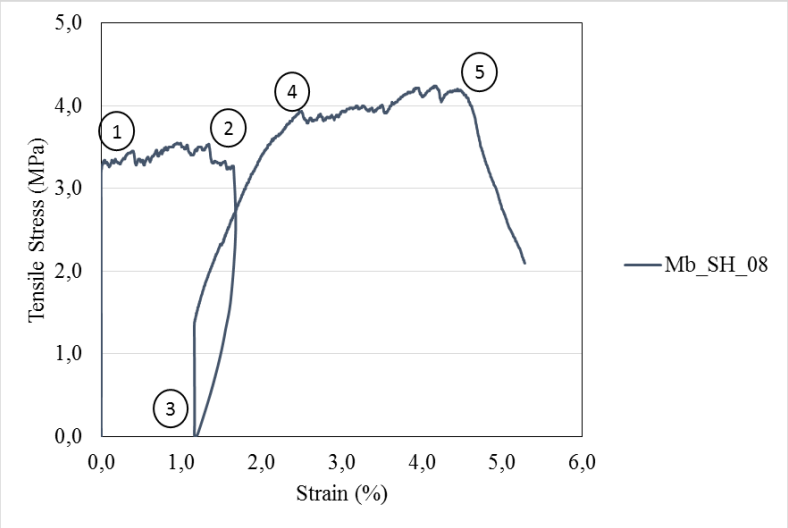

Figure 4. 25- Self-healing behaviour of one specimen cured in seawater and pre-loaded at 1.5%.

In this case, the initial stiffness recovery remained up to higher stresses than previously, of about 1.3 MPa. The number of cracks formed is not so high as previously, which implies greater crack widths, as shown in Figure 4. 26.

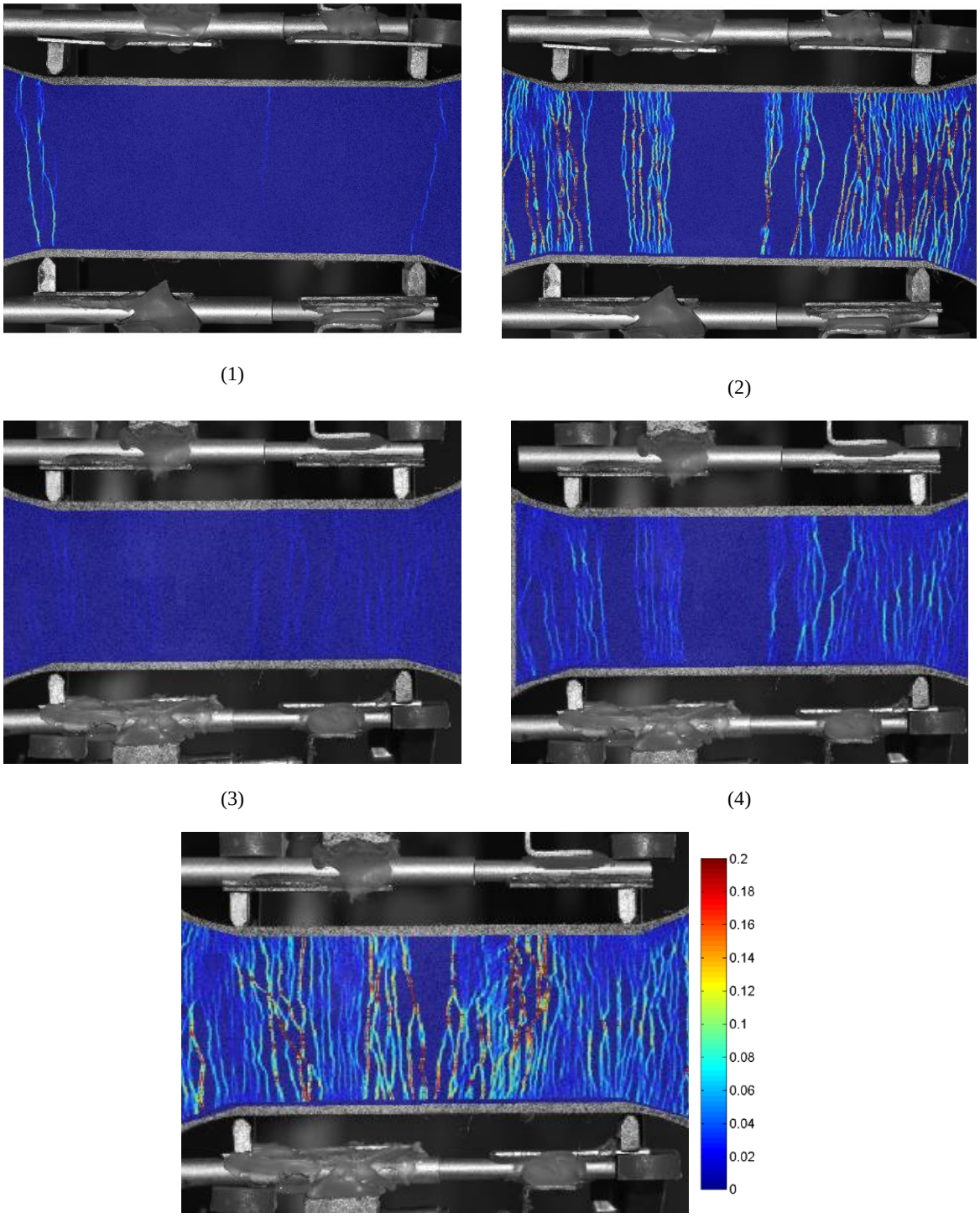

(1) (2)

(3) (4)

(5)

Figure 4. 26- Crack pattern of Mixture B specimen cured in seawater and pre-load at 1.5%

Mixture C

Figure 4. 27 is represents the tensile response obtained after conducting the experimental procedure already explained to assess the self-healing behaviour of one specimen prepared with salted water cured in air, when pre-loaded up to 0.75% of tensile strain.

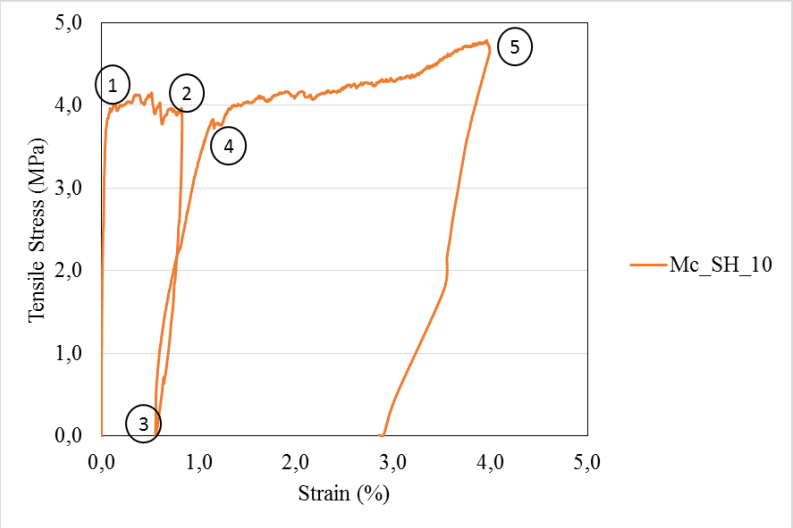

Figure 4. 27- Self-healing behaviour of one specimen cured in air and pre-loaded at 0.75%.

The image analysis showed that, when the specimen was pre-loaded a significant number of fine cracks emerged. As shown in Figure 4.28, the final crack pattern obtained after the second loading stage showed well distributed cracks, in great number and very finely spaced, and as a consequence with very tight crack openings.

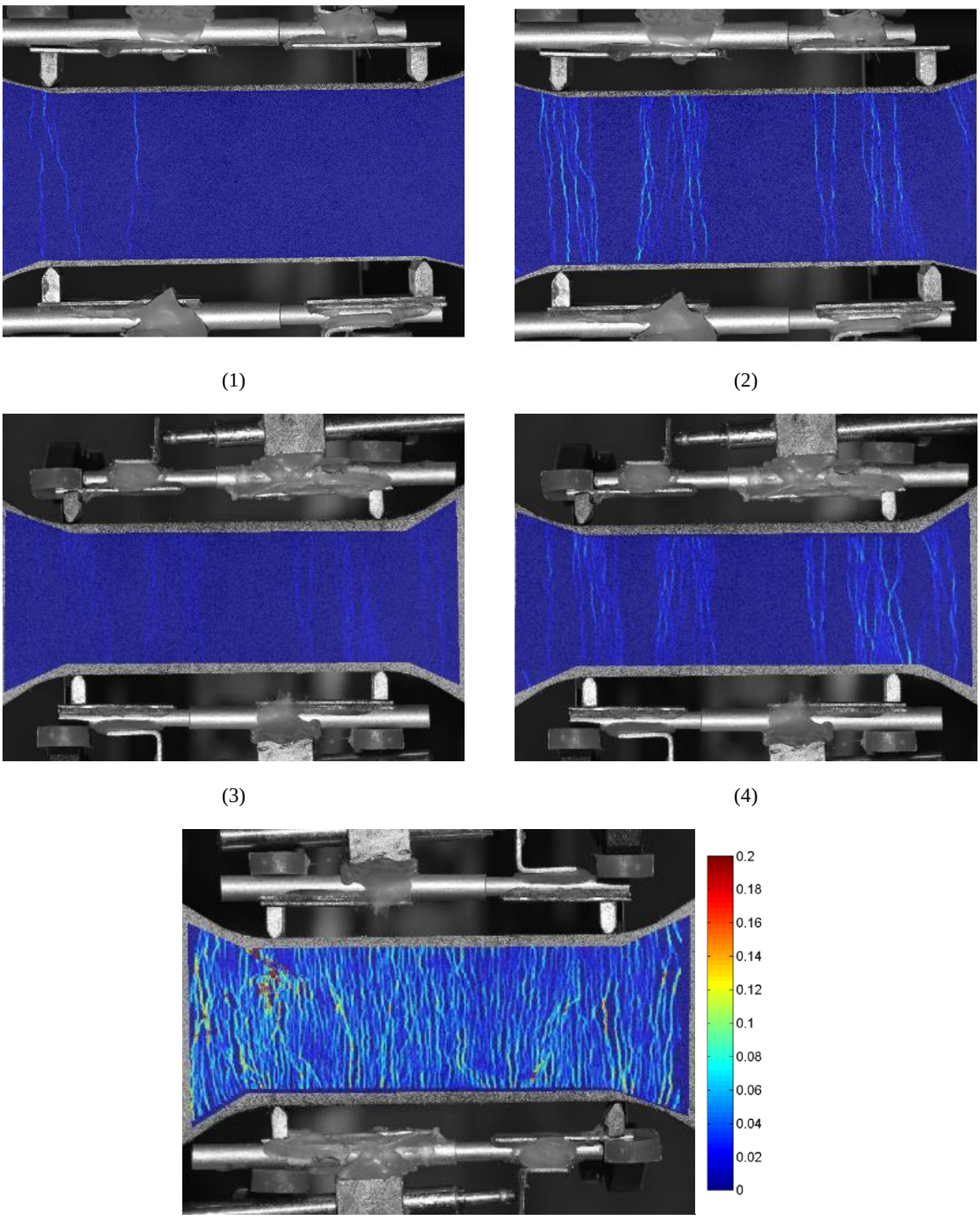

(1) (2)

(3) (4)

(5)

Figure 4. 28- Crack pattern of Mixture C specimen cured in air and pre-load at 0.75%

Figure 4. 29 represents the tensile response of Mixture C specimen, this time cured in salted water and pre-loaded up to 0.75% of tensile strain.

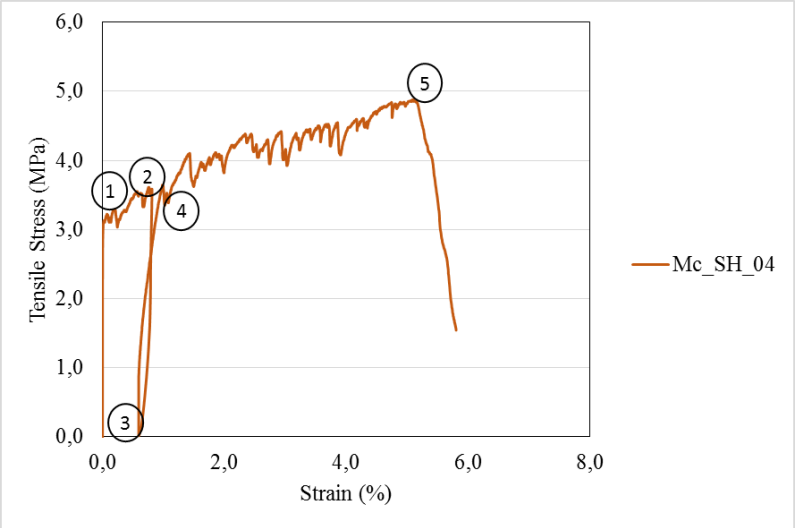

Figure 4. 29-. Self-healing behaviour of one specimen cured in seawater and pre-loaded at 0.75%.

Figure 4. 30 shows the image analysis obtained during testing. As shown, the number of cracks formed in each stage was high but not as high as previously observed. As a consequence, also crack widths are higher. The images also show that the closing stage led to cracks with a slightly greater crack opening. Before the failure the specimen showed a very uniform crack pattern.

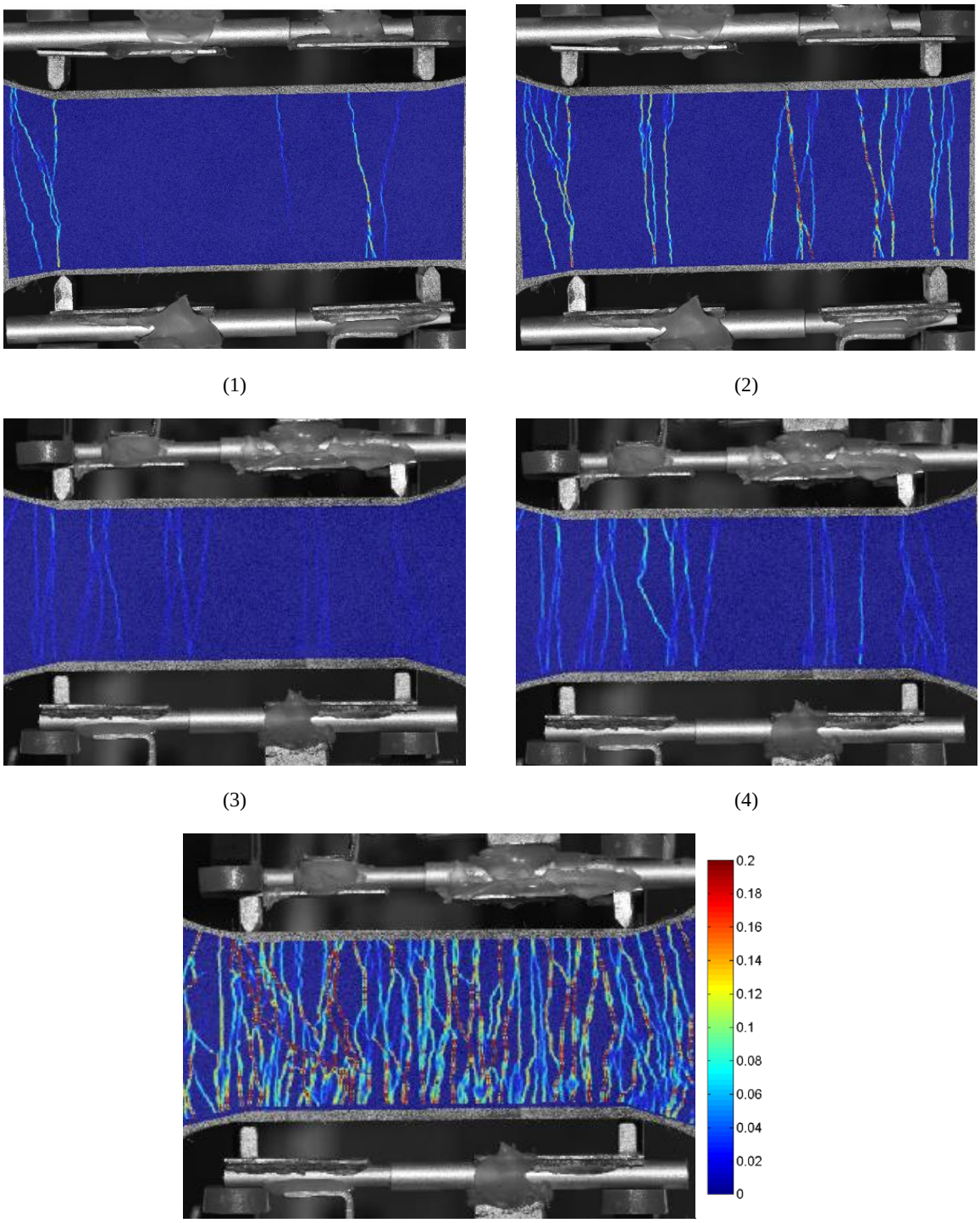

Figure 4. 30- Crack pattern of Mixture C specimen cured in salted water and pre-load at 0.75%

Figure 4. 31 shows the tensile response of one specimen cured in air, but in this case pre-loaded up to 1.5% of tensile strain.

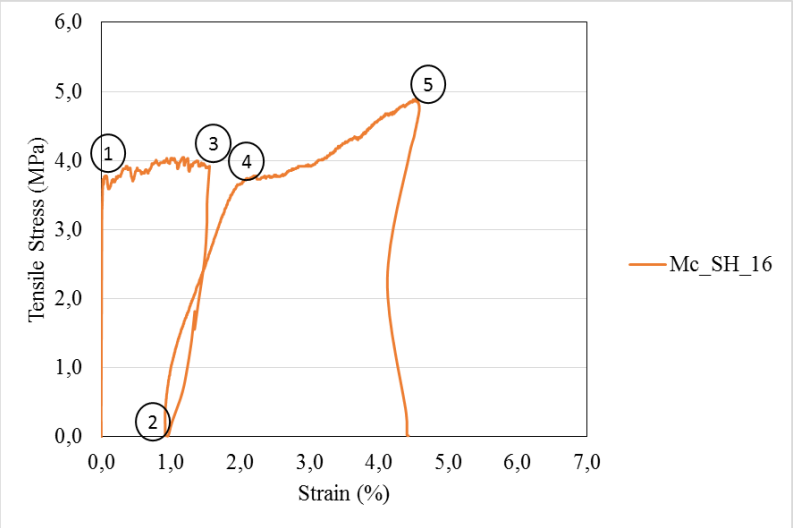

Figure 4. 31- Self-healing behaviour of one specimen cured in air and pre-loaded at 1.5%.

The image analysis shows that during the pre-cracking stage the number of cracks formed was very high, which implied very tight crack openings and a smooth transition to the second stage of strain hardening. In the end of the test, the specimen showed a distributed pattern of very fine cracks across the surface with very small crack widths, as can be confirmed in Figure 4. 32.

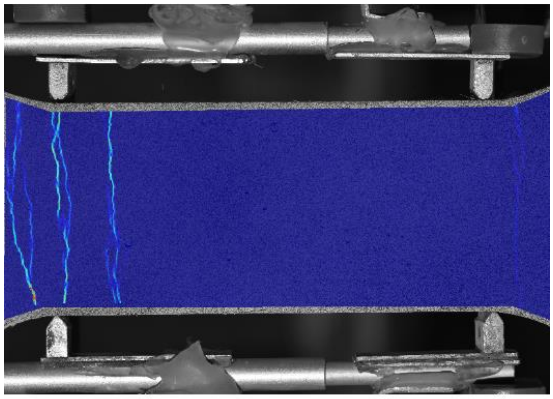

(1)

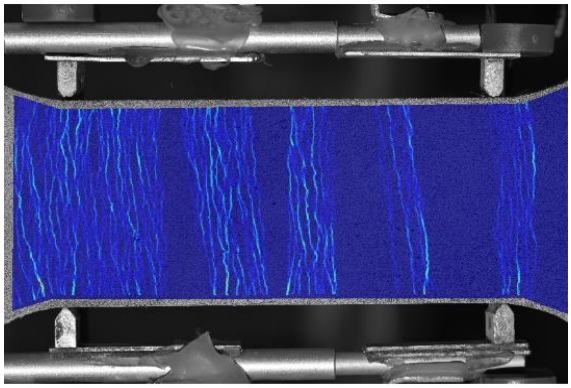

(2)

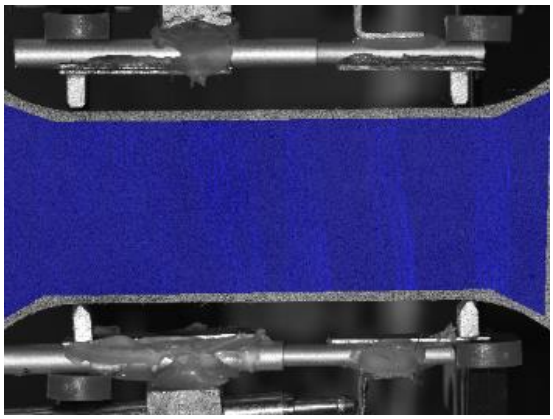

(3)

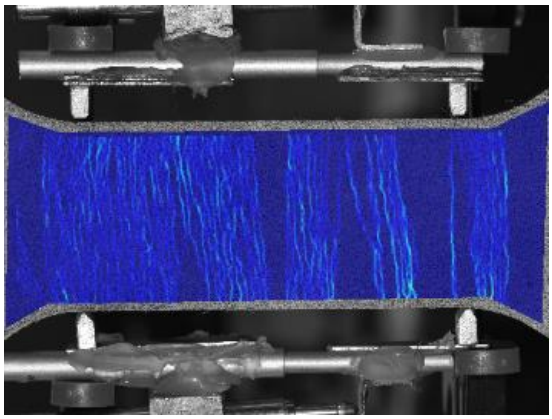

(4)

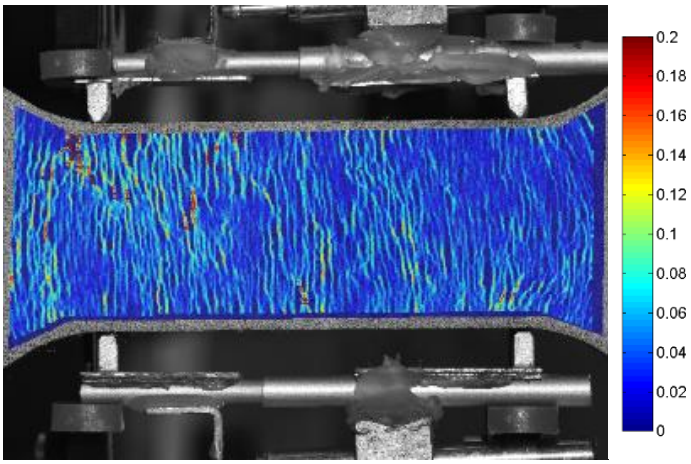

(5)

Figure 4. 32- Crack pattern of Mixture C specimen cured in air and pre-loaded at 1.5%

The results represented in Figure 4. 33 show the tensile response of Mixture C specimen cured in salted water and pre-loaded up to 1.5% of tensile strain.

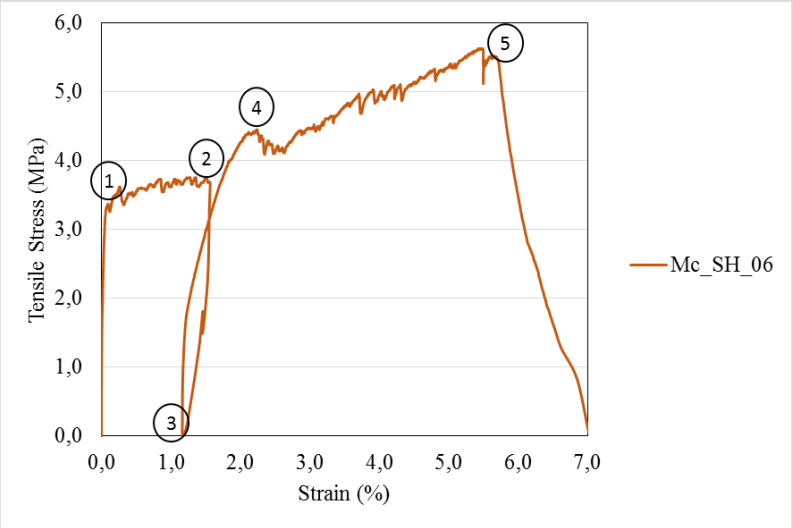

Figure 4. 33- Self-healing behaviour of one specimen cured in salted water and pre-loaded at 1.5%.

As shown in Figure 4. 34, once again the number of cracks formed during the pre-cracking stage is not so expressive. After the additional 28 days of curing in salted water, during the second cycle of loading the specimen retained the recovered initial stiffness until the tensile stress of about 1.5 MPa was again reached. Before failure the specimen showed a very uniform crack pattern, crack openings seem to be somewhat larger and therefore crack spacing is also greater. Although the number of cracks is less expressive, crack saturation seems to have been reached again, as previously.

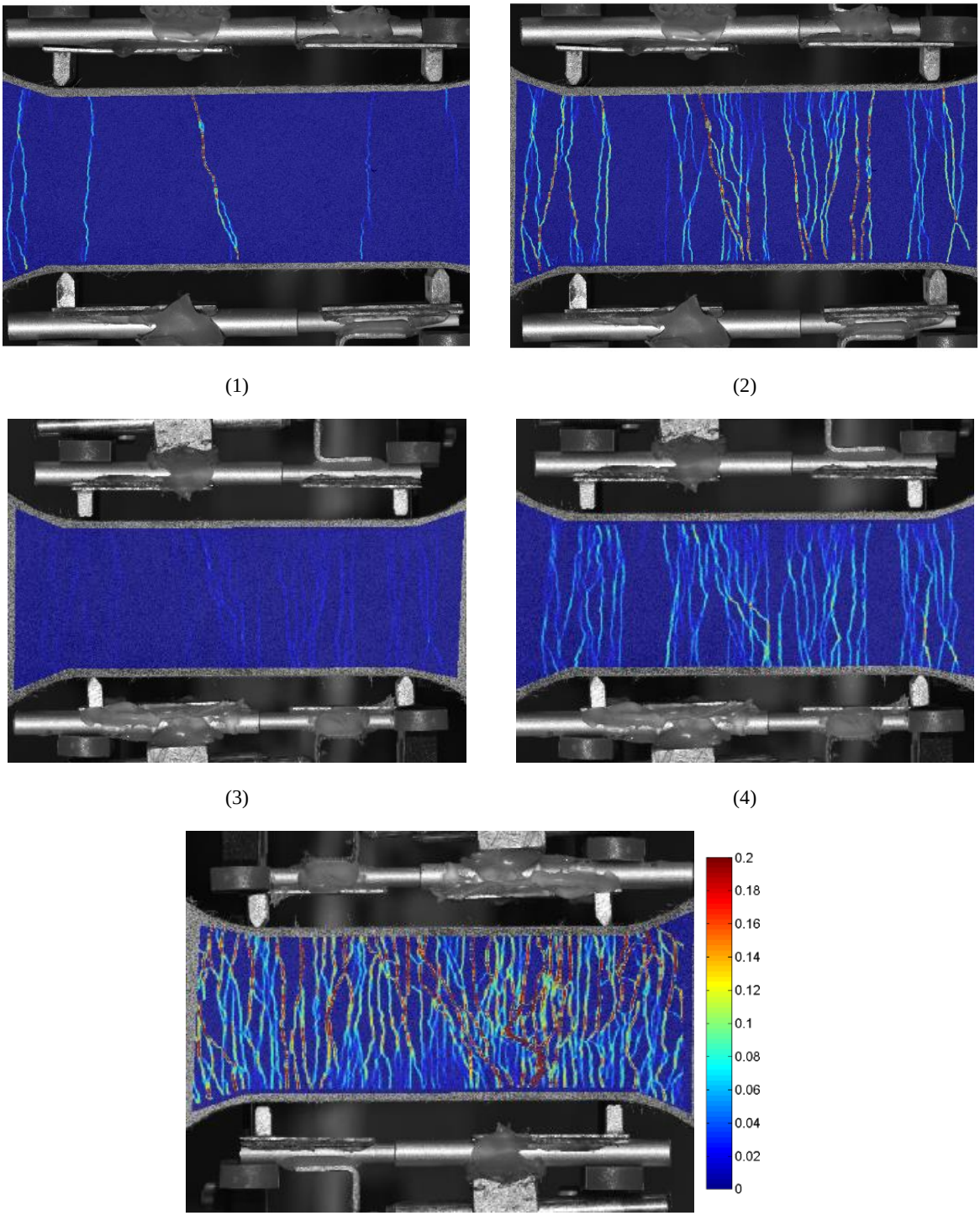

(1) (2)

(3) (4)

(5)

Figure 4. 34- Crack pattern of Mixture C specimen cured in salted water and pre-load at 1.5%

4.7 Conclusions

This study allowed to conclude that it is possible prepare ECC mixtures using seawater and salted water and still achieve self-healing behaviour. One of the most surprising outcomes of this research was to verify that ECCs prepared with seawater develop cracks that remain very tight and controlled at very small openings under tension, when compared with ECC mixtures prepared in salted water or even the conventional mixtures.

The amount of pre-load applied in the specimen and the type of curing have shown to have great influence both at the level of the mechanical responses in tension and the cracking processes development during testing. For these reasons and probably due to other mechanisms that need further research for full clarification, the self-healing behaviour was also influenced. Additionally, it was possible to verify that the specimens subjected to lower preloading levels and cured in the same water used to prepare the mixtures have almost fully recovered their initial mechanical characteristics.

Self-healing ability is a very attractive characteristic in this type of materials, and the results obtained allowed to understand that the design of these materials can be oriented to the optimization of this characteristic. The expectations relatively to what is still possible to achieve with these materials are quite high, considering what has been obtained in this research.

CHAPTER 5

Alternative Binder System

Recent developments have shown that it is possible to obtain acceptable mechanical characteristics with alternative binder systems that do not contain Portland cement. The main motivation for the development of these alternative binder systems is the additional stability and resistance to the aggressiveness of harsh environments. Other advantages may lie on the use of wastes or by-products of other industries.

Geopolymer materials is a term used to describe inorganic polymers based on aluminosilicates and can be produced by synthesizing pozzolanic compounds or aluminosilicate source of ceramic-like properties with highly alkali solutions [53]. Normally waste materials are used as a resource of aluminosilicates. However, in this research, metakoalin (a calcined product of a clay mineral kaolinite) was used. In this chapter, the term geopolymer is used to describe the alternative binder system.

The attaining of strain hardening and multiple cracking typical of ECC materials using these alternative binder systems is very attractive from a conceptual point of view, since additional resistance to harsh environments and enhanced durability are expected as main outcome. In this chapter the main objective is to attempt to attain a tensile hardening and multiple cracking behaviour under direct tension resourcing to alternative binder systems not containing Portland cement. In the present case, metakaolin was chosen as the basic fine material for defining the alternative binding system which will be used for the matrix phase.

5.1 Materials and Compositions

Within the scope of this chapter, three different matrix compositions have been developed. The materials commons in to all mixtures are: sand, metakaolin, activator (prepared with sodium hydroxide and sodium silicate), VMA (Viscosity Modifying Agent) and super-plasticizer. The ratio of the activator was prepared using one third of sodium hydroxide and two thirds of sodium silicate or waterglass.

This experimental work aims to obtain tensile strain-hardening behaviour in fibre reinforced geopolymeric materials. To achieve that goal, two types of fibres were used in this work: PVA

fibres and metallic fibres. The PVA fibres used in this study are 8 mm long and the diameter is 40 μm. The tensile strength of this type of fibre is 1600 MPa and the density is 1350 kg/m^3.

Corrosion resistance, flexibility and high mechanical strength are the essential properties of the metallic fibres used. They are 15.2 mm long and 1.0 mm wide. The tensile strength is 1400 MPa and the density is 7250 kg/m^3.

In this research work, metakaolin with a maximum grain size below 5 μm, specific gravity of 2.5 g/cm^3 and specify surface of 10150 cm^3/g.

The compositions of the three mixtures are presented in Table 5. 1.

Table 5. 1- Alternative binder system compositions for a volume of 2 dm^3.

	GP_2.0_Metallic	***GP_1.5_Metallic***	***GP_2.0_PVA***
Materials	M (g)	M (g)	M (g)
Metakoalin	1976,4	1987,8	1976,4
Sand	260	260	260
Sodium Hidroxide	439,2	441,7	439,2
Sodium Silicate	878,4	883,4	878,4
SP Sika 3002HE	20	20	20
VMA	6	6	6
PVA Fibres			52
Metallic Fibres	314	235,5	

Two mixtures of fibre reinforced geopolymer were prepared using metallic fibres. The difference between the two mixtures lies in the percentage of fibres used. The GP_2.0_Metallic has 2% of the total volume of the mixture of metallic fibres, and the mixture GP_1.5_Metallic has 1.5% of fibres by volume. The GP_2.0_PVA was prepared using 2% of PVA fibres by volume.

One of the mixtures previously used for preparing ECC was used now but replacing the PVA fibres with metallic fibres, in order to compare the behaviour of both types of mixtures. This was mixture A, considering that tap water was used in the mixture. The ingredients and quantities used to prepare the Ma_Metalic mixture are presented in Table 5. 2.

Table 5. 2- Ma_Metallic composition for a volume of 2 dm^3.

	Ma_Metallic

Materials	g
Cement	836,9
Fly Ash	1653,7
Sand	292,9
Filler	292,9
Water	657,9
SP 3002	31,6
VMA	2,5
Metallic Fibres	314

5.2 Mixing Procedure

The procedure adopted to mix all the ingredients for Ma_Metallic was already explained in section 3.1.2.

In the case of the three geopolymeric mixtures, a mixer with 3L capacity was used and the following procedure was adopted: firstly all the materials were collected and weighted. Solid ingredients, including metakoalin, sand and VMA were placed inside a bowl and mixed for one minute in slow speed. 90% of the activator and the super-plasticizer were added into the bowl while mixing for another 2 minutes. After that, the mixer was stopped in order to test the fresh properties of the mortar.

The mixer was restarted and all the fibres were then added to the mortar and mixed until the fibres were homogeneously distributed, for about 2 minutes. Then the remainder activator was added into the bowl and mixed for another 2 minutes. The fresh properties were tested, before casting.

The specimens were cast in different moulds and then vibrated in the shaking table, in order to reduce the air entrapped in the mixture and covered with cling film.

Two types of specimens were made: dogbone shaped and cubes. The dogbone moulds were used to perform the tensile test and the cubes were for the compression test. After one day of curing at 80º and RH=0% the specimens were demoulded and kept in dry atmosphere conditions, at about 20º +/- 2º of temperature.

5.3 Fresh Properties

The fresh properties were studied before and after the fibres were added to the mortar. The mini-slump time and the mini-slump spread were measured. The procedure adopted was explained in Section 3.1.3 of Chapter 3.

Table 5. 3- Fresh properties of each mixture.

	GP_2.0_Metallic	***GP_1.5_Metallic***	***GP_2.0_PVA***	***Ma_Metallic***
t20 (s)	no data	n.d	n.d	5.1
dxd (cm)	14x14	15x16	15x15	20x21
t20 (s) (with fibre)	n.d	n.d	n.d	n.d
dxd (cm) (with fibres)	10x10	14x13	13x12	20x19

As expected, the ingredients and quantities used affect the fresh properties of the mixtures.

As show in Table 5. 3, as expected all mixtures are more fluid without the fibres. Figure 5. 1 shows the fresh properties obtained in Ma_Metallic mixture, which has shown very similar behaviours with and without fibres.

Figure 5. 1- Images of fresh Ma_Metallic mixture spread with and without fibres.

Figure 5. 2 presents the fresh properties of GP_2.0_Metallic mixture. The percentage of fibres in the mortar is very high and affects the fresh behaviour in a much more evident way than before.

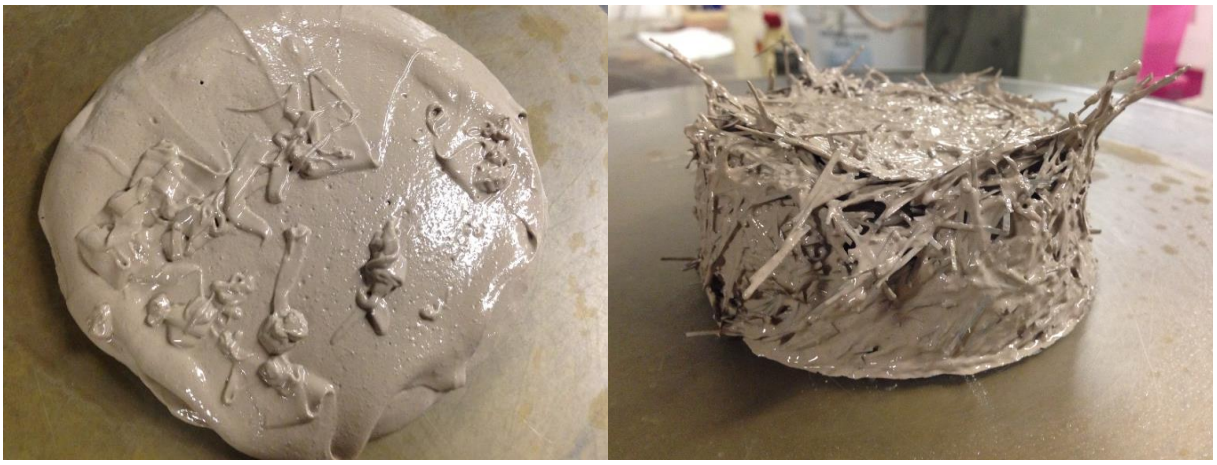

Figure 5. 2 – Images of fresh GP_2.0_Metallic spread mixture with and without fibres.

Figure 5. 3 represents the fresh properties of GP_1.5_Metallic mixture. This mixture showed better fresh behaviour when compared with mixture GP_2.0_Metallic. The fibres also seem to be better distributed.

Figure 5. 3- Images of fresh GP_1.5_Metallic spread mixture with and without fibres.

Figure 5. 4 represents the fresh properties of GP_2.0_PVA mixture. After adding the fibres to the mixture it exhibited a viscous behaviour and needed much more time to spread in the Plexiglass plate.

Figure 5. 4- Images of fresh GP_2.0_PVA spread mixture with and without fibres.

5.4 Mechanical Characterization

In order to characterize the hardened behaviour of the mixtures developed, compression and direct tension tests were performed according to the previously described procedures.

5.4.1 Compression testing

In this section the compression test results of each mixture are presented. The specimens used in this test were cubes measuring 50x50x50 mm^3. The setup and procedure used in this chapter was explained in section 3.2.3.

Mixture Ma_Metallic

Three cubic specimens were tested. Figure 5. 5 shows the Ma_Metallic compression test responses. Although not as expressive as in the results obtained in chapter three, also in this case the residual compressive stresses are considerable, mostly due to the toughness increase caused by the added fibres.

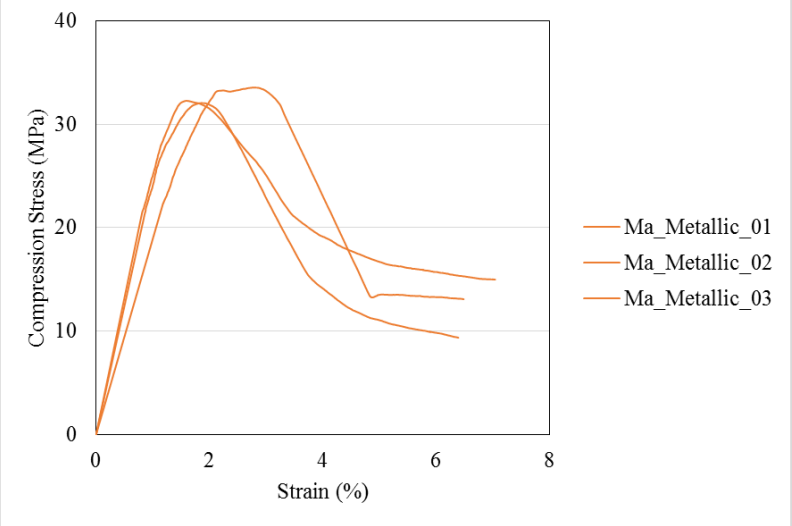

Figure 5. 5- Compressive responses of all Ma_Metallic specimens tested.

Table 5. 5 shows the compressive strength obtain in each specimen tested, which varied between 32 MPa and 34 MPa and resulted in a very low coefficient of variation.

Mixture	Specimen	Compressive strength (Mpa)	Average (Mpa)	Standard Deviation (Mpa)	Coefficient of Variation (%)
Ma_Metallic	1	33,54	32,62	0,66	2
	2	32,05			
	3	32,26			

Table 5. 4- Compression test results of Ma_Metallic specimens.

Mixture GP_2.0_Metallic

Figure 5. 6 shows the results of the compression tests. Three cubic specimens were tested.

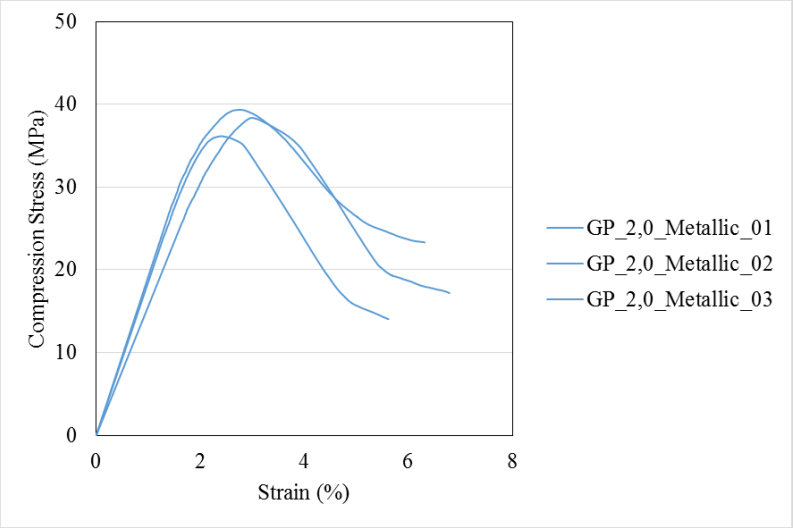

Figure 5. 6- Compressive responses of GP_2.0_Metallic specimens.

In Table 5. 5 the compressive strengths obtained are presented, ranging between 35 MPa and 40 MPa.

Table 5. 5- Compression test results of GP_2.0_Metallic specimens.

Mixture	Specimen	Compressive Strength (Mpa)	Average (Mpa)	Standard Deviation (Mpa)	Coefficient of Variation (%)
GP_2,0_Metallic	1	36,16	37,97	1,34	4
	2	38,37			
	3	39,36			

Mixture GP_1.5_Metallic

Figure 5.7 shows the compressive behaviour of the three specimens tested. The specimens showed generally distinct behaviours, which resulted in a higher coefficient of variation.

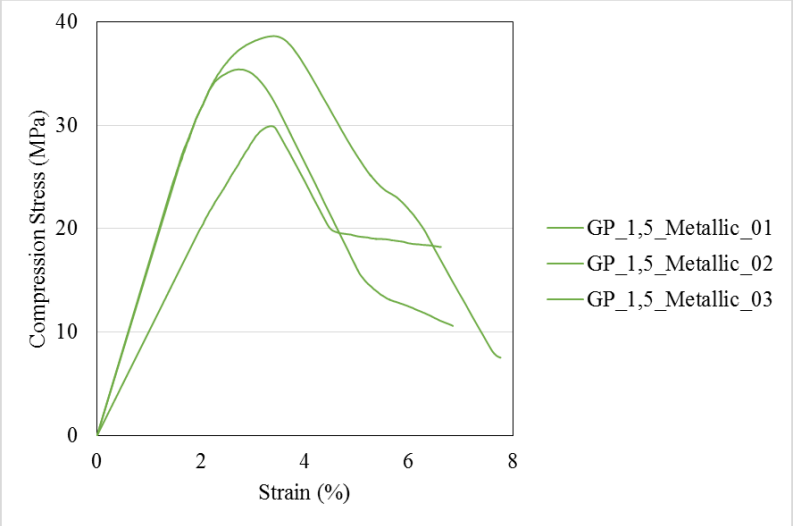

Figure 5.7- Compressive responses of GP_1.5_Metallic specimens.

Table 5. 6 shows the compressive strengths obtained, which varied between 29 MPa and 39 MPa. Probably the casting procedure or the preparation of the even surfaces on the cubic specimens prior to testing was not accurate, which created some heterogeneity on the results.

Table 5. 6- Compression test results of GP_1.5_Metallic specimens.

Mixture	Specimen	Compressive strength (Mpa)	Average (Mpa)	Standard Deviation (Mpa)	Coefficient of Variation (%)
GP_1,5_Metallic	1	29,90	34,64	3,60	10
	2	35,39			
	3	38,62			

Mixture GP_2.0_PVA

Three specimens of each mixture were tested. Figure 5. 8 shows the compressive response of all specimens tested. One of the specimens showed a different inclination in the elastic phase of the response, which means a lower stiffness. However, the compressive strengths obtained

were very similar, which suggests that, most likely, the creation of the even surfaces by rectifying the specimens prior to testing may not have been totally accurate.

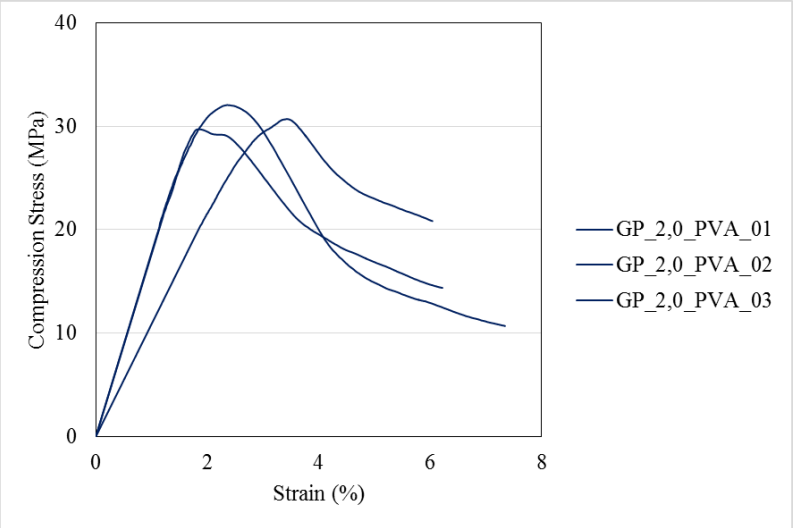

Figure 5. 8- Compressive responses of GP_2.0_PVA specimens.

Table 5. 7 presents the compressive strengths obtained, which ranged between 29 MPa and 33 MPa.

Table 5. 7- Compression test results of GP_2.0_PVA specimens.

Mixture	Specimen	Compressive strength (Mpa)	Average (Mpa)	Standard Deviation (Mpa)	Coefficient of Variation (%)
GP_2,0_PVA	1	30,70	30,82	0,95	3
	2	32,04			
	3	29,72			

5.4.2 Tensile Stress-Strain Behaviour

Although still considered as a novel topic, the compressive and flexural behaviour of geopolymers and other alkali activated materials is already reasonably well studied. However their tensile behaviour, and mostly their application on tensile strain hardening cementitious composites, is still unexplored. In this section the uniaxial tensile test results of all mixtures previously described are presented. The setup and procedure used in this chapter was explained

in section 3.2.3. All the specimens were rectified to improve the adherence between the specimen surface and the grips.

The main objective of this task was to try to obtain strain hardening and multiple crack development under direct tension on cementitious composites based on an alternative binder system which does not contain Portland cement.

Mixture Ma_Metallic

This mixture was prepared in order to compare the results of both types of mixtures considered in this chapter when using metallic fibres as reinforcement. Figure 5. 9 shows the uniaxial tensile test results of Ma_Metallic mixtures. Three specimens were tested, however one of the specimens was broken before testing.

The tensile results are very different than expected. The goal was obtain the strain hardening behaviour with the formation of multiple cracks. However, as can be confirm in Figure 5. 10, the specimens tested showed only one crack until the failure was reached.

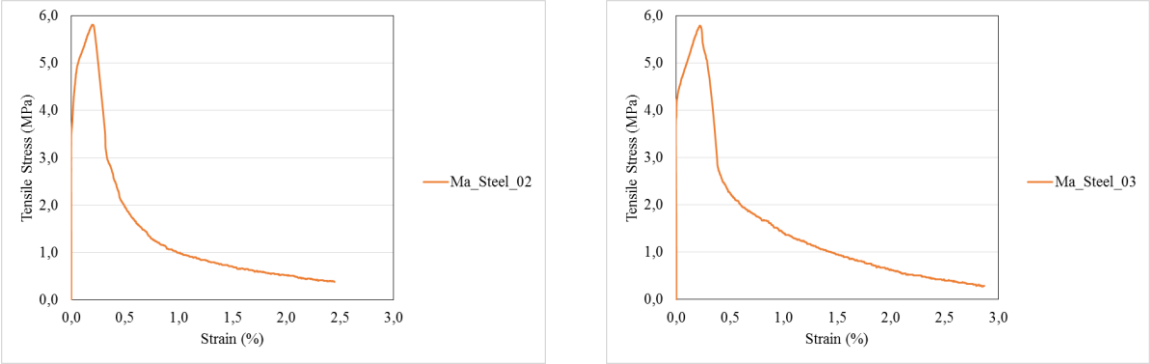

Figure 5. 9- Tensile responses of Ma_Metallic specimens.

The specimens showed high stiffness until 3.5 MPa of tensile stress and, after that, the increase of tensile stress until the failure is achieved for a small total strain.

Figure 5. 10- Photos of one Ma_Metallic specimen after testing.

It was possible to confirm that the use of metallic fibres influence the tensile results, however this is not enough to obtain the tensile strain hardening behaviour typical of ECC materials.

Mixture GP_2.0_Metallic

In this case the geopolymeric matrix was used and combined with the 2% of metallic fibres in volume. However, the multiple cracking behaviour was not achieved. All of the specimens showed only one crack. Figure 5. 11 represents the tensile responses obtained for mixture GP_2.0_Metallic.

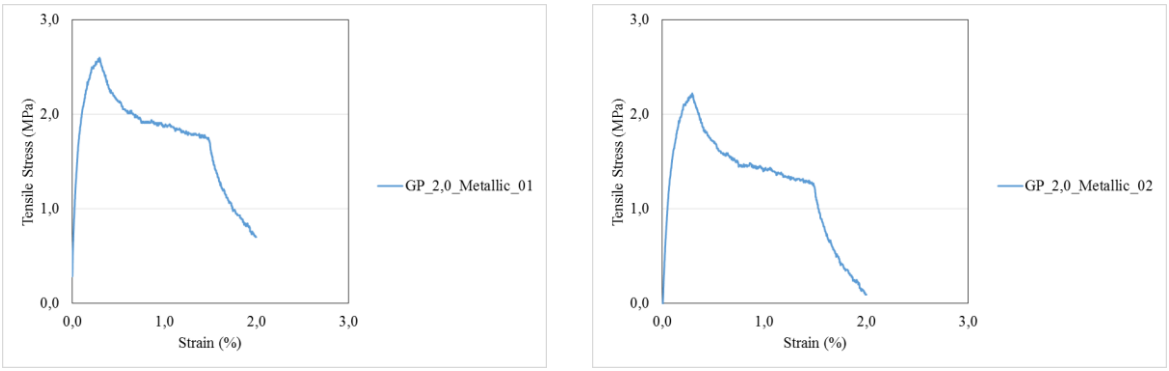

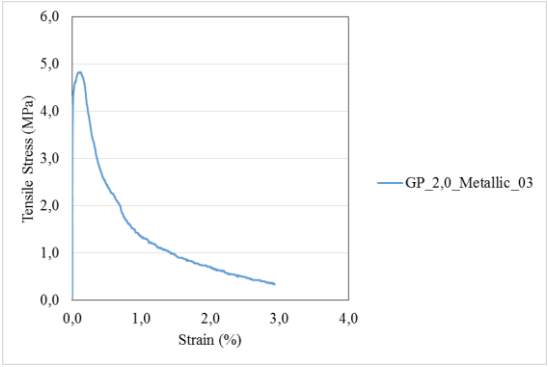

Figure 5. 11- Tensile responses of GP_2.0_Metallic specimens.

Figure 5. 12- Photos of one GP_2.0_Metallic specimen after testing.

In Figure 5. 12 it is possible to confirm that the specimens tested just showed the formation of one crack during the test.

Mixture GP_1.5_Metallic

Figure 5. 13 shows the tensile results of the three specimens tested. The results showed the goal of strain hardening behaviour was not achieved. The maximum tensile strain ranged between 2.0 MPa and 3 MPa. Although a lower volume of steel fibres favoured the fresh properties of the mixture and an easier dispersion of the fibres throughout the mixture, the existing fibres are not sufficient to efficiently bridge the cracks and propitiate the formation of more than one crack during tensile testing.

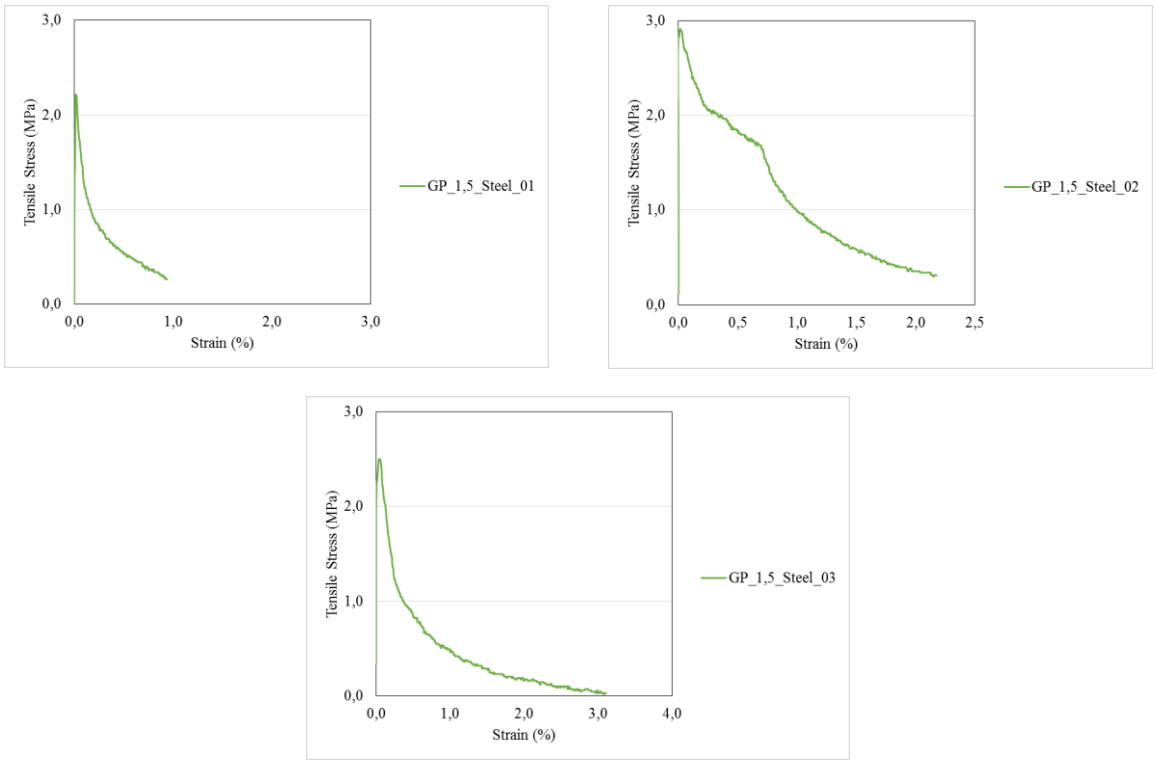

Figure 5. 13- Tensile response of GP_1.5_Metallic specimens.

Figure 5. 14 shows one specimens after the tensile testing.

Figure 5. 14- Photos of one of the GP_1.5_Metallic specimen after testing.

Mixture GP_2.0_PVA

In this mixture, 2% of PVA fibres were used to strengthen the matrix. The three specimens tested exhibited the development of multiple cracks at steadily increasing tensile stresses and

strains, which is typical of the ECC strain-hardening behaviour. In Figure 5. 15 the tensile response obtained for the first specimen is presented (GP_2.0_PVA_01). The specimen showed high stiffness until the formation of the first crack and then the gradual tensile hardening for increasing strains with the formation of multiple cracks. The maximum tensile stress of 3.4 MPa was reached and the maximum tensile strain was 1.8%.

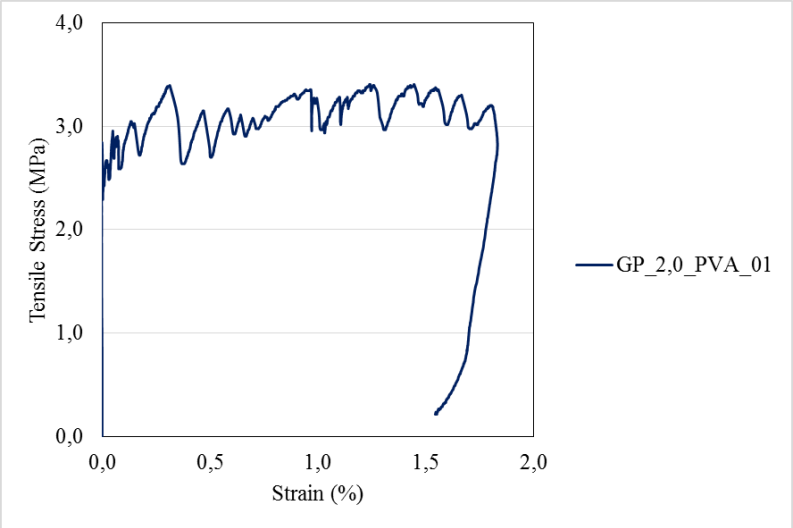

Figure 5. 15- Tensile response of GP_2.0_PVA_01 specimen.

In Figure 5. 16 the crack pattern observed at the surface of the first specimen is showed.

Figure 5. 16- Photos of the first GP_2.0_PVA_specimen after testing.

In Figure 5. 17 the tensile results of GP_2.0_PVA_02 specimen are showed. This specimen also achieved the same type of tensile behaviour. The sudden tensile peaks observed in the tensile hardening multiple cracking phase represent the formation of new cracks. The maximum tensile stress achieved by the specimen was 3.2 MPa and the tensile strain was 2.9 %.

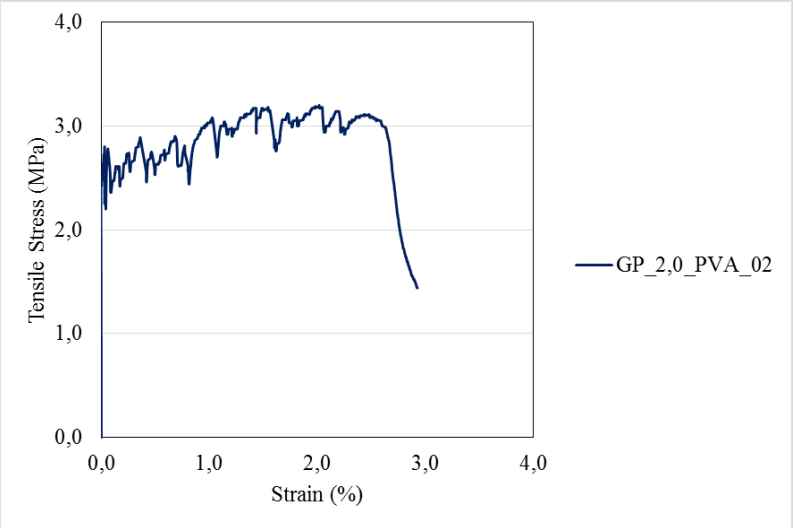

Figure 5. 17- Tensile response of GP_2.0_PVA_02 specimen.

The crack pattern observed on specimen GP_2.0_PVA_02 is showed in Figure 5. 18.

Figure 5. 18- Photos of GP_2.0_PVA_02 specimen after testing.

In Figure 5. 19 the tensile response obtained for GP_2.0_PVA_03 specimen are represented. The maximum tensile stress of 2.75 MPa at a maximum tensile strain of about 2% were reached.

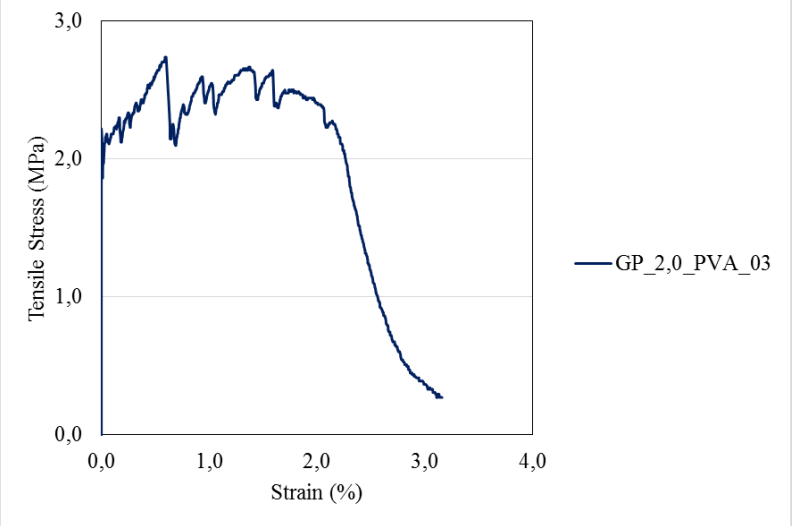

Figure 5. 19- Tensile response of GP_2.0_PVA_03 specimen.

In Figure 5. 20 the crack pattern of the GP_2.0_PVA_03 specimen is showed.

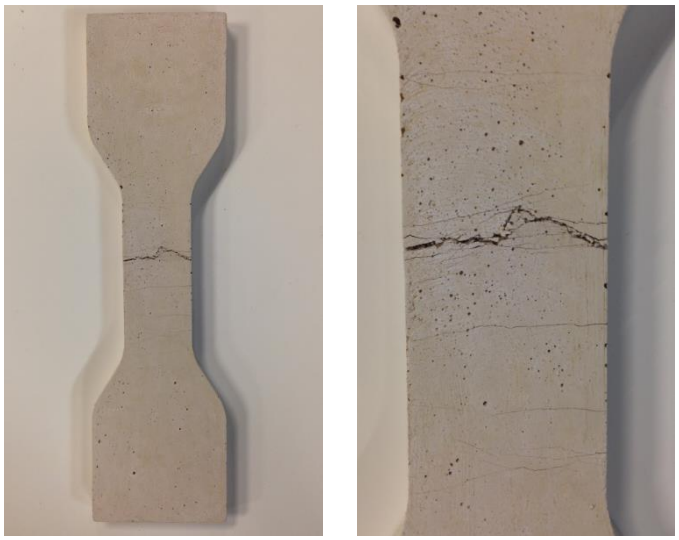

Figure 5. 20- Photos of GP_2.0_PVA_03 specimen after testing.

5.5 Conclusions

ECC materials, which typically contain ordinary Portland cement in the composition, show a special behaviour when subjected to uniaxial tensile loading, which is characterized by a moderate tensile hardening for a substantial increase in tensile strain while multiple cracks form. The fact that this material shows the ability to develop multiple cracks under tensile loading has two significant advantages: while more cracks develop at the same tensile deformation, the individual crack openings are significantly smaller.

The goal of the study reported in this chapter was to try to obtain the same type of behaviour but with an alternative binder system, in this case a metakoalin based geopolymer. That behaviour was reached by GP_2.0_PVA mixture. The mixtures that were reinforced with metallic fibres did not achieve multiple cracking behaviour in tension, even when the same type of matrix used in ECC compositions was employed. However this study was just a first incursion in this topic, due to time limitations. Additional studies must be carried out in order to fully explore the ideas and concepts discussed.

The development of fibre reinforced geopolymer materials may still be considered as a novel topic and has showed great potential for achieving important developments for Civil Engineering and structural applications.

CHAPTER 6

Final Remarks

The present investigation concerning the mechanical behaviour of Engineered Cementitious Composites showed that the main properties of ECC materials, including multi-cracking behaviour at increasing tensile strains when subjected to direct tension, is very sensitive to variations of the curing environment or the type of water used in the composition, considering mostly the seawater influence. However, although the differences in the tensile behaviour are clearly distinguishable, the tensile properties including tensile strain hardening or multiple cracking were never compromised. The differences became clear mostly when the cracking processes were analysed, which shows that the effects studied have a greater influence at the micromechanical level.

The most important accomplishments of this research are related to the Engineered Cementitious Composites and may be summarized by the following:

- One of the main conclusion of this research is that it was confirmed that is possible to replace the water used in ECC materials by seawater and salted water without substantially compromising the typical strain hardening behaviour of ECC materials;

- This research revealed that ECC mixtures prepared with seawater develop cracks that remain very tight and controlled at very small openings under tension, when compared with ECC mixtures prepared with salted water, or even the conventional ones prepared with tap water.

- The results obtained showed also that the salted water does not represent well the effect of seawater on ECC mechanical characteristics, since in all perspectives the responses obtained when seawater or salted water were considered have been quite different.

Self-healing ability is a very attractive characteristic in this type of materials, and the results obtained allowed to understand that the design of these materials can be oriented to the optimization of this characteristic. The main conclusion are:

- It is possible prepare ECC mixtures using seawater and salted water and still achieve self-healing behaviour;

- The pre-loading level and the type of curing have shown to have great influence both at the level of the mechanical responses in tension and at the cracking processes development during testing;

- It was possible to verify that the specimens subjected to lower pre-loading levels and cured immersed in the same type of water used to prepare the mixtures have almost fully recovered their initial mechanical characteristics.

ECC materials, which typically contain ordinary Portland cement in their composition, have special behaviour when subjected to uniaxial loading, which is characterized by a moderate tensile hardening for a substantial increase in tensile strain while multiple cracks form. Another important goal of this study was to try to obtain the same type of behaviour but with an alternative binder system, in this case a metakoalin based geopolymer. That behaviour was reached by the mixture prepared with PVA fibres. The mixtures that were reinforced with metallic fibres did not achieve multiple cracking behaviour in tension, even when the same type of matrix used in ECC compositions was employed.

The geopolymer material is a more sustainable option due to the utilization of by-products and/or waste materials when compared to the cementitious matrix composite based on Portland cement. The development of fibre reinforced geopolymer materials may still be considered as a novel research topic and showed to have great potential for creating new and interesting developments for Civil Engineering and structural applications.

Bibliography

[1] S. Islan, M. Islan and B. C. Mondal, "Deterioration of Concrete in Ambiente Marine Environment," *International Journal of Enginnering,* 2012.

[2] P. K. Mehta, Concrete in the Marine Environment, Elsevier, 2003.

[3] B. C. Gerwick Jr., Construction of Marine and Offshore Structures, CRC Press, 2007.

[4] L. N. Phillips, Designe with Advanced Composite Materials, Springer, 1989.

[5] Available:https://commons.wikimedia.org/wiki/File%3AOceans_and_seas_boundaries_map-en.svg. [Accessed 7 10 2015].

[6] J. Jaszewski and H. Costa, "National Geografic," 2014. [Online].

[7] S. D. Q. M. M. Z. C. M. M. K. A. M. a. H. M. Solomon, "Climate Change 2007: The Physical Science Basis. Contribution of Working Group I to the Fourth Assessment Report of the Intergovernmental Panel on Climate Change," Cambridge University Press, Cambridge, Cambridge, United Kingdom and New York, NY, USA, IPCC, 2007.

[8] "Global Climate Change," [Online]. Available: http://climate.nasa.gov/vital-signs/sea-level/. [Accessed 10 10 2015].

[9] R. J. Nicholls, F. M. Hoozemans and M. Marchand, "Increasing flood risk and wetland losses due to global sea-level rise: regional and global analyses," *Global Environmental Change,* 4 June 1999.

[10] Available: http://www.topchinatravel.com/china-attractions/yangshan-deep-water-port.htm. [Accessed 10 10 2015].

[11] A. Govarets and B. Lauwerts, "Assement of impact of coastal defence structures," 2009.

[12] P. A. Frieze, "Offshore Structure Design and Construction," in *Ships and offshore structures,* 2011.

[13] Available: https://www.rt.com/news/224371-oil-rig-berkut-extraction/. [Accessed 11 10 2015].

[14] "Study on deepening understanding of potencial blue growth in the EU members states on Europe's atlantic arc," March 2014. [Online].

[15] Available: http://www.logisticaetransporteshoje.com/porto-de-sines-marca-presenca-no-port-efficiency-forum/. [Accessed 15 10 2015].

[16] "The Ocean and Temperature - MarineBio Organization," [Online]. Available: http://marinebio.org/oceans/temperature/.

[17] Available: http://aquarius.umaine.edu/cgi/ed_act.htm?id=18. [Accessed 12 10 2015].

[18] E. Pereira, Processes of cracking in strain hardening in cementitious composites, 2012.

[19] Available: http://www.mirror.co.uk/news/uk-weather-environment-agency-issues-2648561. [Accessed 12 10 2015].

[20] A. Costa and J. Appleton, "Case studies of concrete deterioration in a marine environment in Portugal," *Elsevier,* 2002.

[21] A. K. H. Kwan and H. H. C. Wong, "Durability of Reinforced Concrete Structures, Theory vs Practice," Department of Civil Engineering, The University of Hong Kong, 2005.

[22] P. C. Liu, "Damage to concrete structures in a marine environment," *Materials and Structures,* 2007.

[23] C. C. Staff, "Concrete Constrution," 1 February 1966. [Online]. Available: http://www.concreteconstruction.net/concrete-articles/watertight-concrete.aspx.

[24] Available:http://www.corrosionclinic.com/corrosion_courses/advanced_course_in_concrete_durability.htm. [Accessed 20 10 2015].

[25] R. Ferreira, "Probability-based durability analysis of concrete structures in marine environment," 2004.

[26] Available:http://expcep.com/en/bulletin/concrete-degradation-in-infrastructures/. [Accessed 16 10 2015].

[27] Available: http://masqueingenieria.com/blog/durabilidad-del-hormigon/. [Accessed 12 10 2015].

[28] Available: http://www.phys.tue.nl/nfcmr/damage-crys.html. [Accessed 13 10 2015].

[29] P. Pullar-Strecker, Concrete Reinforcement Corrosio: From Assessment to Repair Decisions, Technologia & Engineering, 2002.

[30] S. F. Daily, "Undestanding Corrosion and Cathodic Protection of Reinforced Concrete Structures," Corrpro Companies, Inc., 2011.

[31] C. K. R. Christodoulou, “The word's first hybrid corrosion protection systems for prestressed concrete bridges,” in *Corrosion and Prevention 2013*, Brisbane, 2013.

[32] Available: http://www.concrete-repairs.co.uk/kyle-of-tongue.php. [Accessed 13 10 2015].

[33] V. C. Li, “Engineered Cementitious Composites (ECC) - Material, Structural, and Durability Performance,” Michigan, 2007.

[34] V. C. Li, “On Engineered Cementitious Composites (ECC),” 2003.

[35] M. Sahmaran and V. C. Li, “Engineered Cementitious Composites,” *Transportation Research Board of the National Academies*, 2010.

[36] G. P. van Zijl and F. H. Wittmann, “Durability of Strain-Hardening Fiber Reinforced Cement-Based Composites (SHCC),” 2009.

[37] V. C. Li, “Reflections on The Research And Development of Engineered Cementitious Composites (ECC),” 2002.

[38] K. Li and S. Hui-sheng, “Investigation of self-healing behavior of Engineered Cementitious Composites (ECC) materials,” *Constrution and Building Materials*, 2011.

[39] Z. Li, Z. Ding and Y. Zhang, “Development of Sustainable Cementitious,” Department of Civil Engineering, Hong Kong University of Science and Technology, Hong Kong, 2004.

[40] N. Saidi, B. Samet and S. Baklouti, “Effect of Composition on Structure and Mechanical Properties of Metakaolin Based PSS-Geopolymer,” *International Journal Of Materials Science*, 2013.

[41] P. Duxson, J. L. Provis, G. C. Lukey and J. S. J. van Deventer, “The role of innorganic polymer tecnology in yjr development of "green concrete",” *Cement and Concrete Research*, 2007.

[42] F. Pacheco-Torgal, J. A. Labrincha, C. Leonelli, A. Palomo and P. Chindaprasirt, Alkali-activated Cements, Mortars and Concretes, Woodhead Publishing, 2015.

[43] X. Yao, Z. Zhang, H. Zhun and Y. Chen, “Geopolymerization process of alkali-metakaolinite charecterized by isothermal calorimetry,” *Thermochimica Acta*, 2009.

[44] A. Palomo, P. Krivenko, I. Garcia-Lodeiro, E. Kavalerova, O. Maltseva and A. Fernández-Jiménez, “A review on alkaline activation: new analytical perspectives,” in *Materiales de Construcción*, 2014.

[45] P. Duxon, A. Fernández-Jiménez, J. L. Provis, G. C. Lukey, A. Palomo and J. S. J. van Deventer, "Geopolymer tecnology: the current state of the art," 2006.

[46] D. Bondar, "Geo-polymer Concrete as a New Type of Sustainable Constructin Materials," in *Third International Conference on Sustainable Construction Materials and Technologies*.

[47] Available: http://www.hassellstudio.com/en/cms-projects/detail/the-university-of-queensland-global-change-institute/. [Accessed 22 10 2015].

[48] D. Bondar, C. J. Lynsdale, N. B. Milestone, N. Hassani and A. A. Ramezanianpour, "Enhineering Properties of Alkali Activated Natural Pozzolan Concrete," in *International Conference on Sustainanble Construction Materials and Technologies*.

[49] B. Y. Lee, C.-G. Cho, H.-J. Lim, J.-K. Song, K.-H. Yang and V. C. Li, "Strain hardening fiber reinforced alkali-activated mortar – A feasibility study," *Construction and Building Materials,* 2012.

[50] M. Ohno and V. C. Li, "A feasibility study of strain hardening fibers reinforced fly ash-based geopolymer composites," *Constrution and Building Materials,* 2014.

[51] R. Reis, R. Malheiro, A. Camões and M. Ribeiro, "Carbonation resistance of high volume fly ash concrete," *Susteinable Constrution Materials,* 2015.

[52] E. B. Pereira, G. Fisher and J. A. O. Barros, "Direct assessment of tensile stress-crack opening behavior of Strain Hardening Cementitious Composites," *Cement and Concrete Research,* 2002.

[53] D. L. Y. Kong, J. G. Sanjayan and K. Sagoe-Crentsil, "Comparative performace of geopolymers made with metakaolin and fly ash after exposure to elevated temperatures," *Cement and Concrete Research,* 2006.